

CHAPTER 15

THE CHEMISTRY OF COASTAL CLOUDS AND AEROSOL IN
THE SANTA BARBARA CHANNEL

by

J. William Munger[†], Jeff Collett, Jr.,[‡]
Bruce C. Daube, Jr., and Michael R. Hoffmann^{*}

Environmental Engineering Science
W. M. Keck Laboratories, 138-78
California Institute of Technology
Pasadena, CA 91125, U.S.A.

[†] *Present Addresses*

[†] Dept. of Earth and Planetary Sciences, Harvard
University, Pierce Hall, 29 Oxford St., Cambridge MA 02138

[‡] Atmosphärenphysik ETH, Höggerberg HPP, CH-8093 Zürich, Switzerland

Submitted to:

Environmental Science & Technology

27 February 1989

* To whom correspondence should be addressed.

* Address from 3-15 to 9-1-89: EAWAG, CH-8600 Dübendorf, Switzerland

Abstract

Marine stratus clouds in the Santa Barbara Channel area were found to be consistently acidic with $\text{pH} \leq 4$, $[\text{SO}_4^{2-}] \geq 500 \mu\text{N}$ and $[\text{NO}_3^-] \geq 1000 \mu\text{N}$. The airmass over the Santa Barbara Channel was found to have an excess of acidity with aerosol concentrations of excess sulfate and total nitrate ($\text{NO}_3^- + \text{HNO}_3$) in the range of $100 - 200 \text{ neq m}^{-3}$. Excess acidity in the atmosphere appeared to effectively remove Cl^- from sea-salt aerosol by displacement of HCl , although most of the HCl was rescavenged by the clouds at night. Concentrations of acids at a site above the inversion base were found to be similar to those observed at lower elevations. Atmospheric acidity in the Channel area appeared to arise from the oxidation of local SO_2 and NO_x emissions from nearby urban centers and offshore oil platforms and from transport of polluted air from the Los Angeles basin.

Introduction

Stratiform clouds are prevalent along the eastern coasts of the subtropical oceans. The combination of a temperature inversion induced by subsidence about quasi-stationary high pressure systems and cold sea surface temperatures is conducive to the formation of stratus and stratocumulus clouds. In addition to their influence on local climate, these stratiform clouds influence global climate and circulation because of their large areal extent. Stratus clouds process aerosol, but do not usually remove it via precipitation. Thus, they have a significant influence on aerosol properties.

The summertime weather along the California coast typifies these conditions. A persistent high pressure system is located over the eastern Pacific. High temperatures over the inland deserts in California and Arizona generate a region of low pressure. Northerly winds result from this pressure gradient. Subsidence about the high pressure system leads to a temperature inversion. Calculations of divergence and vertical motion (1) indicate that subsidence should depress the inversion. Convective mixing at the surface offsets the vertical motion, however, preventing the inversion from being pushed to the surface. The average height of the summertime inversion base along the Southern California coast is 400 – 600 m. The inversion is lowest at the coastline and slopes upward away from the coast in either direction (1).

The radiation, dynamic, and thermodynamic structure of the marine stratocumulus have been studied extensively off the coast of California (2–5). Cloud-topped boundary layers are unique in that their mixing is driven by radiative cooling at the top of the layer (6–9) rather than by heating at the surface. Cool air at the cloud top tends to sink. Dry air from above the cloud is entrained by the descending air parcel. Additional cooling of the cloud layer is caused by evaporation of droplets when dry air is mixed into the cloud.

The chemistry of the marine layer and associated stratus clouds along the California coast is of considerable interest. Cloud dynamics and microphysics play a major role in determining the chemical composition of the cloud droplets. Furthermore, cloud microphysics may be influenced

by the chemical composition of the air mass. Cloudwater concentrations of species that are formed or transported above the inversion base are increased by entrainment. Conversely, cloudwater concentrations of species that are absent above the inversion are reduced by entrainment.

Pollutant concentrations may build up along the coast, since ventilation is limited by the temperature inversion and by recirculation associated with a land/sea breeze cycle. Coastal cloudwater may be prone to acidification because sources of atmospheric alkalinity are limited (10). The Santa Barbara Channel area is of special interest in this regard because it is subject to frequent cloud cover, the coastal plain is undergoing rapid urban development, and there is pressure to accelerate exploration and utilization of offshore oil resources in the Channel.

We have studied the cloudwater and aerosol composition at several sites along the Santa Barbara Channel coast over two summers. Our objectives were to determine the acid/base balance of the Santa Barbara Channel air mass and to observe the chemical and physical mechanisms that control the chemical composition of coastal stratus clouds.

Experimental Procedures

• Sampling Sites

The sampling sites used in this study are indicated in Figure 1, which provides a map of the Santa Barbara Channel area. La Jolla Peak (LP) {elev. 475 m} is located 3.4 km inland from the coast near Point Mugu, at the southeastern end of the Channel. The site, which is normally used as a Federal Aviation Administration Communication Station, was on the SE side of the hill, facing a valley; a row of 300 m high hills at the coastline separated it from the ocean. The immediate surroundings were covered by undisturbed grass and shrub. Samples were collected from the roof of a one story building, just below the top of the peak.

The Casitas Pass (CP) site was located at an air quality monitoring station operated by the California Air Resources Board. The site was at a saddle point (elev. \approx 300 m) at the head of a valley extending west (\sim 7 miles) toward the ocean. Nearby this site there were avocado and

citrus groves (below the pass) and chaparral or oak forest (the hillsides above the pass to the north and south). The site had excellent exposure to the west, but a water tank and the crest of the pass restricted the exposure to the east.

During the second summer of our study, four sites (Laguna Peak, Ventura, Casitas Pass, and El Capitan) were used (see Fig. 1). Laguna Peak is 1.6 km SW of La Jolla Peak at an elevation of 450 m. Laguna Peak (LP) is 2 km from the ocean, with no intervening hills. This site was located at a U. S. Navy communication and tracking facility; its surroundings consisted of shrub and grass. The sampling equipment, a cloudwater collector and aerosol filter pack, were positioned on the roof of an unfinished radar pedestal about 5 m above the ground. A secondary site referred to as Laguna Road (LR), used for cloudwater collection only, was located on the west side of Laguna Peak at an elevation of ≈ 240 m, 0.5 km from the summit. The stand for the cloudwater collector was placed on the ground on a level grassy area. The collector was operated on 12 V battery power at this site.

Two sites were used in Ventura. At Emma Wood State Beach (referred to as Beach site or EW), aerosol and gas samples were collected on the roof of an air quality monitoring station operated by the Ventura County Air Pollution Control Department (APCD). The site was within 200 m of the beach. A major highway ran within 100 m of the site on the landward side and a railroad track passed between the sampling site and the beach. The second site in Ventura (referred to as Hill site or TV) was at a cable TV receiving station (elev. 170 m) on a hill about 2.4 km ENE of the Emma Wood site. The immediate surroundings were undeveloped grass or tree covered hillsides. The cloudwater and aerosol samplers used at the Hill site were positioned on the roof of a one story building on the edge of the hill.

The El Capitan site was at an air quality monitoring station operated by the Santa Barbara County APCD. It was located in a State Park campground on a bluff immediately above the beach. Only aerosol and gas samples were collected at this site.

• *Collection Methods*

Cloudwater samples were collected with a Rotating Arm Collector (RAC) during the

summer of 1985 (11). Droplets are collected by the RAC by inertial impaction in slots in a Teflon coated steel rod and accumulated in polyethylene bottles attached to the ends of the rod. The RAC was mounted on a stand 1.4 m above the ground. At the La Jolla Peak site in 1985 and at all sites in 1986, cloudwater was collected with the Caltech Active Strand Cloudwater Collector (CASC) (12) mounted on a 2 m high stand. A fan draws air at 9 m s^{-1} across a bank of inclined Teflon strands, which collect droplets by inertial impaction. Gravity and aerodynamic drag propel the droplets down the strands where they accumulate in a Teflon trough and drain to a collection bottle. The CASC has a theoretical 50% lower droplet size-cut of $3.5 \mu\text{m}$ (diameter), whereas the RAC appears to have a size-cut near $20 \mu\text{m}$, based on a scale model calibration (11). Collett et al. (13) observed in a comparison of the two collectors that samples from the RAC were enhanced in sea salt and soil dust-derived species which are predominantly present in coarse aerosol (14). The CASC appeared to collect a more representative sample of the entire cloud droplet spectrum. A comparison of sample collection rates gave no evidence of increased evaporation on the CASC, despite the longer residence time of droplets on the strands. Because the CASC collects smaller droplets more efficiently and has a significantly higher collection rate, it sampled thin clouds more effectively.

The collection surfaces were rinsed thoroughly with distilled water before and after sampling. The samplers were kept covered when not in use to minimize contamination by dust. Water collected during the first 15 minutes of each sampling period was discarded to avoid inclusion of residual rinse water and to allow the collection surface to equilibrate with the ambient cloudwater.

Aerosol and gaseous compounds were collected using filter pack methods. A timer was used to control the filter pack during 1986 so three samples could be obtained without operator attention. Open-faced Teflon filters (Gelman Zeflour, $1 \mu\text{m}$ pore size) were used to collect aerosol for inorganic analysis. Nitric acid was collected on a nylon filter (Gelman Nylasorb) placed behind one Teflon filter. Ammonia was collected on an oxalic acid-impregnated glass fiber filter placed behind another Teflon filter. Flow rates through the filters

were controlled by critical orifices, which were periodically checked with a calibrated rotameter. A rain shield above the filters excluded sedimenting droplets and large debris. Aerosol sampling during cloud events presents special problems. In windy conditions, droplet collection may be enhanced or diminished depending on the orientation of the filter. We observed non-uniform coverage by droplets on the filters during cloudy periods. Filter pack methods are recognized to produce artifacts by volatilization of collected aerosol (15-16). We attempted to minimize this problem by using short sampling intervals and by not sampling during periods of rapid temperature change.

• *Analytical Methods*

Immediately after the end of a collection interval, the sample was weighed to determine its volume and an aliquot was removed to determine pH using a Radiometer PHM80 meter and a combination electrode (Radiometer GK2320C). The meter was calibrated using pH 4 and 7 buffers. Additional aliquots were removed from the sample and treated to preserve unstable species. S(IV) was preserved as hydroxymethanesulfonate by adding buffered CH_2O (17). CH_2O was reacted with NH_4^+ -acetylacetone (18) to form 3,5-diacetyl-1,4-dilutidine (DDL), which is stable for weeks (19). A buffered solution of p-OH phenylacetic acid (POPA) and peroxidase was used to preserve peroxides (H_2O_2 and ROOH) (20) by formation of the dimer. Carboxylic acids were preserved from bacterial decomposition by addition of CHCl_3 to an aliquot of sample (21). Carbonyls were derivatized with 2,4-dinitrophenylhydrazine in acidic solution (22). The samples and preserved aliquots were stored at 4 °C until analysis.

The samples were analyzed by standard methods used previously (23-24). A brief summary of the analytical methods follows. Complete details are given elsewhere (25). Anions were determined by ion chromatography, metal cations were determined by atomic absorption spectrometry, and NH_4^+ was determined by colorimetric flow injection analysis. The stabilized CH_2O was determined spectrophotometrically at 412 nm. I_2 was added to eliminate interference by S(IV). The CH_2O determined by the Nash method is total CH_2O ; recovery of $\text{NaCH}_2\text{OHSO}_3$ standards was 90 - 100% compared to CH_2O . The preserved S(IV) was determined by the

pararosaniline method (26) adapted for use with a flow injection analyzer. This method determines total S(IV); standards prepared from Na_2SO_3 or $\text{NaCH}_2\text{OH}\text{SO}_3$ gave comparable responses. Peroxide was determined from the fluorescence of POPA dimer (20). The method is sensitive to H_2O_2 and some organic peroxides; however, because they have significantly lower Henry's Law coefficients, CH_3OOH and peroxyacetic acid are unlikely to be important in cloudwater (20). Carboxylic acids were determined by ion exclusion chromatography, with a 2.5 mM HCl eluent, and in parallel by normal ion chromatography, with a 5 mM $\text{Na}_2\text{B}_4\text{O}_7$ eluent. The derivatized carbonyls were extracted in $\text{CH}_2\text{Cl}_2/\text{C}_6\text{H}_{14}$ and determined by reverse phase HPLC using a C18 column and aqueous $\text{CH}_3\text{CN}/\text{THF}$ (tetrahydrofuran) eluent. The aldehydes and ketones were monitored at 365 nm; the analysis was repeated at 430 nm to identify dicarbonyl compounds, which have a higher wavelength absorption maximum.

The inorganic ions on the Teflon filters were extracted by shaking with H_2O (Corning Megapure) after wetting the filter with 200 μl of $\text{CH}_3\text{CH}_2\text{OH}$. The oxalic acid-impregnated filters were extracted in H_2O . The nylon filters were extracted in $\text{HCO}_3^-/\text{CO}_3^{2-}$ solution (IC eluent). The filter extracts were analyzed by the same methods as the cloudwater samples with the exception that the buffer strength of the NH_4^+ reagents was adjusted to account for the presence of oxalic acid in the filter extract. Reported inorganic aerosol concentrations are the average of results from two separate filters.

Results

• Meteorology and Sampling Conditions

During the summer of 1985 the La Jolla Peak site was operated from July 23 to September 18. Sampling at Casitas Pass did not begin until August 7. The stratus layer was often below the sites. Extended cloud interception events occurred at La Jolla Peak on the mornings of July 24 – 26 and on August 21. Brief cloud interception episodes were also sampled on the mornings of July 30, September 4 and September 17. The interception event on July 24 was discontinuous; the stratus layer dropped after 2 hours of sampling and then lifted again after sunrise. Cloud

interception was continuous the following night from 2230 until 0820. Interception was continuous the morning of July 26, but the cloud top was just above the site.

Temperature profiles measured at Pt. Mugu for the period August 4–6, 1986, which are representative of the profiles on other cloudy days as well, are shown in Figure 2. Profiles for the other sampling days are given in the Appendix of Supplemental Material. The inversion base, which is generally coincident with the cloud top, reached a maximum elevation near sunrise. During the day the inversion base dropped, with a concomitant heating of the inversion layer. The mixed layer also warmed slightly due to surface heating. The inversion base was highest on the morning of July 25, 1985 during the most extensive cloud interception event at La Jolla Peak. Clouds briefly covered the site on the morning of July 30, but did not rise much past the top of the peak. Clouds were present below La Jolla Peak on August 20, when there was a weak surface-based temperature inversion. Over the course of the day a more pronounced inversion developed at 300 – 500 m. Stratus formed the following night and rose well above the level of La Jolla Peak. The peak intercepted clouds from 0000 to 0800. The intercepted clouds on September 4 and 17 were thin and did not yield large sample volumes; both events ended before sunrise.

Intercepted clouds were sampled at Casitas Pass on the mornings of August 7, 8, and 9, 1985. The site was near the top of the stratus layer on August 7 and 8; samples were collected intermittently as the cloud top moved up and down. Clouds moved back and forth between the two valleys on either side of Casitas Pass as the height of the inversion base oscillated. After sunrise on August 8 and 9, the cloud top rose well above the pass, as surface heating induced upslope winds and pushed the cloud layer upward. The largest sample volumes, which are proportional to cloud liquid water content (LWC), were obtained during an extended interception event on August 8. Even though Casitas Pass (elev. 300 m) appeared to be near the inversion base, based on cloud-top observations, temperature profiles from Point Mugu for the period Aug 6 – 9 show that the inversion base exceeded 500 m each morning. Clouds were present at La Jolla Peak on the morning of August 9, but were not sampled.

The summer of 1986 was noted for the frequency and persistence of the nocturnal marine stratus clouds. Clouds formed nearly every night for several weeks in July and August. Three or four day periods during three consecutive weeks were selected for intensive study. The presence of clouds at the four sampling sites and the height of the inversion base at Pt. Mugu during these periods is indicated in Figure 3. Temperature profiles for these periods (see Fig. 2 and the Appendix of Supplemental Material) indicate the presence of a strong and very persistent temperature inversion. As in 1985, a diurnal cycle was observed in the height of the inversion base. At Laguna Peak sampling began at the lower site (LR). When the cloud rose above that site, sampling continued at the summit (LP). Initial samples at Laguna Peak were collected near the top of the clouds. Later samples are from the interior of the stratus layer.

The wind direction profiles at Point Mugu for the period August 4 – 6, 1986, are shown in Figure 4. Profiles for the other intensive sampling periods (see Appendix of Supplemental Material) were similar. In the mixed layer, winds were controlled by the diurnally varying sea/land breeze. Westerly winds predominated in the afternoon; the direction of nighttime wind was variable. The wind in the inversion layer frequently had an easterly component, and was usually different from the surface wind. Westerly winds dominated above the inversion layer, where the flow was controlled by circulation around the Pacific High.

• *Chemical Composition: Aerosol*

The average concentrations and ranges of concentrations of aerosol components are presented in Table 1 for day and nighttime samples collected at each site during 1986. Concentrations are not adjusted for changes in pressure with elevation in order to allow direct comparison of cloudwater and aerosol loadings. The pressure correction term would be 1.06 at the highest sites, Laguna and La Jolla Peaks. Complete results are presented in the Appendix of Supplemental Material. Because the number of samples was small and the variability in concentration high, none of the differences between day and night were statistically significant. Consistent with the proximity to the ocean, Na^+ was a major component of the aerosol. The Na^+ concentration decreased away from the coastline. Except at the two sites adjacent to the beach

(El Capitan and Emma Wood), the concentration of Cl^- was less than expected if all the Na^+ was due to sea salt. In addition to the sea salt, appreciable concentrations of SO_4^{2-} , NO_3^- , and NH_4^+ were present. Gaseous HNO_3 and NH_3 were major contributors to the total N(V) and N(-III) . Most of the SO_4^{2-} observed in these samples was "non-sea salt" or "excess" SO_4^{2-} ($\text{SO}_4^{2-}_{\text{xs}}$). Even at the two coastal sites sampled in 1986, the $\text{SO}_4^{2-}_{\text{xs}}$ to SO_4^{2-} ratio exceeded 60%. In 1985 the N(V) concentration exceeded that of $\text{SO}_4^{2-}_{\text{xs}}$ at both sites. In 1986, however, neither species was clearly dominant. Concentrations of $\text{SO}_4^{2-}_{\text{xs}}$ and N(V) tended to be higher at Laguna or La Jolla Peaks than at the other sites. The other sites all had similar concentrations.

• Cloudwater Composition

The average chemical composition of the sampled cloudwater and the range of values observed during the study are given in Table 2 for each sampling site over the sampling period. (Data for each cloud interception event sampled during the study are presented in the Appendix of Supplemental Material). The ion balances, $\Sigma\text{A}^-/\Sigma\text{M}^+$, ($\Sigma\text{A}^- = [\text{Cl}^-] + [\text{NO}_3^-] + [\text{SO}_4^{2-}]$; $\Sigma\text{M}^+ = [\text{H}^+] + [\text{NH}_4^+] + [\text{Na}^+] + [\text{Ca}^{2+}] + [\text{Mg}^{2+}]$) { K^+ was excluded because it was insignificant relative to the other cations} and liquid water contents (LWC) estimated from collection rate also are given.

Cloudwater collected during this study was consistently acidic as shown in Figures 5 and 6 for 1985 and 1986, respectively. H^+ , Na^+ , NH_4^+ , Cl^- , NO_3^- , and SO_4^{2-} were the major ions in the cloudwater. Only a few samples had S(IV) concentrations above the detection limit of $1\ \mu\text{M}$. CH_2O concentrations ranged from $10 - 50\ \mu\text{M}$, with average values closer to $10\ \mu\text{M}$. In most samples, the H_2O_2 concentration was less than $20\ \mu\text{M}$.

Representative values of the concentrations of organic species found in typical time series of cloudwater samples are presented in Table 3. Formic acid was found to be the dominant organic species; however, the $[\text{CH}_3\text{CHO}]$ appeared to exceed the $[\text{CH}_2\text{O}]$. This result is surprising since the solubility of CH_3CHO is three orders of magnitude less than that of CH_2O (27); thus, it should be of much less importance than CH_2O in the aqueous phase for typical observed gas-phase concentrations. The possibility that the peak identified as CH_3CHO is something else

(e.g. HOCH_2CHO) can not be excluded. Acetic acid, glyoxal (CHOCHO) and methylglyoxal ($\text{CH}_3\text{C}(\text{O})\text{CHO}$) were also found to be important. Other carboxylic acids and carbonyls were not present at detectable levels. The CH_2O concentrations determined by the Nash and DNPH-derivatization methods disagree for several samples. There is no obvious explanation for this discrepancy.

The concentrations of the major inorganic ions are plotted versus time in Figure 7 for the sampling period of July 24–26, 1985. In general, the cloudwater concentrations decreased over the 3-day period. During the events on July 24 and 25, however, the concentrations doubled from beginning to end. On the morning of July 26, concentrations were fairly constant. The concentrations during the August 21 event were similar to those observed on July 24. Cloudwater concentrations at Casitas Pass followed the same pattern of increasing over the course of the event, but were lower than those observed at La Jolla Peak.

Time-series data from cloudwater samples taken simultaneously at several sites are shown in Figures 8 and 9. The concentrations of chemical components in the Laguna Road cloudwater were appreciably higher than those in the Laguna Peak cloudwater, which were collected a short time later. Over the course of each event, the Laguna Peak cloudwater became chemically more concentrated. On August 5 and 6, the cloudwater concentrations at Ventura were between the cloudwater concentrations at Laguna Peak and Laguna Road. The Ventura cloudwater samples also showed a pattern of increasing concentrations over the course of the event. During the August 13 and 14 events, the Ventura cloudwater was more concentrated than the Laguna Peak cloudwater. During all cloud events Casitas Pass cloudwater had lower concentrations of the principal chemical components. Cloudwater collected at the Laguna Road site on July 31 was comparable chemically to cloudwater collected during the August 13 to 14 event. The concentration versus time profile was concave with the highest concentrations at the beginning and end of the event. Similar results were obtained for the cloud interception event at Ventura on August 1.

Aerosol and cloudwater loadings at Laguna Peak, Ventura, and Casitas Pass for the period

August 4 – 6, 1986, are shown in Figures 10 – 15. Plots for the other intensive sampling periods are presented in the Appendix of Supplemental Material. Cloudwater loading (neq m^{-3}) is the product of concentration (μN) and LWC (ml m^{-3}). At Laguna Peak some of the highest concentrations of N(-III) , N(V) , and SO_4^{2-} occur when the site is in the inversion layer. Lower concentrations are observed when the site is immersed in stratus clouds. Most of the N(V) is present as HNO_3 during clear periods. Na^+ also has its maximum values during the cloud-free periods, but Cl^- does not follow this trend. When clouds intercepted Laguna Road, the cloudwater loading of N(-III) , N(V) and SO_4^{2-} was usually less than the aerosol concentration in the clear air at the summit. The loadings of Na^+ and Cl^- in the lower elevation clouds were often greater than in the aerosol above the clouds. Over the course of a typical event both aerosol and cloudwater loading decreased. When the clouds intercepted Laguna Peak, the cloudwater loading was comparable to the aerosol loading. This pattern is predicted to occur if air from the mixed layer, which is high in sea salt, is mixed with inversion layer air, which is high in NO_3^- , SO_4^{2-} , and NH_4^+ . The short duration cloud events were often thin or patchy. Cloudwater loadings during these events were usually lower than the aerosol loadings. Cloudwater loadings in the final LR samples were comparable to the first LP samples. The observed concentration differences were primarily due to differences in LWC.

At Ventura N(-III) , N(V) , and SO_4^{2-} were well mixed from sea level up to the TV site. When there was a gradient in the aerosol concentrations of these species, sea level concentrations were slightly higher. Na^+ and Cl^- were not well mixed; their concentrations were always much higher at the beach than on the hill. The difference is more than would be caused by the difference in pressure at the two sampling sites. Aerosol concentrations at Ventura were variable, but there were no clear patterns in the variation. On several days the maximum Na^+ concentrations occurred in the early evening, which is opposite to the expected maximum during the afternoon when the sea breeze is strongest. With the exception of the August 5 event, the cloudwater loadings of the primary species were equal to the aerosol concentrations during the extended cloud events. Cloudwater loadings of N(-III) , N(V) , and SO_4^{2-} were less than the

aerosol concentrations during the thin cloud event on August 13.

The behavior of sea-salt aerosol is illustrated in Figures 16 – 19. At Ventura and Casitas Pass, Cl^- was moderately depleted relative to Na^+ in the aerosol. Even at high Na^+ concentrations in the Emma Wood samples, the Cl^- concentrations are $\leq 75\%$ of the expected value if sea salt was the sole source of Na^+ . The Na^+ and Cl^- gradient between the beach and hill sites in Ventura is shown in Figure 18. However, in the Ventura, cloudwater the $\text{Cl}^-:\text{Na}^+$ ratio was very close to the value for seawater. The aerosol at Laguna Peak was severely depleted in Cl^- . The samples with the highest Na^+ had little or no Cl^- . The cloudwater from Laguna Road still exhibited an apparent Cl^- deficiency at high concentration, though at low concentrations the $\text{Cl}^-:\text{Na}^+$ ratio is close to the seawater value. The cloudwater collected at the summit of Laguna Peak often had a Cl^- excess.

Discussion

The strongest temperature inversions appear to be associated with the most extensive cloudiness. In all of the cloud events studied, the inversion base rose during the night and lowered in the day, which is contrary to the usual pattern over land. This result is in accordance with predictions from a model of radiant and turbulent heat transfer in low-level marine stratus (28). Turbulence, driven by radiative cooling, allows the cloud top to propagate upwards during the night. Subsidence heating would continually warm the inversion layer and depress the inversion base. If the competing effect of convective mixing at night (induced by warm ocean water, relative to the air, or radiative and evaporative cooling at the cloud top) were stronger, the depth of the mixed layer would increase. The observed changes in the height of the inversion base are consistent with this explanation. The consequence of this process would be the transfer of aerosol and gases across the inversion.

The composition of aerosol and cloudwater in the Santa Barbara Channel area appears to be a mixture of sea salt and anthropogenic aerosol. Nitrate and non-sea salt sulfate concentrations

in the Santa Barbara Channel are at least a factor of 10 higher than concentrations observed at mid-ocean sites in the North Pacific (29). Harrison and Pio (30) observed similar concentrations of the major aerosol components at a coastal site in northwestern England where ammonium nitrate and sulfate aerosol was mixed with sea salt aerosol. Saltzman et al. (31) report comparable levels of SO_4^{2-} in aerosol off the Peruvian coast that they attribute to smelter emissions. Total SO_4^{2-} concentrations observed in this study are similar to the concentrations reported at Santa Catalina Island (32), which is ≈ 32 km off the Los Angeles coast and is affected by advection from Los Angeles. Maximum SO_4^{2-} concentrations at two coastal stations in Los Angeles (32) were 3 times the highest value observed for SO_4^{2-} at Laguna Peak.

Acidic components ($\text{NO}_3^- + \text{SO}_4^{2-}$) in the cloudwater were found to exceed NH_4^+ . This observation is consistent with the previous observations of Jacob et al. (10). Much of the atmospheric acidity was due to HNO_3 in the gas phase. In general, the excess of acidic anions over cations in the aerosol was small. In most samples from Laguna and La Jolla Peaks the concentration of N(V) exceeded that of SO_4^{2-} on an equivalents basis. At the remaining sites, however, neither species was consistently in excess. However, NO_3^- usually exceeded SO_4^{2-} in cloudwater. The $\text{NO}_3^-:\text{SO}_4^{2-}$ ratios of the volume-weighted average concentrations (expressed in equivalents) ranged from 1.1 to 1.6. This is considerably less than the typical value of 2.5, which is commonly observed in clouds and fogs collected in Los Angeles (22,33). In the Channel area, NO_x emissions reported from stationary sources exceed SO_x emissions by a factor of 15 (California Resources Board Emission Inventory). Vehicular emissions add to this excess. Active photochemistry, which would rapidly convert NO_x to HNO_3 , is indicated by peak O_3 concentrations of up to 100 ppb at the coastline and in the Channel at Anacapa Island (Ventura County APCD data), while up to 140 ppb was measured inland at Casitas Pass. Therefore, $\text{HNO}_{3(g)}$ or $\text{NO}_{3(a)}^-$ appears to be lost from the air mass at a faster rate than the SO_4^{2-} .

The geographical distribution of Na^+ , Mg^{2+} and Cl^- (with a few exceptions) in the aerosol and cloudwater is consistent with their derivation from sea spray. The high concentrations of Na^+ , Mg^{2+} , and Cl^- at Emma Wood and El Capitan probably are due to a few large sea-salt

aerosol or sea-spray droplets. These would not remain suspended long enough to penetrate far inland or rise more than a few meters above sea level. The deposition of large sea-salt particles could account for the large concentration gradient for sea salt-derived ions observed between Emma Wood and the TV site a short distance away. A further decrease in sea salt-derived ions is observed between the TV site and Casitas Pass or Laguna Peak. Comparison of the Laguna Road and Laguna Peak samples indicates a sea salt gradient within the stratus layer. Concentrations (and total loading) of Na^+ and Mg^{2+} were greater near the cloud base (Laguna Road samples) than near the cloud top (Laguna Peak samples). The increasing dominance of NH_4^+ and its associated anions over Na^+ and Mg^{2+} in cloudwater with increasing height is consistent with the observation that sea salt aerosol are not the dominant source of cloud condensation nuclei (34).

The highest concentrations of N(V) and $\text{SO}_4^{2-}\text{xs}$ were observed at Laguna and La Jolla Peaks, which are the sites furthest east and at the highest elevations. This pattern could be explained by transport of the polluted air mass from the Los Angeles basin, which is situated southeast of the Santa Barbara Channel area, by upper level winds. As noted previously, winds in the inversion layer frequently had an easterly component. Shair et al. (35) have documented transport from Los Angeles to sites as far north as Ventura. In that study a power plant plume was followed by means of SF_6 tracer. At night the plume was transported over the ocean by the land breeze. The following morning it returned to shore on the sea breeze. The plume remained near the inversion base during most of the night. However, around 0500 it was dispersed throughout the mixed layer by convection over the ocean. Transport over the length of the Channel by the sea/land breeze cycle has been observed as well (36). It is unlikely that the highest concentrations of N(V) and $\text{SO}_4^{2-}\text{xs}$ would be found at Laguna or La Jolla Peak if their primary source were oxidation of locally emitted NO_x and SO_2 . Furthermore, the concentrations of N(V) and $\text{SO}_4^{2-}\text{xs}$ were not higher when the inversion base was lower during the July 29 – August 1 sampling period, which might be expected if they were derived from local sources. The comparable concentrations of these species for this particular sampling period indicate that there

may have been effective mixing from one end of the channel to the other.

The volatilization of HCl from the acidification of sea salt aerosol is well known (37-39). Theoretical calculations (40) indicate that most of the HCl is lost from the smallest aerosol. The loss of Cl^- decreases rapidly with increasing relative humidity above 99%. Thus droplets retain their Cl^- , even at low pH. This mechanism would account for the Cl^- deficiency observed in aerosol from the Santa Barbara Channel area. Small Cl^- deficiencies were observed at the coastal sites (Emma Wood and El Capitan) where, presumably, large sea salt aerosol and sea-spray droplets are present. Substantial aerosol depletion of Cl^- was observed at Laguna Peak where most of the sea salt should be present as small aerosol and where the humidity was the lowest. In most cases, the Santa Barbara Channel area has excess atmospheric acidity, which is primarily gas-phase HNO_3 .

HCl volatilization by HNO_3 has some important consequences for the size distribution of NO_3^- and Cl^- aerosol, which may in turn affect the fate of those species in the atmosphere. In the absence of sea salt, NO_3^- is present in the atmosphere as gas-phase HNO_3 or sub-micron aerosol (NH_4NO_3) formed by gas-to-particle conversion processes. Deposition of HNO_3 on sea salt particles, which are mainly in the size range $1 - 40 \mu\text{m}$ (diameter), transfers NO_3^- mass from the gas phase to large diameter particles; at the same time Cl^- is transferred to the gas phase. If NH_3 is available, HCl may react to form NH_4Cl aerosol (41). NO_3^- and SO_4^{2-} in polluted marine air were found to have bimodal distributions (30). The portion having a mode at about $1 \mu\text{m}$ was associated with NH_4^+ ; a second mode around $3.5 \mu\text{m}$ was associated with Na^+ (30). The transport of both gases and particles to the surface layer is limited by turbulent transfer. The deposition velocities for small particles ($0.01 \mu\text{m} < d \leq 1 \mu\text{m}$) is typically $\leq 0.1 \text{ cm s}^{-1}$ where d is the particle diameter, while reactive gases such as HNO_3 have deposition velocities of $1 - 3 \text{ cm s}^{-1}$ (41). Deposition velocity for large particles ($d > 1 \mu\text{m}$) increases with size. Over water surfaces, particle growth in the humid boundary layer enhances deposition of large particles ($d > 1 \mu\text{m}$) up to the limit imposed by turbulent transfer (43).

Unless the gaseous HCl is separated from the air mass during the day, it will be rescavenged

totally by cloud droplets at night. Thus, the $\text{Na}^+:\text{Cl}^-$ ratio in cloudwater will be close to the seawater ratio. Deposition of $\text{HCl}_{(\text{g})}$ to land surfaces may slightly exceed that of the smaller sea-salt aerosol, which could account for the slight Cl^- deficiency we observed occasionally in cloudwater at Laguna Road. The Na^+ and Cl^- need not necessarily be in the same droplets, however. HCl will be scavenged by all the droplets present according to their surface area. Droplet scavenging provides a second mechanism for the formation of Cl^- aerosol in addition to direct gas-to-particle reactions. Future studies of aerosol and gas-phase species in coastal settings should include measurements of HCl to verify that this exchange occurs.

Theoretical considerations suggest that the scavenging efficiency of aerosol by stratus clouds should be near 100%. Hygroscopic aerosol larger than about $0.1\ \mu\text{m}$ (34) should be activated at the supersaturations found in stratus clouds. Gaseous species should partition into the droplet phase according to their Henry's Law coefficients. At the pH observed in the Santa Barbara Channel cloudwater, both HNO_3 and NH_3 should be partitioned almost completely into the droplet phase. The characteristic time for interfacial mass transfer is seconds to minutes (44). Previous studies of scavenging by stratus clouds indicate nearly 100% scavenging of SO_4^{2-} and light-scattering particles (45).

Scavenging ratios, defined as $R_s = [\text{C}]_{\text{cloud}} / [\text{C}]_{\text{aerosol}}$, have been calculated for the periods with concurrent (or consecutive) aerosol and cloudwater data (Table 4). The scavenging ratios for NH_4^+ and NO_3^- are computed from $\text{N}(-\text{III})$ and $\text{N}(\text{V})$, respectively, to eliminate the effect of gas/aerosol partitioning. Two major sources of uncertainty are inherent in this method. The sampling intervals (2 – 4 hours typically) are long relative to the time for changes in cloudwater composition or microphysics. If the cloud is inhomogeneous, or patchy, the average scavenging ratio obtained will be less than the instantaneous ratio for the cloud parcels. Secondly, the estimate of LWC derived from the sampler collection rate and theoretical collection efficiency is subject to some uncertainty, which propagates to the derived cloudwater loading. These uncertainties should affect all species in the cloud equally. Differences in scavenging ratios for different ions imply that they are affected by different processes.

The scavenging ratios at Laguna Peak and Ventura were close to 1. The exceptions with low scavenging ratios were generally short-duration cloud events that often were patchy. Low scavenging ratios, however, also were observed during the first interval on August 5 at Laguna Peak, when the site was near the cloud top. The ratio for N(V) was consistently greater than the ratio for SO_4^{2-} . As noted previously, NO_3^- may be present as large aerosol derived from sea salt or as $\text{HNO}_{3(g)}$, both of which will be scavenged more rapidly by droplets than the smaller SO_4^{2-} aerosol.

The scavenging ratios computed for the Casitas Pass samples were consistently less than 1. The events on July 31 and August 1 were of short duration. The others extended over several hours. Casitas Pass was usually near the top of the stratus layer and it is likely that clear patches were entrained into the cloud. The sampler at Casitas Pass was only 2 m above the ground, whereas, at the other sites, the samplers were located on buildings. Heating at the warm ground surface may have evaporated some of the cloud droplets at this site; thus the material collected as aerosol may have included the freshly evaporated droplets, thereby reducing the scavenging ratio.

Because very little of the stratus cloudwater is removed at the ground, the solutes in the droplets remain in the atmosphere as aerosol and gases after the clouds dissipate. Hoppel et al. (46) suggest that non-precipitating clouds increase the size of the aerosol by transferring small aerosol and gas to droplets, which then evaporate to form particles larger than the original condensation nuclei.

The organic species found in the Santa Barbara Channel cloudwater may arise from two sources. Formaldehyde and other carbonyls are well known primary pollutants; they are also formed from the reaction of hydrocarbons, which come from incomplete combustion, fuel and solvent evaporation, or from vegetation (47). Toluene and related aromatic compounds are a major source of the dicarbonyls, glyoxal and methyl glyoxal (48). Natural emissions may account for the carboxylic acids observed in the troposphere. In particular, isoprene, a major biogenic product of plants, reacts with O_3 to give HCOOH and $\text{CH}_3\text{C}(\text{O})\text{CHO}$ (49), observed in

cloudwater samples, among other products, which were not observed. Anthropogenic emissions are also direct and indirect sources of these carboxylic acids (50). The $\text{HCOOH}/\text{CH}_3\text{COOH}$ ratio near 2 that was observed in the Santa Barbara Channel cloudwater is close to the average value of 2.4 reported for rainwater at marine sites (51). The lower concentrations of carbonyls than carboxylic acids are consistent with the faster rates of photochemical degradation for carbonyls in the atmosphere.

Acknowledgements

This research was supported by the California Air Resources Board. We gratefully acknowledge the assistance and cooperation of the United States Navy Pacific Missile Test Center at Point Mugu, the Federal Aviation Administration, the California Air Resources Board Monitoring Branch, the Ventura County Air Pollution Control District, and Avenue Cable TV for allowing us access to their facilities for use as sampling sites. Rawinsonde and meteorological data for Point Mugu were provided by the U. S. Navy. Additional meteorological data were provided by the California Air Resources Board. The CARB and Ventura County APCD provided pollutant data for the sampling periods. Assistance in the field and laboratory was provided by S. Gomez, C. Choy, and G. Gibb.

References

1. Nieburger, M., Johnson, D. S., and Chien. C.-W. *Studies of the structure of the atmosphere over the eastern Pacific Ocean in summer I. The inversion over the eastern North Pacific Ocean*. University of California Press: Berkeley 1961.
2. Allbrecht, B. A., Penc, R. S., and Schubert, W. *J. Atmos. Sci.* 1985, 42, 800-822.
3. Brost, R. A., Lenschow, D. H., and Wyngaard, J. C. *J. Atmos. Sci.* 1982, 39, 800-817.
4. Brost, R. A., Wyngaard, J. C., and Lenschow, D. H. *J. Atmos. Sci.* 1982, 39, 818-836.
5. Mahrt, L. and Paumier, J. *J. Atmos. Sci.* 1982, 39, 622-634.
6. Deardroff, J. W. *Quart. J. R. Met. Soc.* 1976, 102, 563-582.
7. Deardroff, J. W. *Quart. J. R. Met. Soc.* 1981, 107, 191-202.
8. Randall, D. R. *J. Atmos. Sci.* 1980, 37, 125-130.
9. Randall, D. R. *J. Atmos. Sci.* 1980, 37, 148-159.
10. Jacob, D. J., Waldman, J. M., Munger, J. W., and Hoffmann, M. R. *Environ. Sci. Technol.* 1985, 19, 730-736.
11. Jacob, D. J., Wang, R.-F. T. and Flagan, R. C. 1984 *Environ. Sci., Technol.* 18, 827-833.
12. Daube, B. C., Jr., Flagan, R. C., and Hoffmann, M. R. *Active Cloudwater Collector*, United States Patent # 4,697,462, Oct. 6, 1987.
13. Collett, J., Jr., Daube, B., Jr., Munger, J. W., and Hoffmann, M. R. *Atmos. Environ* 1989, in review.
14. Seinfeld, J. H. *Atmospheric Chemistry and Physics of Air Pollution*, John Wiley: New York, 1986. 738 pp..
15. Appel, B. R., Wall, S. M., Tokiwa, Y., and Haik, M. *Atmos. Environ.* 1979, 13, 319-325.
16. Spicer, C. W., Howes, J. E., Jr., Bishop, T. A., Arnold, L. H., and Stevens, R. K. *Atmos. Environ.* 1982, 16, 1487-1500.
17. Dasgupta, P. K., DeCesare, K. and Ullrey, J. C. *Anal. Chem.* 1980, 52, 1912-1922.
18. Nash, T. *Biochem. J.* 1953, 55, 416-421.
19. Reitz E. B. *Analyt. Lett.* 1980, 13, 1073-1084.
20. Lazrus, A., Kok, G. L., Gitlin, S. N., Lind, J. A., and McLaren, S. E. *Anal. Chem.* 1985, 57, 917-922.

21. Keene, W. C. and Galloway, J. N. *Atmos. Environ.* 1984, 18, 2491–2497.
22. Grosjean, D. and Wright, B. *Atmos. Environ.* 1983, 17, 2093–2096
23. Munger, J. W., Jacob, D. J., Waldman, J. M., and Hoffmann, M. R. *J. Geophys. Res.* 1983, 88, 5109–5121.
24. Jacob, D. J., Munger, J. W., Waldman, J. M., and Hoffmann, M. R. *J. Geophys. Res.* 1986, 91, 1073–1088.
25. Munger, J. W. *Chemical Composition of Fogs and Clouds in Southern California*, Ph. D. Thesis, California Institute of Technology, Pasadena, CA 1989.
26. Dasgupta, P. K. *J. Air Pollut. Cont. Assoc.* 1981, 31, 779–782.
27. Betterton, E. A., Hoffmann, M. R. *Environ. Sci. Technol.* 1988, 22, 1415–1418.
28. Oliver, D. A., Lewellen, W. S., and Wialliamson, G. G. *J. Atm. Sci.* 1978, 35, 301–316.
29. Prospero, J. M., Savoie, D. L., Nees, R. T., Duce, R. A., and Merrill, J. *J. Geophys. Res.* 1985, 90, 10,586–10,596.
30. Harrison, R. M. and Pio, C. A. *Atmos. Environ.* 1983, 17, 1733–1738.
31. Saltzman, E. S., Savoie, D. L., Prospero, J. M., Zika, R. G., and Mosher, B. *J. Geophys. Res.* 1986, 91, 7913–7918.
32. Cass, G. R. and Shair, F. H. *Atmos. Environ.* 1984, 89, 1429–1438
33. Munger, J. W., Collett, J., Daube, B., Jr., and Hoffmann, M. R. *Atmos. Environ.* 1989 in press.
34. Pruppacher, H. R. and Klett, J. D. *Microphysics of clouds and precipitation*, D. Reidel: Dordrecht 1978; pp. 139–140.
35. Shair, F. H., Sasaki, E. J., Carlan, D. E., Cass, G. R., Goodin, W. R., Edinger, J. G., and Schacher, G. E. *Atmos. Environ.* 1982, 16, 2043–2053.
36. Angell, J. K., Pack, D. H., Holzworth, G. C., and Dickson, C. R. *J. Appl. Met.* 1966. 5. 565–572.
37. Eriksson, E. *Tellus* 1960, 12, 63–109.
38. Martens, C. S., Wesolowski, J. J., Harriss, R. C., and Kaifer, R. *J. Geophys. Res.* 1973, 78, 8778–8791.
39. Hitchcock, D. R., Spiller, L. L., and Wilson, W. E. *Atmos. Environ.* 1980, 14, 165–182.
40. Clegg, S. L. and Brimblecombe, P. *Atmos. Environ.* 1985, 19, 465–470.
41. Harrison, R. M. and Pio, C. A. *Envir. Sci. Technol.* 1983, 17, 169–174.
42. Huebert, B. J. and Roberts, C. H. *J. Geophys. Res.* 1985, 90, 2085–2090.

43. Slinn, S. A. and Slinn, W. G. N. *Atmos. Environ.* 1980, 14, 1013-1016.
44. Schwartz, S. E. and Freiberg, J. E. *Atmos. Environ.* 1981, 15, 1129-1144.
45. ten Brink, H. M., Schwartz, S. E., And Daum, P. H. *Atmos. Environ.* 1987, 21, 2035-2052.
46. Hoppel, W., A., Frick, G. M., and Larson, R. E. *Geophys. Res. Lett.* 1986, 13, 125-128.
47. Graedel, T. E., Hawkins, D. T., and Claxton, L. D. *Atmospheric chemical compounds: Sources, occurrence, and bioassay.* Academic Press: New York, 1986.
48. Tuazon, E. C., MacLeod, H., Atkinson, R., and Carter, W. P. *Environ. Sci. Technol. Env. Sci. Technol.* 1986, 20, 383-387.
49. Lloyd, A. C., Atkinson, R., Lurmann, F. W., and Nitta, B. *Atmos., Environ.* 1983, 17, 1931-1950.
50. Talbot, R. W., Beecher, K. M., Harriss, R. C., and Cofer, W. R., III. *J. Geophys. Res.* 1988, 93, 1638-1652.
51. Keene, W. C. and Galloway, J. N. *J. Geophys. Res.* 1986, 91, 14466-14474.

Table 1. Range and average of concentrations in aerosol samples collected at several sites along the Santa Barbara Channel in 1986

<u>Laguna Peak 1986</u>												
	Na ⁺	NH ₄ ⁺	Ca ²⁺	Mg ²⁺	Cl ⁻	NO ₃ ⁻	SO ₄ ²⁻	SO ₄ ^{2-*}	NH ₃	HNO ₃	N(-III)	N(V)
	← neq m ⁻³ →								← nmole m ⁻³ →			
<i>Day (N = 8)</i>												
Min	9.2	39.2	5.0	0.9	0.0	18.1	90.1	89.0	0.0	16.3	39.2	74.5
Max	87	176	47	17	25	112	386	381	34	202	189	244
Avg	52	118	19	10	8	46	224	218	7	134	125	180
S	23	39	7	5	8	14	90	89	11	53	39	60
<i>Night (N = 12)</i>												
Min	7.0	42.2	6.4	1.2	0.0	22.3	57.6	56.4	0.0	7.5	46.3	88.7
Max	49	156	49	11	45	138	193	187	101	355	182	412
Avg	22	84	19	5	17	72	128	125	19	124	102	196
S	15	34	14	3	14	39	38	37	29	117	44	98

<u>Ventura (Hill) 1986</u>												
	Na ⁺	NH ₄ ⁺	Ca ²⁺	Mg ²⁺	Cl ⁻	NO ₃ ⁻	SO ₄ ²⁻	SO ₄ ^{2-*}	NH ₃	HNO ₃	N(-III)	N(V)
	← neq m ⁻³ →								← nmole m ⁻³ →			
<i>Day (N = 15)</i>												
Min	16.1	25.0	12.8	3.9	0.0	18.0	42.4	25.7	0.0	11.6	25.0	37.9
Max	167	303	62	41	126	146	295	286	42	139	313	236
Avg	71	105	29	15	35	49	159	151	8	78	114	127
S	41	63	14	10	38	31	63	65	11	40	66	49
<i>Night (N = 19)</i>												
Min	23.9	43.1	9.7	2.7	2.4	41.7	66.1	39.4	0.0	5.7	47.3	47.5
Max	239	177	52	53	200	205	169	164	19.5	51	181.4	218
Avg	105	100	22	23	77	97	113	100	2.8	20	107.5	118
S	66	41	11	15	58	51	28	32	5	13	39	49

Table 1. (continued).

<u>Ventura (Beach) 1986</u>												
	Na ⁺	NH ₄ ⁺	Ca ²⁺	Mg ²⁺	Cl ⁻	NO ₃ ⁻	SO ₄ ²⁻	SO ₄ ^{2-*}	NH ₃	HNO ₃	N(-III)	N(V)
	← neq m ⁻³ →								← nmole m ⁻³ →			
<i>Day (N = 11)</i>												
Min	121	42.9	4.8	21.1	73.3	37.3	108	48.2	0.0	5.6	42.9	42.9
Max	490	210	57	98	432	93	261	243	37	144	217	230
Avg	254	107	23	55	198	69	170	139	11	54	117	124
S	118	49	12	23	119	18	50	61	15	432	45	53
<i>Night (N = 12)</i>												
Min	90	32.1	9.0	19	19	33	45	0.0	0.0	4.2	53	39
Max	1001	146	79	201	1051	114	176	165	82	112	167	193
Avg	396	82	34	85	348	75	132	87	16	26	99	101
S	297	34	17	55	307	24	39	49	24	30	35	44

	<u>Casitas Pass 1986</u>											
	Na ⁺	NH ₄ ⁺	Ca ²⁺	Mg ²⁺	Cl ⁻	NO ₃ ⁻	SO ₄ ²⁻	SO ₄ ^{2-*}	NH ₃	HNO ₃	N(-III)	N(V)
	← neq m ⁻³ →								← nmole m ⁻³ →			
	<i>Day (N = 14)</i>											
Min	4.7	42.7	11.3	0.0	0.0	28.2	55.7	44.6	0.0	0.0	20.0	66.4
Max	123	168	36	27	51	81	189	189	145	133	288	192
Avg	51	123	20	11	16	48	133	126	46	62	161	115
S	33	28	7	8	16	13	32	34	38	30	54	32
	<i>Night (N = 21)</i>											
Min	4.8	24.1	5.2	0.5	0.0	30.6	32.1	24.8	0.0	0.0	29.2	40.7
Max	129	201	34.5	30	101	105	156	153	74	36	222	119
Avg	45	113	13.7	9	30	65	81	75	13	12	122	78
S	39	45	7	9	31	22	27	29	18	8	50	22

Table 1. (continued).

<u>El Capitan 1986</u>												
	Na ⁺	NH ₄ ⁺	Ca ²⁺	Mg ²⁺	Cl ⁻	NO ₃ ⁻	SO ₄ ²⁻	SO ₄ ^{2-*}	NH ₃	HNO ₃	N(-III)	N(V)
	← neq m ⁻³ →							← nmole m ⁻³ →				
<i>Day (N = 4)</i>												
Min	404	18.0	27.1	87.9	422	36.7	72.0	23.0	0.0	10.2	57.0	46.9
Max	1079	106	85	215	867	133	289	159	39	29	106	162
Avg	612	74	48	133	554	92	181	107	16	22	90	114
S	273	34	22	49	183	35	82	56	16	8	19	42
<i>Night (N = 8)</i>												
Min	50.2	11.3	6.1	10.8	36.6	11.8	21.5	12.9	0.0	4.9	34.2	16.7
Max	335	136	69	73	297	140	149	114	42	22	136	162
Avg	217	76	34	48	186	64	87	61	20	11	91	76
S	93	44	20	22	92	41	41	34	15	6	35	45

* "Excess" (non-sea salt) Sulfate

$$[\text{SO}_4^{2-*}] = [\text{SO}_4^{2-}] - [\text{Na}^+] \frac{[\text{SO}_4^{2-}]_{\text{sw}}}{[\text{Na}^+]_{\text{sw}}}$$

S = standard deviation

Table 2. Cloudwater Composition at Elevated Sites Along the Santa Barbara Channel Coast

La Jolla Peak Cloudwater Samples 24 July – 17 September 1985.

<u>RAC Samples</u>										
	Vol ml	pH	Na ⁺	NH ₄ ⁺	Ca ²⁺	Mg ²⁺	Cl ⁻	NO ₃ ⁻	SO ₄ ²⁻	SO ₄ ^{2-*} _{xs}
			← μN →				← →			
N	27	26	25	26	26	26	26	25	26	23
Min	1.1	2.36	30	105	10.5	12.5	70	201	132	128
Max	70	3.79	1550	882	275	816	1210	2750	1980	1792
Avg	31	3.12	396	372	83.8	143	363	973	630	582
Avg _{vol wt}		2.95	301	308	57	86	247	681	472	436

	S(IV)	CH ₂ O	H ₂ O ₂	-/+	H ⁺	LWC
	← μM →				μM	g m ⁻³
N	23	16	23	19	26	26
Min	0	9	3.2	0.38	162	0.03
Max	6.6	50	79	1.19	6607	0.53
Avg	1.1	19.8	16.4	0.70	1788	0.19
Avg _{vol wt}	0.97	16	18	0.75	1126	

La Jolla Peak Cloudwater 25 July – 04 September 1985.

<u>CASC Samples</u>										
	Vol ml	pH	Na ⁺	NH ₄ ⁺	Ca ²⁺	Mg ²⁺	Cl ⁻	NO ₃ ⁻	SO ₄ ²⁻	SO ₄ ^{2-*} _{xs}
			← μN →				← →			
N	26	22	26	25	26	26	25	25	25	22
Min	19.4	2.24	46.1	92.9	15.8	17.3	94	203.2	167.5	162
Max	381	4.94	2980	1070	370	1110	2200	4730	2000	1639
Avg	128	3.33	521	442	79	194	474	901	658	595
Avg _{vol wt}		2.83	248	345	44	81	253	647	484	454

Table 2. (continued)

La Jolla Peak Cloudwater 25 July – 04 September 1985.CASC Samples

	S(IV) ← μM →	CH ₂ O	H ₂ O ₂	-/+	H ⁺ μM	LWC gm ⁻³
N	15	3	16	20	23	25
Min	0	13	2.8	0.37	11.5	0.02
Max	5.7	15	36.3	1.07	6166	0.47
Avg	1	14	12	0.67	1789	0.13
Avg _{vol wt}	0.96	—	12	0.63	1464	

Casitas Pass Cloudwater 7 August – 9 August 1985RAC Samples

	Vol ml	pH	Na ⁺	NH ₄ ⁺	Ca ²⁺	Mg ²⁺	Cl ⁻	NO ₃ ⁻	SO ₄ ²⁻	SO ₄ ^{2-*} _{xs}
			← μN →							
N	10	10	10	10	8	10	10	10	10	10
Min	6	3.28	46	113	28	19	60	141	84	0
Max	40	4.93	>1000	1450	672	842	1600	>2800	2150	1736
Avg	19	3.77	401	467	169	209	448	>731	407	325
Avg _{vol wt}		3.75	>218	282	71	83	315	>414	206	165

	S(IV) ← μM →	CH ₂ O	H ₂ O ₂	-/+	H ⁺ μM	LWC g m ⁻³
N	7	0	6	7	10	10
Min	0	NA	3	0.64	12	0.03
Max	0	NA	17	1.32	525	0.33
Avg	0	NA	8	1.05	255	0.19
Avg _{vol wt}	0	—	6		178	0.16

Table 2. (continued)

Laguna Peak Cloudwater 5 August - 14 August 1986

	Vol ml	pH	Na ⁺	NH ₄ ⁺	Ca ²⁺	Mg ²⁺	Cl ⁻	NO ₃ ⁻	SO ₄ ²⁻	SO ₄ ^{2-*} _{xs}
			← μN →					→		
N		20	20	20	20	20	20	20	20	20
Min		2.69	9	143	4	3	46	344	276	275
Max		3.46	318	686	73	88	350	1410	1340	1335
Avg		3.07	68	337	16	20	122	702	590	582
Avg _{vol wt}		3.16	47	276	11	15	105	579	472	466
			S(IV)CH ₂ O	H ₂ O ₂	HFo	HAc	H ⁺	-/+	LWC	
			← μM →						g m ⁻³	
N			15	15	15	16	16	20	20	20
Min			0	7	0	24	12	347	0.75	0.02
Max			0	33	6	103	44	2042	1.57	0.39
Avg			0	17	2	42	18	941	1.05	0.21
Avg _{vol wt}			0	17	1	39	17	775	1.02	

Laguna Road Cloudwater 5 August - 14 August 1986

	Vol ml	pH	Na ⁺	NH ₄ ⁺	Ca ²⁺	Mg ²⁺	Cl ⁻	NO ₃ ⁻	SO ₄ ²⁻	SO ₄ ^{2-*} _{xs}
			← μN →					→		
N	20	20	20	20	20	20	20	20	20	20
Min		2.58	119	445	21	28	102	612	425	407
Max		3.49	1070	1780	162	247	758	2140	2630	2500
Avg		3.06	367	857	65	90	325	1030	1000	956
Avg _{vol wt}		3.12	319	807	59	79	299	926	860	822
			S(IV)CH ₂ O	H ₂ O ₂	HFo	HAc	H ⁺	-/+	LWC	
			← μM →						g m ⁻³	
N			18	18	18	17	16	20	20	20
Min				0	4	0	21	7	324	0.81
Max				12	15	21	74	34	2630	1.31
Avg				2	11	7	40	15	1054	1.03
Avg _{vol wt}				2	10	7	29	11	872	

Table 2. (continued)

Ventura Hill Cloudwater 30 July – 14 August 1986

	Vol ml	pH	Na ⁺	NH ₄ ⁺	Ca ²⁺	Mg ²⁺	Cl ⁻	NO ₃ ⁻	SO ₄ ²⁻	SO ₄ ^{2-*} _{xs}
			$\longleftrightarrow \mu\text{M} \longleftrightarrow$							
N	32	32	32	32	32	32	32	32	32	32
Min	33	2.74	74	405	18	23	104	247	267	246
Max	188	4.92	5720	2990	1400	1450	4290	6480	3220	2528
Avg	111	3.12	745	959	154	181	684	1430	948	858
Avg _{vol wt}		3.05	471	833	87	112	463	1161	797	740

			S(IV) CH ₂ O	H ₂ O ₂	HFo	HAc	H ⁺	-/+	LWC
			$\longleftrightarrow \mu\text{M} \longleftrightarrow$					g m ⁻³	
N			30	30	29	16	17	32	32
Min			0	5	0	31	3	12	0.58
Max			0	27	29	96	173	1820	1.08
Avg			0	13	11	60	32	971	0.99
Avg _{vol wt}			0	13	10	56	30	896	0.10

Casitas Pass Cloudwater 31 July – 14 August 1986

	Vol ml	pH	Na ⁺	NH ₄ ⁺	Ca ²⁺	Mg ²⁺	Cl ⁻	NO ₃ ⁻	SO ₄ ²⁻	SO ₄ ^{2-*} _{xs}
			$\longleftrightarrow \mu\text{M} \longleftrightarrow$							
N		32	32	32	32	32	32	32	32	32
Min		3.33	12	149	8	6	22	147	108	106
Max		4.52	176	1130	170	52	164	892	769	753
Avg		3.97	47	613	29	18	58	406	329	277
Avg _{vol wt}		3.90	41	552	24	15	53	369	295	290

			S(IV) CH ₂ O	H ₂ O ₂	HFo	HAc	-/+	H ⁺	LWC
			$\longleftrightarrow \mu\text{M} \longleftrightarrow$				μM	g m ⁻³	
N			32	30	22	25	25	32	32
Min			0	3	3	16	4	0.83	30
Max			0	13	16	58	15	1.02	468
Avg			0	8	6	27	10	0.93	131
Avg _{vol wt}			0	7	4	19	7	0.94	126

Table 3. Organic Compound Concentrations in
Santa Barbara Channel Stratus Cloudwater.

				CH ₂ O*	CH ₃ COOH	CH ₃ CHO	CH ₃ C(O)CHO			
				HCOOH		CH ₂ O†		CHOCHO		
				←————— μM —————→						
<u>Casitas Pass</u>										
Date	Seq	Start	Stop							
08/13	A	03:21	04:00	3	29	8	17.7	13.1	8.0	3.9
08/13	C	04:40	06:05	4	19	6	8.2	11.8	5.2	2.8
08/13	D	06:05	06:55	5	25	7	7.5	9.1	6.3	3.1
08/14	B	00:00	01:00	13	58	4	9.9	25.2	6.4	3.8
08/14	C	01:00	02:00	10	36	14	10.8	16.2	8.3	4.0
08/14	D	02:00	04:00	7	23	11	7.3	16.5	6.4	3.7
08/14	E	04:00	05:00	8	26	10	10.0	16.6	7.1	3.9
08/14	F	05:00	06:00	9	27	10	9.9	14.1	7.1	4.0
08/14	G	06:00	07:00	10	NA	NA	12.3	11.6	7.0	4.1
08/14	H	07:00	08:00	9	NA	NA	12.1	16.0	7.6	4.2
08/14	I	08:00	09:00	11	NA	NA	12.4	17.7	9.6	5.0
08/14	J	09:00	09:15	12	NA	NA	13.4	22.8	11.0	5.4
<u>Ventura</u>										
Date	Seq	Start	Stop							
08/13	A	22:45	00:00	27	92	28	15.3	37.2	11.8	4.2
08/14	B	00:00	01:00	18	85	30	14.0	41.4	14.4	3.0
08/14	C	01:00	02:00	19	74	173	16.6	33.6	5.9	5.2
08/14	D	02:00	03:00	15	69	34	19.1	33.7	11.7	5.7
08/14	E	03:00	04:00	21	64	24	16.9	31.8	8.9	5.5
08/14	F	04:00	05:00	23	61	23	15.2	31.2	27.2	7.1
08/14	G	05:00	06:00	11	64	23	15.1	24.0	11.6	5.6
08/14	H	06:00	07:00	18	54	33	11.6	18.4	9.0	4.9
08/14	I	07:00	08:00	14	60	27	12.9	1.5	8.7	4.1
<u>Laguna Road/Peak</u>										
Date	Seq	Start	Stop							
08/13	A	05:21	06:10	4	26	11	11.5	11.5	11.2	4.7
08/13	A	08:30	09:00	7	37	19	15.1	16.3	22.4	7.2

* Total formaldehyde determined by the Nash (colorimetric) procedure.

† Formaldehyde determined by DNPH derivatization followed by HPLC analysis.

Table 4. Cloudwater Scavenging Ratios

Date	Start	Stop	Na ⁺	Mg ²⁺	Cl ⁻	SO ₄ ²⁻	N(-III)	N(V)
------	-------	------	-----------------	------------------	-----------------	-------------------------------	---------	------

Laguna Peak

Date	Start	Stop	Na ⁺	Mg ²⁺	Cl ⁻	SO ₄ ²⁻	N(-III)	N(V)
08/05	03:33	05:30	0.39	1.17	0.29	0.54	0.45	0.65
08/05	05:30	08:30	0.72	0.87	2.71	0.69	0.79	0.98
08/06	06:40	11:10	0.42	1.32	—	1.01	1.18	1.34
08/14	02:30	05:00	0.67	1.50	1.48	1.16	1.10	1.39
08/14	05:05	07:00	3.33	1.22	0.83	1.28	1.49	1.76
08/14	07:00	09:00	0.34	0.98	1.02	0.80	0.77	1.06

Ventura

Date	Start	Stop	Na ⁺	Mg ²⁺	Cl ⁻	SO ₄ ²⁻	N(-III)	N(V)
07/30	06:30	08:15	0.48	0.95	0.74	0.59	0.70	0.60
08/01	00:20	03:20	1.12	0.86	0.79	0.74	<0.86	0.88
08/01	03:20	06:20	1.16	1.15	0.90	0.67	0.77	0.80
08/05	02:45	05:45	0.58	0.51	0.90	0.57	0.64	0.51
08/06	01:55	04:00	0.38	0.91	1.31	0.79	0.89	0.99
08/13	03:45	06:30	0.77	0.80	1.20	0.39	0.33	0.67
08/13	22:45	00:00	0.95	0.72	1.06	0.50	0.45	0.63
08/14	04:00	08:50	0.59	0.58	1.21	0.65	0.69	0.68

Casitas Pass

Date	Start	Stop	Na ⁺	Mg ²⁺	Cl ⁻	SO ₄ ²⁻	N(-III)	N(V)
07/31	06:30	06:30	0.12	0.39	0.07	0.34	0.42	0.56
08/01	02:45	05:00	0.45	0.65	0.50	0.44	0.61	0.61
08/05	02:20	03:00	0.42	0.53	0.36	0.53	0.57	0.59
08/06	02:00	06:20	0.29	0.60	4.83	0.56	0.65	0.71
08/06	06:20	07:46	0.17	0.39	1.04	0.56	0.69	0.67
08/13	03:21	06:05	1.09	5.82	—	0.48	0.44	0.60
08/13	06:05	08:40	0.36	0.89	0.19	0.37	0.29	0.41
08/14	00:00	04:00	0.51	0.64	0.46	0.45	0.50	0.51
08/14	04:00	08:05	0.44	1.03	3.90	0.57	0.64	0.65

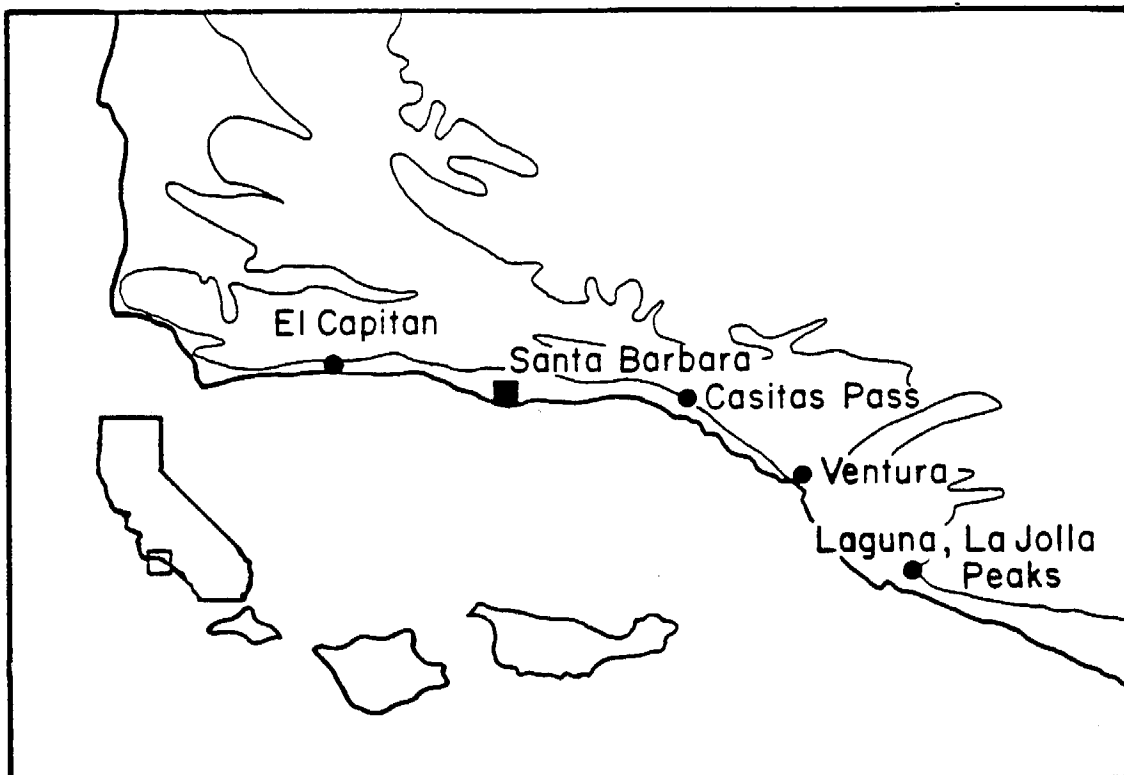


Figure 1

Map of the Santa Barbara Channel Area showing the location of sampling sites. La Jolla Peak and Casitas Pass were used in 1985. In 1986 the sites were Laguna Peak, Ventura, Casitas Pass and El Capitan. Two elevations were used at Laguna Peak. At Ventura one site was at the coast and a second was in the hills a few km inland. The near-shore contour line is at 300 meters and the inland contour line is at 500 meters.

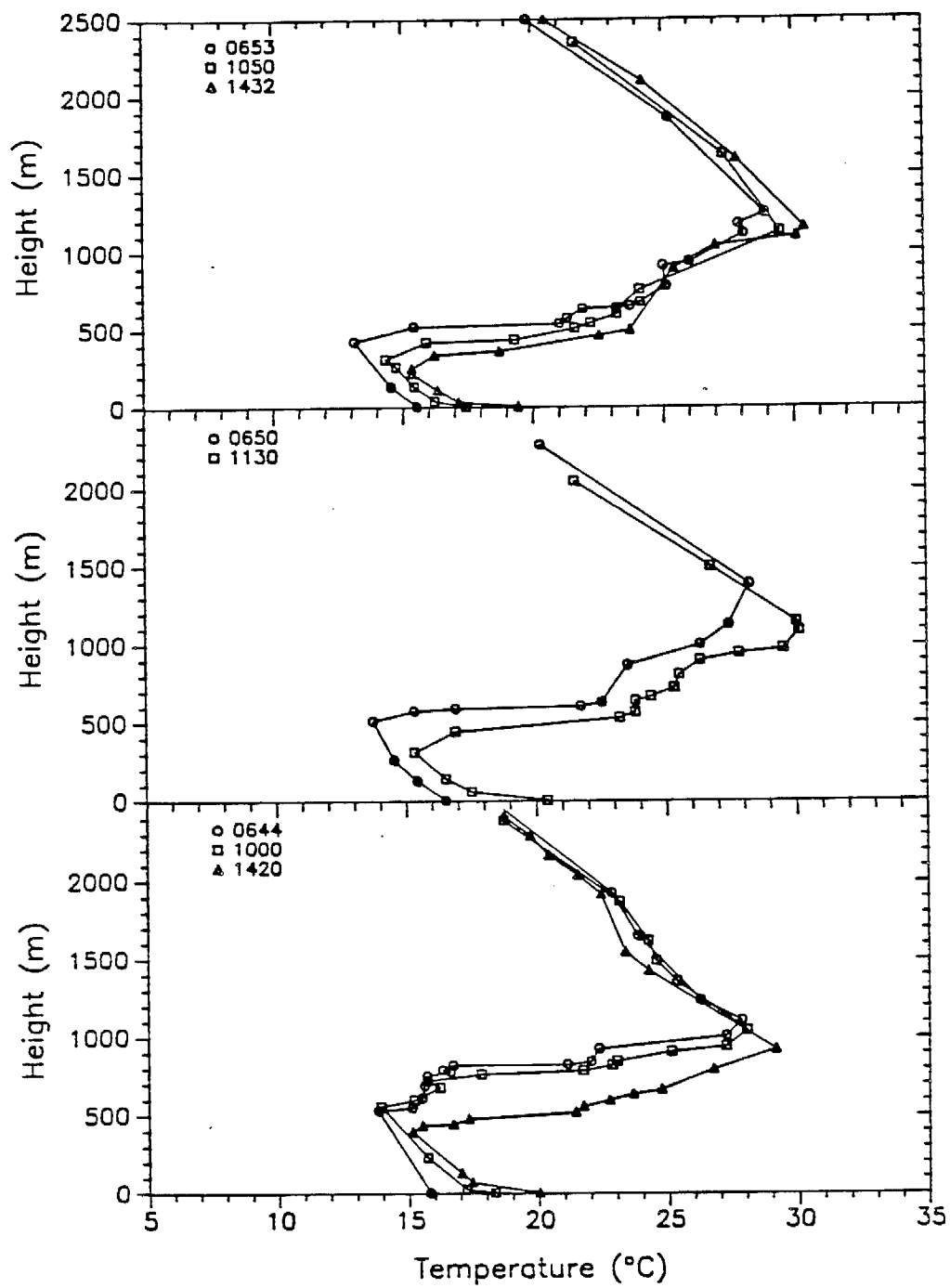


Figure 2

Temperature profiles for the period August 4 – 6, 1986 taken at Point Mugu by rawinsonde.

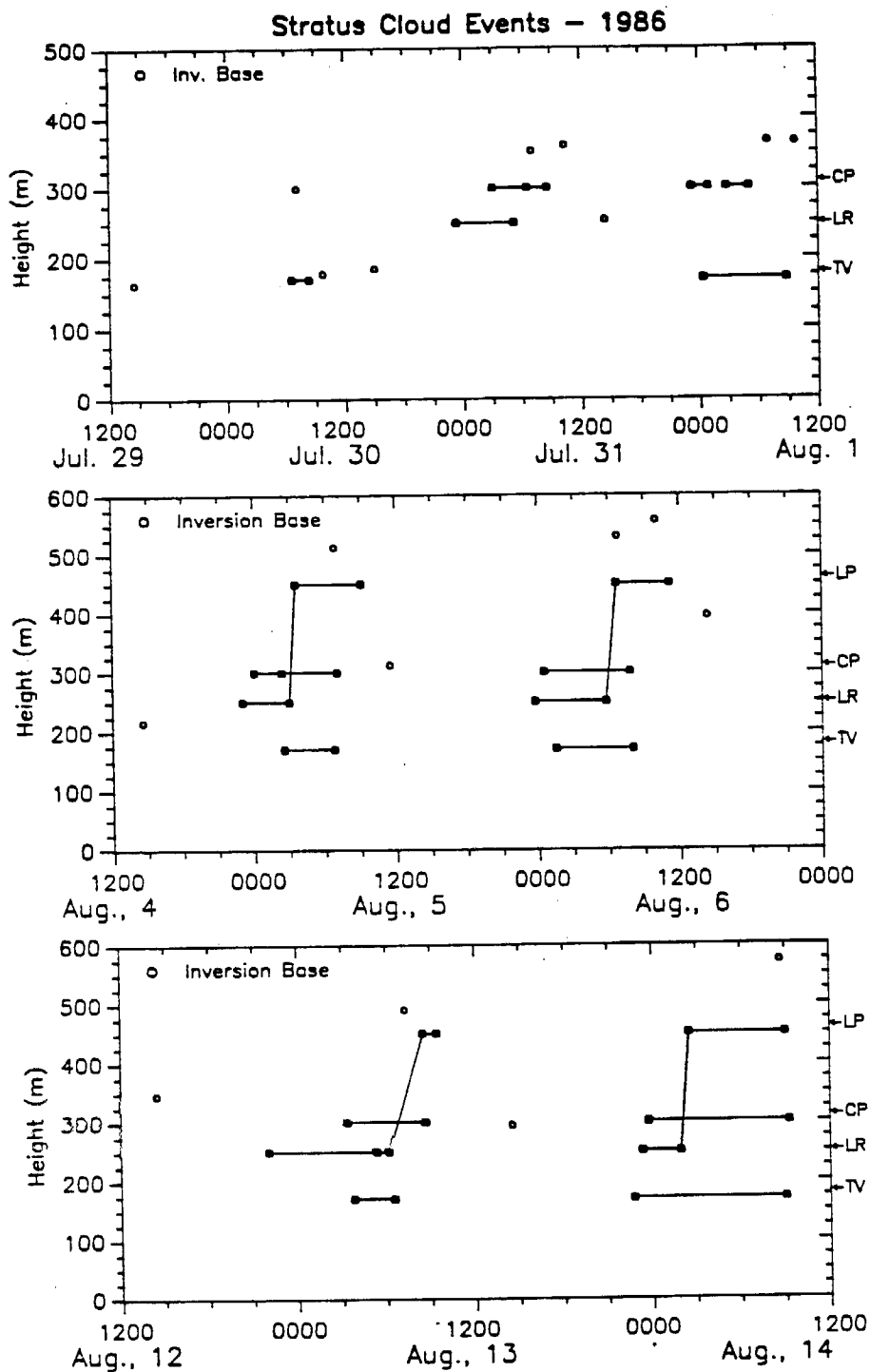


Figure 3

The presence of clouds at each sampling site used in 1986 is shown by a line. The square symbols indicate the beginning and end of cloud impactation at the site. The open squares indicate that cloud was present, but not sampled; the closed squares show the beginning of the sampling period. The heights of the inversion base derived from the Point Mugu rawinsonde data are shown by the open circles (o).

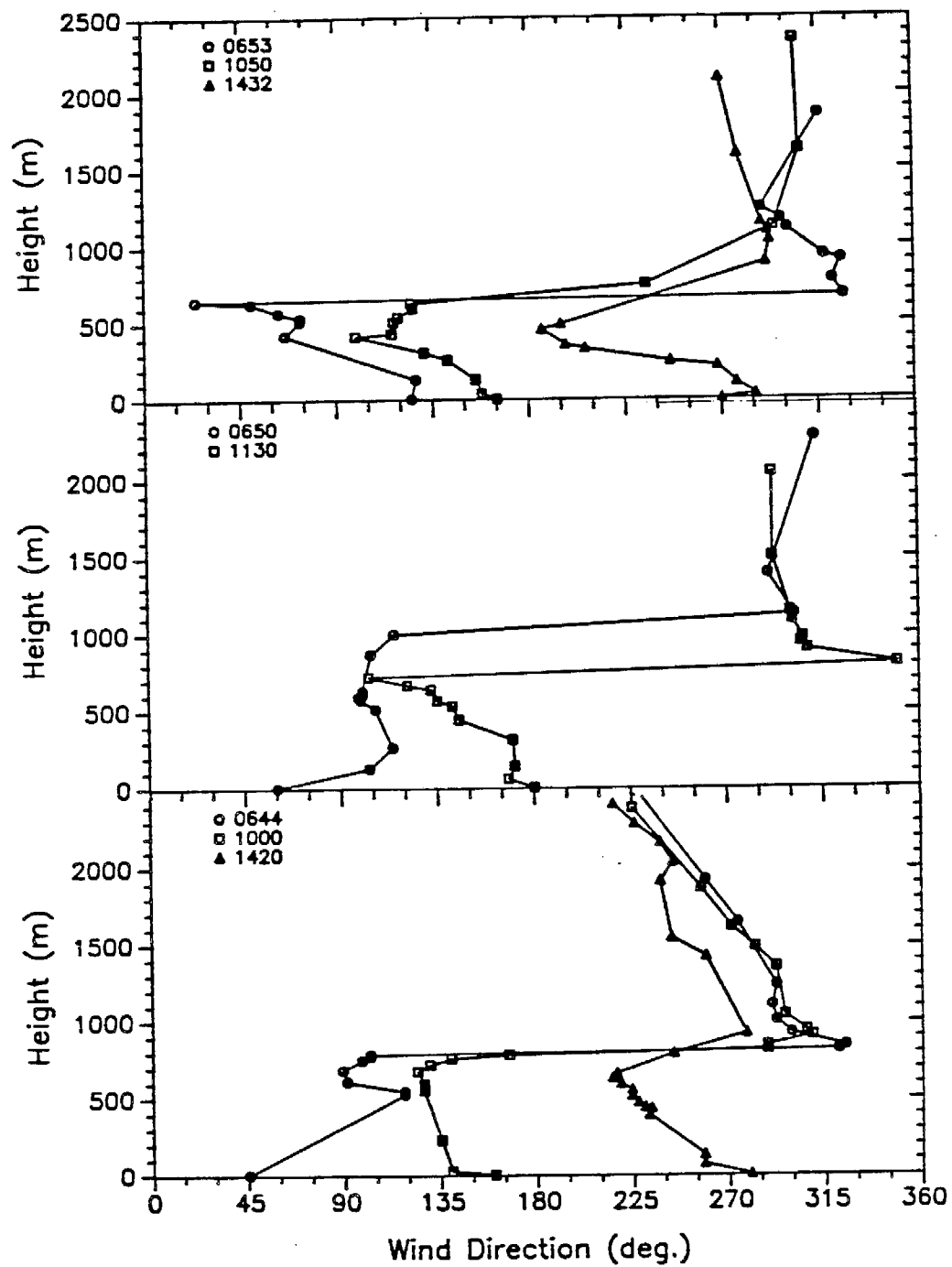


Figure 4

Wind direction profiles taken at Point Mugu for the period August 4 – August 6, 1986.

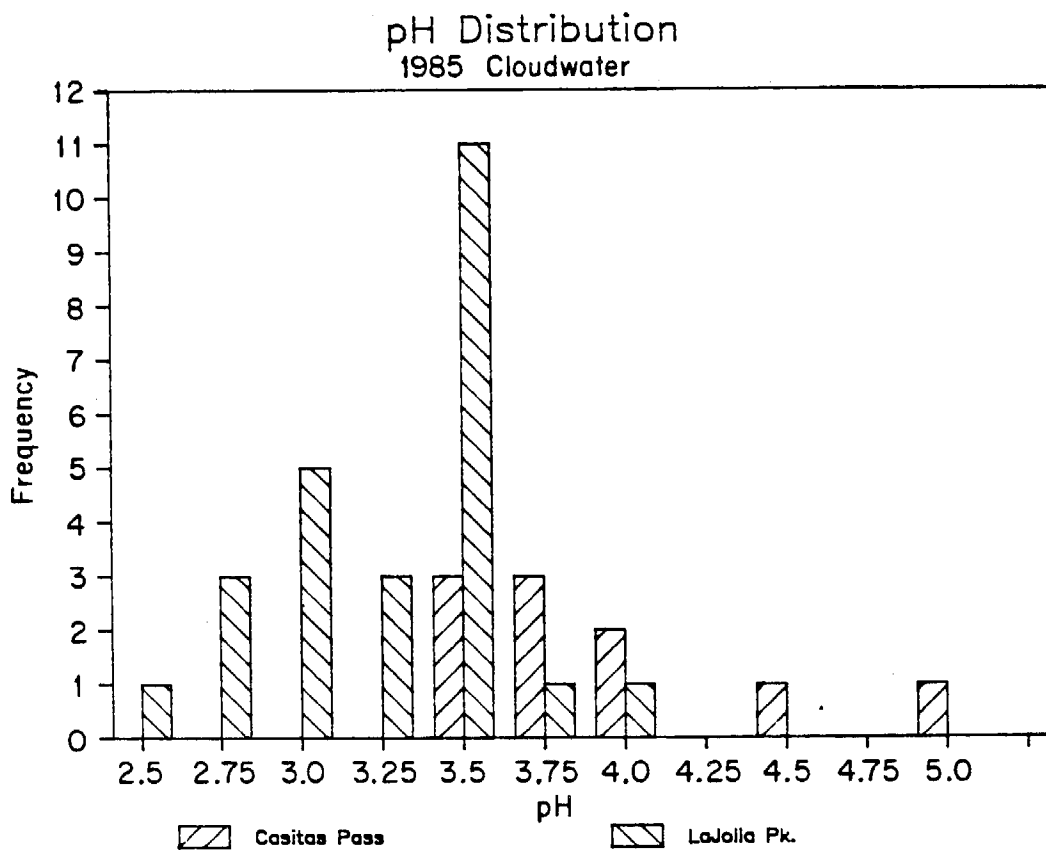


Figure 5

Distribution of cloudwater pH in samples collected at La Jolla Peak and Casitas Pass during the summer of 1985. The pH of suspect samples from La Jolla Peak has been adjusted to achieve a proper ion balance.

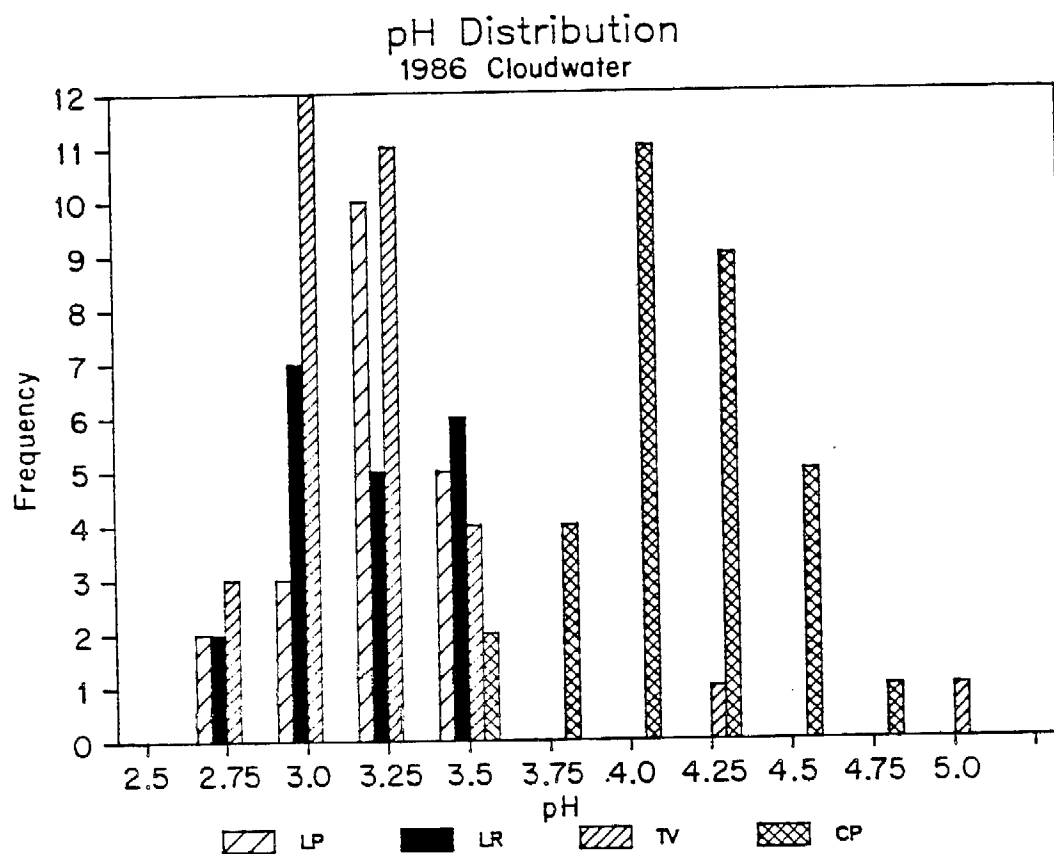


Figure 6

Distribution of cloudwater pH in samples collected at four sites along the Santa Barbara Channel coast during the summer of 1986. LP is Laguna Peak, LR is Laguna Road, TV is the hill site in Ventura, CP is Casitas Pass.

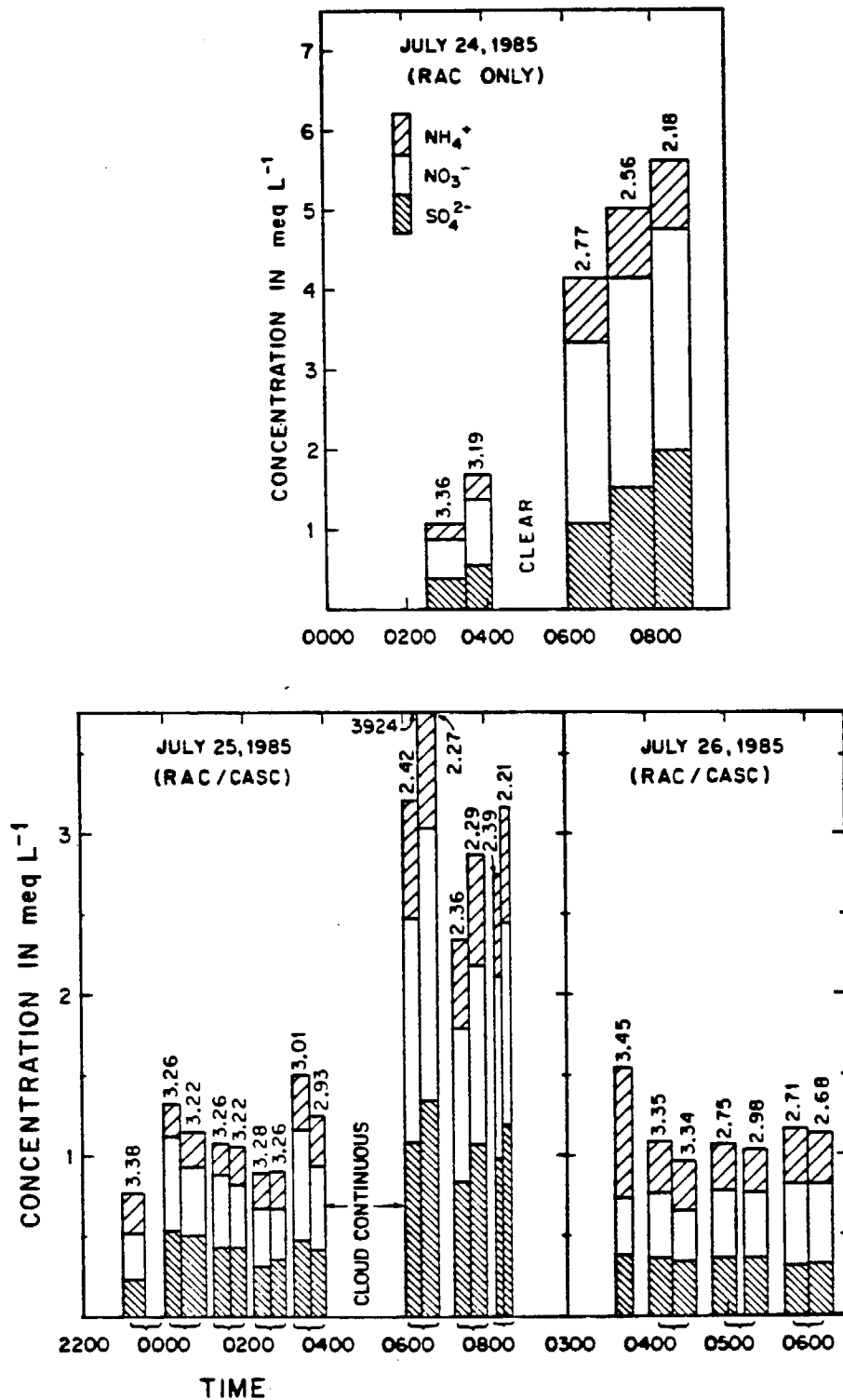


Figure 7

Concentrations of major ions in cloudwater collected at La Jolla Peak in July 1985. Cloudwater pH is indicated by the number above each bar. RAC and CASC samples were collected simultaneously; the point of the brace indicates the time of collection. Sample duration is indicated by the width of each bar.

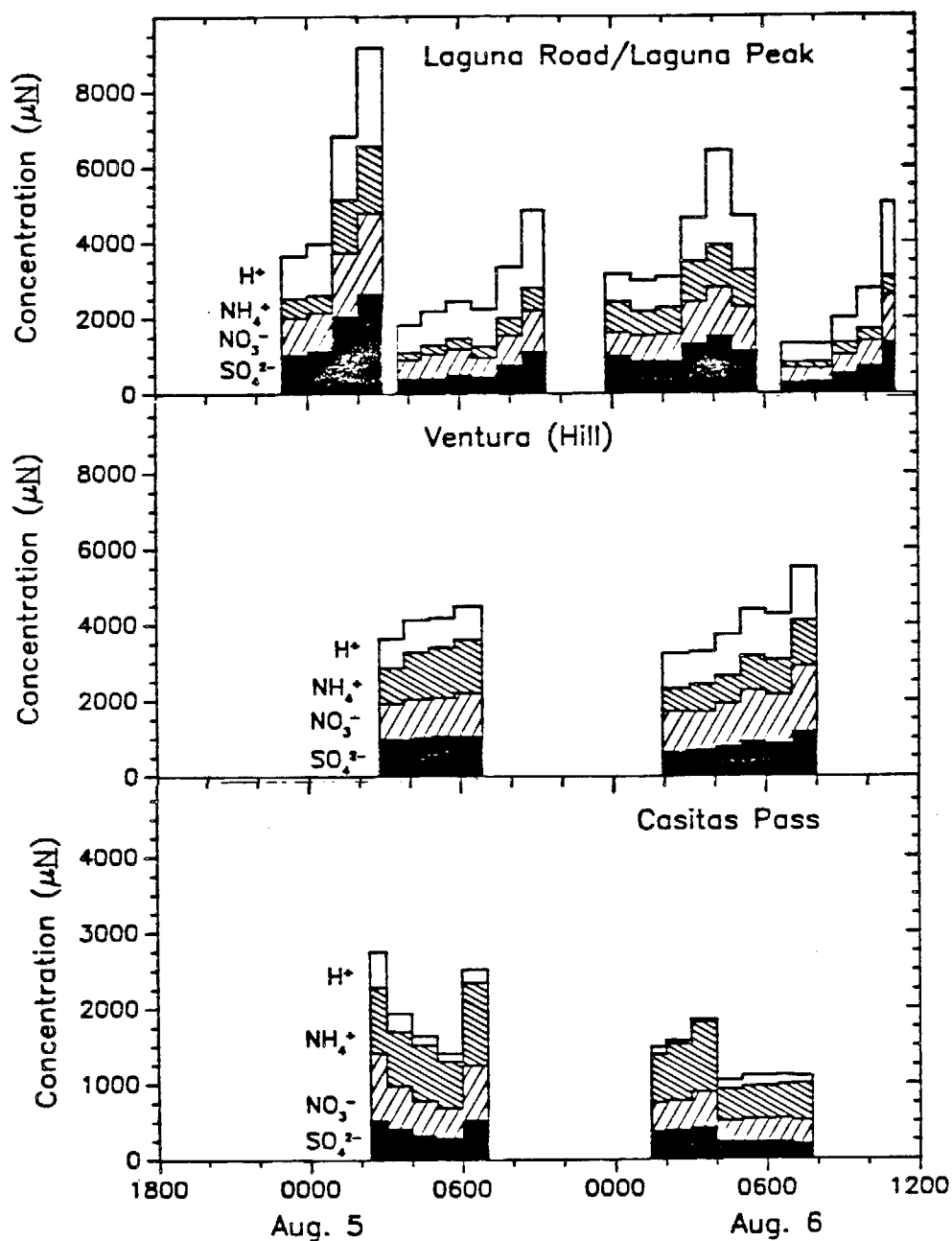


Figure 8

Concentrations of major ions in cloudwater samples collected at four sites along the coast of the Santa Barbara Channel on the mornings of August 5 and 6, 1986. Note the change in scale for the Casitas Pass samples. The Laguna Road samples (23:00–02:55; 23:45–5:45) were collected before the Laguna Peak (03:33–09:05; 06:40–11:10) during each event.

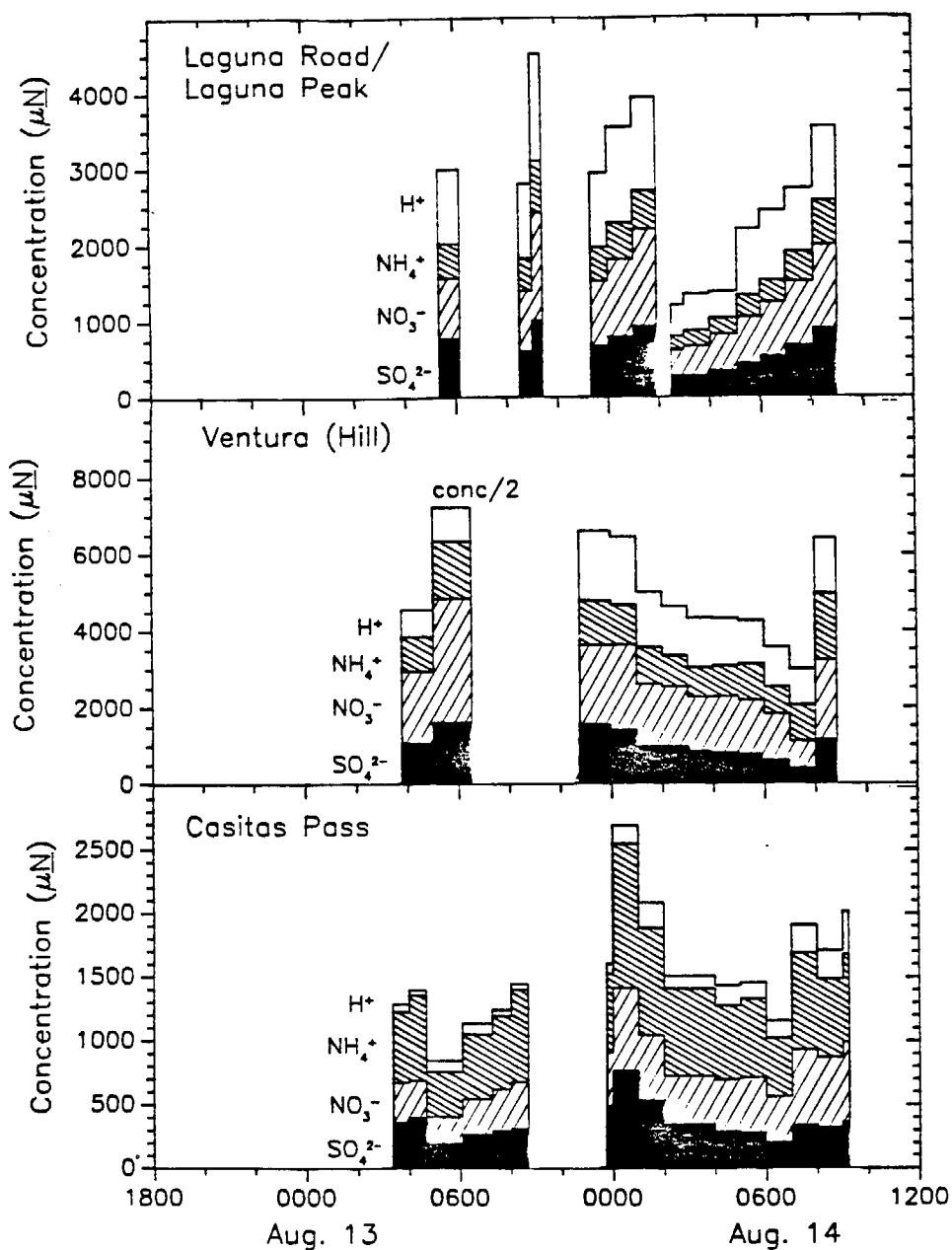


Figure 9

Concentrations of major ions in cloudwater samples collected at four sites along the coast of the Santa Barbara Channel on the mornings of August 13 and 14. Note the differences in scale for each site and the change in scale for the August 13 samples from Ventura. The Laguna Road samples (05:21–06:10; 00:00–01:55) were collected before the Laguna Peak (08:30–09:25; 02:30–09:00) during each event.

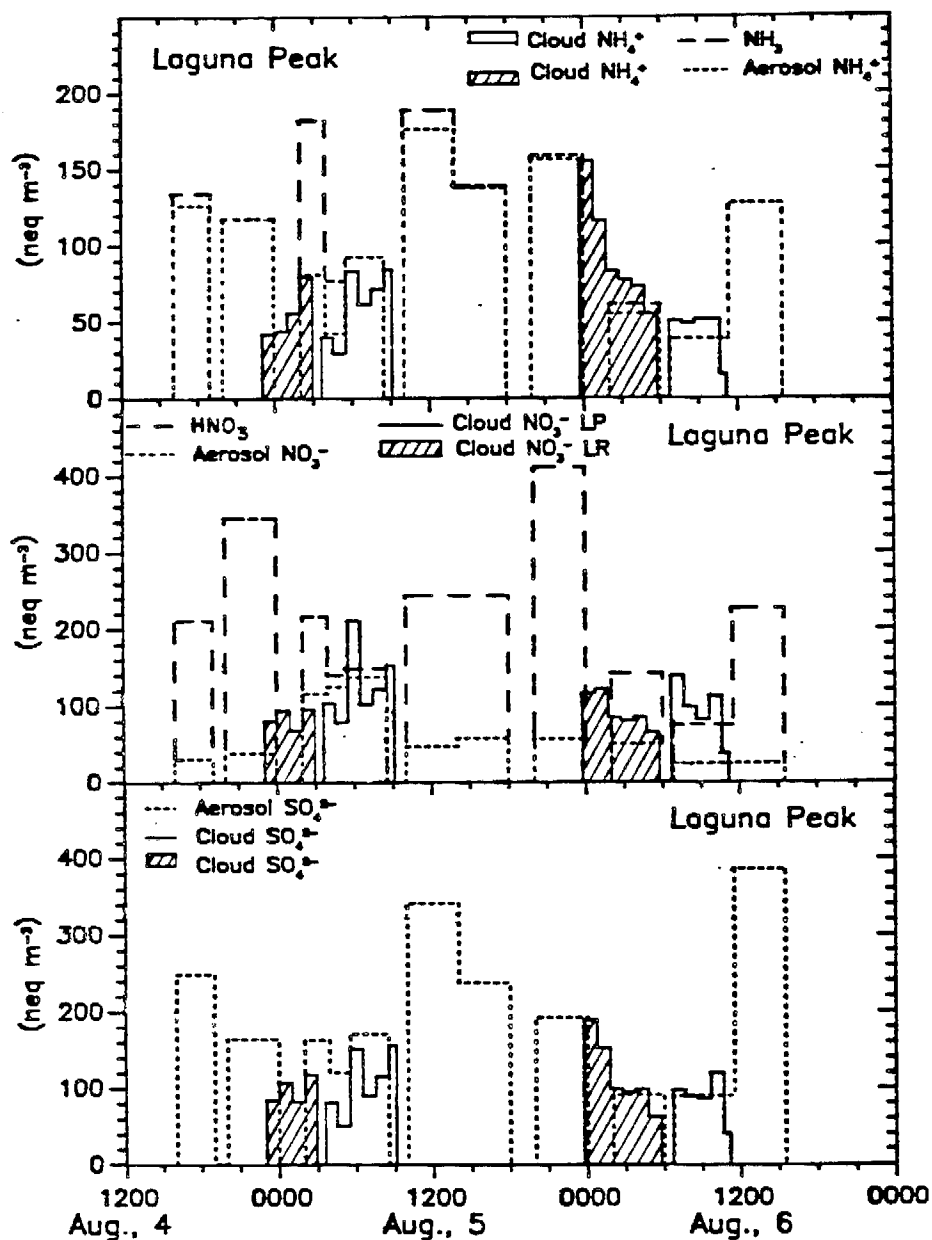


Figure 10

Aerosol and cloudwater loadings of major ions at Laguna Peak on August 4 – 6, 1986.

Cloudwater loading is the product of aqueous-phase concentration and estimated LWC. The cross-hatched regions (LR) indicate Laguna Road samples whereas the other regions correspond to Laguna Peak samples.

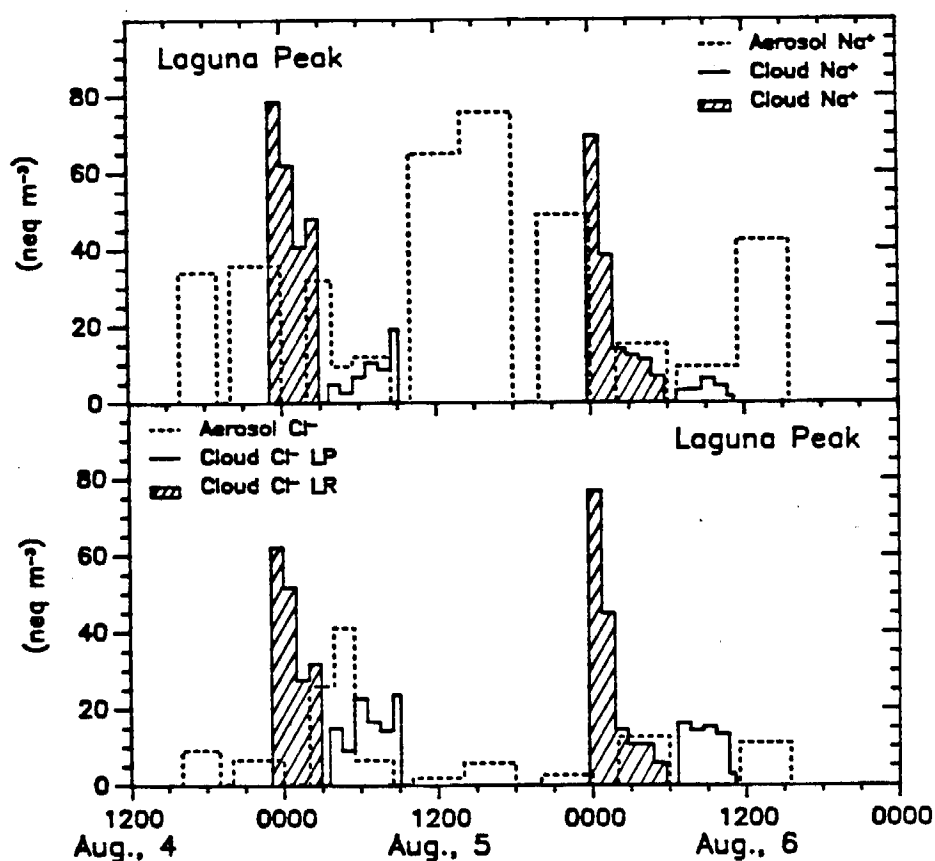


Figure 11

Aerosol and cloudwater loadings of sea salts at Laguna Peak on August 4 – 6, 1986.

Cloudwater loading is the product of aqueous-phase concentration and estimated LWC. The cross-hatched regions (▨) indicate Laguna Road samples whereas the other regions correspond to Laguna Peak samples.

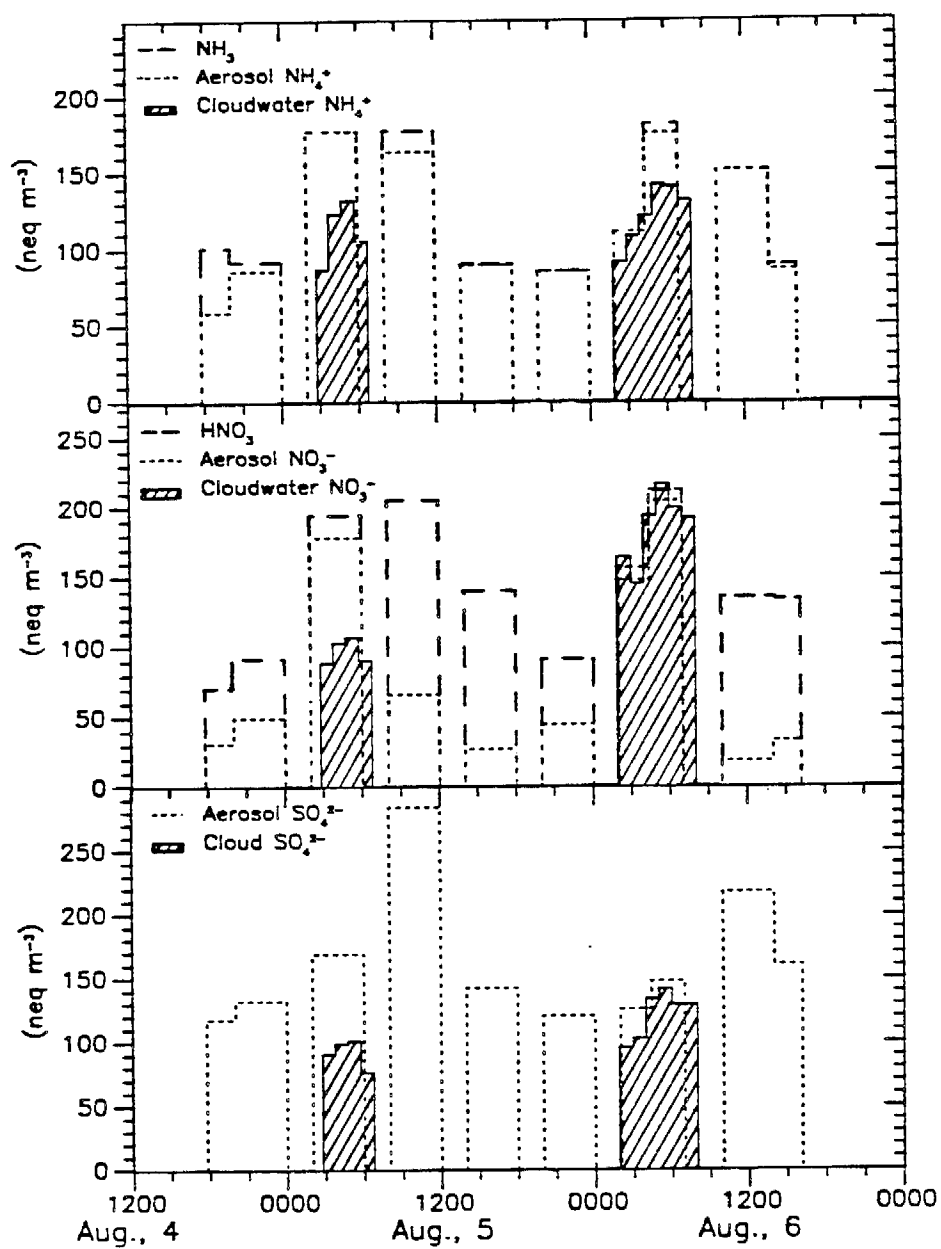


Figure 12

Aerosol and cloudwater loadings of major ions at Ventura on August 4 – 6, 1986. Cloudwater loading is the product of aqueous-phase concentration and estimated LWC.

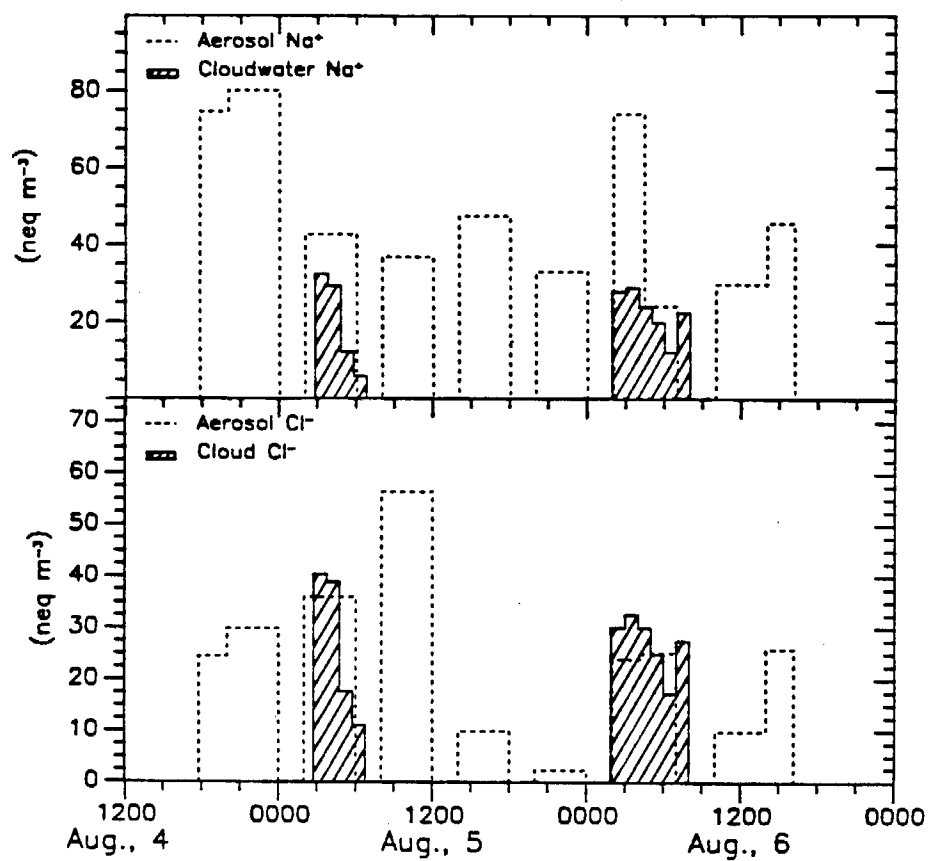


Figure 13

Aerosol and cloudwater loadings of sea salts at Ventura on August 4 – 6, 1986. Cloudwater loading is the product of aqueous-phase concentration and estimated LWC.

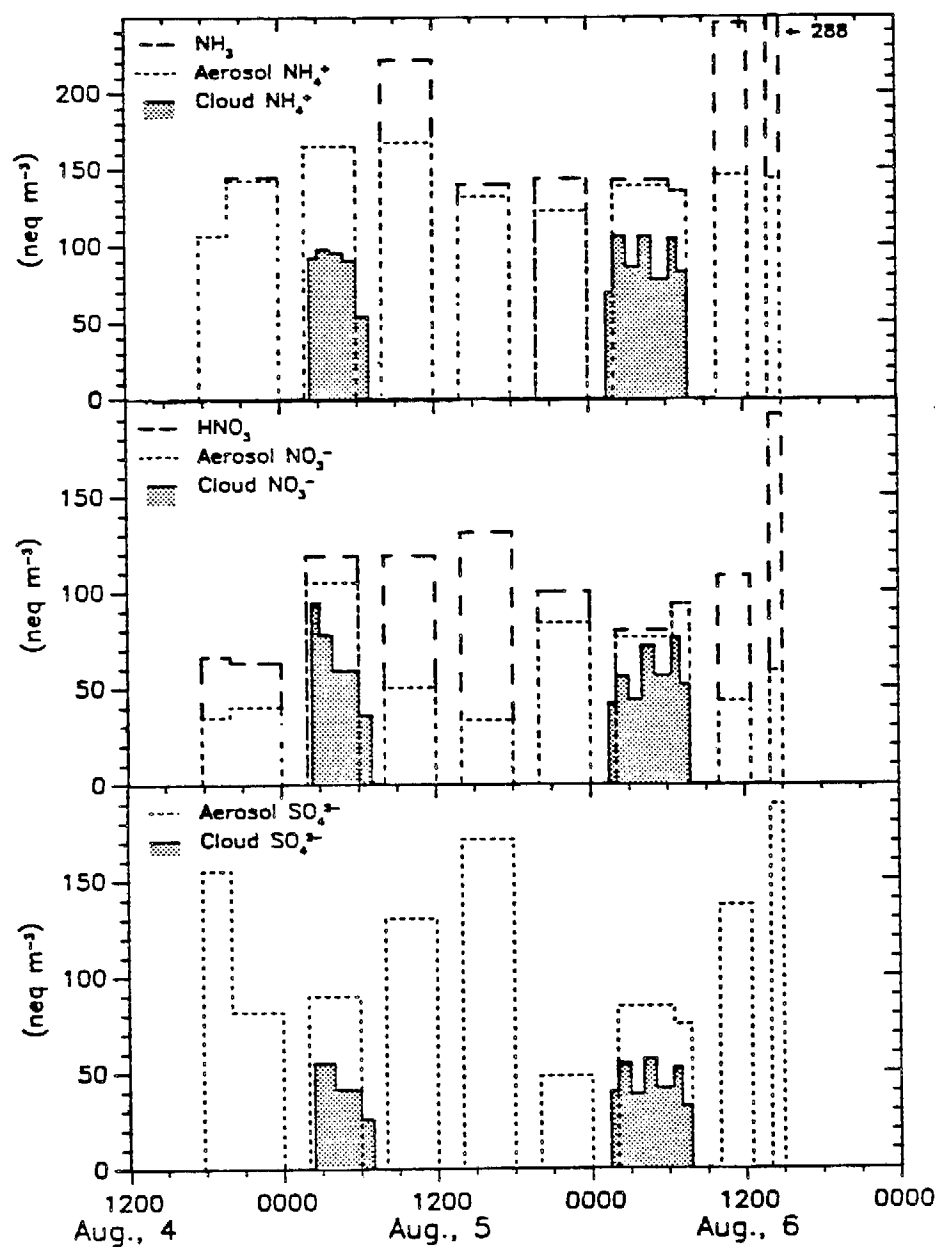


Figure 14

Aerosol and cloudwater loadings of major ions at Casitas Pass on August 4 – 6, 1986. Cloudwater loading is the product of aqueous-phase concentration and estimated LWC.

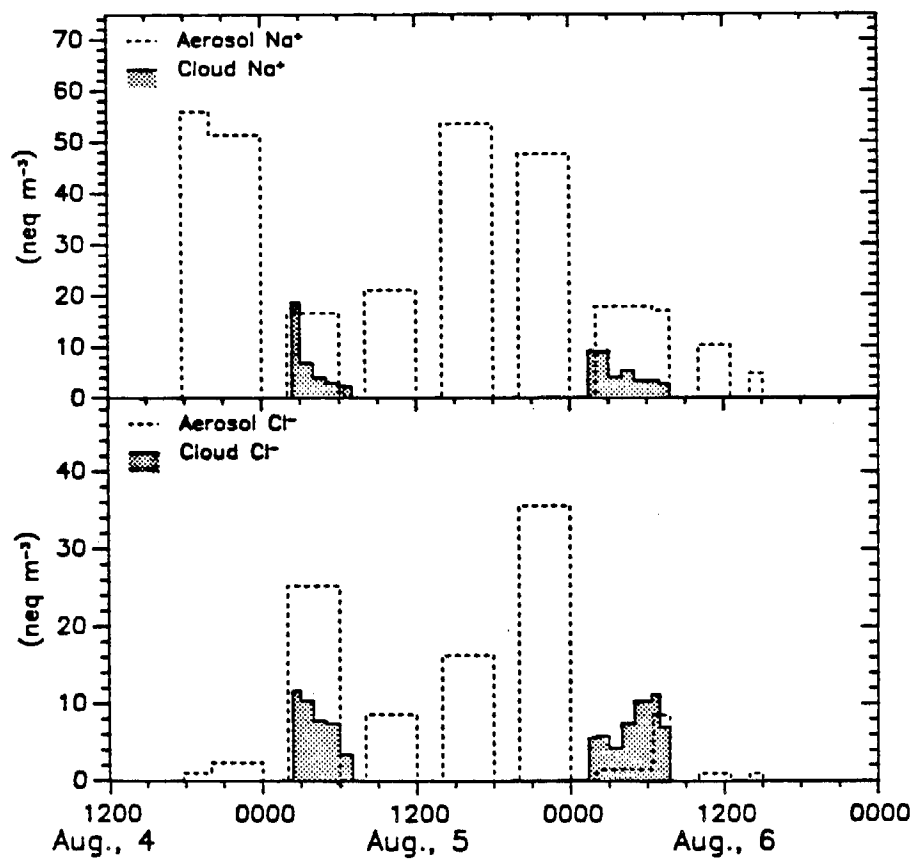


Figure 15

Aerosol and cloudwater loadings of sea salts at Casitas Pass on August 4 - 6, 1986. Cloudwater loading is the product of aqueous-phase concentration and estimated LWC.

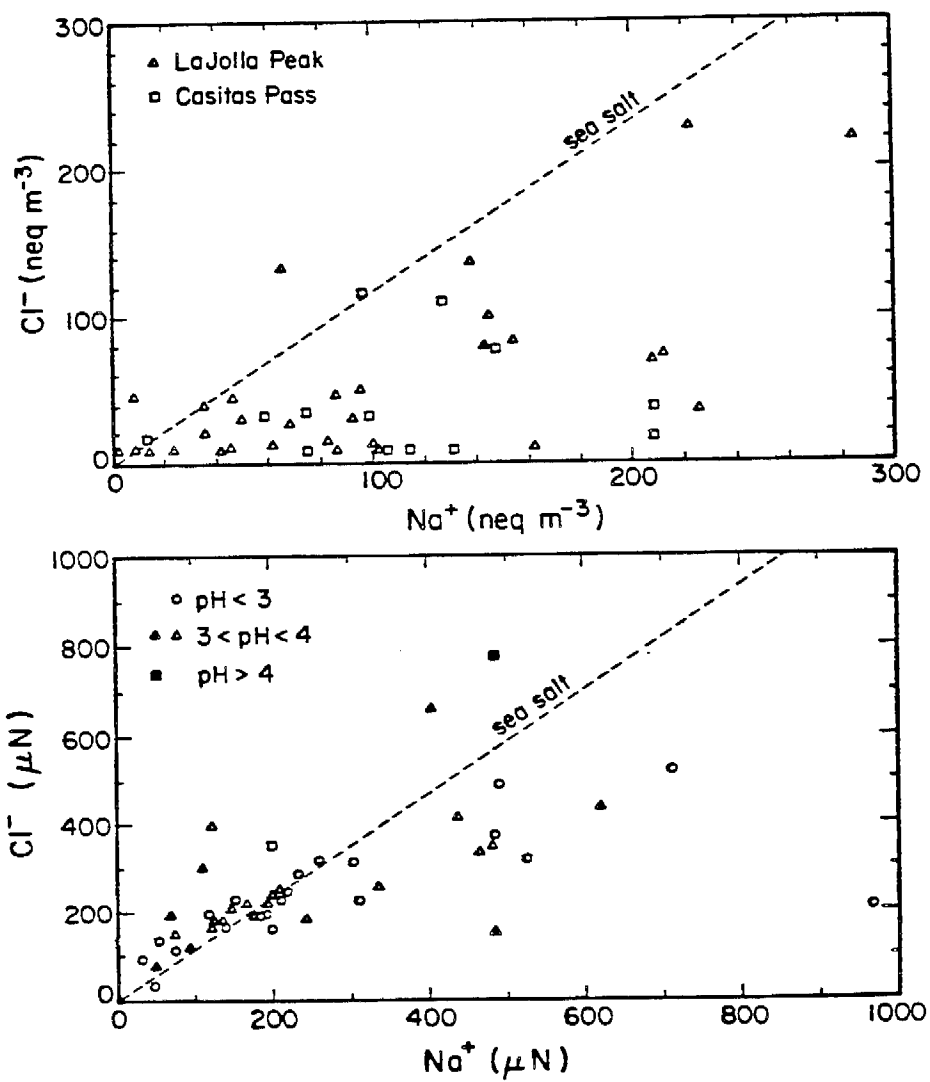


Figure 16

A. Plot of Cl^- concentration vs. Na^+ in aerosol samples collected at La Jolla Peak and Casitas Pass during July and August 1985 B. Plot of Cl^- concentrations vs Na^+ in cloudwater samples collected at La Jolla Peak (\circ, Δ) and Casitas Pass ($\blacktriangle, \blacksquare$).

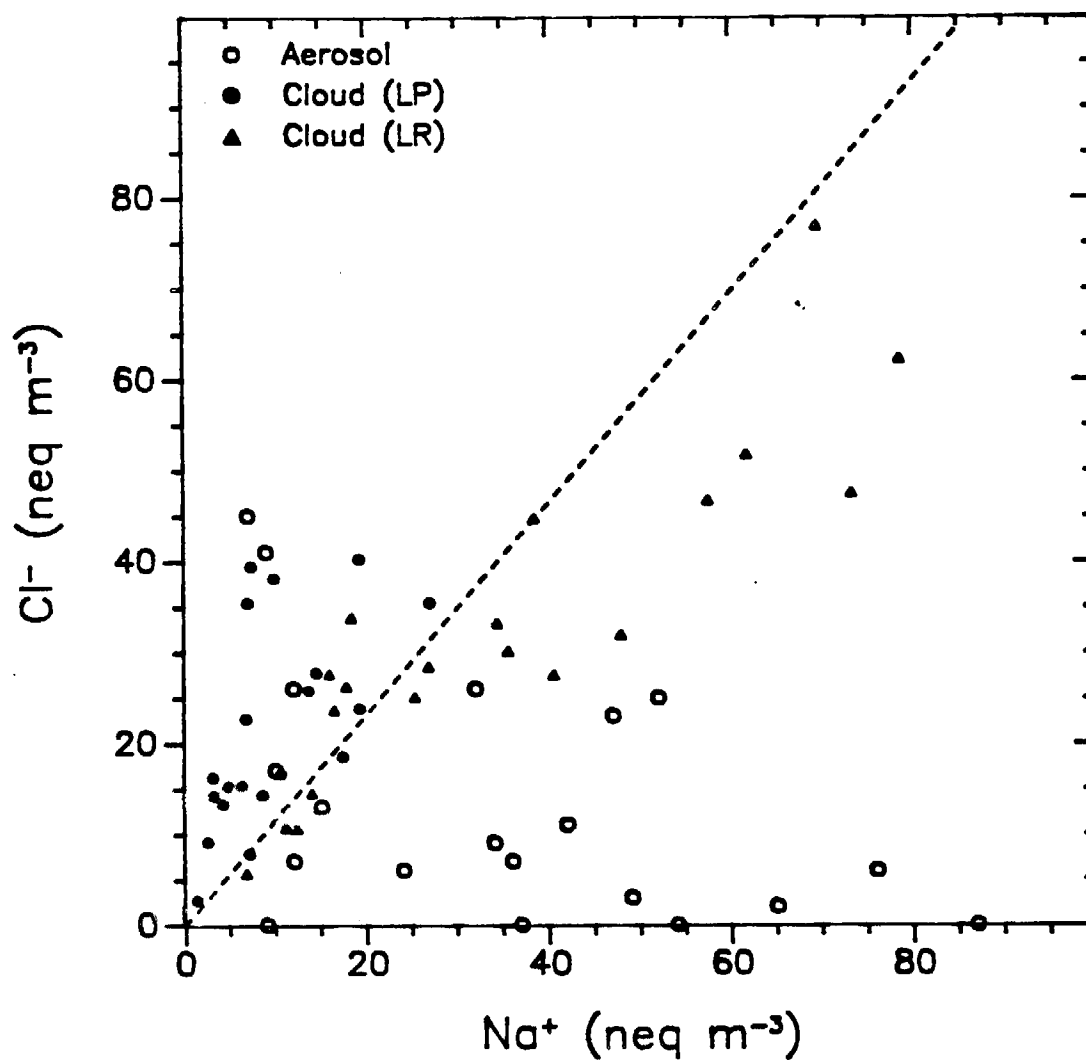


Figure 17

Plot of Cl^- concentrations vs Na^+ in aerosol and cloudwater samples from the upper and lower sites collected at Laguna Peak during July and August 1986. Cloudwater concentrations are given as loading, which is the product of aqueous-phase concentration and LWC.

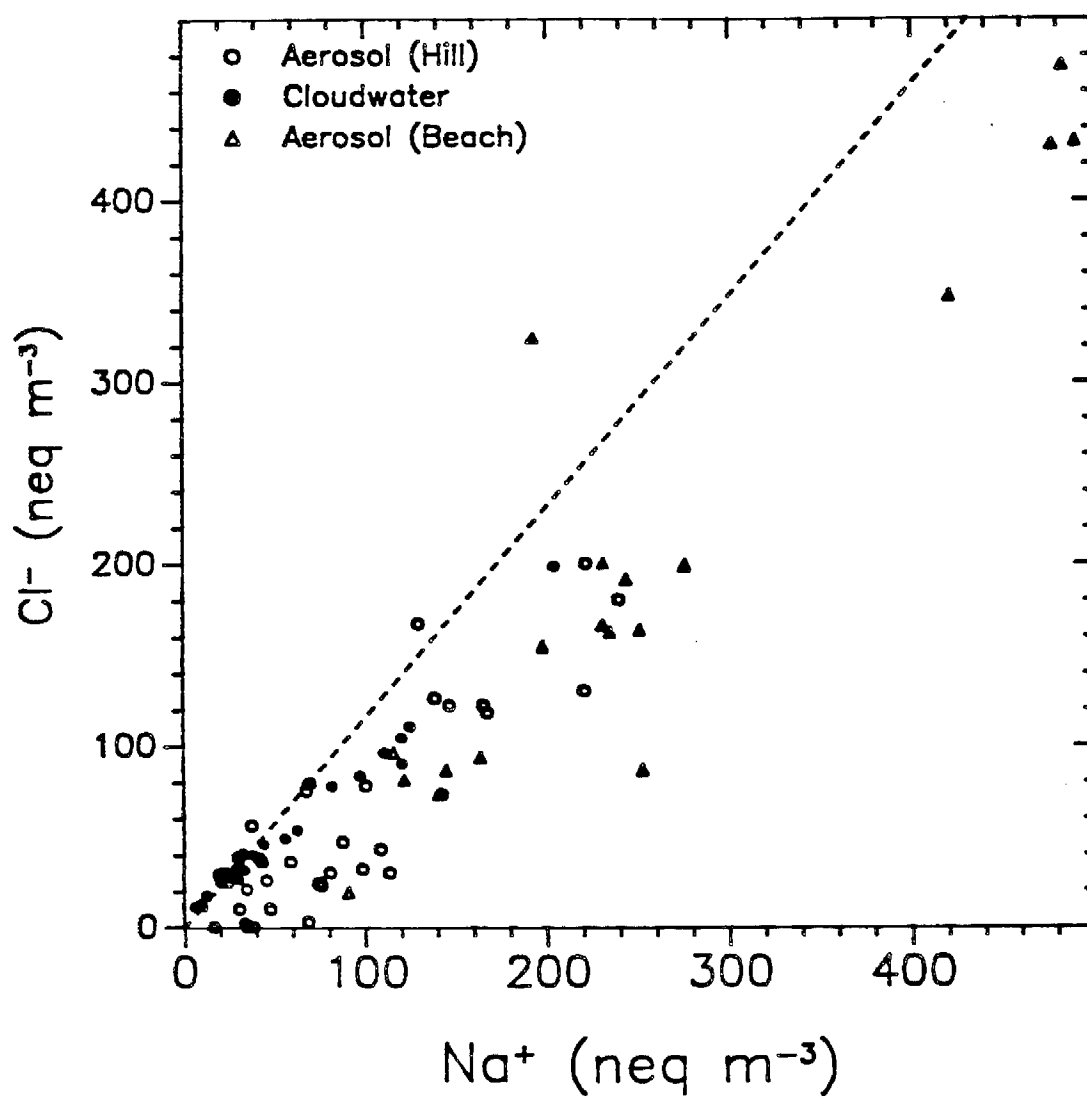


Figure 18

Plot of Cl^- concentrations vs Na^+ in aerosol and cloudwater samples collected at Ventura during July and August 1986. Cloudwater concentrations are given as loading, which is the product of aqueous-phase concentration and LWC.

APPENDIX OF SUPPLEMENTAL MATERIAL

Meteorology and Chemical Composition of Aerosol and Cloudwater Samples Collected at Sites Along the Santa Barbara Channel

for

The Chemistry of Coastal Clouds and Aerosol in the Santa Barbara Channel

by

J. William Munger[†], Jeff Collett, Jr.,[‡]

Bruce C. Daube, Jr., and Michael R. Hoffmann*

*Environmental Engineering Science
W. M. Keck Laboratories, 138-78
California Institute of Technology
Pasadena, CA 91125, U.S.A.*

Present Addresses:

[†]Dept. of Earth and Planetary Sciences, Harvard
University, Pierce Hall, 29 Oxford St., Cambridge MA 02138

[‡] Atmosphärenphysik ETH, Hönggerberg HPP
CH-8093 Zürich, Switzerland

Submitted to:

Environmental Science & Technology

23 February 1989

* To whom correspondence should be addressed.

* Address from 3-15 to 9-1-89: EAWAG, CH-8600 Dübendorf, Switzerland

List of Tables

Table	Title	Page
A.1	1985 LaJolla Peak Aerosol Concentrations	3
A.2	1985 Casitas Pass Aerosol Concentrations	3
A.3	1985 La Jolla Peak Cloudwater Concentrations – RAC Collector	4
A.4	1985 La Jolla Peak Cloudwater Concentrations – CASC Collector	6
A.5	1985 La Jolla Peak Cloudwater (RAC) Loading	8
A.6	1985 La Jolla Peak Cloudwater (CASC) Loading	9
A.7	1985 Casitas Pass Cloudwater Concentrations	10
A.8	1985 Casitas Pass Cloudwater Loading	10
A.9	1986 Laguna Peak Cloudwater Concentrations	11
A.10	1986 Laguna Peak Cloudwater Loading	12
A.11	1986 Laguna Road Cloudwater Concentrations	14
A.12	1986 Laguna Road Cloudwater Loading	15
A.13	1986 Ventura Hill Cloudwater Concentrations	16
A.14	1986 Ventura Hill Cloudwater Loading	18
A.15	1986 Casitas Pass Cloudwater Concentrations	20
A.16	1986 Casitas Pass Cloudwater Loading	22
A.17	1986 Laguna Peak Aerosol Concentrations	24
A.18	1986 Ventura Hill Aerosol Concentrations	25
A.19	1986 Emma Wood State Beach Aerosol Concentrations	26
A.20	1986 West Casitas Pass Aerosol Concentrations	27
A.21	1986 El Capitan State Beach Aerosol Concentrations	28

List of Figures

Figure	Title	Page
A.1.	Temperature profiles (rawinsonde) for 24–26 July 1985 at Point Mugu.	
A.2	Temperature profiles (rawinsonde) for 29–30 July 1985 at Point Mugu.	
A.3	Temperature profiles (rawinsonde) for 7–9 August 1985 at Point Mugu.	
A.4	Temperature profiles (rawinsonde) for 20–21 August 1985 at Point Mugu.	
A.5	Temperature profiles (rawinsonde) for 7–29 to 8–1–1986 at Point Mugu.	
A.6	Temperature profiles (rawinsonde) for 12–14 August 1986 at Point Mugu.	
A.7	Wind direction profiles taken at Point Mugu for July 30 – August 1, 1986.	
A.8	Wind direction profiles taken at Point Mugu for 13–14 August 1986.	
A.9	Aerosol and cloudwater loadings of major ions at Laguna Peak on August 12 – August 14, 1986.	
A.10	Aerosol and cloudwater loadings of sea salts at Laguna Peak on August 12 – 14, 1986.	
A.11	Aerosol and cloudwater loadings of major ions at Ventura on July 29 – August 1, 1986.	
A.12	Aerosol and cloudwater loadings of sea salts at Ventura on July 29 – August 1, 1986.	
A.13	Aerosol and cloudwater loadings of major ions at Ventura on August 12 – 14, 1986.	
A.14	Aerosol and cloudwater loadings of sea salts at Ventura on August 12 – 14, 1986.	
A.15	Aerosol and cloudwater loadings of major ions at Casitas Pass on July 29 – August 1, 1986.	
A.16	Aerosol and cloudwater loadings of sea salts at Casitas Pass on July 29 – August 1, 1986.	
A.17	Aerosol and cloudwater loadings of major ions at Casitas Pass on August 12 – 14, 1986.	
A.18	Aerosol and cloudwater loadings of sea salts at Casitas Pass on August 12 – 14, 1986.	

Table A.1 1985 LaJolla Peak Aerosol Concentrations

Date ID	Start	Stop	Na ⁺	NH ₄ ⁺	Ca ²⁺	Mg ²⁺	Cl ⁻	NO ₃ ⁻	SO ₄ ²⁻	NH ₃	HNO ₃
← neq m ⁻³ →										← nmole m ⁻³ →	
07/23 A	12:00	15:54	99	62	7.3	18.4	4.1	59	173	66	101
07/24 A	02:30	05:53	14	65	3.9	2.7	0.0	24	107	19	61
07/24 B	06:00	09:33	4	52	0.0	0.8	0.8	22	53	36	94
07/25 A	12:00	15:52	41	73	6.9	5.6	16.6	38	132	22	119
07/26 A	12:00	15:52	23	78	1.7	4.1	0.0	16	176	12	4
07/27 B	03:30	06:20	1	18	16.8	0.0	0.0	31	71	31	NA
07/29 A	15:30	19:40	95	0	0.0	21.0	41.2	39	32	8	21
07/30 A	01:45	04:18	284	20	6.9	35.0	211	34	153	68	24
07/30 B	05:00	09:27	86	14	3.0	18.1	38.3	39	42	30	9
07/30 C	13:00	16:57	225	66	5.5	51.2	26.9	152	148	23	71
07/31 A	20:47	11:44	92	33	12.7	22.7	22.7	77	52	16	28
08/06 A	23:00	03:00	137	166	41.7	34.5	128	111	66	21	85
08/07 B	16:15	20:09	128	239	37.0	33.4	126	99	97	14	83
08/07 A	23:00	03:01	79	80	31.7	22.8	6.0	142	80	56	186
08/08 B	12:40	16:01	101	142	NA	30.1	0.0	68	304	7	386
08/14 B	02:00	05:55	NA	NA	NA	NA	107	95	67	19	34
08/19 A	17:02	20:02	45	34	0.0	9.7	2.2	40	34	33	37
08/20 A	12:00	15:56	65	48	1.1	13.9	124	34	63	8	82
08/21 A	00:11	04:10	8	14	10.6	8.1	36.3	29	81	8	30
08/21 B	04:25	07:51	162	33	15.7	6.8	1.7	153	111	4	37
08/26 A	16:00	19:07	86	95	37.4	23.5	1.3	72	129	29	77
08/28 A	14:40	21:19	61	46	17.5	20.3	4.5	57	57	42	99

Table A.2 1985 Casitas Pass Aerosol Concentrations

Date ID	Start	Stop	Na ⁺	NH ₄ ⁺	Ca ²⁺	Mg ²⁺	Cl ⁻	NO ₃ ⁻	SO ₄ ²⁻	NH ₃	HNO ₃
← neq m ⁻³ →										← nmole m ⁻³ →	
08/07 A	02:00	02:36	207	78	0.0	58.3	107	43	75	97	22
08/07 B	13:00	17:00	130	68	6.5	32.1	24.4	99	89	53	44
08/08 A	00:00	04:36	74	61	26.6	22.3	0.0	97	63	15	29
08/08 B	05:55	08:37	12	107	38.9	6.2	0.0	69	79	11	27
08/08 A	12:00	16:06	NA	NA	NA	NA	NA	NA	NA	21	136
08/09 B	00:00	03:45	96	65	32.4	26.4	9.1	122	109	8	25
08/09 C	06:00	09:12	57	185	43.2	20.6	0.0	148	141	28	43
08/14 A	00:00	04:00	100	35	34.6	32.7	75.0	52	61	12	16
08/14 B	12:00	16:12	113	22	3.4	28.4	26.8	73	59	37	28
08/28 A	16:30	19:30	207	68	38.6	55.0	50.0	172	95	94	24
08/29 A	14:20	15:56	105	57	40.6	22.4	14.6	82	53	115	163
09/03 A	16:20	19:48	146	0	2.9	31.0	101	10	43	0	11
09/04 A	16:00	19:36	73	7	19.7	19.0	23.8	34	55	31	15
09/05 A	00:00	04:00	195	38	33.3	54.2	115	110	77	16	18
09/16 A	19:30	23:12	116	46	5.4	37.8	123	126	85	22	23
09/17 A	03:30	06:36	126	98	30.4	35.2	37.4	153	97	20	23
09/17 B	14:00	18:12	NA	NA	NA	NA	NA	NA	NA	21	84
09/17 A	22:00	02:18	99	36	13.8	29.1	43.8	114	54	10	11

NA indicates sample not analyzed

Table A.3 1985 La Jolla Peak Cloudwater Concentrations
RAC Collector

Date ID	Start	Stop	Vol ml	pH	Na ⁺	NH ₄ ⁺	Ca ²⁺	Mg ²⁺	Cl ⁻	NO ₃ ⁻	SO ₄ ²⁻	SO ₄ ²⁻ * _{xs}
					←----- μN -----→							
07/24 A	02:35	03:35	49	3.36	193	214	62	57	196	509	370	347
07/24 B	03:35	04:10	20	3.19	199	311	82	65	217	844	532	508
07/24 C	06:05	07:05	14	2.77	302	801	259	111	290	2260	1050	1013
07/24 D	07:07	08:10	17	2.56	710	882	192	236	495	2610	1500	1414
07/24 E	08:10	09:05	13	2.18	>300	873	102	153	1100	2750	1980	1905
07/24 A	23:02	00:00	36	3.38	480	253	77	125	322	481	225	167
07/25 B	00:02	01:00	48	3.26	464	196	106	116	309	600	537	481
07/25 C	01:02	02:00	53	3.26	259	192	136	72	272	449	433	402
07/25 D	02:02	03:00	58	3.28	243	210	42	64	161	370	310	281
07/25 E	03:02	04:00	70	3.01	335	333	53	88	234	687	481	440
07/25 F	06:00	07:00	18	2.42	310	719	52	92	202	1410	1080	1042
07/25 G	07:00	08:00	22	2.36	192	546	25	54	170	967	826	803
07/25 H	08:00	08:20	6	2.39	NA	632	69	92	242	1150	970	925
07/26 A	03:35	04:00	40	3.45	483	294	12	34	126	365	371	313
07/26 B	04:00	04:45	57	3.35	122	319	22	37	125	402	361	346
07/26 C	04:48	05:30	58	2.75	74	284	12	23	87	426	359	350
07/26 D	05:30	06:17	46	2.71	30	323	11	13	70	511	322	318
07/30 A	05:00	05:45	11	3.50	>870	310	76	816	1120	844	568	167
08/21 A	00:19	01:02	52	3.79	166	119	25	37	197	201	132	111
08/21 B	01:02	01:35	22	3.72	147	109	22	34	183	208	139	122
08/21 C	02:10	03:10	47	3.14	436	238	52	115	389	677	395	342
08/21 D	03:10	04:10	16	2.64	965	591	139	259	185	NA	1010	1046
08/21 F	05:10	06:10	34	2.81	211	402	51	46	203	1460	557	532
08/21 G	06:10	07:10	23	2.55	525	418	103	144	294	2540	1110	1046
08/21 H	07:10	07:50	1	2.21	NA	NA	NA	NA	NA	NA	NA	
09/17 A	00:00	00:45	15	3.46	1500	105	121	321	1030	558	358	177
09/17 B	03:15	04:00	4	NA	1550	>150	275	523	1210	1050	410	222

Table A.3 1985 La Jolla Peak Cloudwater Concentrations (continued)
RAC Samples

Date	ID	Start	Stop	S(IV) ←— μM —→	CH ₂ O	H ₂ O ₂	-/+
07/24	A	02:35	03:35	0	13	19	1.08
07/24	B	03:35	04:10	0	16	4	1.19
07/24	C	06:05	07:05	1	29	11	1.10
07/24	D	07:07	08:10	3	44	5	0.95
07/24	E	08:10	09:05	2	50	4	NA
07/24	A	23:02	00:00	3	16	79	0.75
07/25	B	00:02	01:00	2	13	12	1.00
07/25	C	01:02	02:00	0	15	24	0.95
07/25	D	02:02	03:00	0	9	33	0.77
07/25	E	03:02	04:00	0	13	21	0.78
07/25	F	06:00	07:00	2	21	3	0.54
07/25	G	07:00	08:00	7	21	5	0.38
07/25	H	08:00	08:20	NA	NA	NA	NA
07/26	A	03:35	04:00	6	10	22	NA
07/26	B	04:00	04:45	0	13	12	0.92
07/26	C	04:48	05:30	0	16	12	0.40
07/26	D	05:30	06:17	0	17	6	NA
07/30	A	05:00	05:45	0	NA	21	NA
08/21	A	00:19	01:02	0	NA	22	1.03
08/21	B	01:02	01:35	0	NA	22	1.04
08/21	C	02:10	03:10	0	NA	15	0.93
08/21	D	03:10	04:10	0	NA	11	NA
08/21	F	05:10	06:10	0	NA	10	0.98
08/21	G	06:10	07:10	0	NA	5	0.98
08/21	H	07:10	07:50	NA	NA	NA	NA
09/17	A	00:00	00:45	NA	NA	NA	0.80
09/17	B	03:15	04:00	NA	NA	NA	NA

Table A.4 1985 La Jolla Peak Cloudwater Concentrations
CASC Collector

Date ID	Start	Stop	Vol ml	pH	Na ⁺	NH ₄ ⁺	Ca ²⁺	Mg ²⁺	Cl ⁻	NO ₃ ⁻	SO ₄ ²⁻	SO ₄ ^{2-*} _{xs}
					←————— μN —————→							
07/25 B	00:02	01:00	143	3.22	207	224	51	86	229	427	500	475
07/25C1	01:00	01:30	114	NA	124	223	41	52	153	362	436	421
07/25C2	01:30	02:00	114	3.22	134	233	34	55	160	398	469	453
07/25 D	02:00	03:00	NA	3.26	121	236	36	39	138	327	349	334
07/25E1	03:00	03:30	115	NA	138	260	33	41	144	365	317	300
07/25E2	03:30	04:00	98	2.93	184	390	31	56	167	675	509	487
07/25 F	06:00	07:00	79	2.27	231	888	37	37	NA	NA	NA	
07/25 G	07:00	08:00	119	2.29	117	678	66	67	174	1140	1040	1026
07/25 H	08:00	08:20	19	2.21	151	716	32	45	204	1250	1190	1172
07/26 B	04:00	04:45	381	3.34	73	303	16	17	126	320	332	323
07/26 C	04:48	05:30	355	2.98	52	265	19	18	112	411	356	350
07/26 D	05:30	06:17	301	2.68	46	319	19	17	94	495	329	323
07/30 A	05:00	05:45	34	3.43	870	430	54	661	2200	949	717	611
08/21 A	00:19	01:02	208	3.70	175	134	30	23	168	225	172	
08/21 B	01:02	01:35	89	3.68	133	131	19	19	154	203	168	
08/21 C	02:10	03:10	23	NA	259	282	43	57	293	605	396	
08/21 D	03:10	04:10	103	2.68	488	525	67	113	463	745	894	
08/21 E	04:10	05:10	87	2.48	483	745	107	135	345	2230	1380	1322
08/21 F	05:10	06:10	150	2.63	198	568	53	38	138	1860	833	809
08/21 G	06:10	07:10	167	2.54	218	562	55	43	222	1990	922	895
08/21 H	07:10	07:50	31	2.2	781	NA	158	211	1370	4730	2000	1905
09/03 A	23:00	00:00	50	4.94	2980	795	256	775	909	378	734	373
09/04 B	00:00	01:00	56	4.85	2510	712	212	582	1050	325	653	349
09/04 C	01:00	03:00	49	4.27	764	1070	370	1110	738	732	1020	928
09/17 A	00:00	00:45	71	3.47	843	93	76	392	901	390	290	188
09/17 B	03:15	04:00	27	3.41	1270	260	140	356	1190	992	448	294

Table A.4 1985 La Jolla Peak Cloudwater (continued)
CASC Collector

Date ID	Start	Stop	S(IV)	CH ₂ O	H ₂ O ₂	-/+
			$\longleftrightarrow \mu\text{M} \longrightarrow$			
07/25 B	00:02	01:00	6	NA	36	0.96
07/25C1	01:00	01:30	NA	NA	NA	NA
07/25C2	01:30	02:00	NA	NA	NA	0.95
07/25 D	02:00	03:00	NA	NA	NA	0.81
07/25E1	03:00	03:30	NA	NA	NA	NA
07/25E2	03:30	04:00	NA	NA	NA	0.72
07/25 F	06:00	07:00	NA	NA	5	NA
07/25 G	07:00	08:00	5	NA	3	0.39
07/25 H	08:00	08:20	0	NA	4	0.37
07/26 B	04:00	04:45	0	13	10	0.89
07/26 C	04:48	05:30	0	14	5	0.62
07/26 D	05:30	06:17	4	15	9	0.37
07/30 A	05:00	05:45	0	NA	10	NA
08/21 A	00:19	01:02	0	NA	22	0.99
08/21 B	01:02	01:35	0	NA	21	1.02
08/21 C	02:10	03:10	0	NA	17	NA
08/21 D	03:10	04:10	0	NA	13	0.64
08/21 E	04:10	05:10	0	NA	12	0.82
08/21 F	05:10	06:10	0	NA	11	0.88
08/21 G	06:10	07:10	0	NA	5	0.83
08/21 H	07:10	07:50	0	NA	3	NA
09/03 A	23:00	00:00	NA	NA	NA	NA
09/04 B	00:00	01:00	NA	NA	NA	NA
09/04 C	01:00	03:00	NA	NA	NA	NA
09/17 A	00:00	00:45	NA	NA	NA	0.89
09/17 B	03:15	04:00	NA	NA	NA	1.07

Table A.5 1985 La Jolla Peak Cloudwater (RAC) Loading

Date ID	Start	Stop	LWC	H ⁺	Na ⁺	NH ₄ ⁺	Ca ²⁺	Mg ²⁺	Cl ⁻	NO ₃ ⁻	SO ₄ ²⁻
			g m ⁻³	← neq m ⁻³ →							
07/24 A	02:35	03:35	0.27	119	52	58	16.8	15.5	53.3	138	101
07/24 B	03:35	04:10	0.19	125	38	60	15.9	12.5	41.9	163	103
07/24 C	06:05	07:05	0.08	136	24	64	20.7	8.9	23.2	181	84
07/24 D	07:07	08:10	0.09	253	65	81	17.7	21.7	45.5	240	138
07/24 E	08:10	09:05	0.08	502	>4	66	7.8	11.6	83.6	209	150
07/24 A	23:02	00:00	0.20	85	98	52	15.7	25.5	65.7	98	46
07/25 B	00:02	01:00	0.27	151	127	54	29.1	31.8	84.7	164	147
07/25 C	01:02	02:00	0.30	167	79	58	41.5	21.8	82.7	136	132
07/25 D	02:02	03:00	0.33	174	80	70	13.8	21.1	53.3	122	103
07/25 E	03:02	04:00	0.40	392	134	134	21.3	35.3	93.8	275	193
07/25 F	06:00	07:00	0.10	384	31	73	5.3	9.3	20.4	142	109
07/25 G	07:00	08:00	0.12	537	24	67	3.0	6.7	20.9	119	102
07/25 H	08:00	08:20	0.09	375	NA	58	6.3	8.5	22.3	106	89
07/26 A	03:35	04:00	0.53	187	254	155	6.5	17.9	66.3	192	195
07/26 B	04:00	04:45	0.42	189	52	135	9.3	15.6	52.9	170	153
07/26 C	04:48	05:30	0.46	823	34	131	5.7	10.7	40.3	197	166
07/26 D	05:30	06:17	0.32	632	10	105	3.4	4.1	22.7	166	104
07/30 A	05:00	05:45	0.08	27	>12	26	6.4	68.5	94.1	71	48
08/21 A	00:19	01:02	0.40	65	66	48	9.9	14.6	78.9	80	53
08/21 B	01:02	01:35	0.23	43	33	25	5.0	7.6	41.3	47	31
08/21 C	02:10	03:10	0.26	189	114	62	13.6	30.0	102	177	103
08/21 D	03:10	04:10	0.09	197	83	51	12.0	22.3	15.9	NA	87
08/21 F	05:10	06:10	0.19	293	40	76	9.6	8.7	38.3	276	105
08/21 G	06:10	07:10	0.13	358	67	53	13.0	18.3	37.3	323	141
08/21 H	07:10	07:50	0.01	55	NA	NA	NA	NA	NA	NA	NA
09/17 A	00:00	00:45	0.11	37	161	11	12.9	34.3	110	60	38
09/17 B	03:15	04:00	0.03	NA	50	>1	8.8	16.7	38.7	34	13
N				26	25	26	26	26	26	25	27
Min				27	0.0	0.0	3.0	4.1	15.9	33.6	0.0
Max				823	254	155	41	69	110	323	177
Avg				250	69	68	13	19	55	155	92

Table A.6 1985 La Jolla Peak Cloudwater (CASC) Loading

Date ID	Start	Stop	LWC	H ⁺	Na ⁺	NH ₄ ⁺	Ca ²⁺	Mg ²⁺	Cl ⁻	NO ₃ ⁻	SO ₄ ²⁻
			g m ⁻³	← neq m ⁻³ →							
07/25 B	00:02	01:00	0.14	83	29	31	7.1	11.9	31.6	59	69
07/25C1	01:00	01:30	0.21	NA	26	47	8.7	11.0	32.6	77	93
07/25C2	01:30	02:00	0.21	128	29	50	7.2	11.7	34.1	85	100
07/25 D	02:00	03:00	NA	NA	NA	NA	NA	NA	NA	NA	NA
07/25E1	03:00	03:30	0.22	NA	30	56	7.0	8.9	31.0	78	68
07/25E2	03:30	04:00	0.18	215	34	71	5.7	10.3	30.6	124	93
07/25 F	06:00	07:00	0.07	397	17	66	2.7	2.8	NA	NA	NA
07/25 G	07:00	08:00	0.11	569	13	75	7.4	7.4	19.3	127	115
07/25 H	08:00	08:20	0.05	333	8	39	1.7	2.5	11.0	68	64
07/26 B	04:00	04:45	0.47	217	34	144	7.5	8.2	59.7	152	157
07/26 C	04:48	05:30	0.47	495	25	125	8.8	8.7	53.0	194	168
07/26 D	05:30	06:17	0.36	750	17	115	7.0	6.2	33.7	178	118
07/30 A	05:00	05:45	0.04	16	>37	18	2.3	27.8	92.4	40	30
08/21 A	00:19	01:02	0.27	54	47	36	8.0	6.1	45.5	61	47
08/21 B	01:02	01:35	0.15	32	20	20	2.8	2.9	23.4	31	25
08/21 C	02:10	03:10	0.22	NA	57	62	9.4	12.4	64.4	133	87
08/21 D	03:10	04:10	0.10	201	47	50	6.4	10.8	44.4	72	86
08/21 E	04:10	05:10	0.08	268	39	60	8.6	10.9	27.9	181	112
08/21 F	05:10	06:10	0.14	328	28	80	7.5	5.3	19.3	260	117
08/21 G	06:10	07:10	0.16	450	34	88	8.5	6.7	34.7	310	144
08/21 H	07:10	07:50	0.04	253	34	NA	7.0	9.3	60.3	208	88
09/03 A	23:00	00:00	0.05	1	137	37	11.8	35.7	41.8	17	34
09/04 B	00:00	01:00	0.05	1	131	37	11.0	30.3	54.6	17	34
09/04 C	01:00	03:00	0.02	1	18	25	8.5	25.5	17.0	17	23
09/17 A	00:00	00:45	0.09	30	74	8	6.7	34.5	79.3	34	26
09/17 B	03:15	04:00	0.03	13	42	9	4.6	11.7	39.3	33	15
N				22	25	24	25	25	24	24	24
Min				0.5	0.0	8.2	1.7	2.5	11.0	16.8	14.8
Max				750	137	144	12	36	92	310	168
Avg				220	39	56	7	13	41	106	80

Table A.7 1985 Casitas Pass Cloudwater Concentrations

Date ID	Start	Stop	Vol ml	pH	Na ⁺	NH ₄ ⁺	Ca ²⁺	Mg ²⁺	Cl ⁻	NO ₃ ⁻	SO ₄ ²⁻	SO ₄ ^{2-*} xs
					← μN →				→			
08/07 A	02:55	03:16	16	4.38	200	113	35	51	333	141	100	76
08/07 B	03:30	03:40	8	4.93	480	209	69	131	751	299	195	137
08/08 A	05:02	05:21	19	3.88	46	170	28	19	60	232	118	112
08/08 B	05:40	06:15	33	3.61	90	221	34	29	99	382	131	120
08/08 C	06:15	06:55	40	3.80	66	310	34	23	172	367	142	134
08/08 D	07:07	08:00	34	3.61	110	413	44	32	276	191	84	71
08/08 E	08:00	08:39	10	3.28	400	NA	149	108	628	956	422	374
08/09 A	06:00	07:00	13	3.36	620	847	268	222	411	1540	562	487
08/09 B	07:00	08:00	8	3.31	>1000	NA	362	842	1600	>2800	2150	1736
08/09 C	08:00	09:00	6	3.57	>1000	1450	672	637	155	401	162	0

Date ID	Start	Stop	S(IV)	CH ₂ O	H ₂ O ₂	-/+
			← μM →			
08/07 A	02:55	03:16	NA	NA	NA	1.25
08/07 B	03:30	03:40	NA	NA	NA	1.32
08/08 A	05:02	05:21	0	NA	3	1.01
08/08 B	05:40	06:15	0	NA	7	0.95
08/08 C	06:15	06:55	0	NA	3	1.13
08/08 D	07:07	08:00	0	NA	12	0.64
08/08 E	08:00	08:39	0	NA	17	NA
08/09 A	06:00	07:00	0	NA	8	1.03
08/09 B	07:00	08:00	0	NA	NA	NA
08/09 C	08:00	09:00	NA	NA	NA	NA

Table A.8 1985 Casitas Pass Cloudwater Loading

Date ID	Start	Stop	LWC	H ⁺	Na ⁺	NH ₄ ⁺	Ca ²⁺	Mg ²⁺	Cl ⁻	NO ₃ ⁻	SO ₄ ²⁻
			g m^{-3}	← neq m^{-3} →							
08/07 A	02:55	03:16	0.25	11	50.8	28.7	9.0	12.9	84.6	35.8	25.5
08/07 B	03:30	03:40	0.27	3	128	55.6	18.3	34.8	199.8	79.6	51.8
08/08 A	05:02	05:21	0.32	43	14.9	55.1	9.1	6.2	19.4	75.3	38.2
08/08 B	05:40	06:15	0.31	76	27.8	68.3	10.4	9.0	30.6	118	40.5
08/08 C	06:15	06:55	0.33	53	21.8	103	11.2	7.5	57.2	122	47.3
08/08 D	07:07	08:00	0.21	52	23.5	88.4	9.5	6.9	59.0	40.9	18.1
08/08 E	08:00	08:39	0.09	45	34.0	NA	12.7	9.2	53.4	81.2	35.9
08/09 A	06:00	07:00	0.07	31	44.6	61.0	19.3	16.0	29.6	111	40.4
08/09 B	07:00	08:00	0.04	22	>7.0	NA	15.9	37.0	70.4	>20	94.6
08/09 C	08:00	09:00	0.03	9	>6.0	47.9	22.2	21.0	5.1	13.2	5.3

Table A.9 1986 Laguna Peak Cloudwater Concentrations

Date ID	Start	Stop	Vol ml	pH	Na ⁺	NH ₄ ⁺	Ca ²⁺	Mg ²⁺	Cl ⁻	NO ₃ ⁻	SO ₄ ²⁻	SO ₄ ²⁻ * xs
					$\xleftarrow{\mu\text{N}} \xrightarrow{\hspace{1.5cm}}$							
08/05 A	03:33	04:30	210	3.14	24	195	13	9	74	504	395	392
08/05 B	04:30	05:30	131	3.05	21	238	11	8	75	639	410	407
08/05 C	05:30	06:30	327	3.01	22	273	6	7	75	693	496	493
08/05 D	06:30	07:30	218	3.01	52	300	10	15	82	500	439	433
08/05 E	07:30	08:30	166	2.87	56	460	16	17	92	790	744	737
08/05 F	08:30	09:05	88	2.69	137	599	27	39	169	1090	1110	1093
08/06 A	06:40	07:40	378	3.30	9	143	4	3	46	394	276	275
08/06 B	07:40	08:40	304	3.33	12	170	5	4	50	345	310	309
08/06 C	08:40	09:40	174	3.18	39	315	10	12	94	500	524	519
08/06 D	09:40	10:40	180	2.97	25	305	8	8	79	672	716	713
08/06 E	10:40	11:10	16	2.71	45	502	14	16	92	1250	1340	1335
08/13 A	08:30	09:00	69	3.01	106	425	23	31	200	792	607	594
08/13 B	09:00	09:25	10	2.85	318	686	73	88	350	1410	1010	972
08/14 A	02:30	03:00	186	3.39	20	171	7	8	102	344	279	277
08/14 B	03:00	04:00	423	3.32	25	205	8	9	97	381	280	277
08/14 C	04:00	05:00	346	3.46	23	211	7	10	122	475	342	339
08/14 D	05:05	06:00	265	3.06	72	286	15	24	149	601	442	433
08/14 E	06:00	07:00	227	3.04	128	290	18	32	167	710	528	513
08/14 F	07:00	08:01	185	3.08	85	388	19	27	163	848	665	655
08/14 G	08:05	09:00	113	3.01	151	578	27	40	161	1100	888	870

Date ID	Start	Stop	S(IV)	CH ₂ O	H ₂ O ₂	HFo	HAc	H ⁺	-/+
					$\xleftarrow{\mu\text{M}} \xrightarrow{\hspace{1.5cm}}$				
08/05 A	03:33	04:30	0	15	2	24	14	724	1.01
08/05 B	04:30	05:30	0	18	0	26	16	891	0.95
08/05 C	05:30	06:30	0	18	0	25	15	977	0.98
08/05 D	06:30	07:30	0	18	1	28	17	977	0.75
08/05 E	07:30	08:30	0	17	1	36	19	1349	0.85
08/05 F	08:30	09:05	0	18	1	41	14	2042	0.83
08/06 A	06:40	07:40	0	20	2	40	13	501	1.08
08/06 B	07:40	08:40	0	20	3	48	14	468	1.07
08/06 C	08:40	09:40	0	26	5	58	23	661	1.08
08/06 D	09:40	10:40	0	33	6	63	26	1072	1.03
08/06 E	10:40	11:10	—	—	—	—	—	1950	1.06
08/13 A	08:30	09:00	0	7	2	37	19	977	1.02
08/13 B	09:00	09:25	—	—	—	—	—	1413	1.07
08/14 A	02:30	03:00	—	—	—	—	—	407	1.18
08/14 B	03:00	04:00	—	—	—	—	—	479	1.04
08/14 C	04:00	05:00	—	—	—	32	12	347	1.57
08/14 D	05:05	06:00	0	9	1	27	12	871	0.94
08/14 E	06:00	07:00	0	9	2	34	13	912	1.01
08/14 F	07:00	08:01	0	11	4	48	20	832	1.24
08/14 G	08:05	09:00	0	13	4	103	44	977	1.21

Table A.10 1986 Laguna Peak Cloudwater Loading

Date ID	Start	Stop	LWC	H ⁺	Na ⁺	NH ₄ ⁺	Ca ²⁺	Mg ²⁺	Cl ⁻	NO ₃ ⁻	SO ₄ ²⁻
			g m ⁻³	← neq m ⁻³ →							
08/05 A	03:33	04:30	0.21	149.4	4.8	40.2	2.6	1.8	15.2	104.0	81.5
08/05 B	04:30	05:30	0.12	108.9	2.5	29.1	1.4	1.0	9.1	78.1	50.1
08/05 C	05:30	06:30	0.31	298.2	6.8	83.3	1.9	2.3	22.7	211.5	151.4
08/05 D	06:30	07:30	0.20	198.8	10.6	61.0	2.1	3.0	16.6	101.7	89.3
08/05 E	07:30	08:30	0.15	209.0	8.6	71.3	2.4	2.7	14.3	122.4	115.3
08/05 F	08:30	09:05	0.14	287.5	19.3	84.3	3.8	5.5	23.8	153.5	156.3
08/06 A	06:40	07:40	0.35	176.8	3.1	50.5	1.4	1.0	16.2	139.0	97.4
08/06 B	07:40	08:40	0.28	132.8	3.3	48.2	1.3	1.1	14.2	97.9	88.0
08/06 C	08:40	09:40	0.16	107.3	6.3	51.2	1.7	1.9	15.3	81.2	85.1
08/06 D	09:40	10:40	0.17	180.1	4.2	51.2	1.4	1.3	13.3	112.9	120.3
08/06 E	10:40	11:10	0.03	58.2	1.3	15.0	0.4	0.5	2.7	37.3	40.0
08/13 A	08:30	09:00	0.13	125.8	13.7	54.7	2.9	4.0	25.8	102.0	78.2
08/13 B	09:00	09:25	0.02	31.7	7.1	15.4	1.6	2.0	7.8	31.6	22.6
08/14 A	02:30	03:00	0.35	141.3	7.0	59.4	2.5	2.7	35.4	119.4	96.9
08/14 B	03:00	04:00	0.39	189.1	9.9	80.9	3.1	3.5	38.1	150.4	110.5
08/14 C	04:00	05:00	0.32	112.1	7.4	68.1	2.2	3.3	39.4	153.4	110.4
08/14 D	05:05	06:00	0.27	235.0	19.3	77.2	4.0	6.5	40.2	162.2	119.3
08/14 E	06:00	07:00	0.21	193.2	27.1	61.4	3.8	6.8	35.4	150.4	111.9
08/14 F	07:00	08:01	0.17	141.3	14.5	65.9	3.2	4.6	27.7	144.0	112.9
08/14 G	08:05	09:00	0.12	112.4	17.4	66.5	3.1	4.6	18.5	126.6	102.2
N			20	20	20	20	20	20	20	20	20
Min			0.02	31.7	1.3	15.0	0.4	0.5	2.7	31.6	22.6
Max			0.39	298	27.1	84.3	4.0	6.8	40	212	156
Avg			0.21	159	9.7	57	2.3	3.0	21.6	119	97

Table A.10 1986 Laguna Peak Cloudwater Loading (continued)

Date ID	Start	Stop	S(IV)	CH ₂ O	H ₂ O ₂	HFo	HAc
				← nmole m ⁻³ →			
08/05 A	03:33	04:30	0	3.05	0.37	4.93	2.97
08/05 B	04:30	05:30	0	2.21	0.00	3.18	1.93
08/05 C	05:30	06:30	0	5.59	0.13	7.54	4.61
08/05 D	06:30	07:30	0	3.64	0.22	5.60	3.50
08/05 E	07:30	08:30	0	2.63	0.08	5.57	2.94
08/05 F	08:30	09:05	0	2.51	0.15	5.78	2.03
08/06 A	06:40	07:40	0	7.02	0.53	14.20	4.62
08/06 B	07:40	08:40	0	5.79	0.82	13.53	4.09
08/06 C	08:40	09:40	0	4.25	0.80	9.35	3.72
08/06 D	09:40	10:40	0	5.46	0.97	10.57	4.38
08/06 E	10:40	11:10	0	0.00	0.00	0.00	0.00
08/13 A	08:30	09:00	0	0.93	0.22	4.80	2.43
08/13 B	09:00	09:25	0	NA	NA	NA	NA
08/14 A	02:30	03:00	0	NA	NA	NA	NA
08/14 B	03:00	04:00	0	NA	NA	NA	NA
08/14 C	04:00	05:00	0	NA	NA	10.4	3.7
08/14 D	05:05	06:00	0	2.43	0.23	7.4	3.3
08/14 E	06:00	07:00	0	1.86	0.44	7.2	2.8
08/14 F	07:00	08:01	0	1.85	0.66	8.2	3.4
08/14 G	08:05	09:00	0	1.53	0.51	11.8	5.1
N			20	20	20	20	20
Min			0	0	0	0	0
Max			0	7.02	0.97	14.2	5.09
Avg	0	2.54	0.31	6.5	2.78		

Table A.11 1986 Laguna Road Cloudwater Concentrations

Date ID	Start	Stop	Vol	pH	Na ⁺	NH ₄ ⁺	Ca ²⁺	Mg ²⁺	Cl ⁻	NO ₃ ⁻	SO ₄ ²⁻	SO ₄ ^{2-*} _{xs}
	ml				← μN →							
07/30 A	23:45	00:00	43	3.41	456	1350	152	109	296	1110	806	751
07/31 B	00:30	01:30	125	3.49	304	1150	79	83	258	891	596	559
07/31 C	01:30	02:30	190	3.44	151	722	33	42	160	651	425	407
07/31 D	02:30	03:30	159	3.41	232	760	47	67	224	754	457	429
07/31 E	03:30	04:30	136	3.34	453	982	68	98	368	1050	604	549
07/31 F	04:30	05:10	68	3.36	266	821	47	73	264	867	498	466
08/04 A	23:00	00:00	88	2.95	957	512	132	217	758	978	1030	914
08/05 B	00:00	01:00	101	2.87	655	468	80	137	548	1000	1140	1061
08/05 C	01:00	02:00	43	2.77	1010	1390	142	239	684	1690	2040	1918
08/05 D	02:00	02:55	44	2.58	1070	1780	162	247	711	2140	2630	2501
08/05 A	23:45	00:45	204	3.13	365	816	36	88	404	612	996	952
08/06 B	00:45	01:45	194	3.09	212	639	21	52	247	674	842	816
08/06 C	01:45	02:45	125	3.09	119	709	21	28	124	722	846	832
08/06 D	02:45	03:45	77	2.94	171	1070	34	42	147	1110	1310	1289
08/06 E	03:45	04:45	70	2.60	170	1110	34	41	164	1300	1510	1489
08/06 F	04:45	05:45	60	2.84	119	974	24	29	102	1160	1110	1096
08/13 A	05:21	06:10	92	3.01	157	456	29	44	225	790	776	757
08/13 B	23:20	00:00	81	3.01	157	445	50	51	232	854	670	651
08/14 B	00:00	01:00	137	2.90	144	476	45	48	264	1020	793	776
08/14 C	01:00	01:55	87	2.91	180	504	59	61	312	1280	925	903

Date ID	Start	Stop	S(IV)	CH ₂ O	H ₂ O ₂	HFO	HAc	H ⁺	-/+
			← μM →						
07/30 A	23:45	00:00	0	11	18	—	—	389	1.12
07/31 B	00:30	01:30	0	13	17	41	21	324	1.12
07/31 C	01:30	02:30	0	15	19	21	9	363	1.07
07/31 D	02:30	03:30	0	13	20	33	29	389	1.05
07/31 E	03:30	04:30	0	15	21	36	13	457	1.03
07/31 F	04:30	05:10	—	—	—	—	—	437	1.02
08/04 A	23:00	00:00	1	6	7	29	11	1122	1.08
08/05 B	00:00	01:00	0	6	4	34	13	1349	1.01
08/05 C	01:00	02:00	4	12	2	56	NA	1698	1.03
08/05 D	02:00	02:55	5	12	2	74	34	2630	1.09
08/05 A	23:45	00:45	12	11	0	24	7	741	1.02
08/06 B	00:45	01:45	6	9	0	30	13	813	0.99
08/06 C	01:45	02:45	3	7	1	34	8	813	1.01
08/06 D	02:45	03:45	2	11	2	47	10	1148	0.97
08/06 E	03:45	04:45	1	12	2	52	14	2512	1.31
08/06 F	04:45	05:45	0	15	4	51	16	1445	1.10
08/13 A	05:21	06:10	0	4	1	26	11	977	0.93
08/13 A	23:20	00:00	0	12	1	42	15	977	0.96
08/14 B	00:00	01:00	0	12	0	NA	NA	1259	0.95
08/14 C	01:00	01:55				44	14	1230	0.81

Table A.12 1986 Laguna Road Cloudwater Loading

Date ID	Start	Stop	LWC	H ⁺	Na ⁺	NH ₄ ⁺	Ca ²⁺	Mg ²⁺	Cl ⁻	NO ₃ ⁻	SO ₄ ²⁻
			g m ⁻³	← neq m ⁻³ →							
07/30 A	23:45	00:00	0.16	62.4	73.2	216.7	24.4	17.5	47.5	178.2	129.4
07/31 B	00:30	01:30	0.12	37.8	35.5	134.2	9.2	9.7	30.1	104.0	69.5
07/31 C	01:30	02:30	0.18	64.4	26.8	129.9	5.8	7.4	28.4	115.4	75.4
07/31 D	02:30	03:30	0.15	57.7	34.4	112.8	7.0	9.9	33.2	111.9	67.8
07/31 E	03:30	04:30	0.13	58.0	57.5	124.6	8.6	12.5	46.7	133.3	76.7
07/31 F	04:30	05:10	0.10	41.6	25.3	78.2	4.5	6.9	25.1	82.5	47.4
08/04 A	23:00	00:00	0.08	92.2	78.6	42.1	10.8	17.8	62.3	80.3	84.6
08/05 B	00:00	01:00	0.09	127.2	61.7	44.1	7.5	12.9	51.7	94.3	107.5
08/05 C	01:00	02:00	0.04	68.1	40.5	55.8	5.7	9.6	27.5	67.8	81.9
08/05 D	02:00	02:55	0.04	117.8	47.9	79.7	7.3	11.1	31.9	95.9	117.8
08/05 A	23:45	00:45	0.19	141.1	69.5	155.4	6.8	16.7	76.9	116.5	189.6
08/06 B	00:45	01:45	0.18	147.2	38.4	115.7	3.7	9.5	44.7	122.0	152.5
08/06 C	01:45	02:45	0.12	94.9	13.9	82.7	2.4	3.3	14.5	84.2	98.7
08/06 D	02:45	03:45	0.07	82.5	12.3	76.9	2.5	3.0	10.6	79.8	94.1
08/06 E	03:45	04:45	0.07	164.1	11.1	72.5	2.2	2.7	10.7	84.9	98.7
08/06 F	04:45	05:45	0.06	80.9	6.7	54.5	1.3	1.6	5.7	65.0	62.2
08/13 A	05:21	06:10	0.11	102.7	16.5	47.9	3.1	4.6	23.7	83.1	81.6
08/13 A	23:20	00:00	0.11	110.8	17.8	50.5	5.7	5.8	26.3	96.8	76.0
08/14 B	00:00	01:00	0.13	161.0	18.4	60.9	5.7	6.2	33.8	130.4	101.4
08/14 C	01:00	01:55	0.09	109.0	15.9	44.6	5.2	5.4	27.6	113.4	81.9
Min			0.04	38	6.7	42.1	1.3	1.6	5.7	65.0	47.4
Max			0.19	164	78.6	217	24.4	17.8	77	178	190
Avg			0.11	96.1	35.1	88.9	6.5	8.7	32.9	102	95

Date ID	Start	Stop	S(IV)	CH ₂ O	H ₂ O ₂	HFo	HAc
			← neq m ⁻³ →				
07/30 A	23:45	00:00	0.00	1.73	2.89	0.00	0.00
07/31 B	00:30	01:30	0.00	1.47	2.01	4.83	2.45
07/31 C	01:30	02:30	0.00	2.62	3.44	3.79	1.65
07/31 D	02:30	03:30	0.00	1.88	2.89	4.84	4.27
07/31 E	03:30	04:30	0.00	1.95	2.64	4.59	1.70
07/31 F	04:30	05:10	0.00	0.00	0.00	0.00	0.00
08/04 A	23:00	00:00	0.09	0.48	0.53	2.40	0.92
08/05 B	00:00	01:00	0.00	0.60	0.33	3.17	1.19
08/05 C	01:00	02:00	0.15	0.48	0.10	2.25	0.00
08/05 D	02:00	02:55	0.23	0.55	0.09	3.31	1.52
08/05 A	23:45	00:45	2.25	2.13	0.00	4.58	1.39
08/06 B	00:45	01:45	1.16	1.67	0.07	5.50	2.28
08/06 C	01:45	02:45	0.32	0.83	0.13	3.98	0.89
08/06 D	02:45	03:45	0.11	0.79	0.11	3.36	0.73
08/06 E	03:45	04:45	0.07	0.81	0.12	3.39	0.91
08/06 F	04:45	05:45	0.00	0.81	0.24	2.83	0.90
08/13 A	05:21	06:10	0.00	0.43	0.09	2.75	1.20
08/13 A	23:20	00:00	0	1.39	0.07	4.82	1.70
08/14 B	00:00	01:00	0	1.47	0.06	0	0
08/14 C	01:00	01:55	NA	NA	NA	3.85	1.24

Table A.13 Ventura Hill Cloudwater Concentrations

Date ID	Start	Stop	Vol ml	pH	Na ⁺	NH ₄ ⁺	Ca ²⁺	Mg ²⁺	Cl ⁻	NO ₃ ⁻	SO ₄ ²⁻	SO ₄ ^{2-*} _{xs}
					← μN →							
07/30 A	06:30	07:30	188	4.92	171	539	65	43	150	247	267	246
07/30 B	07:30	08:15	107	4.24	189	520	57	47	203	284	325	302
08/01 A	00:20	01:20	97	3.13	2240	405	199	519	2180	1290	998	727
08/01 B	01:20	02:20	115	3.17	1030	416	91	225	896	898	676	551
08/01 C	02:20	03:20	122	3.16	1050	514	90	232	914	902	707	580
08/01 D	03:20	04:20	147	3.21	907	426	69	193	806	739	620	510
08/01 E	04:20	05:20	108	3.33	548	533	48	116	482	673	554	488
08/01 F	05:20	06:20	87	3.34	765	811	79	169	659	814	668	575
08/01 G	06:45	07:45	75	3.44	1160	966	198	267	1110	1030	870	730
08/01 H	07:45	08:45	76	3.43	611	960	217	147	642	948	855	781
08/05 A	02:45	03:45	100	3.11	349	931	62	47	435	952	976	934
08/05 B	03:45	04:45	106	3.07	295	1240	45	71	392	1040	998	962
08/05 C	04:45	05:45	107	3.11	121	1320	24	29	175	1070	1010	995
08/05 D	05:45	06:45	80	3.06	78	1400	26	23	146	1200	1010	1001
08/06 A	01:55	03:00	177	3.03	183	598	32	48	198	1080	630	608
08/06 B	03:00	04:00	158	3.06	196	734	25	48	222	985	700	676
08/06 C	04:00	05:00	182	2.96	139	712	18	32	176	1140	787	770
08/06 D	05:00	06:00	169	2.91	124	896	18	30	157	1370	897	882
08/06 E	06:00	07:00	164	2.92	78	913	25	24	112	1300	842	833
08/06 F	07:00	08:00	118	2.85	203	1190	157	69	250	1740	1170	1145
08/13 A	03:45	05:00	34	2.85	3880	1800	771	1010	3330	3730	2170	1701
08/13 B	05:00	06:30	33	2.75	5720	2990	1400	1450	4290	6480	3220	2528
08/13 A	22:45	00:00	51	2.74	1060	1160	297	254	989	2100	1530	1402
08/14 B	00:00	01:00	55	2.75	823	1030	281	199	757	2240	1400	1300
08/14 C	01:00	02:00	94	2.84	429	964	100	94	451	1620	973	921
08/14 D	02:00	03:00	81	2.89	440	814	87	95	415	1560	967	914
08/14 E	03:00	04:00	110	2.89	194	778	49	54	259	1420	839	816
08/14 F	04:00	05:00	130	2.91	248	798	51	65	304	1480	804	774
08/14 G	05:00	06:00	143	2.95	228	952	50	62	282	1410	762	734
08/14 H	06:00	07:00	150	2.98	135	698	31	38	204	1220	594	578
08/14 I	07:00	08:00	126	3.03	74	946	61	29	104	708	387	378
08/14 J	08:00	08:50	50	2.84	175	1730	209	69	208	2100	1130	1109

Table A.13 Ventura Hill Cloudwater Concentration (continued)

Date ID	Start	Stop	S(IV)	CH ₂ O	H ₂ O ₂	HFo	HAc	H ⁺	-/+
←-----μM-----→									
07/30 A	06:30	07:30	0	13	2	—	—	12	0.80
07/30 B	07:30	08:15	0	18	0	—	—	58	0.92
08/01 A	00:20	01:20	0	8	6	40	6	741	1.07
08/01 B	01:20	02:20	0	6	6	31	3	676	1.00
08/01 C	02:20	03:20	0	7	5	15	?—	692	0.97
08/01 D	03:20	04:20	0	5	6	35	16	617	0.97
08/01 E	04:20	05:20	0	10	11	33	14	468	0.99
08/01 F	05:20	06:20	0	7	11	52	30	457	0.93
08/01 G	06:45	07:45	0	7	8	54	16	363	1.01
08/01 H	07:45	08:45	0	8	0	—	—	372	1.05
08/05 A	02:45	03:45	0	6	5	—	—	776	1.08
08/05 B	03:45	04:45	0	9	5	—	—	851	0.96
08/05 C	04:45	05:45	0	11	6	—	—	776	0.99
08/05 D	05:45	06:45	0	13	6	—	—	871	0.98
08/06 A	01:55	03:00	0	19	29	—	—	933	1.06
08/06 B	03:00	04:00	0	17	19	—	—	871	1.01
08/06 C	04:00	05:00	0	12	0	—	—	1096	1.05
08/06 D	05:00	06:00	0	12	0	—	—	1230	1.05
08/06 E	06:00	07:00	0	15	0	—	—	1202	1.00
08/06 F	07:00	08:00	0	12	—	—	—	1413	1.04
08/13 A	03:45	05:00	—	—	—	—	—	1413	1.03
08/13 B	05:00	06:30	—	—	—	—	—	1778	1.03
08/13 A	22:45	00:00	0	27	17	92	28	1820	1.00
08/14 B	00:00	01:00	0	18	22	85	30	1778	1.06
08/14 C	01:00	02:00	0	19	22	74	173	1445	1.00
08/14 D	02:00	03:00	0	15	23	69	34	1288	1.07
08/14 E	03:00	04:00	0	21	24	64	24	1288	1.06
08/14 F	04:00	05:00	0	23	20	61	23	1230	1.08
08/14 G	05:00	06:00	0	11	18	64	23	1122	1.01
08/14 H	06:00	07:00	0	18	15	54	33	1047	1.03
08/14 I	07:00	08:00	0	14	12	60	27	933	0.58
08/14 J	08:00	08:50	0	23	10	96	45	1445	0.94

Table A.14 1986 Ventura Hill Cloudwater Loading

Date ID	Start	Stop	LWC	H ⁺	Na ⁺	NH ₄ ⁺	Ca ²⁺	Mg ²⁺	Cl ⁻	NO ₃ ⁻	SO ₄ ²⁻
			g m ⁻³	← neq m ⁻³ →							
07/30 A	06:30	07:30	0.18	2.1	29.9	94.3	11.4	7.6	26.3	43.2	46.7
07/30 B	07:30	08:15	0.13	7.7	25.1	69.2	7.6	6.3	27.0	37.8	43.2
08/01 A	00:20	01:20	0.09	67.4	203.8	36.9	18.1	47.2	198.4	117.4	90.8
08/01 B	01:20	02:20	0.11	72.3	110.2	44.5	9.8	24.1	95.9	96.1	72.3
08/01 C	02:20	03:20	0.11	78.9	119.7	58.6	10.3	26.4	104.2	102.8	80.6
08/01 D	03:20	04:20	0.14	84.5	124.3	58.4	9.5	26.4	110.4	101.2	84.9
08/01 E	04:20	05:20	0.10	47.3	55.3	53.8	4.9	11.7	48.7	68.0	56.0
08/01 F	05:20	06:20	0.08	37.0	62.0	65.7	6.4	13.7	53.4	65.9	54.1
08/01 G	06:45	07:45	0.07	25.4	81.2	67.6	13.9	18.7	77.7	72.1	60.9
08/01 H	07:45	08:45	0.07	26.4	43.4	68.2	15.4	10.4	45.6	67.3	60.7
08/05 A	02:45	03:45	0.09	72.2	32.5	86.6	5.8	4.3	40.5	88.5	90.8
08/05 B	03:45	04:45	0.10	84.2	29.2	122.8	4.4	7.0	38.8	103.0	98.8
08/05 C	04:45	05:45	0.10	77.6	12.1	132.0	2.4	2.9	17.5	107.0	101.0
08/05 D	05:45	06:45	0.08	65.3	5.8	105.0	2.0	1.7	11.0	90.0	75.8
08/06 A	01:55	03:00	0.15	141.8	27.8	90.9	4.9	7.2	30.1	164.2	95.8
08/06 B	03:00	04:00	0.15	128.0	28.8	107.9	3.7	7.1	32.6	144.8	102.9
08/06 C	04:00	05:00	0.17	186.3	23.6	121.0	3.0	5.5	29.9	193.8	133.8
08/06 D	05:00	06:00	0.16	194.3	19.6	141.6	2.9	4.7	24.8	216.5	141.7
08/06 E	06:00	07:00	0.15	183.9	11.9	139.7	3.8	3.7	17.1	198.9	128.8
08/06 F	07:00	08:00	0.11	155.4	22.3	130.9	17.3	7.6	27.5	191.4	128.7
08/13 A	03:45	05:00	0.03	35.3	97.0	45.0	19.3	25.3	83.3	93.3	54.3
08/13 B	05:00	06:30	0.02	37.3	120.1	62.8	29.4	30.5	90.1	136.1	67.6
08/13 A	22:45	00:00	0.04	69.2	40.3	44.1	11.3	9.7	37.6	79.8	58.1
08/14 B	00:00	01:00	0.05	90.7	42.0	52.5	14.3	10.1	38.6	114.2	71.4
08/14 C	01:00	02:00	0.09	127.2	37.8	84.8	8.8	8.2	39.7	142.6	85.6
08/14 D	02:00	03:00	0.08	97.9	33.4	61.9	6.6	7.2	31.5	118.6	73.5
08/14 E	03:00	04:00	0.10	132.7	20.0	80.1	5.1	5.6	26.7	146.3	86.4
08/14 F	04:00	05:00	0.12	148.8	30.0	96.6	6.2	7.8	36.8	179.1	97.3
08/14 G	05:00	06:00	0.13	149.2	30.3	126.6	6.7	8.3	37.5	187.5	101.3
08/14 H	06:00	07:00	0.14	146.6	18.9	97.7	4.4	5.3	28.6	170.8	83.2
08/14 I	07:00	08:00	0.12	110.1	8.8	111.6	7.1	3.4	12.3	83.5	45.7
08/14 J	08:00	08:50	0.06	80.9	9.8	96.9	11.7	3.9	11.6	117.6	63.3
N			32	32	32	32	32	32	32	32	32
Min			0.02	2.1	5.8	36.9	2.0	1.7	11.0	37.8	43.2
Max			0.18	194	204	142	29.4	47.2	198	216	142
Avg			0.10	92.6	48.7	86.1	9.0	11.6	47.9	120	82.4

Table A.14 Ventura Hill Cloudwater Loadings (continued)

Date ID	Start	Stop	S(IV)	CH ₂ O	H ₂ O ₂	HFo	HAc
← nmole m ⁻³ →							
07/30 A	06:30	07:30	0.0	2.3	0.3	NA	NA
07/30 B	07:30	08:15	0.0	2.4	0.0	NA	NA
08/01 A	00:20	01:20	0.0	0.7	0.6	3.7	0.6
08/01 B	01:20	02:20	0.0	0.7	0.6	3.3	0.4
08/01 C	02:20	03:20	0.0	0.8	0.5	NA	1.7
08/01 D	03:20	04:20	0.0	0.7	0.8	4.7	2.2
08/01 E	04:20	05:20	0.0	1.0	1.1	3.3	1.4
08/01 F	05:20	06:20	0.0	0.6	0.9	4.2	2.4
08/01 G	06:45	07:45	0.0	0.5	0.6	3.8	1.1
08/01 H	07:45	08:45	0.0	0.5	0.0	0.0	0.0
08/05 A	02:45	03:45	0.0	0.6	0.5	NA	NA
08/05 B	03:45	04:45	0.0	0.9	0.5	NA	NA
08/05 C	04:45	05:45	0.0	1.1	0.6	NA	NA
08/05 D	05:45	06:45	0.0	1.0	0.4	NA	NA
08/06 A	01:55	03:00	0.0	2.9	4.4	NA	NA
08/06 B	03:00	04:00	0.0	2.4	2.8	NA	NA
08/06 C	04:00	05:00	0.0	2.0	0.1	NA	NA
08/06 D	05:00	06:00	0.0	1.9	0.0	NA	NA
08/06 E	06:00	07:00	0.0	2.3	0.1	NA	NA
08/06 F	07:00	08:00	0.0	1.3	0.0	NA	NA
08/13 A	03:45	05:00	0.0	0.0	0.0	NA	NA
08/13 B	05:00	06:30	0.0	0.0	0.0	NA	NA
08/13 A	22:45	00:00	0.0	1.0	0.6	3.5	1.1
08/14 B	00:00	01:00	0.0	0.9	1.1	4.3	1.5
08/14 C	01:00	02:00	0.0	1.7	1.9	6.5	15.2
08/14 D	02:00	03:00	0.0	1.2	1.7	5.3	2.6
08/14 E	03:00	04:00	0.0	2.2	2.4	6.5	2.5
08/14 F	04:00	05:00	0.0	2.8	2.5	7.4	2.7
08/14 G	05:00	06:00	0.0	1.5	2.4	8.5	3.1
08/14 H	06:00	07:00	0.0	2.6	2.1	7.5	4.6
08/14 I	07:00	08:00	0.0	1.6	1.4	7.0	3.2
08/14 J	08:00	08:50	0.0	1.3	0.5	5.4	2.5
N			30	30	29	16	17
Min			0	0.5	0	3.3	0.4
Max			0	2.9	4.4	8.5	15.2
Avg			0	1.4	1.1	5.3	2.9

Table A.15 1986 Casitas Pass Cloudwater Concentrations

Date ID	Start	Stop	Vol ml	pH	Na ⁺	NH ₄ ⁺	Ca ²⁺	Mg ²⁺	Cl ⁻	NO ₃ ⁻	SO ₄ ²⁻	SO ₄ ²⁻ *
					← μ N →				→			
07/31 A	06:30	07:30	303	3.87	18	149	10	7	35	147	108	106
07/31 B	07:30	08:30	130	4.06	16	283	18	9	38	171	138	136
08/01 A	02:45	03:45	199	4.07	82	330	18	23	73	229	211	201
08/01 B	03:45	05:00	212	4.26	48	358	9	14	40	196	177	171
08/05 A	02:20	03:00	76	3.33	176	869	49	50	110	892	521	500
08/05 B	03:00	04:00	146	3.62	49	718	16	17	76	570	404	398
08/05 C	04:00	05:00	138	3.92	29	736	16	11	60	458	320	316
08/05 D	05:00	06:00	157	3.96	19	612	12	8	50	402	280	278
08/05 E	06:00	07:00	52	3.76	43	1090	27	17	68	729	523	518
08/06 A	01:25	02:00	68	4.02	83	636	25	27	51	386	369	359
08/06 B	02:00	03:00	152	4.32	62	748	19	19	41	394	387	380
08/06 C	03:00	04:00	99	4.52	42	930	16	14	45	474	419	414
08/06 D	04:00	05:00	272	3.92	21	418	9	7	29	283	225	222
08/06 E	05:00	06:20	258	3.85	17	429	9	6	57	310	230	228
08/06 F	06:20	07:00	167	3.91	14	448	8	6	48	326	224	222
08/06 G	07:00	07:46	135	4.07	16	502	11	7	42	314	197	195
08/13 A	03:21	04:00	73	4.21	137	552	48	40	110	317	359	342
08/13 B	04:00	04:20	29	4.42	57	669	26	21	51	290	401	394
08/13 C	04:40	06:05	356	4.06	23	354	12	9	34	209	195	192
08/13 D	06:05	06:55	105	4.07	23	508	11	9	34	278	268	265
08/13 E	07:15	08:00	108	4.32	26	575	32	14	44	326	297	294
08/13 F	08:00	08:40	58	4.34	47	721	48	22	67	369	314	308
08/13 A	23:45	00:00	26	4.11	146	618	170	49	164	417	496	478
08/14 B	00:00	01:00	107	3.84	132	1130	80	52	141	649	769	753
08/14 C	01:00	02:00	103	3.70	50	840	39	24	65	508	536	530
08/14 D	02:00	04:00	346	4.01	19	684	14	9	22	381	347	345
08/14 E	04:00	05:00	133	3.80	14	579	15	9	33	409	289	287
08/14 F	05:00	06:00	164	3.90	16	616	13	8	37	437	280	278
08/14 G	06:00	07:00	187	3.87	12	460	13	7	33	357	204	203
08/14 H	07:00	08:00	101	3.66	23	757	37	18	33	594	339	336
08/14 I	08:00	09:00	122	3.65	19	612	43	18	68	551	318	316
08/14 J	09:00	09:15	23	3.47	18	688	47	20	65	624	367	365

Table A.15 1986 Casitas Pass Cloudwater Concentrations (continued)

Date	ID	Start	Stop	S(IV)	CH ₂ O	H ₂ O ₂	HFo	HAc	H ⁺	-/+
				← μM →						
07/31	A	06:30	07:30	0	6	4	NA	NA	135	0.91
07/31	B	07:30	08:30	0	7	5	24	9	87	0.83
08/01	A	02:45	03:45	0	5	3	17	8	85	0.94
08/01	B	03:45	05:00	0	5	3	20	10	55	0.85
08/05	A	02:20	03:00	0	11	16	57	14	468	0.94
08/05	B	03:00	04:00	0	8	10	23	14	240	1.01
08/05	C	04:00	05:00	0	8	7	18	7	120	0.91
08/05	D	05:00	06:00	0	8	6	16	8	110	0.96
08/05	E	06:00	07:00	0	8	6	27	11	174	0.97
08/06	A	01:25	02:00	0	9	7	21	10	96	0.93
08/06	B	02:00	03:00	0	8	6	25	9	48	0.91
08/06	C	03:00	04:00	0	9	4	32	14	30	0.91
08/06	D	04:00	05:00	0	8	5	17	10	120	0.93
08/06	E	05:00	06:20	0	9	5	21	9	141	0.99
08/06	F	06:20	07:00	0	8	6	16	9	123	0.99
08/06	G	07:00	07:46	0	8	6	21	10	85	0.89
08/13	A	03:21	04:00	0	3	3	29	8	62	0.91
08/13	B	04:00	04:20	0	4	3	31	9	38	0.91
08/13	C	04:40	06:05	0	4	6	19	6	87	0.90
08/13	D	06:05	06:55	0	5	5	25	7	85	0.91
08/13	E	07:15	08:00	0	NA	6	NA	NA	48	0.95
08/13	F	08:00	08:40	0	NA	8	NA	NA	46	0.83
08/13	A	23:45	00:00	0	9	NA	44	15	78	0.98
08/14	B	00:00	01:00	0	13	NA	58	4	145	1.01
08/14	C	01:00	02:00	0	10	NA	36	14	200	0.96
08/14	D	02:00	04:00	0	7	NA	23	11	98	0.91
08/14	E	04:00	05:00	0	8	NA	26	10	158	0.94
08/14	F	05:00	06:00	0	9	NA	27	10	126	0.96
08/14	G	06:00	07:00	0	10	NA	NA	NA	135	0.94
08/14	H	07:00	08:00	0	9	NA	NA	NA	219	0.91
08/14	I	08:00	09:00	0	11	NA	NA	NA	224	1.02
08/14	J	09:00	09:15	0	12	NA	NA	NA	339	0.95

Table A.16 1986 Casitas Pass Cloudwater Loading

Date ID	Start	Stop	LWC	H ⁺	Na ⁺	NH ₄ ⁺	Ca ²⁺	Mg ²⁺	Cl ⁻	NO ₃ ⁻	SO ₄ ²⁻
			g m ⁻³	← neq m ⁻³ →							
07/31 A	06:30	07:30	0.28	38.2	5.2	42.2	2.7	2.0	9.8	41.6	30.6
07/31 B	07:30	08:30	0.12	10.5	1.9	34.2	2.1	1.1	4.6	20.7	16.7
08/01 A	02:45	03:45	0.19	15.8	15.3	61.4	3.4	4.4	13.6	42.6	39.2
08/01 B	03:45	05:00	0.16	8.7	7.6	56.6	1.4	2.2	6.3	31.0	28.0
08/05 A	02:20	03:00	0.11	49.6	18.7	92.1	5.2	5.3	11.7	94.6	55.2
08/05 B	03:00	04:00	0.14	32.6	6.7	97.6	2.2	2.3	10.3	77.5	54.9
08/05 C	04:00	05:00	0.13	15.5	3.8	94.9	2.1	1.4	7.7	59.1	41.3
08/05 D	05:00	06:00	0.15	16.1	2.8	90.0	1.8	1.1	7.4	59.1	41.2
08/05 E	06:00	07:00	0.05	8.5	2.1	53.4	1.3	0.8	3.3	35.7	25.6
08/06 A	01:25	02:00	0.11	10.4	9.1	69.3	2.7	2.9	5.5	42.1	40.2
08/06 B	02:00	03:00	0.14	6.8	8.8	106.2	2.7	2.7	5.8	55.9	55.0
08/06 C	03:00	04:00	0.09	2.8	3.9	85.6	1.5	1.3	4.2	43.6	38.5
08/06 D	04:00	05:00	0.25	30.5	5.3	106.2	2.3	1.8	7.4	71.9	57.2
08/06 E	05:00	06:20	0.18	25.6	3.1	77.6	1.5	1.1	10.3	56.1	41.6
08/06 F	06:20	07:00	0.23	28.8	3.3	104.8	1.9	1.3	11.2	76.3	52.4
08/06 G	07:00	07:46	0.16	14.0	2.5	82.3	1.8	1.1	6.9	51.5	32.3
08/13 A	03:21	04:00	0.11	6.5	14.4	58.0	5.1	4.2	11.5	33.3	37.7
08/13 B	04:00	04:20	0.08	3.1	4.6	54.2	2.1	1.7	4.1	23.5	32.5
08/13 C	04:40	06:05	0.24	20.5	5.5	83.2	2.8	2.1	8.0	49.1	45.8
08/13 D	06:05	06:55	0.12	10.0	2.7	59.9	1.3	1.1	4.0	32.8	31.6
08/13 E	07:15	08:00	0.13	6.4	3.4	77.1	4.3	1.9	5.9	43.7	39.8
08/13 F	08:00	08:40	0.08	3.7	3.8	58.4	3.9	1.7	5.5	29.9	25.4
08/13 A	23:45	00:00	0.10	7.5	14.2	59.9	16.5	4.8	15.9	40.4	48.1
08/14 B	00:00	01:00	0.10	14.5	13.2	113.0	8.0	5.2	14.1	64.9	76.9
08/14 C	01:00	02:00	0.10	19.2	4.8	80.6	3.7	2.3	6.2	48.8	51.5
08/14 D	02:00	04:00	0.16	15.7	3.1	110.1	2.3	1.4	3.6	61.3	55.9
08/14 E	04:00	05:00	0.12	19.7	1.7	71.8	1.8	1.1	4.1	50.7	35.8
08/14 F	05:00	06:00	0.15	19.3	2.4	94.2	2.1	1.2	5.6	66.9	42.8
08/14 G	06:00	07:00	0.18	23.6	2.1	80.5	2.3	1.2	5.8	62.5	35.7
08/14 H	07:00	08:00	0.09	20.6	2.2	71.2	3.5	1.7	3.1	55.8	31.9
08/14 I	08:00	09:00	0.11	25.5	2.1	69.8	4.9	2.1	7.8	62.8	36.3
08/14 J	09:00	09:15	0.09	29.1	1.5	59.2	4.1	1.7	5.6	53.7	31.6
N			32	32	32	32	32	32	32	32	32
Min.			0.05	2.8	1.5	34.2	1.3	0.8	3.1	20.7	16.7
Max.			0.28	49.6	18.7	113.0	16.5	5.3	15.9	94.6	76.9
Avg.			0.14	17.5	5.7	76.7	3.3	2.1	7.4	51.2	40.9

Table A.16 1986 Casitas Pass Cloudwater Loading (continued)

Date ID	Start	Stop	S(IV)	CH ₂ O	H ₂ O ₂	HFo	HAc
				← nmole m ⁻³ →			
07/31 A	06:30	07:30	0.00	1.75	0.99	NA	NA
07/31 B	07:30	08:30	0.00	0.86	0.58	2.86	1.10
08/01 A	02:45	03:45	0.00	0.87	0.61	3.20	1.49
08/01 B	03:45	05:00	0.00	0.77	0.52	3.18	1.56
08/05 A	02:20	03:00	0.00	1.16	1.72	6.07	1.53
08/05 B	03:00	04:00	0.00	1.10	1.40	3.10	1.96
08/05 C	04:00	05:00	0.00	0.99	0.84	2.38	0.85
08/05 D	05:00	06:00	0.00	1.19	0.94	2.41	1.10
08/05 E	06:00	07:00	0.00	0.39	0.27	1.34	0.51
08/06 A	01:25	02:00	0.00	1.00	0.81	2.32	1.05
08/06 B	02:00	03:00	0.00	1.18	0.82	3.58	1.29
08/06 C	03:00	04:00	0.00	0.79	0.40	2.92	1.29
08/06 D	04:00	05:00	0.00	1.96	1.24	4.19	2.41
08/06 E	05:00	06:20	0.00	1.59	0.92	3.75	1.65
08/06 F	06:20	07:00	0.00	1.80	1.33	3.72	2.13
08/06 G	07:00	07:46	0.00	1.26	0.90	3.44	1.66
08/13 A	03:21	04:00	0.00	0.33	0.36	3.01	0.86
08/13 B	04:00	04:20	0.00	0.30	0.22	2.52	0.75
08/13 C	04:40	06:05	0.00	0.89	1.50	4.44	1.50
08/13 D	06:05	06:55	0.00	0.54	0.53	2.91	0.81
08/13 E	07:15	08:00	0.00	NA	0.83	NA	NA
08/13 F	08:00	08:40	0.00	NA	0.64	NA	NA
08/13 A	23:45	00:00	0.00	0.87	NA	4.28	1.41
08/14 B	00:00	01:00	0.00	1.26	NA	5.79	0.41
08/14 C	01:00	02:00	0.00	0.91	NA	3.47	1.35
08/14 D	02:00	04:00	0.00	1.19	NA	3.71	1.79
08/14 E	04:00	05:00	0.00	0.97	NA	3.16	1.24
08/14 F	05:00	06:00	0.00	1.32	NA	4.11	1.47
08/14 G	06:00	07:00	0.00	1.70	NA	NA	NA
08/14 H	07:00	08:00	0.00	0.86	NA	NA	NA
08/14 I	08:00	09:00	0.00	1.22	NA	NA	NA
08/14 J	09:00	09:15	0.00	1.01	NA	NA	NA
N			30	30	22	25	25
Min.			0	0.3	0.2	1.3	0.4
Max.			0	2.0	1.7	6.1	2.4
Avg.			0	1.1	0.8	3.4	1.3

Table A.17 1986 Laguna Peak Aerosol Concentrations

Date	ID	Start	Stop	Na ⁺ NH ₄ ⁺		Ca ²⁺ Mg ²⁺		Cl ⁻	NO ₃ ⁻	SO ₄ ²⁻	NH ₃ HNO ₃		SO ₂	HFo	HAc
				← neq m ⁻³ →						← nmole m ⁻³ →					
08/04	A	16:00	19:00	34	126	14	6	9	31	249	8	180	247	192	132
08/04	B	20:00	00:00	36	118	13	8	7	39	164	0	306	283	5	3
08/05	A	02:00	03:40	32	81	37	8	26	116	163	101	101	228	141	175
08/05	B	03:55	05:30	9	42	19	1	41	125	120	34	14	237	80	81
08/05	C	05:31	08:30	12	91	10	3	7	138	171	0	11	263	85	76
08/05	D	10:00	14:00	65	176	22	15	2	47	342	13	197	250	165	126
08/05	E	14:01	18:00	76	137	14	16	6	58	237	1	185	274	179	153
08/05	F	20:00	00:00	49	156	17	11	3	57	193	2	355	156	178	92
08/06	A	02:00	06:00	15	55	11	3	13	51	92	6	92	—	122	92
08/06	B	06:45	11:10	9	39	12	1	0	24	90	0	50	161	103	86
08/06	C	11:30	15:30	42	127	5	7	11	25	386	0	202	224	157	147
08/12	A	14:00	18:00	52	133	32	13	25	45	170	3	84	102	102	68
08/12	B	20:00	00:00	10	44	16	3	17	22	58	3	72	96	80	116
08/13	A	02:00	06:00	37	109	22	8	0	32	135	10	220	298	113	97
08/13	B	09:00	12:00	87	147	16	17	0	52	240	3	173	192	105	102
08/13	C	14:00	18:00	54	89	12	13	0	18	168	34	122	140	100	99
08/13	D	20:00	00:00	24	115	12	6	6	39	130	45	176	200	126	122
08/14	A	02:12	05:00	12	64	6	2	26	97	92	1	7	14	40	61
08/14	B	05:13	07:00	7	46	49	5	45	77	90	0	12	19	58	77
08/14	C	07:25	09:00	47	86	47	5	23	112	135	0	16	27	66	79

Table A.18 1986 Ventura Hill Aerosol Concentrations

Date	ID	Start	Stop	Na ⁺ NH ₄ ⁺		Ca ²⁺ Mg ²⁺		Cl ⁻	NO ₃ ⁻	SO ₄ ²⁻	NH ₃	HNO ₃	SO ₂	HFo	HAc
				← neq m ⁻³ →						← nmole m ⁻³ →					
07/29	A	17:39	19:59	138	25	17	25	126	26	42	0	12	47	65	82
07/29	B	20:00	00:00	221	43	23	46	200	42	66	4	6	111	44	53
07/30	A	02:00	06:00	146	67	14	29	122	54	76	7	14	68	99	79
07/30	B	06:45	08:15	58	119	20	7	36	58	77	0	9	36	45	77
07/30	C	09:00	13:00	108	111	50	25	43	55	122	5	28	—	—	—
07/30	D	16:00	19:35	87	80	40	19	47	46	139	0	41	35	68	48
07/30	E	20:00	00:00	220	85	43	49	130	102	134	0	17	72	76	96
07/31	A	02:00	06:00	67	126	18	11	75	60	116	0	23	30	40	60
07/31	B	15:30	19:00	167	82	62	41	118	79	143	NA	61	73	66	65
07/31	C	20:00	23:23	239	64	52	53	180	89	97	NA	18	33	40	49
08/01	A	00:20	03:15	129	54	27	31	167	106	110	NA	14	35	48	48
08/01	B	03:25	06:00	69	73	12	15	79	88	97	4	10	105	38	46
08/01	C	09:00	12:00	98	65	36	20	32	70	137	7	45	42	99	108
08/04	A	17:45	19:30	75	59	21	10	24	31	118	42	40	50	260	96
08/04	B	20:00	00:00	80	86	25	18	30	49	132	6	42	39	140	75
08/05	A	02:00	06:00	43	177	10	9	36	178	169	0	16	137	140	73
08/05	B	08:00	12:00	37	164	25	9	56	66	284	14	139	84	100	100
08/05	C	14:00	18:00	47	89	19	11	10	27	142	0	113	28	113	95
08/05	D	20:00	00:00	33	85	11	8	2	45	121	0	47			
08/06	A	02:00	04:00	74	111	13	8	24	148	126	0	9	33	48	63
08/06	B	04:25	07:00	24	175	10	3	25	205	148	6	8	344	53	66
08/06	C	10:00	13:59	30	151	21	4	10	18	218	0	117	—	—	—
08/06	D	14:00	16:10	45	86	36	5	26	33	161	3	100	47	138	123
08/12	A	14:00	18:00	38	54	15	7	0	29	170	0	92	128	61	72
08/12	B	20:00	00:00	100	87	23	23	78	67	118	0	25	29	43	55
08/13	A	02:00	06:00	142	166	30	35	73	146	159	2	29	28	44	53
08/13	B	08:00	12:00	75	303	42	22	23	146	295	10	90	334	77	102
08/13	C	14:00	18:00	34	98	22	8	0	31	168	1	122	33	122	109
08/13	D	20:00	00:00	42	98	19	13	36	75	116	0	51	38	47	44
08/14	A	04:15	08:50	34	153	38	10	21	202	120	0	16	55	53	57
08/14	B	10:00	12:30	16	122	15	4	0	25	139	4	127	557	119	122
09/08	A	14:02	18:00	68	87	13	18	3	48	111	21	43	87	104	84
09/08	B	20:00	00:00	113	82	18	28	30	74	84	-8	25	67	86	60
09/09	A	02:00	06:00	165	56	15	41	122	63	77	19	11	123	46	36

Table A.19 1986 Emma Wood State Beach Aerosol Concentrations

Date	ID	Start	Stop	Na ⁺ NH ₄ ⁺		Ca ²⁺ Mg ²⁺		Cl ⁻	NO ₃ ⁻	SO ₄ ²⁻	NH ₃	HNO ₃	SO ₂	HFo	HAc
				← neq m ⁻³ →						← nmole m ⁻³ →					
07/23	A	12:00	16:00	490	63	57	98	432	93	108	32	28	—	83	110
07/23	B	20:00	00:00	1001	32	79	201	1051	49	77	21	8	—	40	25
07/24	A	02:00	06:00	115	41	36	31	96	33	45	82	6	—	62	68
07/29	A	17:01	19:59	477	43	31	94	430	37	114	0	6	—	45	17
07/29	B	20:00	00:00	967	52	58	183	834	44	130	1	4	—	33	19
07/30	D	20:00	00:00	483	86	35	105	474	99	159	0	15	—	29	11
07/31	A	02:00	06:00	275	125	27	63	199	104	159	0	35	—	35	22
07/31	B	08:00	12:00	230	129	24	49	200	90	163	0	28	—	46	30
07/31	C	14:35	18:00	275	98	24	59	198	67	159	0	51	—	62	46
07/31	D	20:00	00:00	564	52	33	112	493	86	148	2	9	—	26	13
08/01	A	02:00	06:00	420	119	26	86	347	114	167	0	23	—	42	35
08/01	B	09:45	13:00	250	127	23	55	163	88	155	3	40	—	62	47
08/04	A	17:30	19:30	197	65	20	39	154	45	150	37	24	—	—	—
08/04	B	20:00	00:00	234	85	25	53	162	75	159	0	39	—	—	—
08/05	B	08:45	12:00	144	210	15	34	86	86	261	8	144	—	152	136
08/05	C	14:00	18:00	230	102	21	57	166	79	226	0	75	—	100	104
08/05	D	20:00	00:00	163	89	25	39	93	86	153	0	49	—	41	21
08/06	A	02:00	06:00	90	146	9	19	19	81	176	21	112	—	55	48
08/06	B	08:00	12:00	140	178	21	34	73	68	249	2	133	—	111	89
08/06	C	14:00	15:45	121	80	5	21	81	53	160	2	49	—	95	89
09/08	A	14:00	18:00	243	78	15	61	191	57	121	35	20	—	79	58
09/08	B	20:00	00:00	252	101	31	63	86	77	111	35	5	—	92	51
09/09	A	02:00	06:00	192	60	29	67	324	52	95	35	5	—	41	27

Table A.20 1986 West Casitas Pass Aerosol Concentrations

Date	ID	Start	Stop	Na ⁺ NH ₄ ⁺		Ca ²⁺ Mg ²⁺		Cl ⁻	NO ₃ ⁻	SO ₄ ²⁻	NH ₃	HNO ₃	SO ₂	HFo	HAc
				← neq m ⁻³ →						← nmole m ⁻³ →					
07/23	A	17:15	20:00	92	43	19	18	51	50	56	25	20	40	69	138
07/23	B	20:00	00:00	109	36	14	21	80	31	45	19	10	35	53	142
07/24	A	02:00	06:00	60	24	13	10	46	31	32	14	10	136	52	98
07/29	A	20:00	00:00	129	67	26	29	73	65	68	15	20	45	85	74
07/30	A	02:00	06:00	84	71	24	19	19	73	64	1	36	55	93	75
07/30	B	08:00	12:00	92	99	36	23	44	63	105	73	29	51	114	65
07/30	C	14:00	18:00	123	136	27	27	25	81	126	22	65	58	125	99
07/30	D	20:00	00:00	90	102	17	20	50	56	91	7	13	81	52	56
07/31	A	02:00	06:00	26	76	12	6	10	51	79	0	10	40	40	43
07/31	B	06:37	08:30	29	91	11	4	101	44	70	0	12	23	31	36
07/31	C	09:15	12:00	54	112	25	13	25	48	115	78	47	0	91	69
07/31	D	14:00	18:00	63	131	21	15	20	44	137	36	79	0	129	96
07/31	E	20:00	23:37	126	82	16	30	92	88	91	4	11	0	36	31
08/01	A	00:45	05:00	24	93	6	5	19	51	74	4	8	0	na	na
08/01	B	06:15	09:00	24	177	10	2	11	42	60	19	8	30	49	48
08/04	A	17:45	19:30	56	106	14	9	0	35	155	0	31	64	76	75
08/04	B	20:00	00:00	51	143	16	13	2	40	82	2	23	31	57	41
08/05	A	02:00	06:00	17	165	NA	4	25	105	90	0	14	26	35	31
08/05	B	08:00	12:00	21	168	11	4	9	51	130	54	68	31	78	64
08/05	C	14:00	18:00	53	132	16	11	16	34	172	8	98	38	136	114
08/05	D	20:00	00:00	48	123	14	10	36	84	48	21	16	37	53	70
08/06	A	02:00	06:00	18	139	8	3	1	77	85	3	4	11	27	60
08/06	B	06:25	07:46	17	135	9	3	9	94	75	0	0	23	45	71
08/06	C	10:00	12:30	10	146	11	3	0	43	137	100	65	48	73	82
08/06	D	14:00	15:00	5	144	25	0	0	59	189	145	133	199	180	208
08/12	A	14:30	18:00	32	111	19	7	0	28	150	20	79	180	96	107
08/12	B	20:00	22:10	37	91	17	7	10	50	122	15	18	46	54	69
08/13	A	03:41	06:00	7	112	6	0	0	65	87	54	4	25	24	40
08/13	B	06:40	08:40	9	148	9	2	27	81	88	74	6	17	34	46
08/13	C	10:00	13:59	47	131	21	10	6	43	136	54	65	35	98	66
08/13	D	14:00	18:00	48	125	16	10	22	46	151	36	91	36	151	98
08/13	E	20:00	23:00	24	173	35	9	6	63	156	20	23	23	49	48
08/14	A	00:45	04:00	7	201	7	3	10	103	122	1	10	57	25	25
08/14	B	04:00	08:00	5	124	5	1	1	80	65	0	11	18	28	37
08/14	C	09:00	12:00	15	136	15	3	3	55	97	25	NA	124	74	63
09/08	A	15:30	18:00	20	0	142	105	89							
09/08	B	20:00	00:00	29	0	27	50	42							
09/09	A	02:00	06:00	0	0	29	48	34							

Table A.21 1986 El Capitan State Beach Aerosol Concentrations

Date	ID	Start	Stop	Na ⁺ NH ₄ ⁺		Ca ²⁺ Mg ²⁺		Cl ⁻	NO ₃ ⁻	SO ₄ ²⁻	NH ₃	HNO ₃	SO ₂	HFo	HAc
				← neq m ⁻³ →						← nmole m ⁻³ →					
07/23	A	15:00	18:00	404	18	27	88	427	37	72	39	10	30	68	96
07/23	B	20:00	00:00	236	15	24	52	227	12	41	39	5	92	68	129
07/24	A	02:00	06:00	50	11	6	11	37	13	21	23	7	103	55	57
07/29	A	20:00	00:00	302	56	69	67	297	47	78	42	7	45	107	192
07/30	A	02:00	06:00	125	67	21	26	71	65	69	15	7	137	97	58
07/30	B	08:00	12:00	439	76	34	108	422	99	141	22	20	68	87	67
07/30	C	14:00	18:00	1079	97	85	215	867	133	289	2	29	67	98	81
07/30	D	20:00	00:00	261	97	43	60	237	61	111	15	12	77	76	136
07/31	A	02:00	06:00	142	117	18	29	116	67	98	6	21	71	58	61
07/31	B	20:00	00:00	335	108	58	73	286	108	130	NA	10	85	89	173
08/01	A	02:00	06:00	285	136	32	66	215	140	149	0	22	72	48	45
08/01	B	08:00	12:00	527	106	43	122	499	99	221	0	29	151	92	100

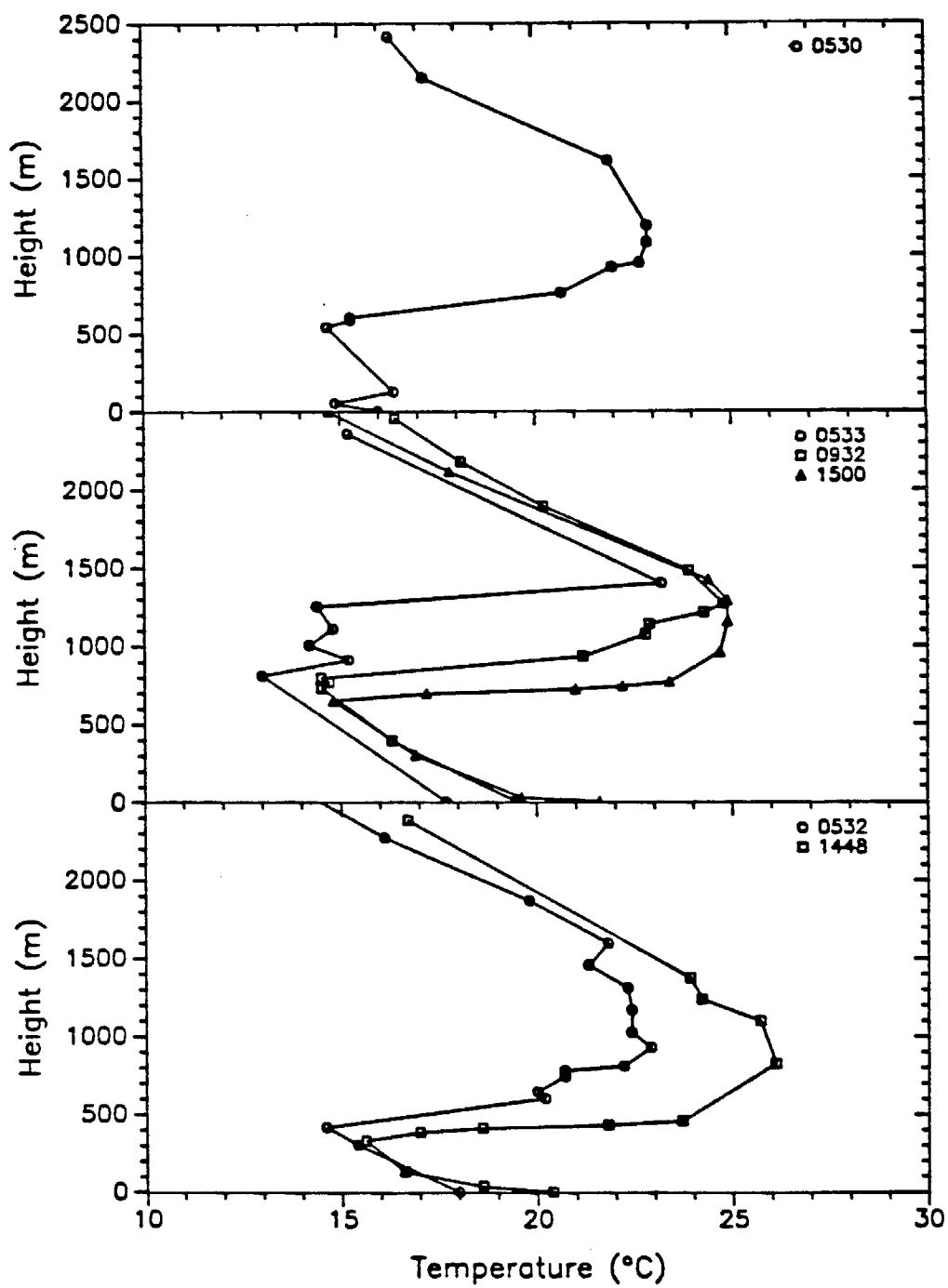


Figure A.1

Temperature profiles on July, 24, 25, and 26, 1985 taken at Point Mugu by rawinsonde. Stratus clouds were present during the late night and early morning of each day shown.

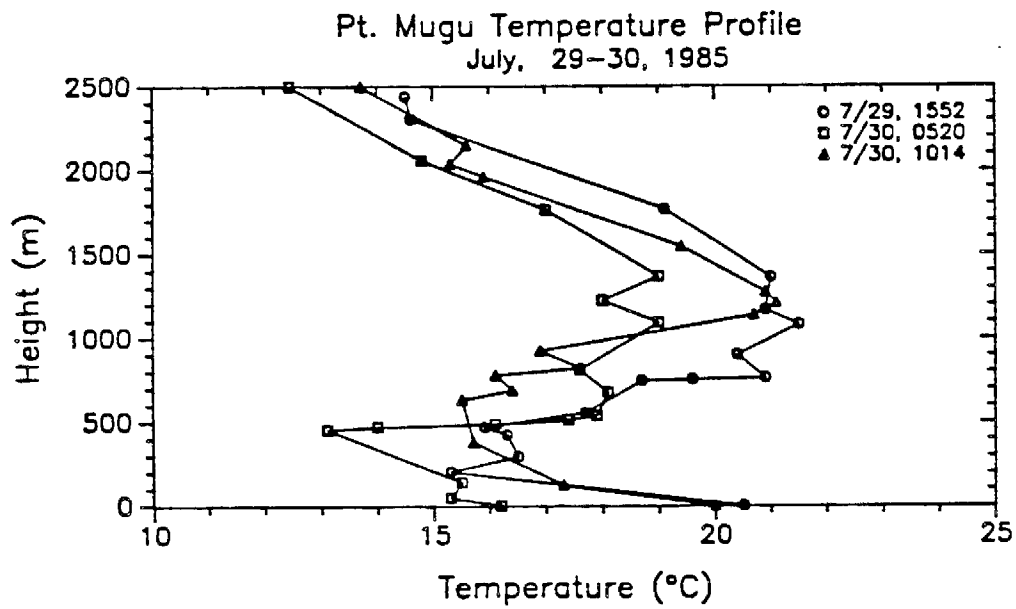


Figure A.2

Temperature profiles on July 29 and 30, 1985, taken at Point Mugu by rawinsonde. Thin stratus was present the morning of July 30 below the level of La Jolla Peak (500 m).

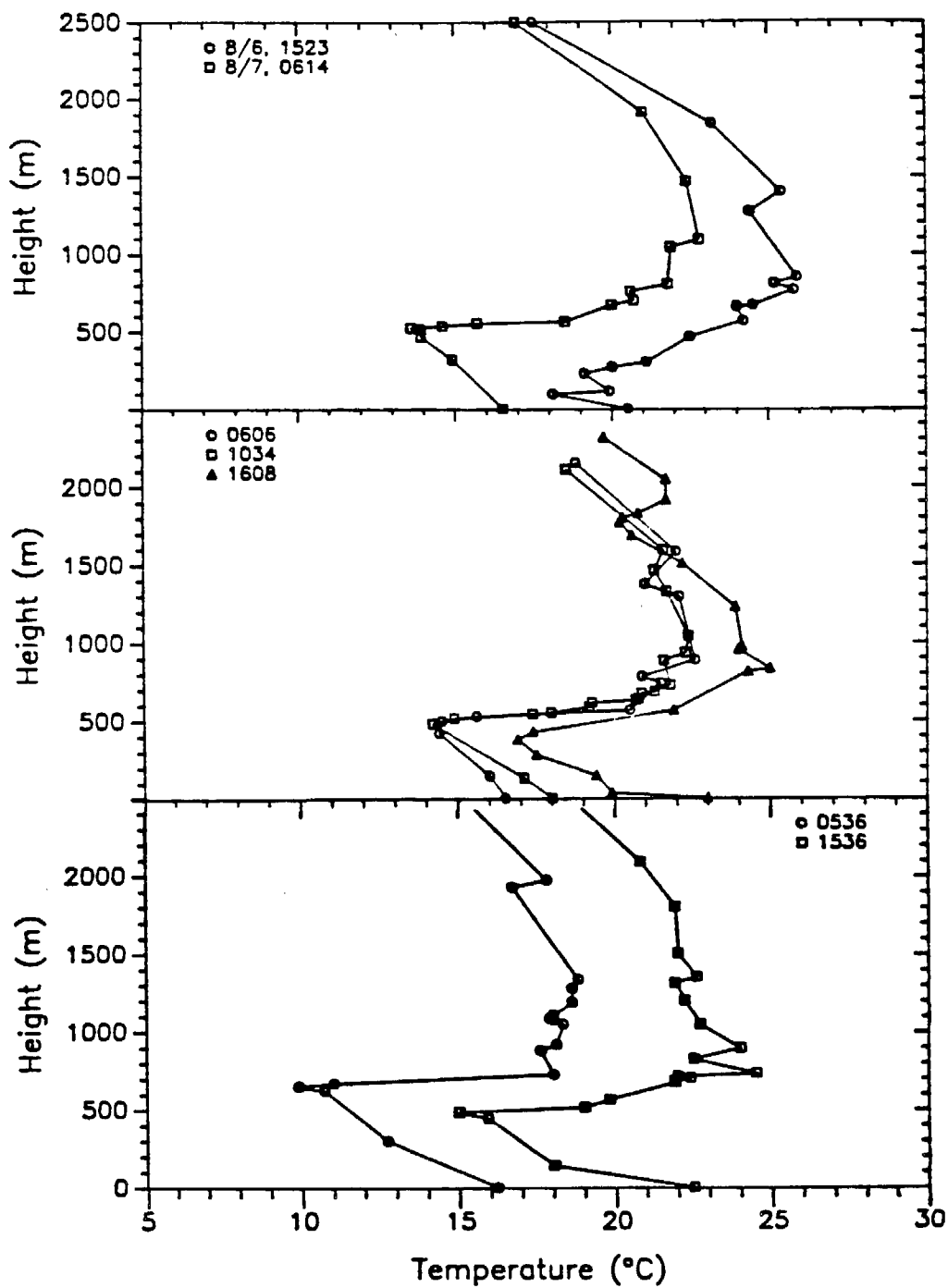


Figure A.3

Temperature profiles on August 7, 8, and 9, 1985 taken at Point Mugu by rawinsonde. Stratus clouds were collected at Casitas Pass on each of the mornings shown.

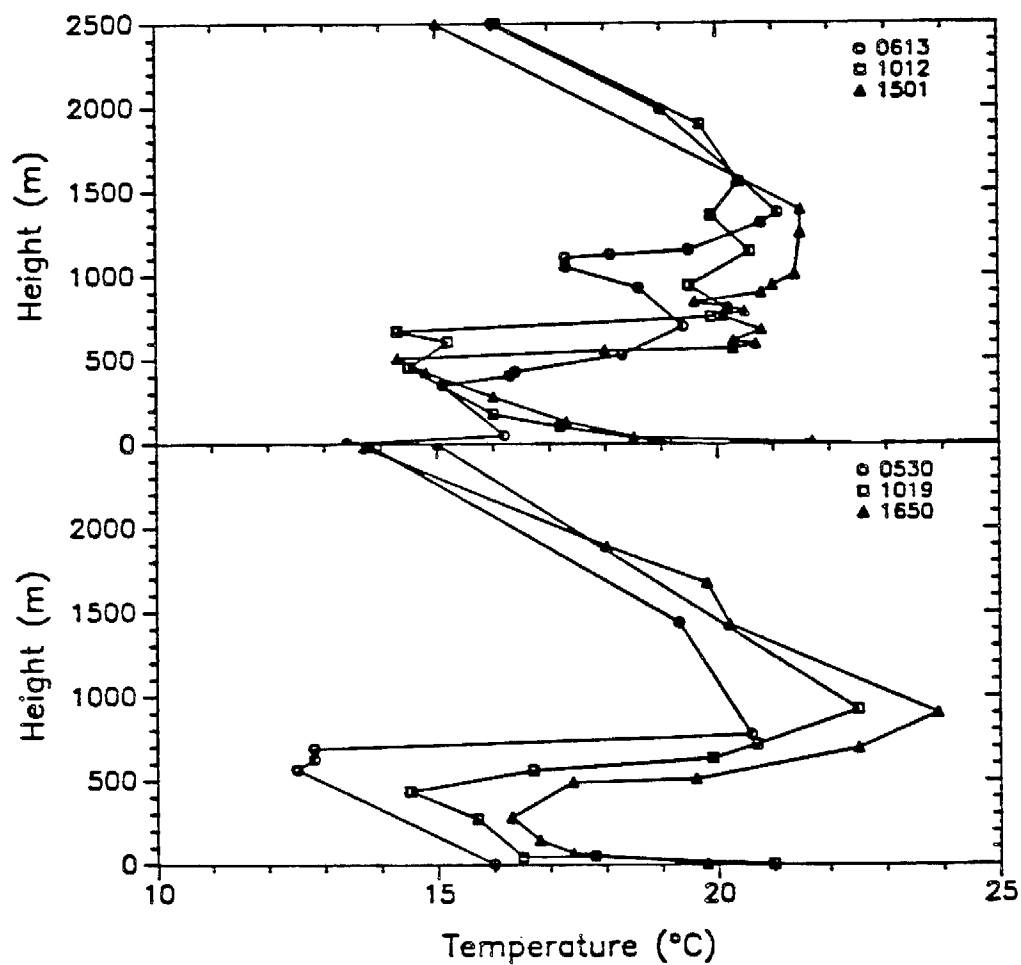


Figure A.4

Temperature profiles on August, 20 and 21, 1985 taken at Point Mugu by rawinsonde. Stratus cloud was present the morning of August 21.

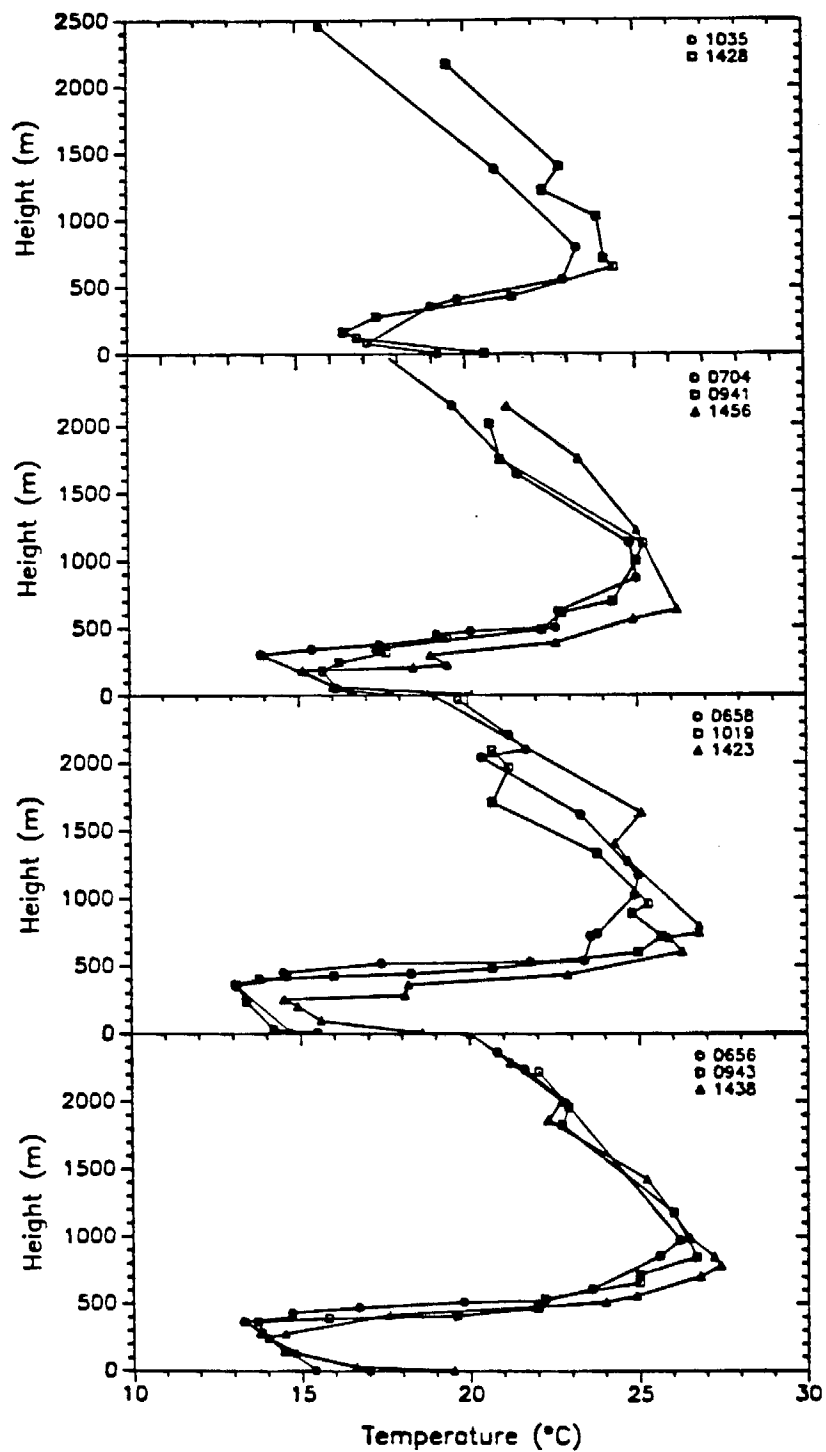


Figure A.5

Temperature profiles for the period July 29 – August 1, 1986 taken at Point Mugu by rawinsonde.

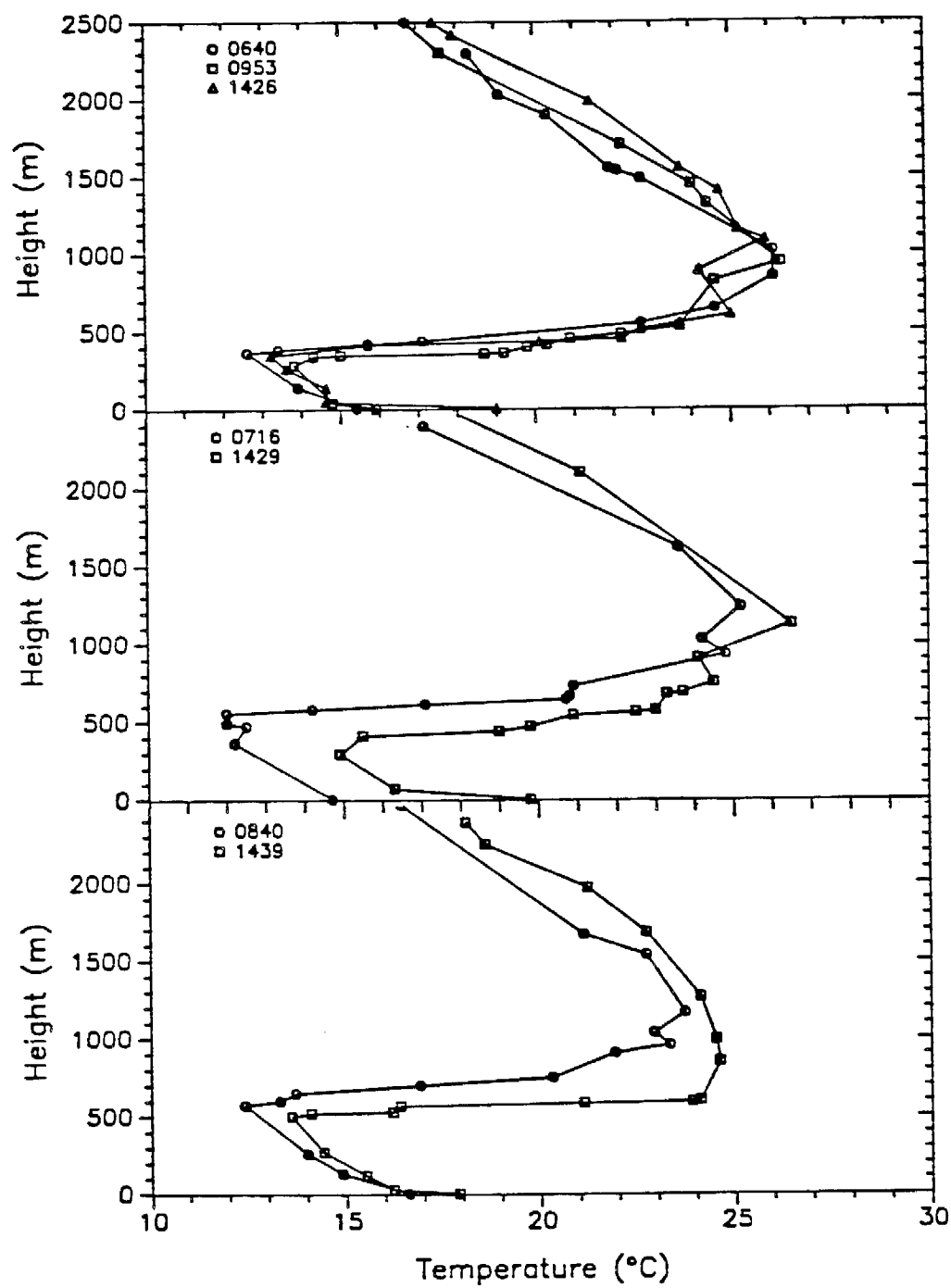


Figure A.6

Temperature profiles for the period August 12 – August 14 , 1986 taken at Point Mugu by rawinsonde.

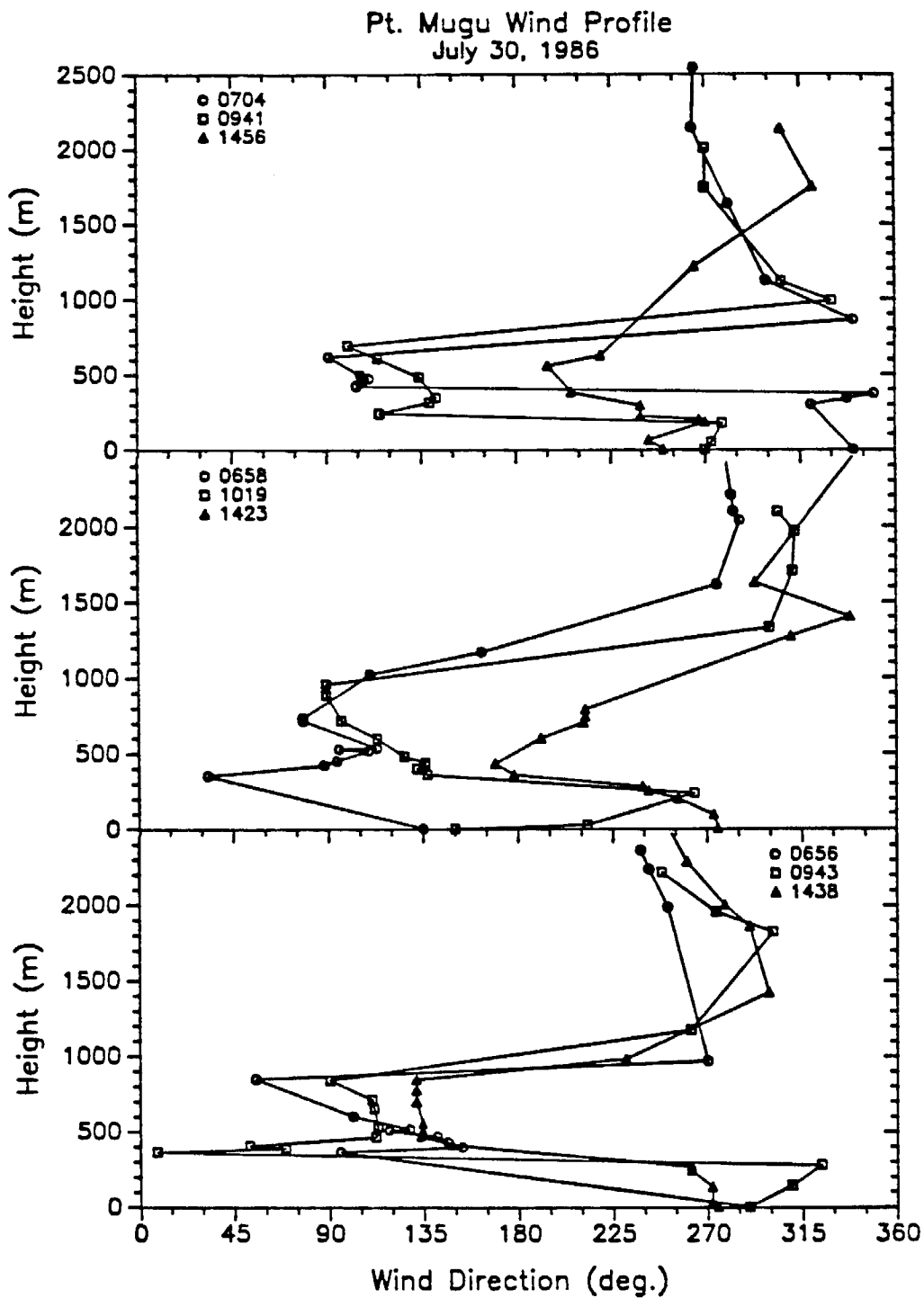


Figure A.7

Wind direction profiles taken at Point Mugu for the period July 30 – August 1, 1986.

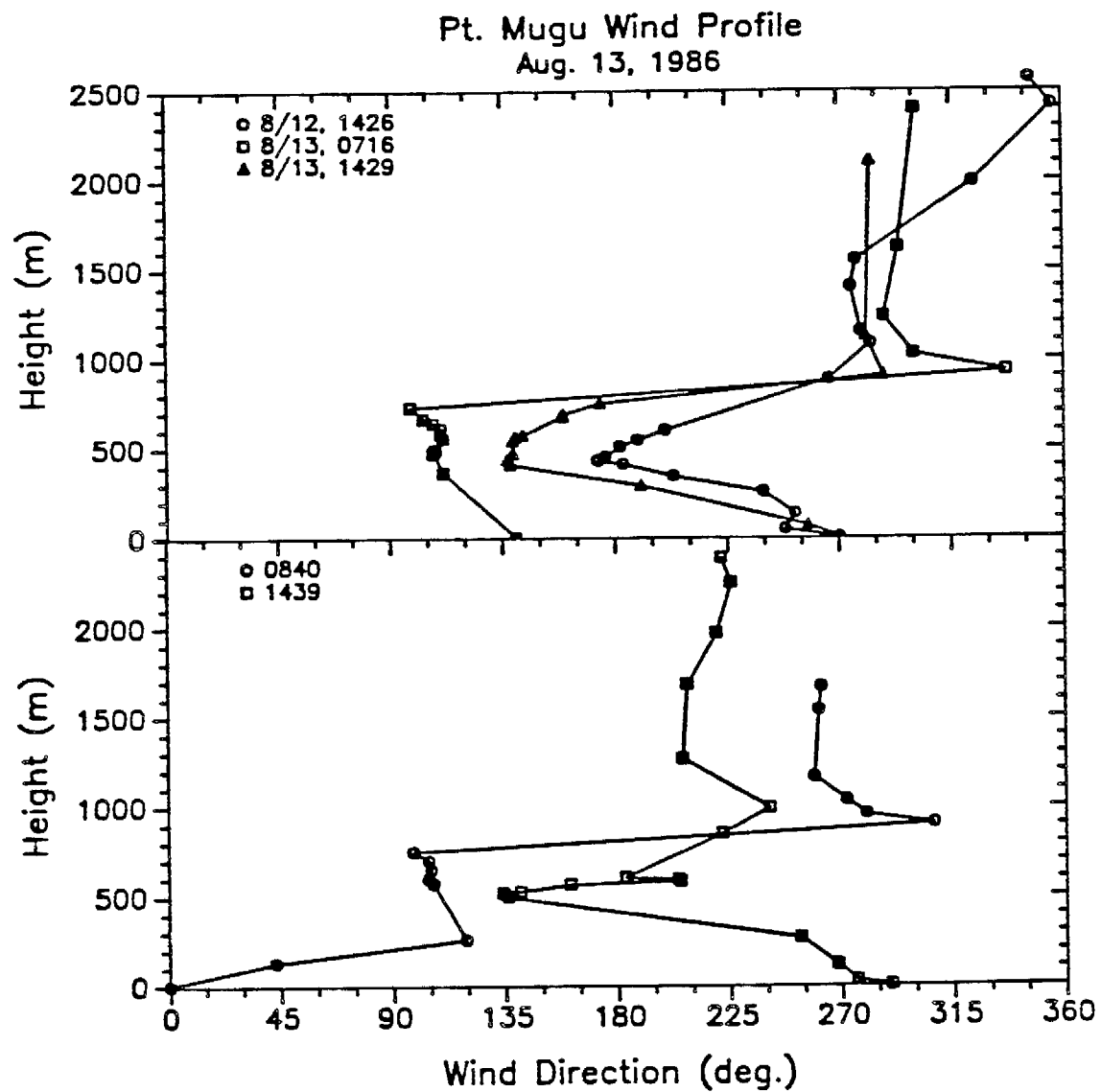


Figure A.8

Wind direction profiles taken at Point Mugu for the period August 13 – August 14, 1986.

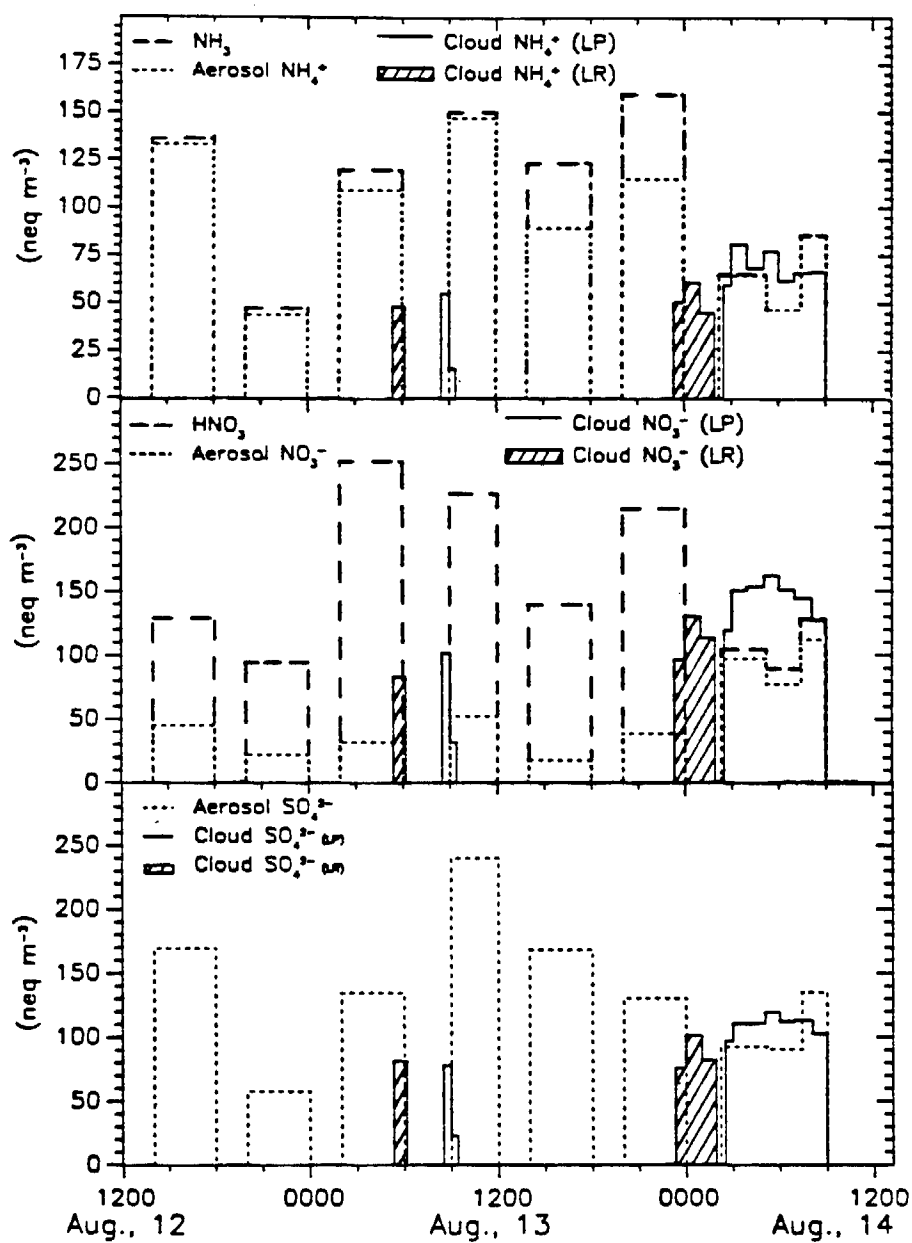


Figure A.9

Aerosol and cloudwater loadings of major ions at Laguna Peak on August 12 – 14, 1986.
 Cloudwater loading is the product of aqueous-phase concentration and estimated LWC.

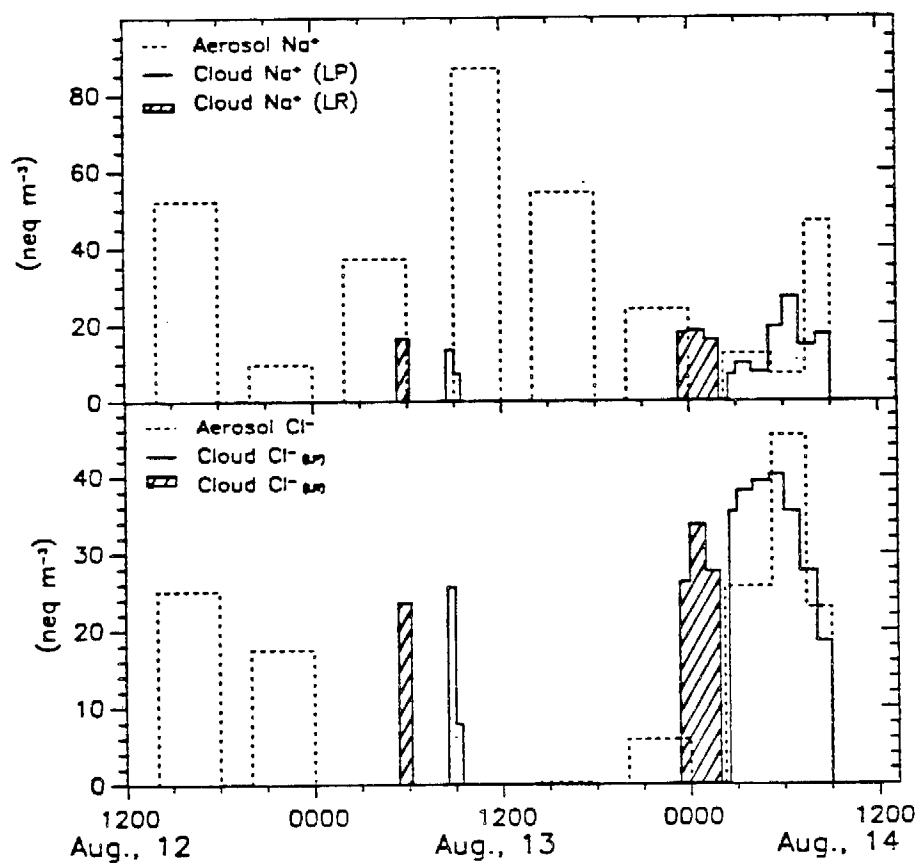


Figure A.10

Aerosol and cloudwater loadings of sea salts at Laguna Peak on August 12 – 14, 1986. Cloudwater loading is the product of aqueous-phase concentration and estimated LWC.

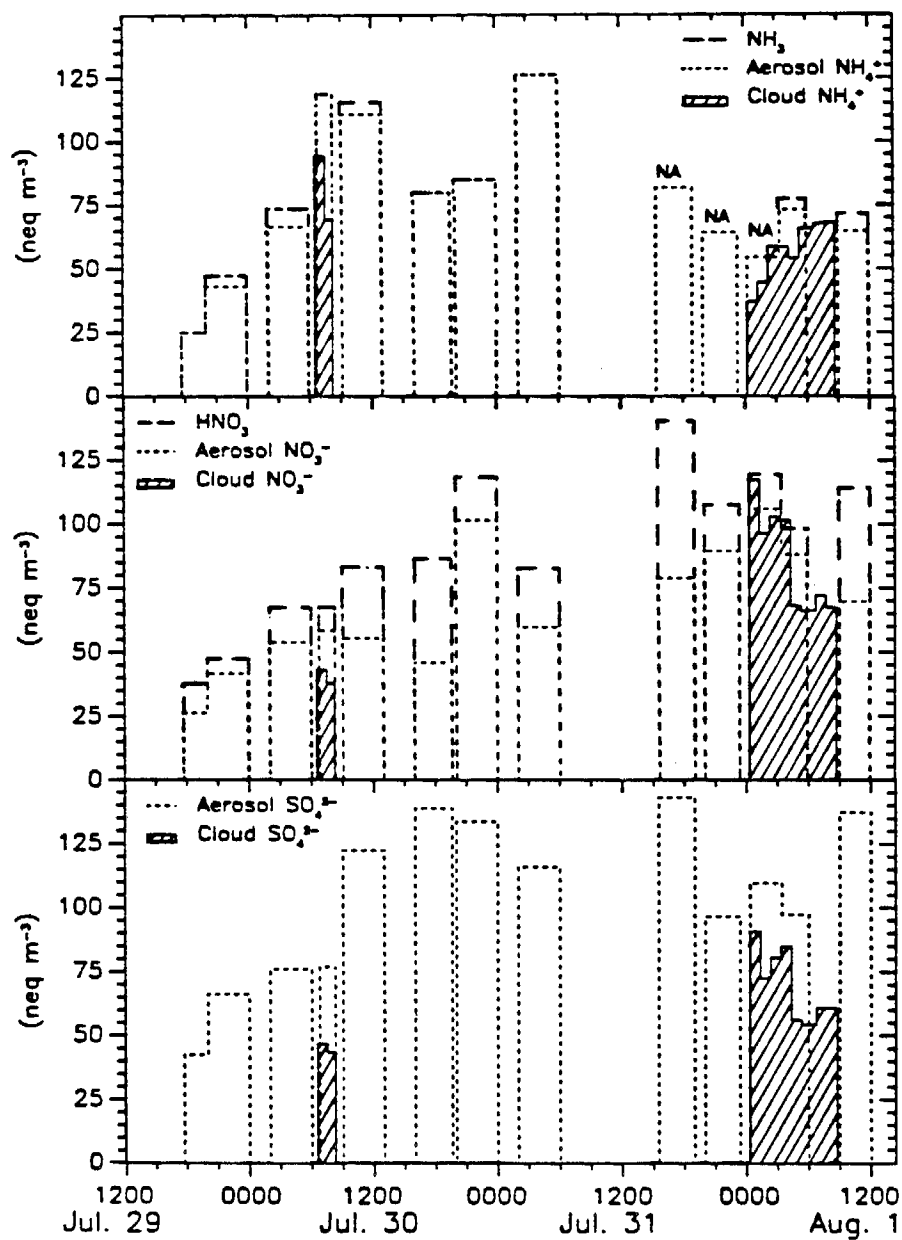


Figure A.11

Aerosol and cloudwater loadings of major ions at Ventura on July 29 – August 1, 1986. Cloudwater loading is the product of aqueous-phase concentration and estimated LWC.

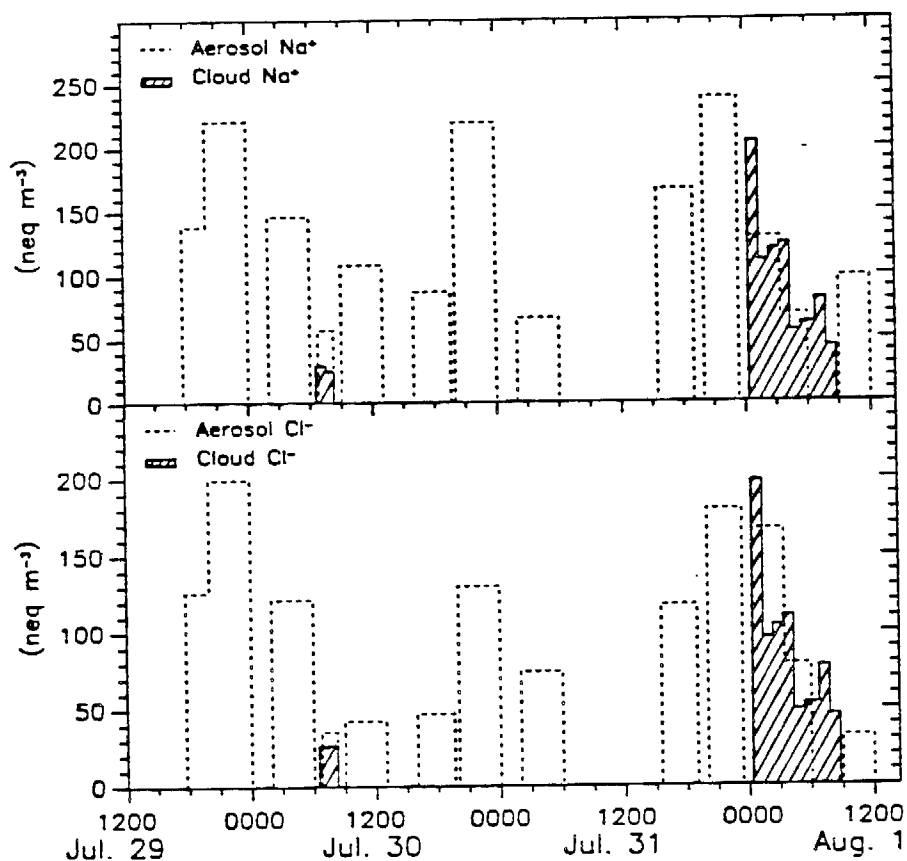


Figure A.12

Aerosol and cloudwater loadings of sea salts at Ventura on July 29 – August 1, 1986. Cloudwater loading is the product of aqueous-phase concentration and estimated LWC.

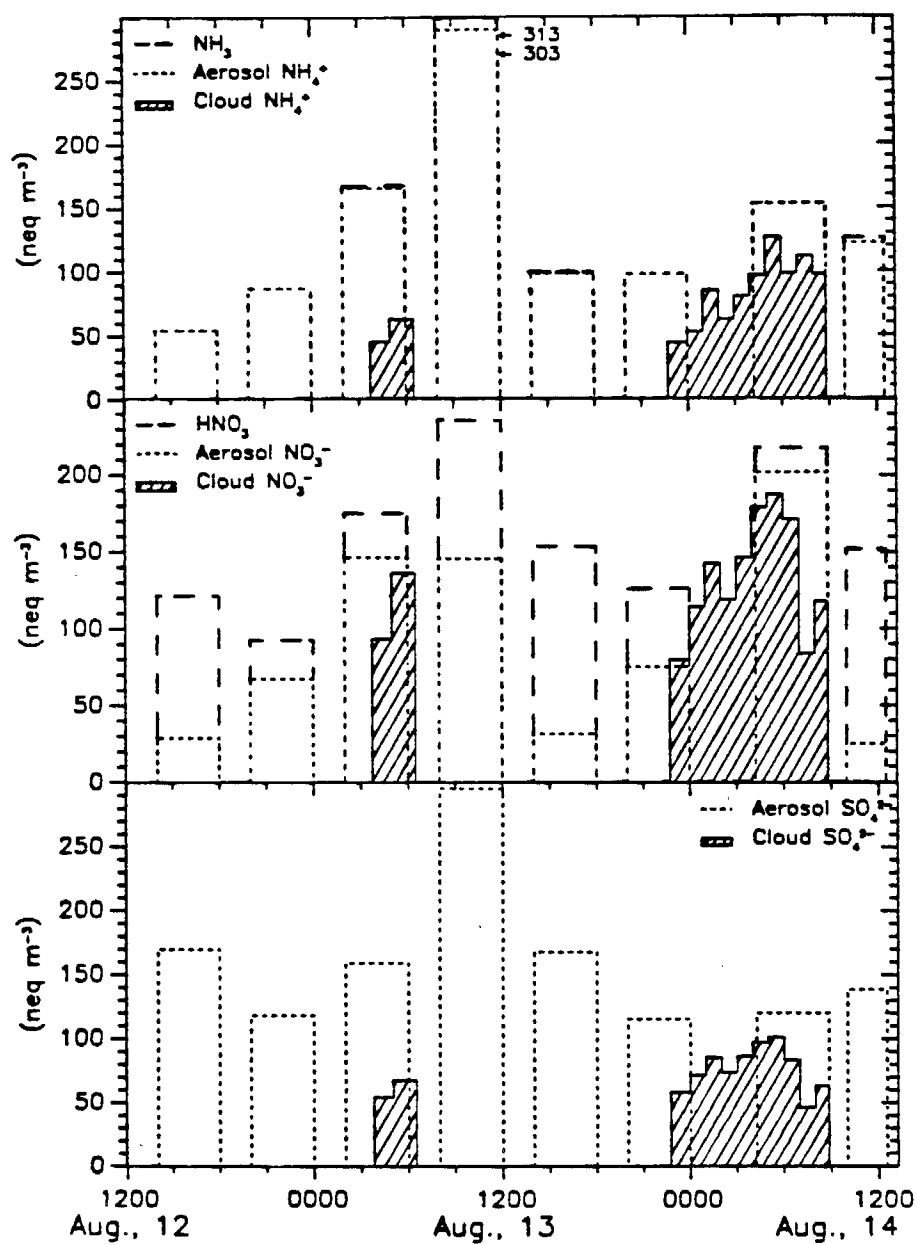


Figure A.13

Aerosol and cloudwater loadings of major ions at Ventura on August 12 – 14, 1986. Cloudwater loading is the product of aqueous-phase concentration and estimated LWC.

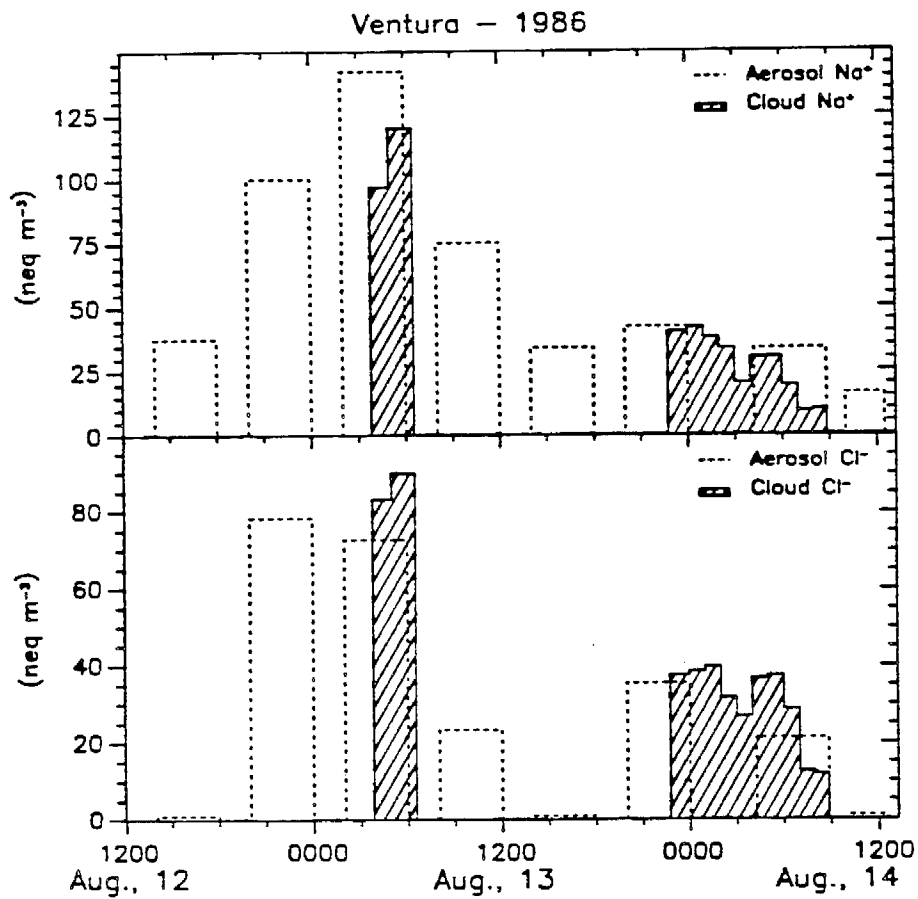


Figure A.14

Aerosol and cloudwater loadings of sea salts at Ventura on August 12 – 14, 1986. Cloudwater loading is the product of aqueous-phase concentration and estimated LWC.

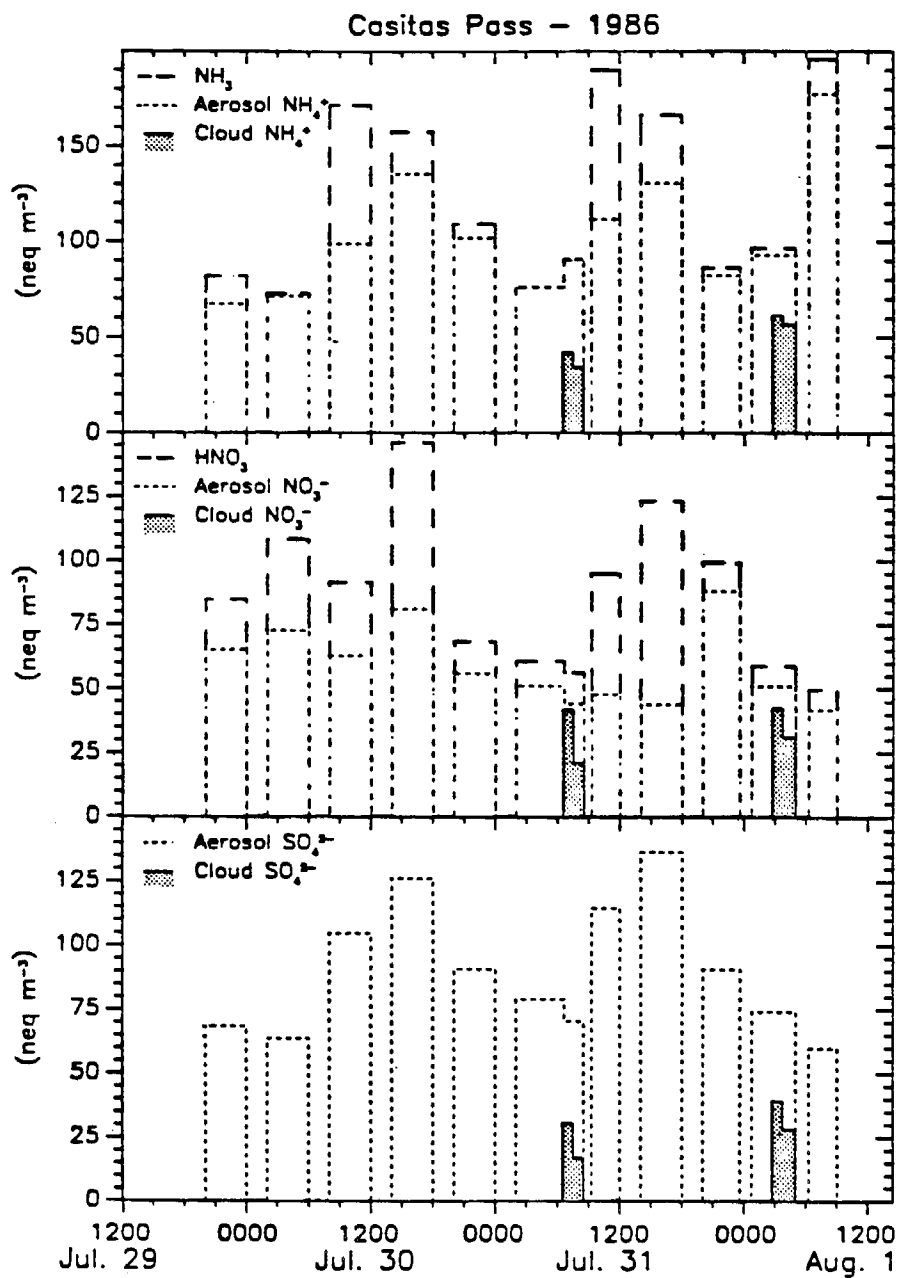


Figure A.15

Aerosol and cloudwater loadings of major ions at Casitas Pass on July 29 - August 1, 1986. Cloudwater loading is the product of aqueous-phase concentration and estimated LWC.

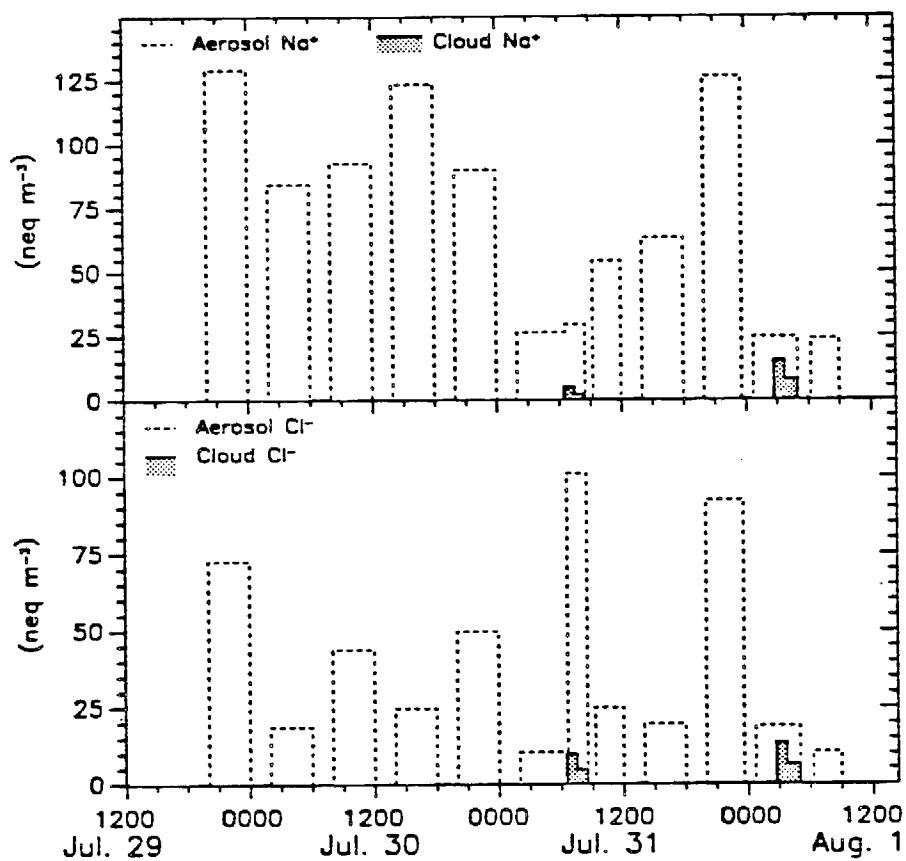


Figure A.16

Aerosol and cloudwater loadings of sea salts at Casitas Pass on July 29 – August 1, 1986. Cloudwater loading is the product of aqueous-phase concentration and estimated LWC.

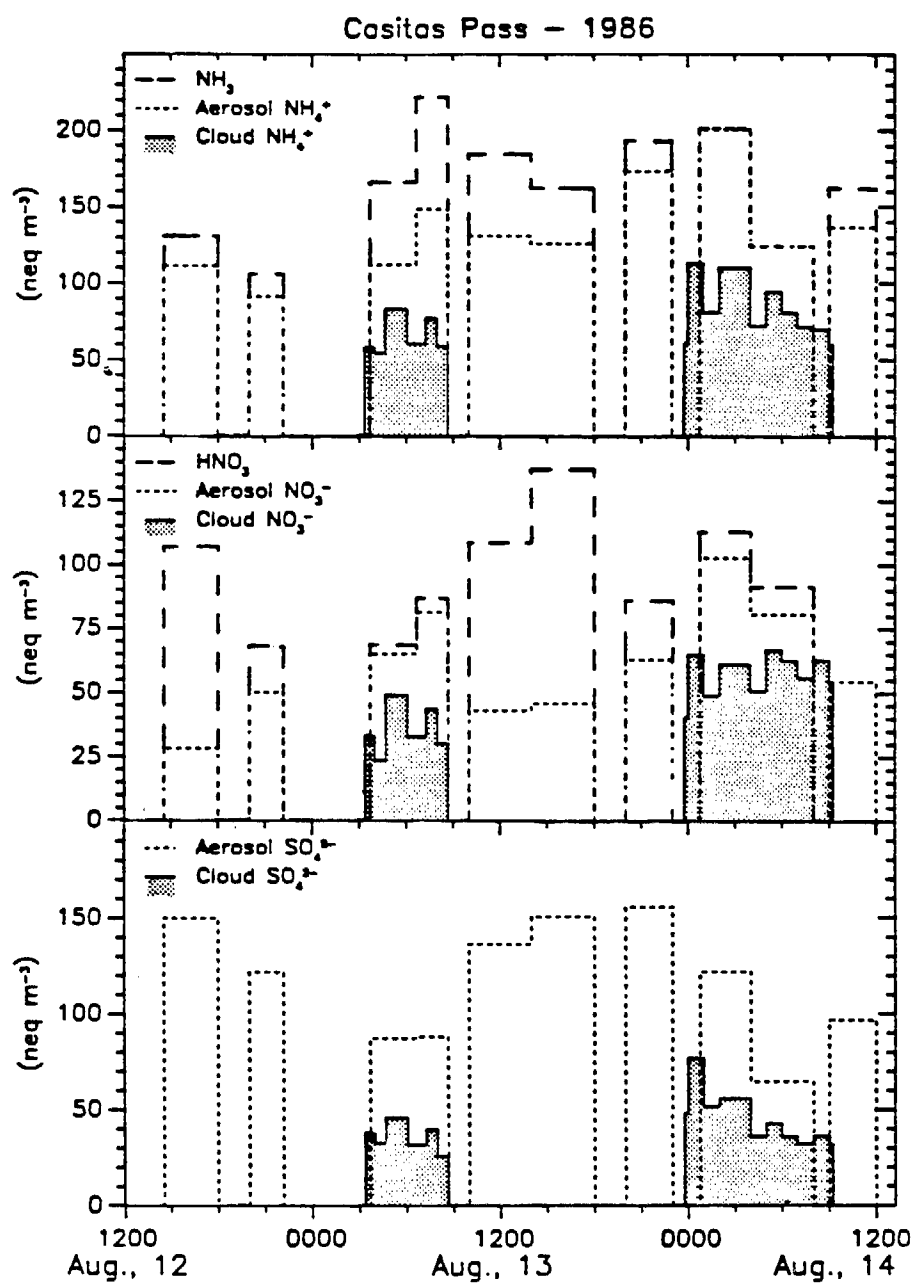


Figure A.17

Aerosol and cloudwater loadings of major ions at Casitas Pass on August 12 - 14, 1986. Cloudwater loading is the product of aqueous-phase concentration and estimated LWC.

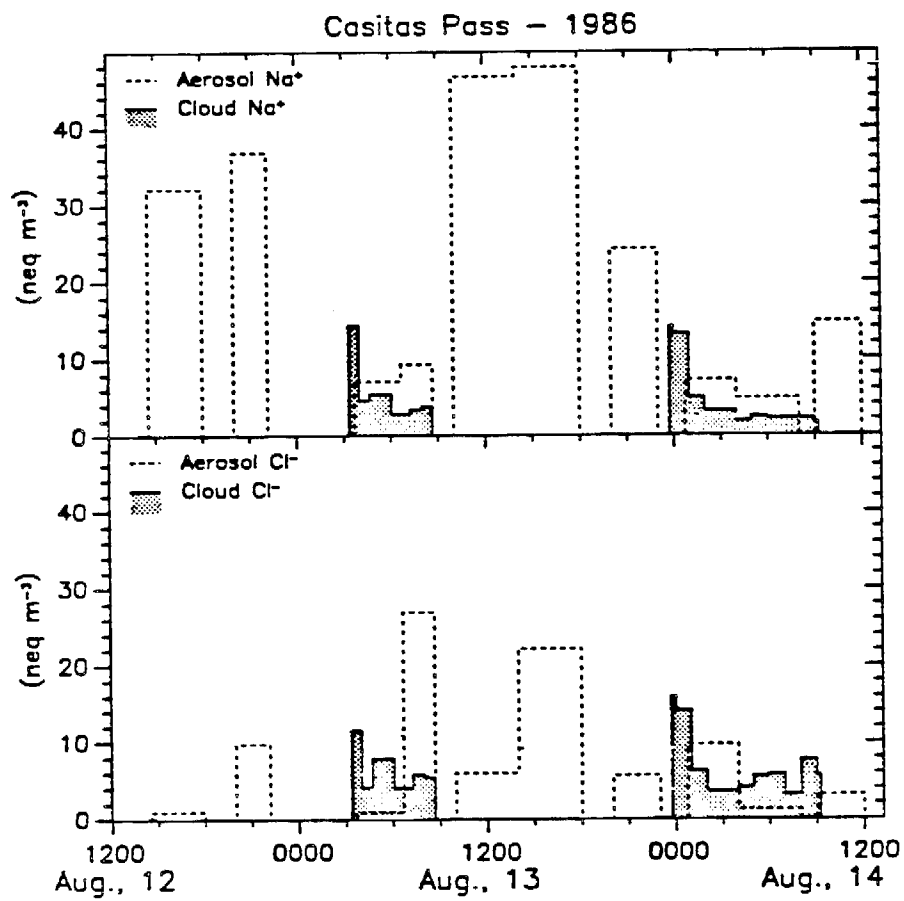


Figure A.18

Aerosol and cloudwater loadings of sea salts at Casitas Pass on August 12 - 14, 1986. Cloudwater loading is the product of aqueous-phase concentration and estimated LWC.

CHAPTER 16

Chemical Composition of Fogwater Collected along the California Coast

Daniel J. Jacob,[†] Jed M. Waldman, J. William Munger, and Michael R. Hoffmann*

Environmental Engineering Science, W. M. Keck Engineering Laboratories, California Institute of Technology, Pasadena, California 91125

■ Fogwater collected at both urban and nonurban coastal sites in California was found to be consistently acidic. Millimolar concentrations of NO_3^- , and fogwater pH values below 3, were observed at sites downwind of the Los Angeles basin. Fogwater composition at remote sites showed evidence of substantial continental and anthropogenic contributions. Acid-neutralizing capacities in coastal air were found to be very low and insufficient to neutralize even small acid inputs. Chloride loss relative to its sea salt contribution was observed at sites furthest from anthropogenic sources.

Introduction

Recent investigations of fogwater chemical composition in the Los Angeles basin (1, 2) have revealed high concentrations of SO_4^{2-} and NO_3^- , usually associated with very high acidities (pH values typically in the range 2–4). Comparable acidities have been observed in low stratus clouds collected by aircraft over the basin (3) and sampled on the slopes of the surrounding mountains (4). These high acidities have raised concern regarding potential damage to materials, vegetation (5), crops (6), and public health (7). Laboratory studies have shown that aqueous-phase oxidation of S(IV) to S(VI) can proceed rapidly under the conditions found in fog droplets (8) and in the precursor aerosol at high humidities (9). Field data suggest that aqueous aerosols are important sites for the conversion of SO_2 to H_2SO_4 in the atmosphere (10–13).

Fogs are frequent seasonal occurrences along the California coast. During the summer, coastal stations may report over 50% foggy days (14). These fogs are often coupled with land breeze/sea breeze systems, which recirculate the same air parcels several times across the shoreline (12). Tracer studies in the Santa Barbara

Channel (15) have shown that emissions from offshore and coastal sources may reside several days along the coast. These humid, poorly ventilated conditions favor pollutant accumulation and H_2SO_4 production.

As part of an extensive fog sampling program in California, we have collected fogwater at a number of coastal sites. Coastal fogs may be a major cause of sulfate pollution episodes in southern California (13). Furthermore, impaction of fog droplets can be an important source of water and chemical loading to the coastal vegetation (16); in some cases, fogwater has important local implications for acid deposition. Recent interest in these problems has been stirred by federal plans to encourage oil exploration and production in the outer continental shelf off California (17).

Sampling Sites and Methods

Fogwater was sampled at eight coastal sites and one island site (Figure 1). The sites, and meteorological conditions during sampling, are described in Table I. Samples were collected with a rotating arm collector over intervals ranging from 30 min to 2 h. The rotating arm collector, which has been described in detail previously (18), collects fog droplets by impaction on a slotted rod rotating at high velocity. Droplets impacting inside the slots flow by centrifugal force to bottles mounted at the ends of the rod. In this way, impacted droplets are immediately sheltered in a quiescent environment, and sample evaporation is prevented (18). The rotating arm collector samples air at a rate of $5 \text{ m}^3 \text{ min}^{-1}$. Model-scale laboratory calibration has indicated a lower size cut (50% collection efficiency) of $20\text{-}\mu\text{m}$ diameter.

A recent intercomparison of fogwater collectors (19) has established that our rotating arm collector provides samples that are representative of ambient fogwater. In that study, no significant differences in ionic concentrations were observed between samples collected concurrently with the rotating arm collector and with a jet impactor devel-

[†] Present address: Center for Earth and Planetary Physics, Harvard University, Cambridge, MA.

Table I. Description of Sampling Sites

site		Conditions during sampling		
		inversion base, ^a m MSL	temp, ^b °C	surface wind, ^b m s ⁻¹
Del Mar	coastal lagoon, residential area, 800 m from shore	surface	11	moderate NW shifting to moderate E
Corona del Mar	residential area; collector set on pier	260	11	calm
Long Beach Harbor	industrial area, ships; collector set on dock, 10 m from water	220	10	calm
Lennox	industrial and residential area; Los Angeles Int'l Airport is 2 km NW, major freeway is 500 m E; ocean is 4 km W; collector set on roof of 1-story building	surface	12 (Dec 7, 1981)	1 NE
		surface	14 (Dec 18, 1981)	1 SE
		220	10 (Jan 7, 1983)	calm
San Nicholas Island	U.S. Navy base, 100 km offshore; no impact from local sources; collector set at 50 m elevation, 400 m from shore	150	14	5 NNW
San Marcos Pass	mountain pass in coastal range, 700-m elevation; no nearby sources	1800	8-15	2 S
Morro Bay	rural town at the base of major power plant; agriculture, ranches; some local traffic; collector set 500 m from shore, on roof of 1-story building	450	11	0-2 SW
Mt. Sutro	250-m elevation hill above San Francisco; radio towers, no local traffic; ocean is 5 km W	570	12	1 W
Pt. Reyes	National Seashore, no nearby sources; collector set at tip of peninsula, 10-m elevation, 50 m from shore	600	12 (Aug 9, 1982)	10-15 N
		420	11-12 (Aug 10, 1982)	10-15 N
		1800	12-14 (Aug 11, 1982)	10-15 N
		240	11-14 (Aug 12, 1982)	2 SE

^aBase of temperature inversion, measured at San Diego, Los Angeles, Vandenberg AFB, or Oakland. ^bMeasured at the site.

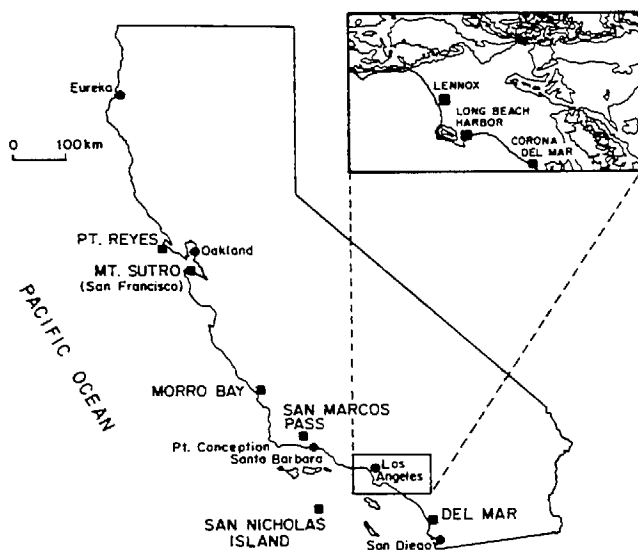


Figure 1. Fogwater sampling sites (■).

oper by the Desert Research Institute, Reno, NV (20). Moreover, it was shown that the rotating arm collector provides chemically reproducible samples; no significant differences in ionic concentrations were found between samples collected by two rotating arm collectors set side by side.

Fogwater pH was measured within 10 min of sample collection with a Radiometer PHM 82 meter and Radiometer GK2320C combination electrode. The pH meter was calibrated before each measurement with pH 1.68, 4, and 7 standards. The pH readings were very stable, as would be expected in view of the high ionic strengths of the samples. Major ions and metals were analyzed in our laboratory following previously described protocol (1). The standard errors on chemical analyses were about 5% and the detection limits, 1 $\mu\text{equiv L}^{-1}$, for all ions reported. Detection limits for metals were 1 $\mu\text{g L}^{-1}$. When the ionic concentrations to be determined were larger than 150 $\mu\text{equiv L}^{-1}$, the samples had to be quantitatively diluted

to bring them within analytical range. Concentrations of Na^+ , K^+ , Ca^{2+} , and Mg^{2+} were determined by atomic absorption spectroscopy on filtered aliquots; at some sites (Del Mar, Long Beach, Lennox, and Morro Bay), we analyzed both filtered and unfiltered aliquots and did not observe significant differences in concentrations. In samples collected at some urban sites, Cl^- determinations by ion chromatography were subject to positive interference from unidentified peaks eluting just before Cl^- . The interference was substantial when Cl^- concentrations were low; Cl^- concentrations reported are then an upper bound of true Cl^- concentrations and are identified as such. The unidentified peaks were likely due to organic acids (21). Formate and acetate at concentrations near 10^{-4} M have been observed by us in inland fogs.

Liquid water content in fog was estimated from the collection rate of the rotating arm collector, assuming that the instrument collects 60% of the incident water. This empirical correction factor of 60%, which is justifiable by the experimental lower size cut of the instrument, leads to liquid water content estimates that are in reasonable agreement (within a factor of 2) with those determined by laser transmissometer and Hi-Vol filter methods (18, 19, 22). It must be stressed that there is at this time no widely accepted method for measuring liquid water content in fog, and discrepancies by a factor of 2 are commonly observed between different methods (22). Estimate of liquid water content from the collection rate of the sampling device presents the advantage of coinciding in time and space with the chemical characterization of fogwater.

The marine, continental, and anthropogenic contributions to the fogwater composition were determined from a source apportionment matrix for primary California aerosol (23) (Table II). Because of the relatively small number of elements analyzed and the large spread in elemental concentrations, a stepwise apportionment approach was used instead of the usual least-squares fitting procedure. First, contributions from automobile exhaust and fuel oil fly ash were determined from the concentrations of the Pb and V, which originate almost exclusively from these two sources, respectively. The sea salt con-

Table II. Source Concentrations of Particulate Matter^a

	% mass				
	sea salt	soil dust	cement dust	fuel oil fly ash	automobile exhaust
Na	30.6	2.5	0.4	5	x ^b
S	2.6	0.1 ^b	0.1 ^b	15 ^b	2 ^b
Ca	1.16	1.5	46.0	1.3	0.02 ^b
Mg	3.7	1.4	0.48	0.06	x
K	1.1	1.5	0.53	0.2	x ^b
V	10 ^{-6c}	0.006	x ^d	7	x
Fe	10 ^{-6c}	3.2	1.09	6	0.4
Pb	10 ^{-6c}	0.02	x	0.07	40

^aData from ref 23 unless otherwise specified. ^bRef 24. ^cRef 25. ^dx, negligible.

tribution was then determined from the remaining Na, and from there the cement dust and soil dust contributions were determined from the remaining Ca and Fe. The calculation was iterated if necessary until observed Na and Ca were accounted for to within 5%. No such constraint was placed on the fit to Fe because of the variability of Fe concentrations in soils (26); it must be kept in mind that, depending on the actual Fe fraction in soil dust, the determined soil contributions may be substantially off. Similarly, fluctuations of the V content of fuel oil will correspondingly alter the fuel oil fly ash contribution from that given in Table IV. The contribution of secondary SO₄²⁻ was calculated by subtraction of primary contributions from the total SO₄²⁻ concentration. All NO₃⁻ was assumed to be of secondary origin.

Results and Discussion

Fogwater Concentrations. Table III gives liquid water weighted average fogwater concentrations for each event; the detailed data set is available elsewhere (27). Results of the source apportionment are given in Table IV in terms of fogwater loadings, which we define as the mass of material in fogwater per cubic meter of air. Fogwater loadings were obtained by multiplying the fogwater concentrations by the liquid water content of the fog.

In Table V elemental ratios in fogwater are compared to those for sea salt. The observed Na/Mg ratios were close to that for sea salt; exceptions were the Long Beach, Lennox, and San Marcos sites, where sea salt constituted only a small fraction of the total loading and significant soil dust contributions of Na and Mg were apparent. Calcium and sulfate were partly of marine origin but usually had larger contributions from dust (calcium) and secondary production (sulfate). The K/Na ratios were close to that for sea salt at Del Mar, San Nicholas Island, and Pt. Reyes; soil dust was an important source of K at other sites.

The sites in and around the Los Angeles basin were by far the most affected by anthropogenic sources (Table IV). The large contribution from automobile exhaust in the fog samples collected at Lennox can be attributed to the nearby freeway and airport traffic. Fogwater collected at Long Beach Harbor on Jan 6, 1983, had the same NO₃⁻ loading as fogwater collected at Lennox on the same night, but SO₄²⁻ loadings at Long Beach Harbor were 6 times higher than at Lennox. The SO₄²⁻/NO₃⁻ equivalent ratio was 1.9 in fogwater at Long Beach Harbor, compared to 0.2–0.5 values usually observed in the Los Angeles basin (1, 2). Cass (10) has shown that SO₄²⁻ concentrations in the Los Angeles basin peak in Long Beach Harbor because of residual oil burning by ships.

The fogs of Dec 7 and Dec 18, 1981, at Lennox and Dec 7, 1983, at Corona del Mar occurred during severe sulfate

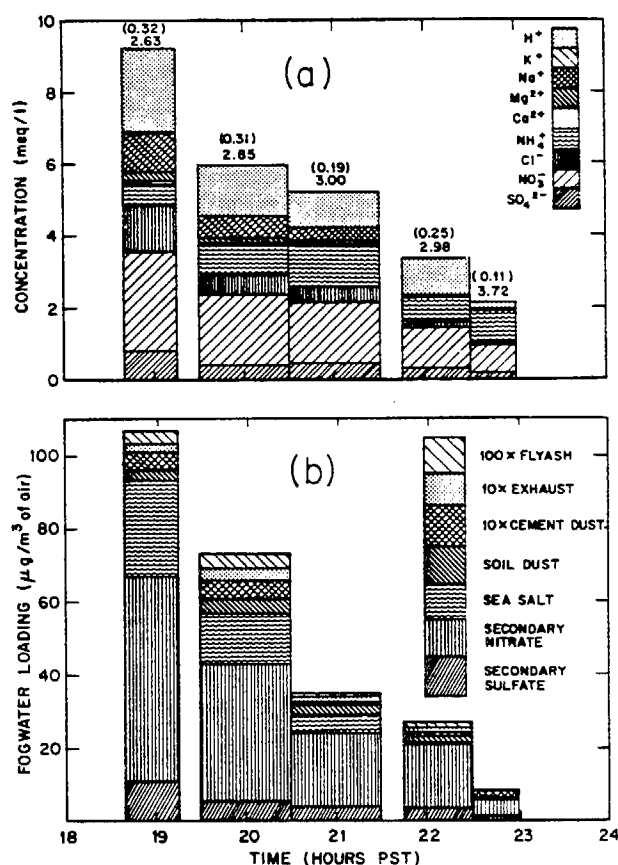


Figure 2. (a) Fogwater concentrations at Del Mar. pH values and liquid water contents (g m⁻³; in parentheses) are indicated on top of each data bar. (b) Source contributions to the fogwater loading at Del Mar; the fogwater loading is defined as the mass of material in fogwater per cubic meter of air. Contributions from soil dust, fly ash, and exhaust were not determined for the last sample.

pollution episodes in the Los Angeles basin. Fogwater pH values below 3 were consistently observed on those nights. On the day following the Corona del Mar event, all coastal stations of the South Coast Air Quality Management District recorded their highest 24-h SO₄²⁻ concentrations for 1982, ranging from 23 to 37 μg m⁻³. Prevailing southward transport of pollutants on the night of Dec 6–7, 1982 (28), explains the extremely high acidities observed at Corona del Mar; a second sample (1 mL) collected following the first as the fog dissipated had a pH of 1.69 (a value which was later confirmed in the laboratory).

High ionic concentrations and acidities were also found in samples collected at Del Mar on Jan 8, 1983 (Figure 2). NW winds over Del Mar at the beginning of the sampling period carried pollutants from the Los Angeles basin, which had been transported offshore by weak NE winds the previous morning (29). Flow was reversed by a developing land breeze between 1900 and 2000 Pacific standard time, and inland air from suburban San Diego County was advected over the site. Sea salt concentrations dropped considerably as the land breeze developed; contributions from anthropogenic sources, and acidities, also decreased as the Los Angeles air was replaced by less polluted air.

Fogwater collected at San Marcos Pass (low stratus), Morro Bay, Mt. Sutro, and Pt. Reyes contained much less NO₃⁻, secondary SO₄²⁻, and automobile exhaust than fogwater collected in the Los Angeles basin or downwind. However, except at Morro Bay, all samples were acidic; fogwater pH ranged from 4.21 to 4.69 at San Marcos Pass and from 3.60 to 5.00 at Pt. Reyes. Significant concen-

Table III. Liquid Water Weighted Average Fogwater Concentrations

site	date ^a	n	L ^b	pH	H ⁺	Na ⁺	K ⁺	NH ₄ ⁺	μequiv L ⁻¹				μg L ⁻¹							
									Ca ²⁺	Mg ²⁺	Cl ⁻	NO ₃ ⁻	SO ₄ ²⁻	n ^c	Fe	Mn	Pb	Cu	Ni	V
Del Mar	Jan 9, 1983, 1840-2300	5	0.24	2.85	1410	511	9	781	49	130	614 ^d	1850	469	4	354	36	310	NA	111	6
Corona del Mar	Dec 7, 1982, 2100-2300	1	0.11	2.16	6920	725	71	2860	197	188	1050	7900	1290	0	NA ^e	NA	NA	NA	NA	NA
Long Beach	Jan 6, 1983, 0400-0500	2	0.25	4.90	12.7	62	12	759	45	26	221 ^d	252	487	2	96	22	152	NA	17	1
Lennox ^f	Dec 7, 1981, 2305-0840	8	0.30	2.96	1100	65	12	1610	111	42	178 ^d	2210	926	8	1440	37	1180	34	10	6
	Dec 18, 1981, 2315-0045	3	0.14	2.66	2190	131	30	1280	127	48	150 ^d	2780	1280	3	1330	51	NA	NA	NA	13
	Jan 6, 1983, 0000-0430	5	0.17	3.63	237	41	8	464	39	18	68 ^d	365	126	5	315	127	447	NA	25	5
San Nicholas Island	Aug 26, 1982, 2115-0755	7	0.052	3.86	138	6060	148	452	450	1500	5490	1580	2080	5	431	93	49	49	99	9
San Marcos Pass/ Morro Bay	Aug 20, 1983, 2340-1200	14	0.43	4.49	32.1	10	3	97	3	4	19	74	55	9	22	3	23	12	6	NA
	July 14, 1982, 0500-0900	2	0.14	6.17	0.67	746	64	107	120	221	1200	114	214	1	192	21	11	57	21	3
Mt. Sutro	Aug 13, 1982, 2125-2225	1	0.056	3.99	102	648	52	183	93	170	851	87	319	1	160	10	24	50	28	NA
Pt. Reyes	Aug 9, 1982, 2200-0000	1	0.054	3.60	251	3520	91	327	242	890	3040	526	1280	1	484	67	67	87	209	NA
	Aug 10, 1982, 0230-1115	3	0.081	4.48	33.4	3150	72	95	153	782	4580	38	463	3	276	12	21	36	66	NA
	Aug 11, 1982, 0200-1155	7	0.13	3.88	132	498	12	59	27	118	645	36	208	4	301	10	38	151	59	NA
	Aug 12, 1982, 0340-0815	6	0.19	4.69	20	42	2	43	3	10	57	6	54	5	265	7	26	48	17	NA

^aDate is that of the a.m. samples or that of the morning following the fog. Time is local time. ^bAverage liquid water content (g m⁻³), calculated from the total volume collected. ^cNumber of samples analyzed for metals. ^dCl⁻ may be overestimated due to interference from organic acids during analysis. At Del Mar, this uncertainty is significant only for the last three samples (see text). ^e1981 events at Lennox have been previously reported (1). ^fStratus cloud. ^gNA, not analyzed.

Table IV. Source Contributions to Fogwater Loading

site	mass loading, $\mu\text{g m}^{-3}$						
	sea salt	secondary NO_3^-	secondary SO_4^{2-}	soil dust	cement dust	fuel oil fly ash	automobile exhaust
Del Mar	9.0	28	4.5	2.9	0.22	0.023	0.21
Corona del Mar	6.1	54	6.4	— ^b	0.80	—	—
Long Beach Harbor	1.1	3.9	5.8	0.58	0.44	0.0036	0.095
Lennox							
Dec 7, 1981	0.64	30	10	8.7	0.94	0.019	0.62
Dec 18, 1981	1.0	25	8.9	5.7	0.64	0.027	—
Jan 6, 1983	0.50	3.9	1.0	1.8	0.25	0.012	0.20
San Nicholas Island	23	5.2	3.4	0.55	0.41	0.0074	0.0064
San Marcos Pass	0.33	1.9	1.1	0.27	0.043	—	0.023
Morro Bay	7.5	1.1	0.9	0.97	0.55	0.0086	0.0055
Mt. Sutro	2.7	0.30	0.64	0.22	0.16	—	0.0033
Pt. Reyes							
Aug 9, 1982	14	1.8	2.2	0.74	0.21	—	0.0090
Aug 10, 1982	17	0.16	0.29	0.79	0.038	—	0.0034
Aug 11, 1982	5.2	0.28	0.9	1.6	0.017	—	0.014
Aug 12, 1982	0.48	0.074	0.45	1.6	0.0051	—	0.013

^a Mass loadings defined as the mass of material in fogwater per cubic meter of air. Numbers given are averages for each event. ^b Missing data. Contributions from soil dust, fly ash, or exhaust were not determined when the concentrations of their respective tracers (Fe, V, and Pb) were missing.

Table V. Ratios of Equivalent Fogwater Concentrations

site	$\text{Mg}^{2+}/\text{Na}^+$	Cl^-/Na^+	$\text{Ca}^{2+}/\text{Na}^+$	$\text{SO}_4^{2-}/\text{Na}^+$	K^+/Na^+
Del Mar	0.25	1.20	0.096	0.92	0.018
Corona del Mar	0.26	1.45	0.27	1.8	0.098
Long Beach Harbor	0.42	3.6	0.73	7.9	0.20
Lennox					
Dec 7, 1981	0.65	2.7	1.7	14	0.19
Dec 18, 1981	0.36	1.15	0.96	9.7	0.23
Jan 6, 1983	0.43	1.66	0.95	3.0	0.21
San Nicholas Island	0.25	0.91	0.074	0.34	0.024
San Marcos Pass	0.40	1.96	0.33	5.6	0.27
Morro Bay	0.30	1.61	0.16	0.29	0.086
Mt. Sutro	0.26	1.31	0.14	0.49	0.080
Pt. Reyes					
Aug 9, 1982	0.25	0.86	0.069	0.36	0.026
Aug 10, 1982	0.25	1.45	0.049	0.15	0.023
Aug 11, 1982	0.24	1.30	0.054	0.42	0.025
Aug 12, 1982	0.24	1.37	0.063	1.29	0.039
sea salt	0.23	1.17	0.043	0.12	0.021

trations of metals and non-sea salt (NSS) Ca at all sites show that the air sampled was of partly continental origin even under onshore wind conditions. Fogwater collected at Pt. Reyes under offshore wind conditions (Aug 12, 1983) contained less sea salt, more soil dust, and more automobile exhaust than fogwater collected on other nights under the more usual onshore N-NW wind conditions.

Nitrate and secondary sulfate loadings at San Nicholas Island were higher than those at other nonurban sites, even though impact of Los Angeles pollutants is very unlikely under the type of wind conditions observed on that night. High concentrations of metals and NSS Ca indicated that the air over the island was of mixed marine/continental origin. The high ratio of fly ash to automobile exhaust at that site (as opposed to the Los Angeles samples) suggests that the acid input could have been mostly due to a plume from either oil drilling operations off Pt. Conception or the Morro Bay power plant, advected over the site by NNW winds; dilution of the plume would have been limited by the low mixing height observed on that night and the slow horizontal dispersion over the ocean (15). Transport from the Pt. Conception area over San Nicholas Island has been previously documented (30).

Acidity of Coastal Fogs in California. Ubiquitous acidic conditions were observed along most of the California coastline. However, the precise origin of the acidity

observed at remote sites is difficult to ascertain from the data available. Acidic species can be transported over long distances with slow dispersion along the coast, because of the sea breeze/land breeze circulation system and the persistent temperature inversions which limit vertical mixing (12, 15). In the case of Mt. Sutro and Pt. Reyes, the low $\text{NO}_3^-/\text{SO}_4^{2-}$ ratios observed suggest a source of acidity especially rich in H_2SO_4 . Two possible sources are sulfate emitted from residual oil combustion by ships, or oxidation of dimethyl sulfide and other reduced sulfur species volatilized from the ocean surface (31, 32).

Fogwater at remote coastal sites was acidic even though the acid input was small. Obviously, there was little alkalinity available in the coastal air to neutralize acid inputs. The nonneutralized fraction of the acidity, $[\text{H}^+]/([\text{NO}_3^-] + 2[(\text{NSS})\text{SO}_4^{2-}])$, was on the average 25% at San Marcos Pass, 31% at Mt. Sutro, and 48% at Pt. Reyes. Ammonia emitted by agricultural sources was found to be the main acid-neutralizing component at inland sites in California (33). An excess of NH_3 ($H = 140 \text{ M atm}^{-1}$; $K_b = 1.6 \times 10^{-5} \text{ M at } 10^\circ\text{C}$) maintains fogwater pH above 5. Fogwater below pH 5, as found along the coast, supports only a very low NH_3 vapor pressure at equilibrium; under those conditions, NH_3 is expected to be nearly 100% scavenged by the fog droplets. The relatively low NH_4^+ fogwater concentrations observed at coastal sites (as com-

Table VI. Chemical Equilibria Involving Cl^- Loss in the $\text{NaCl-H}_2\text{SO}_4\text{-HNO}_3\text{-H}_2\text{O}$ System

no.	reaction	equilibrium constant ^a
1	$\text{HNO}_3(\text{g}) + \text{NaCl}(\text{s}) = \text{HCl}(\text{g}) + \text{NaNO}_3(\text{s})$	3.5
2	$2\text{NO}_2(\text{g}) + \text{NaCl}(\text{s}) = \text{NOCl}(\text{g}) + \text{NaNO}_3(\text{s})$	2.2×10^3
3	$\text{H}^+(\text{aq}) + \text{Cl}^-(\text{aq}) = \text{HCl}(\text{g})$	5.6×10^{-7}
4	$\text{H}^+(\text{aq}) + \text{NO}_3^-(\text{aq}) = \text{HNO}_3(\text{g})$	3.1×10^{-7}
5	$\text{H}^+(\text{aq}) + \text{SO}_4^{2-}(\text{aq}) = \text{HSO}_4^-(\text{aq})$	7.8×10^1

^aEquilibrium constants calculated at 298 K from free enthalpies of formation (39).

pared to NO_3^- and SO_4^{2-} concentrations) show that alkalinity from NH_3 was lacking in coastal air. Soil dust is an alternate source of alkalinity, but the extent of H^+ -neutralizing ion-exchange surface reactions is limited by the small amount of soil dust present in the fogwater (Table IV). These reactions would mostly involve the cations Ca^{2+} and Mg^{2+} , but as mentioned previously we found these ions to be almost totally dissolved. Alkalinity from scavenged soil dust was therefore exhausted.

Volatilization of HCl from Sea Salt Nuclei. Marine aerosols have been observed previously to exhibit Cl^- loss relative to its calculated sea salt contribution. Chloride losses ranging from 0% (no loss) up to 100% (no Cl^- aerosol) have been reported (34, 35). Chloride loss proceeds by incorporation of a strong acid in a sea salt containing aerosol, resulting in pH lowering and volatilization of HCl. The strong acid can be HNO_3 (34) or H_2SO_4 (35, 36). Displacement of Cl^- by $\text{NO}_2(\text{g})$ on $\text{NaCl}(\text{s})$ has also been found to occur (37, 38).

Table VI is a summary of chemical equilibria involving Cl^- loss. Above the deliquescence point, volatilization of HCl is given by the position of equilibrium 3. Both H_2SO_4 and HNO_3 added to a $\text{NaCl}(\text{aq})$ aerosol will displace Cl^- , but HNO_3 is less efficient than H_2SO_4 because it is only slightly less volatile than HCl. Hitchcock et al. (35) inferred from field data that HSO_4^- does not displace Cl^- ; however, equilibria 3 and 5 indicate that HSO_4^- could displace a substantial fraction of Cl^- at the liquid water contents typical of haze ($<10^{-3} \text{ g m}^{-3}$).

Although volatilization of HCl proceeds effectively in acidic haze, consideration of equilibrium 3 indicates that HCl is not volatilized in neutral or acidic fog. This is due to the high liquid water content of fogs and to the lower acidities of fog droplets as compared to the smaller haze droplets. If Cl^- were lost in the precursor aerosol, it should still be recovered in the fog by scavenging of $\text{HCl}(\text{g})$. Chloride deficiency with respect to its sea salt contribution in the fog therefore implies either that diffusion-limited scavenging of $\text{HCl}(\text{g})$ by the fog droplets did not proceed to completion or that the $\text{HCl}(\text{g})$ volatilized from the precursor aerosol was removed from the air parcel during transport before droplet activation.

The fogs sampled in our study were acidic, and Cl^- loss from the precursor aerosol would be expected. However, measured Cl^- concentrations were in excess of the sea salt contribution at most of our sites; this would be due to either anthropogenic sources of Cl^- or interference of organic acids with Cl^- in analysis. Significant Cl^- loss ($>10\%$) was observed in one sample from Del Mar (18%), all samples from San Nicholas Island (12–35%), and four samples from Pt. Reyes (10–28%). Therefore, Cl^- loss was observed in the fogwater only at those sites where a long residence time over the ocean was involved. Transport may have led to separation of $\text{HCl}(\text{g})$ from the nuclei; one way this could occur is if $\text{HCl}(\text{g})$ was removed to the ocean surface faster than aerosol Cl^- . Kritz and Rancher (40)

have reported deposition velocities over the ocean surface of 0.4 cm s^{-1} for aerosol Na and 0.8 cm s^{-1} for gaseous inorganic Cl.

Conclusion

Fogwater samples collected at both urban and nonurban sites along the coast of California were consistently acidic. Substantial continental and anthropogenic influences were determined at remote coastal sites. Acid-neutralizing capacities in coastal air were found to be very low and insufficient to neutralize even low acid inputs. Chloride loss in fogwater relative to its sea salt contribution was observed at sites furthest from anthropogenic sources.

Extremely high fogwater acidities were observed in the Los Angeles basin and downwind. Fogwater pH dropped down to 1.69 at a site downwind of the basin during a high sulfate pollution episode. Millimolar NO_3^- concentrations, and pH values below 3, were associated with the advection of the Los Angeles plume over a site near San Diego.

Acknowledgments

We thank the organizations who provided us with sampling sites: the U.S. Navy, the National Park Service, the South Coast Air Quality Management District, the San Luis Obispo Air Pollution Control District, and the San Diego Air Pollution Control District.

Registry No. H^+ , 12408-02-5; K, 7440-09-7; Na, 7440-23-5; Mg, 7439-95-4; Ca, 7440-70-2; NH_4^+ , 14798-03-9.

Literature Cited

- (1) Munger, J. W.; Jacob, D. J.; Waldman, J. M.; Hoffmann, M. R. *J. Geophys. Res.* 1983, 88, 5109–5123.
- (2) Brewer, R. L.; Ellis, E. C.; Gordon, R. J.; Shepard, L. S. *Atmos. Environ.* 1983, 17, 2267–2271.
- (3) Richards, L. W.; Anderson, J. A.; Blumenthal, D. L.; McDonald, J. A.; Kok, G. L.; Lazrus, A. L. *Atmos. Environ.* 1983, 17, 911–914.
- (4) Waldman, J. M.; Munger, J. W.; Jacob, D. J.; Hoffmann, M. R. *Tellus*, in press.
- (5) Scherbatskoy, T.; Klein, R. M. *J. Environ. Qual.* 1983, 12, 189–195.
- (6) Granett, A. L.; Musselman, R. C. *Atmos. Environ.* 1984, 18, 887–891.
- (7) Hoffmann, M. R. *Environ. Sci. Technol.* 1984, 18, 61–63.
- (8) Martin, L. R. "Acid Precipitation: SO_2 , NO, and NO_2 Oxidation Mechanisms: Atmospheric Considerations"; J. G. Calvert, Ed.; Butterworth: Boston, MA, 1984; pp 63–100.
- (9) Kaplan, D. J.; Himmelblau, D. M. *Atmos. Environ.* 1981, 15, 763–773.
- (10) Cass, G. R. *Atmos. Environ.* 1981, 15, 1227–1249.
- (11) Hegg, D. A.; Hobbs, P. V. *Atmos. Environ.* 1982, 16, 2663–2668.
- (12) Cass, G. R.; Shair, F. H. *J. Geophys. Res.* 1984, 89, 1429–1438.
- (13) Zeldin, M. D.; Davidson, A.; Brunelle, M. F.; Dickinson, J. E. Southern California Air Pollution Control District, El Monte, CA, 1976, Evaluation and Planning Report 76-1.
- (14) deViolini, R. Pacific Missiles Range, Pt. Mugu, CA, 1974, Technical Publication TP/74/1.
- (15) Reible, D. D. Ph.D. Dissertation, California Institute of Technology, Pasadena, CA, 1982.
- (16) Azevedo, J.; Morgan, D. L. *Ecology* 1974, 55, 1135–1141.
- (17) California Air Resources Board "Air Quality Aspects of the Development of Offshore Oil and Gas Resources"; California Air Resources Board: Sacramento, CA, 1982.
- (18) Jacob, D. J.; Wang, R.-F. T.; Flagan, R. C. *Environ. Sci. Technol.* 1984, 18, 827–833.
- (19) Hering, S. V.; Blumenthal, D. L. "Fog Sampler Intercomparison Study: Final Report". Coordinating Research Council, Atlanta, GA, 1985.

- (20) Katz, U. "Communications a la 8^{eme} Conference sur la Physique des Nuages"; Laboratoire Associe de Meteorologie Physique: 63170 Aubiere, France, 1980; pp 697-700.
- (21) Nagamoto, C. T.; Parungo, F.; Reinking, R.; Pueschel, R.; Gerish, T. *Atmos. Environ.* 1983, 17, 1073-1082.
- (22) Waldman, J. M. Ph.D. Dissertation, California Institute of Technology, Pasadena, CA, 1985.
- (23) Friedlander, S. K. *Environ. Sci. Technol.* 1973, 7, 235-240.
- (24) Cooper, J. A.; Watson, J. G., Jr. *J. Air Pollut. Control Assoc.* 1980, 30, 1116-1125.
- (25) Weast, R. C., Ed. "Handbook of Chemistry and Physics", 56th ed.; CRC Press: Cleveland, OH, 1975; p F-199.
- (26) Miller, M. S.; Friedlander, S. K.; Hidy, G. M. *J. Colloid Interface Sci.* 1972, 39, 165-176.
- (27) Jacob, D. J. Ph.D. Dissertation, California Institute of Technology, Pasadena, CA, 1985.
- (28) Unger, C. D. "An Analysis of Meteorological and Air Quality Data Associated with the Occurrence of Fogwater with High Acidity in the Los Angeles Basin"; California Air Resources Board, Sacramento, CA, July 18, 1984, memorandum.
- (29) Brown, H. W. "An Analysis of Air flow over the Southern California Bight and Northern San Diego County on January 8, 1983". San Diego Air Pollution Control District, San Diego, CA, 1983.
- (30) Rosenthal, J.; Battalino, T. E.; Hendon, H.; Noonkester, V. R. Pacific Missiles Test Center, Pt. Mugu, CA, 1979, Technical Publication TP/79/33.
- (31) Atkinson, R.; Perry, R. A.; Pitta, J. N., Jr. *Chem. Phys. Lett.* 1978, 54, 14-18.
- (32) Nguyen, B. C.; Bonsang, B.; Gaudry, A. *J. Geophys. Res.* 1983, 88, 10903-10914.
- (33) Jacob, D. J.; Munger, J. W.; Waldman, J. M.; Hoffmann, M. R. Proceedings of the 77th Annual Meeting of the Air Pollution Control Association, San Francisco, CA, Air Pollution Control Association, Pittsburg, PA, 1984, paper 24-5.
- (34) Martens, C. S.; Welosowski, J. J.; Harriss, R. C.; Kaifer, R. *J. Geophys. Res.* 1973, 78, 8778-8792.
- (35) Hitchcock, D. R.; Spiller, L. L.; Wilson, W. E. *Atmos. Environ.* 1980, 14, 165-182.
- (36) Eriksson, E. *Tellus* 1960, 12, 63-109.
- (37) Robbins, R. C.; Cadle, R. D.; Eckhardt, D. L. *J. Met.* 1959, 16, 53-56.
- (38) Finlayson-Pitts, B. J. *Nature (London)* 1983, 306, 676-677.
- (39) Latimer, W. D. "The Oxidation States of the Elements and Their Potentials in Aqueous Solutions", 2nd ed.; Prentice-Hall: New York, 1952.
- (40) Kritz, M. A.; Rancher, J. *J. Geophys. Res.* 1980, 85, 1633-1639.

Received for review September 17, 1984. Accepted February 12, 1985. This research was funded by the California Air Resources Board (Contract A2-048-32).

CHAPTER 17

NUTRIENT LEACHING FROM PINE NEEDLES IMPACTED BY ACIDIC CLOUDWATER

JED M. WALDMAN

*Department of Environmental and Community Medicine, UMDNJ-Robert Wood Johnson Medical School,
Piscataway, NJ 08854, U.S.A.*

and

MICHAEL R. HOFFMANN

*Department of Environmental Engineering Science, California Institute of Technology (138-78),
Pasadena, CA 91125, U.S.A.*

(Received July 2, 1987; revised November 6, 1987)

Abstract. In coastal and mountainous environments, fog and cloud droplets are frequently deposited onto terrestrial surfaces; this deposition pathway may account for a large fraction of both moisture and chemical loading. Stratus cloudwater was collected for chemical analyses at Henninger Flats (870 m MSL), a site in the foothills of the San Gabriel Mountains, 25 km northeast of downtown Los Angeles. Concurrent samples of intercepted cloudwater were manually removed, drop-by-drop, from needles on various species of pine trees upon which it had deposited. Samples were analyzed for pH, major cations, and anions. Solute concentrations were substantially higher in samples removed from pine needles compared to the suspended cloudwater. For example, cloudwater concentrations for nitrate and sulfate were measured between 0.25 and 4.5 meq L⁻¹ while deposited samples were 0.4 to 90 meq L⁻¹. This solute enhancement was due to evaporation following droplet deposition and to nutrient leaching. Nutrient leaching was indicated by (a) a disproportionate increase in the concentrations of cations such as K and Mg (a factor of 2 to 15 enrichment relative to sulfate), and (b) reductions in the leachate acidity and ammonium relative to the incident droplets. A relationship was observed between the enhancement of Na, Ca, and nitrate in pine needle leachate. This suggests that reactions at the foliar surfaces are occurring which involve gaseous HNO₃ and accumulated soil dust and sea-salt particles.

1. Introduction

Rain or intercepted cloudwater which passes through the forest canopy is known as throughfall, and it is found to be routinely enriched in selected inorganic and organic compounds. The leaching of nutrients from foliage is promoted by acidic deposition which often results in the displacement of cations due to ion exchange (Tukey, 1970). Exposure of a variety of plants has shown nutrient loss as well as tissue damage at threshold pH's between 2 and 3; reduction in plant yields generally were noted for low pH values (Haines *et al.*, 1980). Significant deficiencies of K, Ca, Mg, and Mn in vegetative and soil nutrient pools have been noted by Zoetl and co-workers in the Black Forest of West Germany; replacement in the soil by fertilizing has reversed plant injury in some cases (Zoetl and Huettl, 1985).

Measurements of fog- and cloudwater compositions have shown that droplet chemistry can be strongly altered by the scavenging of ambient pollutants especially in urban-impacted regions such as Los Angeles (Munger *et al.*, 1983). Droplets are acidified by the uptake of strong acid gases (e.g., HNO₃ and SO₂), by acidic aerosols

(e.g., H_2SO_4 and NH_4HSO_4), and by the *in situ* oxidation of S(IV) in the aqueous phase. While these pathways are also important to precipitation chemistry, the smaller droplet sizes of fog and clouds lead to far higher aqueous concentrations than in rainwater.

In coastal and mountainous environments, fog and cloud droplets are frequently deposited directly onto terrestrial surfaces; this deposition pathway may account for a large fraction of both moisture and chemical loading (Kerfoot, 1968). In addition to the total dose of acidity contributed by fog and cloud droplet impaction, the exposure of sensitive plant tissue to the more concentrated droplets may cause additional impacts due to the intensity of acidity. In fact, plant injury in forests has been noted to increase at higher elevations where slope immersion by clouds is most frequent and where other stress factors become important (Johnson and Siccama, 1983).

2. Experimental Method

Stratus cloudwater was collected for chemical analysis at Henniger Flats (870 m MSL), a site in the foothills of the San Gabriel Mountains, 25 km northeast of downtown Los Angeles. Samples were analyzed for pH, major cations, and anions; cloudwater collection and analytical techniques are described in Waldman *et al.* (1984).

In June 1984, concurrent samples of intercepted cloudwater were removed, drop-by-drop into polyethylene vials, by manually touching the vial to droplets on pine needles upon which the cloudwater had deposited. The stand of trees includes primarily Aleppo, Coulter, and Monterey \times Knobcone-hybrid pines, which were first cultivated at the site 50 to 75 yr ago, and has a canopy height of 20 to 30 m.

These pine needle leachate samples were filtered and then analyzed similar to cloudwater samples. Filterable particles in the cloudwater samples were found to make a negligible contribution to solute analyte. However, pine needle leachate needed to be filtered through polycarbonate medium (0.2 μm pore size) immediately after collection to remove particles of plant tissue and other insoluble materials.

3. Results

The ionic compositions of cloudwater (CW) and pine needle leachate (PL) samples are presented in Table I. Volume-weighted mean values are given for CW samples for the indicated intervals on each date. The PL samples were generally many times more concentrated than concurrent CW for most ionic species.

In the canopy, deposited cloudwater droplets aggregate and remain on the pine needles before dripping to the ground. Evaporation takes place because relative humidities in the canopy can drop below 100% when the bulk of condensed-phase water is removed by droplet impaction (Lovett, 1984). Acting alone, evaporation would cause equal increases in the concentrations of all ions. At the low pH's of these samples, weak acids are fully protonated; thus, H^+ would also be a conservation species with respect to volume changes caused by evaporation. Additional contributions to the total solute

TABLE I
Cloudwater^a & pine needle leachate^b samples

	Time	pH	H ⁺	Na ⁺	K ⁺	Milliequivalents per liter						
						NH ₄ ⁺	Ca ²⁺	Mg ²⁺	Cl ⁻	NO ₃ ⁻	SO ₄ ²⁻	-/+
3 June 1984												
FOG: 23:00 to 5:00		2.74	1.8	3.18	0.96	1.5	0.74	0.83	1.2	4.46	2.52	1.01
P. attenuata	4:00	3.00	1.0	24.2	0.9	6.8	26.6	10.0	6.1	54.9	15.4	1.10
P. attenuata	4:15	3.35	0.4	18.0	1.0	4.2	46.4	22.7	9.7	68.4	20.0	1.06
P. halepensis	4:30	2.95	1.1	32.1	2.1	8.0	43.2	17.4	8.8	84.6	17.9	1.07
5 June 1984												
FOG: 8:00 to 12:00		3.23	0.59	0.29	0.006	0.30	0.07	0.08	0.26	0.56	0.51	1.00
P. aleppo	6:05	2.72	1.9	19.7	1.5	5.5	24.5	9.8	7.1	54.6	11.3	1.16
P. coulteri (a)	6:15	2.82	1.5	10.7	1.0	3.3	24.7	10.4	7.3	37.5	10.8	1.08
P. coulteri (d)	6:20	2.78	1.7	9.5	0.8	4.2	12.3	4.6	3.5	26.1	5.6	1.07
P. coulteri (b)	6:30	2.82	1.5	9.7	1.7	0.0	16.3	7.2	6.2	30.8	8.4	1.24
P. attenuata	6:45	2.75	1.8	28.2	1.5	6.6	29.6	13.0	11.2	58.9	16.0	1.07
R. rad. × att.	7:00	2.70	2.0	37.9	2.3	9.7	49.9	17.1	13.3	90.0	19.4	1.03
P. coulteri (a)	11:00	2.90	1.3	8.6	0.5	2.7	15.8	6.4	4.4	26.7	7.9	1.10
P. halepensis	11:15	2.86	1.4	8.2	0.9	3.5	11.6	4.4	3.5	24.8	5.4	1.13
P. rad. × att.	11:30	2.92	1.2	10.9	0.7	3.4	12.0	5.2	4.4	27.3	5.5	1.11
6 June 1984												
FOG: 9:30 to 12:30		3.58	0.26	0.07	0.002	0.16	0.05	0.02	0.07	0.29	0.25	1.08
P. coulteri (a)	0:00	3.08	0.8	11.0	0.8	4.2	19.8	8.4	7.3	34.8	9.9	1.16
P. aleppo	0:00	2.32	4.8	7.3	1.0	1.8	9.9	4.3	4.0	28.8	5.1	1.30
P. coulteri (b)	0:00	3.08	0.8	5.6	1.1	na	9.4	4.1	4.7	18.3	4.1	1.29
P. coulteri (a)	10:15	3.45	0.4	0.6	0.2	na	0.9	0.4	0.5	1.9	0.9	1.38
Pine seedling	10:30	3.23	0.6	0.9	0.1	0.4	1.3	0.5	0.5	3.0	0.8	1.13
P. coulteri (b)	10:45	3.20	0.6	2.1	0.6	0.2	3.9	2.0	1.2	5.3	1.3	0.83
P. rad × att.	11:00	3.50	0.3	0.5	0.1	0.3	0.5	0.2	0.3	1.4	0.4	1.18
Pine seedling	13:30	3.50	0.3	1.0	0.1	0.1	1.5	0.6	0.5	3.1	0.9	1.22
P. coulteri (b)	13:45	3.22	0.6	2.2	0.8	0.2	3.7	1.9	1.8	7.4	1.8	1.17
P. rad × att.	14:00	3.55	0.3	0.9	0.2	0.1	1.2	0.5	0.7	2.7	0.7	1.29
12 June 1984												
FOG: 8:00 to 11:00		3.05	0.89	1.29	0.03	1.05	0.36	0.35	0.57	2.47	1.11	1.05
P. rad. × att.	8:15	3.22	0.6	15.6	0.4	5.3	6.7	4.8	6.6	25.5	5.0	1.11
P. coulteri (c)	8:15	3.22	0.6	12.3	0.4	3.4	7.1	4.2	5.2	20.7	5.2	1.11
P. coulteri (a)	9:30	3.12	0.8	7.6	0.4	2.7	5.2	2.9	3.5	14.2	3.9	1.11
P. rad. × att.	11:00	3.14	0.7	5.6	0.2	1.5	2.8	1.9	2.6	11.3	2.3	1.27

^a Liquid water content-weighted mean concentrations for cloudwater samples during periods of FOG.

^b Samples from different species of *Pinus*; letter in parenthesis indicates repetitive sampling at same location.

in PL relative to CW could originate from (a) the washout of material deposited before the impact of cloudwater, and (b) the exchange of CW ions with plant tissue metabolites.

The concentration of ions in the PL samples did not increase in equal proportions relative to CW samples. This suggests that some ions were selectively lost or gained while the drops were in contact with the pine needles. Fractional compositions of cations in several concurrent CW and PL samples are shown in Figure 1. The pH values among CW and PL samples on a given day were similar, although the PL values were sometimes lower than CW values, presumably because of evaporation. However, the proportion of H^+ was substantially lower in PL samples. This relative loss of acidity points to ion exchange: base cations for protons. For a hardwood canopy, roughly half of the cation leaching can result from cation-exchange reactions, primarily driven by deposited H^+ (Lovett *et al.*, 1985). Similar results may be expected for conifer canopies, although field data are not presently available.

A reduction in the fraction of NH_4^+ in leachate was also noted. Ion exchange involving ammonium is generally not observed in foliar systems (Mengel and Kirby,

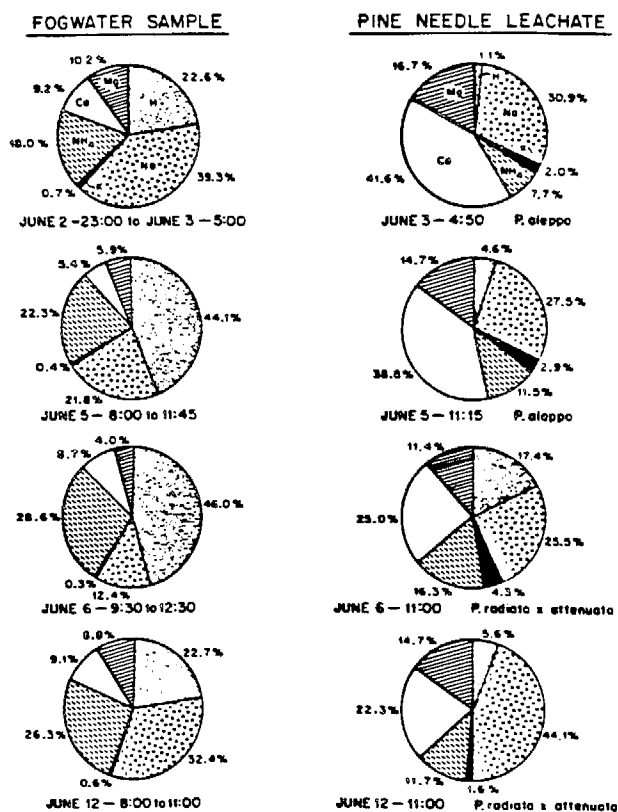


Fig. 1. Cation fractions for concurrent cloudwater and pine needle leachate samples.

1982). In this case, ammonium retention was possibly due to biological assimilation and the activity of fungi or bacteria.

4. Discussion

It appears that there is great variability in the effect of microphysical (i.e., particle deposition and drop evaporation) processes on the chemical composition of PL samples. In an attempt to normalize the effect of evaporation and prior accumulation caused by dry deposition, sulfate ion was taken as a pseudo-conservative tracer for deposition of ions in cloudwater. Sulfate ion was taken as the frame of reference because the amount accumulated on needles prior to each event should be lowest – relative to the other species measured. This is due to the smaller size of sulfate aerosols and their lower deposition; soil dust (Ca and Mg), sea-salt (Na and Cl), and nitrate aerosols are coarser than secondary sulfate aerosols (Whitby and Sverdrup, 1980) and deposit at greater rates under dry condition (Davidson and Friedlander, 1978). Furthermore, nitrate ion deposition will occur rapidly whenever gaseous HNO_3 is present (Huebert and Robert, 1985). Finally, samples were collected during extended periods of clouds immersion, reducing the impact of previously deposited particles.

The increase or decrease in ionic composition of each leachate sample was evaluated using the assumption that sulfate was chiefly deposited with CW. The enhancement in the pine needle leachate, relative to the measured cloudwater concentration for species i , was calculated as follows:

$$\text{Enrichment fraction} = \frac{[C_i]_{\text{PL}}([SO_4^{2-}]_{\text{CW}}/[SO_4^{2-}]_{\text{PL}}) - [C_i]_{\text{CW}}}{[C_i]_{\text{CW}}} \quad (1)$$

where: $[C_i]$ and $[SO_4^{2-}]$ are the concentrations of species i and sulfate, respectively, in concurrent PL and CW samples.

Hence, sulfate values were used to scale PL ion concentrations to those of the incident CW. The relative enrichment of ions by washout or leaching is underestimated to the extent that previously deposited sulfate actually contributed to the measured value of SO_4^{2-} in PL samples. Sulfate from the dry deposition of $SO_2(g)$ has been neglected because concentrations were generally low (≤ 5 ppb) during the study.

Values for the fraction of enrichment or depletion of CW ions are shown in Figure 2. All species were significantly enhanced relative to sulfate, with the exception of H^+ and NH_4^+ . An enrichment fraction below zero represents depletion. As shown in the figure, the strong acidity was almost entirely depleted, and ammonium was depleted by roughly half.

The *amount* of enrichment, i.e., the numerator in Equation (1), for NO_3^- in PL samples was found to be very close or equal to the sum of Na^+ and Ca^{2+} ion enrichment (Figure 3). This suggests that these ions were removed together, perhaps by the washout of neutral salts. The deposition of coarse soil dust and sea-salt aerosols would readily contribute to Ca and Na accumulation on pine needles, respectively. With the sub-

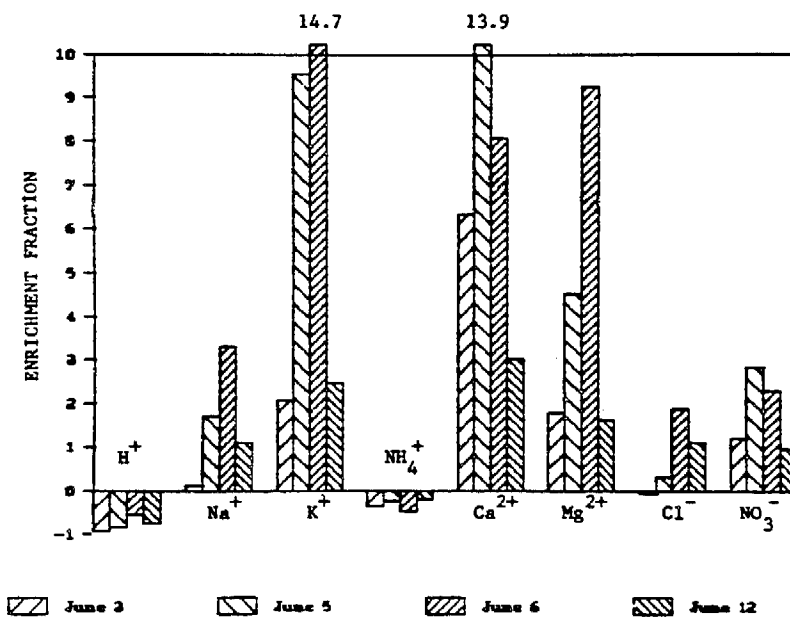


Fig. 2. Fraction of enhancement for ionic species in pine needle leachate compared to concurrent cloudwater samples, taking sulfate as pseudo-conservative.

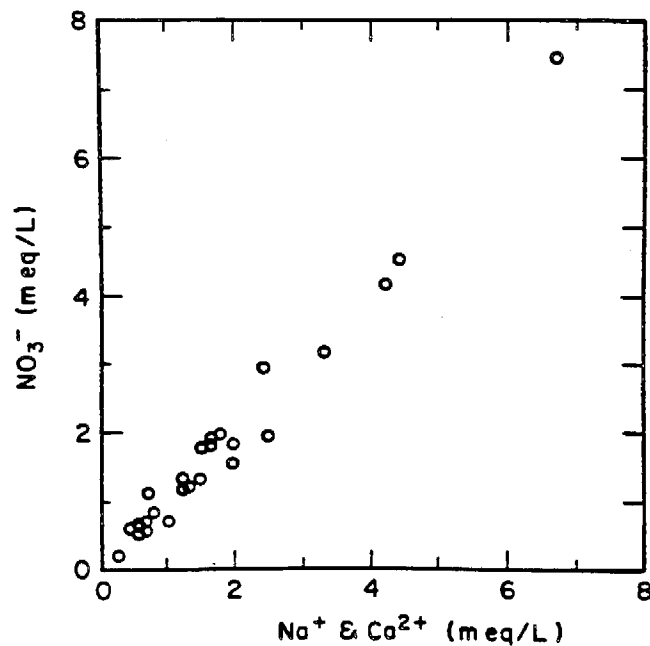
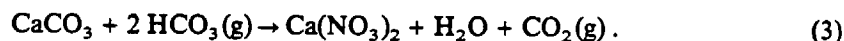
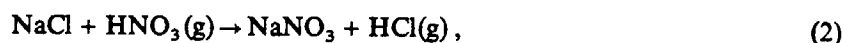


Fig. 3. Comparison of amount of ionic enrichment for all pine needle leachate samples:
 Nitrate = $1.06 \times [Na + Ca] - 0.06$ ($r = 0.986$).

sequent deposition of nitric acid, nitrate could become associated with these ions by the following reactions:



In the former reaction, no net deposition of acidity to the surface occurs. In the latter case, accumulated alkalinity is consumed by the HNO_3 deposited. Also, the reaction in Equation (3) serves to increase Ca solubility considerable. Thus, the amount of HNO_3 deposited to the pine needles may be limited by the availability of alkaline material, since HNO_3 is readily volatilized at daytime temperatures and humidities in the absence of neutralization (Stelson and Seinfeld, 1982).

However, the enrichment observed for K cannot be attributed to dry deposition and the subsequent salt washout. Cloudwater at the site had relatively low K concentrations (Figure 1); dry aerosol samples for the same period were also deficient in K (Waldman, 1986). Thus, the K fraction in PL samples was far higher than would be expected from the prior accumulation of dry particles. Instead, the high factors of enrichment are an indication of nutrient leaching from the needle tissue. Likewise, Mengal *et al.* (1987) demonstrated that substantially higher amounts of K leached from pine needles misted with acidic (pH 2.75) compared to the control (pH 5) solutions.

Knowledge of the chemical loadings to the pine needles before cloudwater impaction would be desirable; however such measurements are difficult to make and often irreproducible (Lindberg *et al.*, 1982). Nonetheless, the analyses of pine needle leachate samples provide a novel complement to cloudwater composition data and give new insights to the interactions occurring at the receptor surfaces. Interestingly, there was a surprising similarity in the fractions of enrichment and depletion in the samples for different dates as well as different species. Finally, the contribution of cloud droplet-deposited acidity has been shown to be similar to the flux from rainfall at this site (Waldman *et al.*, 1984). Thus, considerations of *intensity* and *dose* of cloudwater acidity underscore its potential for substantial impact on forest health in mountainslope ecosystems.

Two years before this study, the same population of pine trees showed a higher-than-normal incidence of needle necrosis and chlorosis, primarily among the Monterey \times Knobcone-hybrid pines (*P. radiata* \times *attenuata*) (Waldman *et al.*, 1984). At that time, it was postulated that O_3 and cloudwater had a synergistic effect on needle surfaces.

Karhu and Huttunen (1986) studied the erosion effects of air pollutants, presumably O_3 , on the epicuticular wax of conifer needles in southern California. Scanning electron micrographs showed chronic injury to the needles of slightly stressed trees. Holes, cracks and erosion of the epicuticular waxes and cuticle may be expected to promote the egress of leaf electrolytes, hence the leaching of buffering ions, such as K^+ , Ca^{2+} , and Mg^{2+} , which exchange with H^+ . Recent studies have identified *in vivo* acid neutralization and buffering of acidic raindrops on foliar surfaces (e.g., Larsen, 1986; Hutchinson *et al.*, 1986).

The hypothesis of a synergism between O_3 (promoting erosion) and acid mist (promoting ion exchange for H^+) has been discussed widely in the debate regarding the forest decline in Europe (e.g. Krouse *et al.*, 1986). Prinz and co-workers (Prinz *et al.*, 1982; Krause *et al.*, 1983) first outlined a plausible mechanism of the impact of ozone and acidic deposition which could lead to nutrient deficiency and, hence, forest decline. In laboratory experiments on conifer species, it was shown that ozone promoted greater efflux of major ions from trees exposed to up to 300 ppb O_3 and subsequent acidic (pH 3.5) mists compared to control cases; the effect was found to be dependent on the O_3 concentration (Krause *et al.*, 1983). As in our study, the ions demonstrating the greatest leaching were K, Ca, Mg, nitrate. Interestingly, sulfate leaching also was shown to be enhanced by the combined exposure to O_3 and acidic mists. As implied previously, underestimation of sulfate leaching would lead to a like undervaluing of the enhancement factors calculated above.

5. Conclusions

This unique data set highlights aspects of the chemical interactions occurring at foliar surfaces in a polluted, cloud-impacted environment. Solute concentrations were substantially higher in water removed from pine needles. This was due to evaporation following droplet deposition and to nutrient leaching. Nutrient leaching was indicated by a disproportionate increase in the concentrations of cations such as K^+ and Mg^{2+} and reductions in leachate acidities relative to the incident droplets. Higher concentrations of Na, Ca, and nitrate appear also to be the result of washout of accumulated deposits of soil dust, sea-salt particles, and gaseous HNO_3 prior to cloudwater impaction.

Acknowledgements

We are grateful to Los Angeles Fire Department Forestry Bureau for their permission and assistance at Henninger Flats. This research was supported by a contract with the California Air Resources Board. We are grateful to our colleagues, Dr Daniel Jacob and Mr Bill Munger, for their assistance, and to Dr Paul Miller and the anonymous reviewers for their helpful comments.

References

- Davidson, C. I. and Friedlander, S. K.: 1978, *J. Geophys. Res.* **83**, 2342.
- Haines, B., Stefani, M., and Hendrix, F.: 1980, *Water, Air, and Soil Pollut.* **14**, 403.
- Huebert, B. J. and Robert, C. H.: 1985, *J. Geophys. Res.* **90D**, 2085.
- Hutchinson, T. C., Adams, C. M., and Gaber, B. A.: 1986, *Water, Air, and Soil Pollut.* **31**, 475.
- Johnson, A. H. and Siccama, T. G.: 1983, *Environ. Sci. Technol.* **17**, 294A.
- Karhu, M. and Huttunen, S.: 1986, *Water, Air, and Soil Pollut.* **31**, 417.
- Kerfoot, O.: 1968, *Forest Abst.* **29**, 8.
- Krause, G. H. M., Prinz, B., and Jung, K. D.: 1983, in: Davis, D. D. and Dochinger, L. (eds.), Proceedings of the Symposium, *Air Pollution and the Productivity of the Forest*. Izaak Walton League, Washington D.C. October 3-4, pp. 297-332.

- Krause, G. H. M., Arndt, U., Brandt, C. J., Bucher, J., Kenk, G., and Matzner, E.: 1986, *Water, Air, and Soil Pollut.* **31**, 647.
- Larsen, B. R.: 1986, *Water, Air, and Soil Pollut.* **31**, 401.
- Lindberg, S. E., Harriss, R. C., and Turner, R. R.: 1982, *Science* **215**, 1609.
- Lovett, G. M.: 1984, *Atmos. Environ.* **18**, 361.
- Lovett, G. M., Lindberg, S. E., Richter, D. D. and Johnson, D. W.: 1985, *Can J. For. Res.* **15**, 1055.
- Mengel, K. and Kirby, E. A.: 1982, *Principles of Plant Nutrition*, Worblaufen-Bern/Switzerland: International Potash Institute, pp. 137-138.
- Mengel, K., Lutz, H. J., and Breininger, M. Th.: 1987, *Z. Pflanzenernähr. Bodenk.* **150**, 61.
- Munger, J. W., Jacob, D. J., Waldman, J. M., and Hoffmann, M. R.: 1983, *J. Geophys. Res.* **88C**, 5209.
- Prinz, B., G. H. M., and Stratmann, H.: 1982, 'Waldschaden in der Bundesrepublik Deutschland', *LIS-Berichte Nr. 28*, Essen 1982.
- Stelson, A. W. and Seinfeld, J. H.: 1982, *Atmos. Environ.* **16**, 983.
- Tukey, Jr., H. B.: 1970, *Ann. Rev. Plant Physiol.* **71**, 305.
- Waldman, J. M.: 1986, 'Depositional Aspects of Pollutant Behavior in Fog', Ph.D. Thesis, California Institute of Technology (also available as W. M. Keck Laboratory Report No. AC-11-85), Pasadena, CA.
- Waldman, J. M., Munger, J. W., Jacob, D. J., and Hoffmann, M. R.: 1984, *Tellus* **37B**, 91.
- Whitby, K. T. and Sverdrup, G. M.: 1980, *Adv. Environ. Sci. Technol.* **9**, 477.
- Zoettl, H. W. and Huettl, R. F.: 1985, *Water, Air, and Soil Pollut.* **31**, 449.

CHAPTER 18

Tellus (1985), 37B, 91–108

Chemical characterization of stratus cloudwater and its role as a vector for pollutant deposition in a Los Angeles pine forest

By JED M. WALDMAN, J. WILLIAM MUNGER, DANIEL J. JACOB, and MICHAEL R. HOFFMANN, *Department of Environmental Engineering Science, W. M. Keck Engineering Laboratories (138-78), California Institute of Technology, Pasadena, CA 91125, USA*

(Manuscript received June 25; in final form December 4, 1984)

ABSTRACT

Highly concentrated, acidic stratus cloudwater was monitored as it intercepted a pine forest (Henninger Flats) 25 km northeast of Los Angeles. Observed pH values ranged from 2.06 to 3.87 for over 100 samples collected in 1982 and 1983 with a median value below pH 3. The ratio of nitrate/sulfate in cloudwater samples was between 1.5 and 2; rainwater at the same site had a ratio of approximately 1. The solute deposition accompanying several light, spring rains (summing to ~1% of annual rainfall) was a disproportionate fraction of the annual total: H^+ , NO_3^- and SO_4^{2-} were ~20% or more. Based on a reasonable estimate of fog precipitation, deposition of sulfate, nitrate and free acidity due to intercepting stratus clouds may be of comparable magnitude as that due to the incident rainfall at Henninger Flats.

Cloudwater that had deposited on local pine needles was collected. It was in general more concentrated than ambient cloudwater but with comparable acidity. Enrichment of K^+ and Ca^{2+} in those samples and in throughfall is believed to be due to leaching from foliar surfaces. Injury to sensitive plant tissue has been noted in the literature when prolonged exposure to this severe kind of micro-environment has been imposed.

1. Introduction

In addition to the orographic enhancement of precipitation at mountain sites, cloud droplet capture can lead to greater pollutant deposition relative to the surrounding lowlands. Fog-derived (sometimes called mist or "occult") precipitation has been determined to be an important hydrological input to some ecosystems (Kerfoot, 1968). Also, measurements of cloudwater composition have shown it to have higher aqueous-phase concentrations compared to precipitation at the same locale (Mrose, 1966; Okita, 1968; Munger et al., 1983b). These two factors combine to suggest the potential for significant pollutant deposition in mountain forests impacted by frequent cloud interception. Often omitted from mass-balance calcu-

lations or regional monitoring, this pathway may represent an important component of the total deposition. By accelerating removal of local emissions, this may be especially significant in urban-impacted environments.

Enhanced precipitation in coastal and mountain forests has been reported for collectors located beneath trees exposed to fog-laden wind. Topography, leaf shape and total area, and canopy structure are important parameters (Kerfoot, 1968). In an early study of fog interception in Japan (Yosida, 1953), an average fogwater deposition rate of 0.5 mm h^{-1} was reported for a coastal forest. Oberlander (1956) measured between 45 and 1500 mm of fog-derived precipitation in less than 6 weeks on the San Francisco peninsula with collectors beneath 5 trees. Although it did not include the frequency or duration of fog,

that study underscored the magnitude of water flux and emphasized the importance of location in addition to the height of the trees in affecting fog-derived precipitation. A number of investigators have employed artificial foliar collectors (Schlesinger and Reiners, 1974) or screen "fog-catchers" (Nagel, 1956; Ekern, 1964; Vogelmann et al., 1968; Vogelmann, 1973; Azevedo and Morgan, 1974) to measure the enhancement of water catchment by horizontal interception. Because of their relatively small interception cross-sections, these collectors may underestimate the flux of fog precipitation induced by the actual forest canopy. The fog-derived precipitation in these studies represented a significant fraction of the total water flux—up to several times the measured incident rainfall.

Following the incorporation of aerosol and gaseous species into cloud and fog droplets, dissolved pollutant species may be brought into contact with vegetative surfaces. The chief mechanisms for deposition are impaction, sedimentation—both strongly enhanced by increased particle inertia—and turbulent transport. Damage to sensitive plant tissue and other elements of the biota caused by direct exposure to aqueous acids has been the subject of field and laboratory research (e.g. Tukey, 1970; Evans, 1982). Cases of specific injury and growth retardation have been reported for several plant and tree species in exposure studies (Wood and Bormann, 1974; Haines et al., 1980; Scherbatskoy and Klein, 1983) with threshold for effects generally noted in the range of pH = 2 to 3.

Our objectives were to characterize the chemical composition of stratus cloudwater and to address the potential that droplet capture may play as a vector for pollutant deposition. In this paper, we report the composition of rainwater, cloudwater, aerosol, bulk deposition, and throughfall samples collected in a Los Angeles pine forest. These are used to compare the relative contributions by these various deposition pathways. Interception of stratus clouds on the mountain slope is evaluated for its role in enhancing pollutant deposition. Our findings are presented as a measure of regional pollution not generally monitored. We also report the composition of deposited cloudwater collected from pine needles. These data are discussed in terms of chemical interactions occurring at the vegetative surfaces.

2. Experimental

Our monitoring site was located at Henninger Flats, a campground and tree nursery located at approximately 780 m MSL on the southern slope of Mount Wilson, 25 km northeast of Los Angeles Civic Center. The site is shown in elevation and plan views in Fig. 1. During the spring and early summer, stratus clouds are common along coastal California, associated with the persistent marine layer (Keith, 1980). An inversion base forms the top of the stratus deck. When drawn inland by an onshore pressure gradient, these low-lying clouds can intercept coastal mountain slopes, leading to frequent, dense fog at elevated sites from late evening through morning hours.

Cloudwater was collected on 8 days in June 1982 and 15 days in May and June 1983. On two of the sampling dates in May 1983, the cloud top was below Henninger Flats, and cloudwater was collected 100–200 m downslope. On most dates sampling proceeded from the time cloud had intercepted the site to the time the fog had dissipated. When fog occurred at the site, it was usually preceded by a relatively strong onshore breeze. The local, nighttime drainage flows inherent to the topography also affected the fog characteristics. Note: we refer to the phenomenon as fog at the site; however on the regional scale, the mountain slope was intercepted by stratus clouds. Hence, we refer to our samples as cloud-, rather than fogwater.

A Caltech rotating arm collector (RAC) was used to collect cloudwater (Jacob et al., 1984b). In essence, the RAC is a rapidly rotating (1700 rpm) propeller with slots and collection bottles located on both ends. The axis of the rotating arm was 1.4 m above ground level. The collector was situated approximately 200 m back from the ridge in a gently sloped, open area, surrounded by dense and tall (30 m) vegetation (Fig. 1). The external collection surfaces of the RAC minimize collection losses for large droplet sizes. Because of the collector design and the rapidity in which impacted droplets are removed from the slots to the bottles, evaporation of collected cloudwater is not a problem. Model-scale calibration of the collector design using solid particles has indicated the lower size-cut (50% collection efficiency) to be approximately 20 μm diameter (Jacob et al., 1984b). Little research has been conducted to determine size-

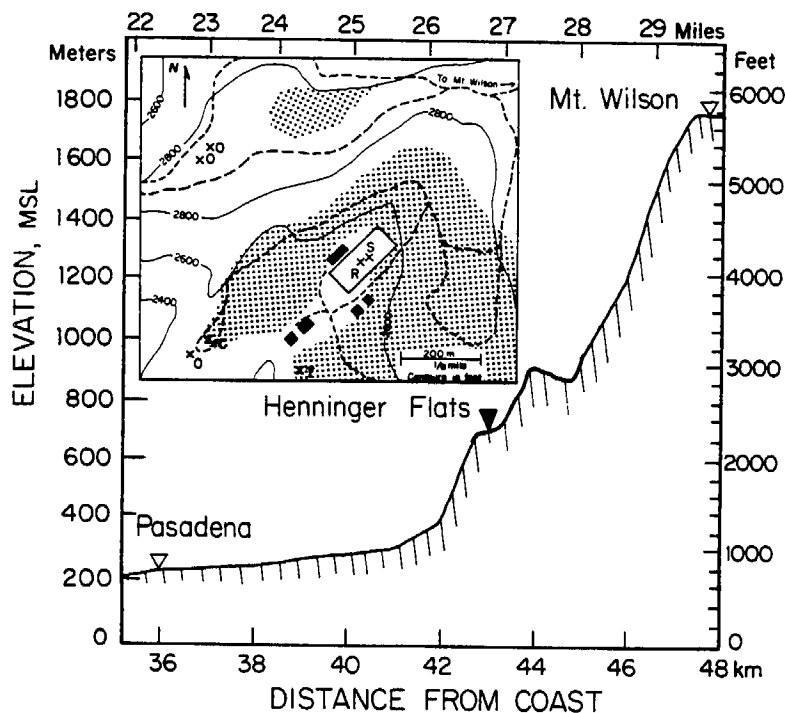


Fig. 1. Profile of southwestern Mount Wilson slope showing location of sampling site. Los Angeles Civic Center is located at 24 km from Pacific Ocean along same profile. On site plan (insert), S is cloudwater sampling site in nursery; R is rainwater collector location; O and C are open (bulk) and canopy (throughfall) bucket collectors; and T is location of tree drop samples. Shading indicates dense pine forest vegetation; dashed lines are dirt roads.

composition relationships of the cloud droplet spectrum experimentally. However, during an intercomparison of fogwater collectors at Henninger Flats (Hering and Blumenthal, 1984), the RAC samples gave consistently very good agreement with those of a jet-impactor having a lower size-cut measured between 2 and 5 μm diameter (Katz, 1980). Hence, the concentrations of the smaller droplets was not sufficiently different to alter the overall composition of simultaneously collected samples.

Sampling intervals generally ranged from 30 to 60 minutes; sample volumes were usually 10–30 ml, although some as small as 1 ml were analyzed. The RAC water collection rate has been found to correlate well with several independent methods (Hering and Blumenthal, 1984). Jacob et al. (1984b) reported that the theoretical RAC collection rate ($5 \text{ m}^3 \text{ min}^{-1}$) gave liquid water content (LWC) which was approximately 60% the value determined by total filter measurements made in

radiation fog. For this study, RAC-derived LWC values were calculated with this empirical correction factor:

$$\text{LWC} = \frac{\text{Sample volume}}{\text{Sample interval}} \times \text{theoretical air volume sampling rate} \times 0.6$$

In an environment where LWC greatly varies, temporally and spatially, the RAC-derived measurements have the advantage that they are collocated with each of the chemical samples and similarly time-averaged. This relationship gave good agreement with the other methods, except for patchy and dissipating fogs (Waldman, 1985).

Immediately after each sample was collected, pH was measured using a Radiometer PHM 82 meter and combination electrode; standard calibration of the electrode was performed at pH 7, 4 and 1.68. Within 30 minutes, aliquots were preserved from each sample for analysis of formaldehyde, S(IV)

and trace metals. For major ion determinations, aliquots were necessarily diluted from 5 to 50:1. Further details of fogwater sample handling and analytical protocols are presented elsewhere (Munger et al., 1983a).

In addition to cloudwater collection as in 1982, ambient aerosol measurements were made during the spring of 1983. Total and fine-fraction aerosol loadings were determined using 47 mm Teflon (Zeflur—1 μm pore size) filters sampling at 10 lpm. Samples—in dry and fog-laden air—were collected simultaneously on an open-faced filter (total) and behind a cyclone separator (fine <3 μm). The concentrations of water soluble ions were determined following aqueous extraction with a reciprocating shaker for 1 hour. Subsequent extractions of the filters produced satisfactory blanks.

Rainwater was monitored at the nursery from November 1982 to June 1983 using a wet-only collector (Liljestrand, 1980). Bulk deposition samples were collected between May and July 1983 in open, plastic buckets. On several occasions droplets that had accumulated on pine needles by cloud droplet capture were collected. This was done by manual, drop-by-drop removal. Selected trees were repeatedly sampled. Further details of these deposition measurements are given in separate sections.

3. Results and discussion

The objective of this field study was to determine the relative contributions of various pathways to the overall pollutant deposition. For clarity, a summary of cloudwater data is first presented and discussed. Several specific fog episodes are described. Wet and bulk deposition data sets are then presented. This is followed by calculations of the magnitude of fog-derived precipitation and the associated pollutant deposition based on the cloudwater composition reported. With these, a comparison of the pollutant fluxes associated with precipitation (incident and occult) and dry deposition pathways is given. Finally, the composition of intercepted cloudwater is presented with a discussion of its potential interactions with foliar surfaces.

3.1 Cloudwater composition

Summaries of 1982 and 1983 results for cloudwater and rainwater chemical analyses are presented

in Table 1. For comparison, values are also given for the 1978–79 volume-weighted mean rainwater concentrations at Pasadena and Mount Wilson (225 and 1800 m MSL, respectively). For most species, the median values for Henninger Flats cloudwater concentrations are 20 or more times those for local rainwater. The ionic balances for cloudwater data are presented in Fig. 2. In general, the results for both years are satisfactory with 1983 data giving very consistent balance. Ionic balance was calculated as a check on both the analytical precision and the completeness of the ion determinations. We are confident that all the major ionic species have been measured. There were a few cases in the 1982 data set which gave poor ionic balance, these for samples with the highest acidities and concentrations (and the smallest sample volumes). For those samples, much of the worse imbalances could be explained by a small analytical error at low pH: e.g. at pH ~ 2 , $d(\text{pH}) = \pm 0.1$ gives $d[\text{H}^+]$ of $\pm 2500 \mu\text{eq}^{-1}$. The better agreement for 1983 data was also due to our experience working with samples of such high concentrations. The protocol for the latter year included a single, quantitative dilution of each sample (5 to 50:1) rather than separate ones for the individual ion determinations, as for the 1982 samples.

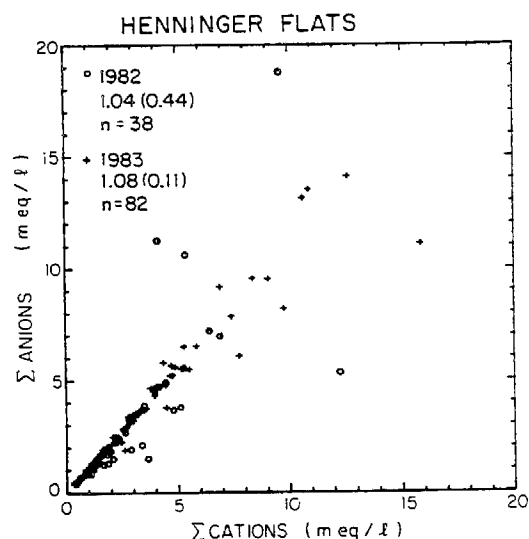


Fig. 2. Total anion versus cation concentrations for cloudwater samples of 1982 and 1983 with mean (std. dev.) of ion balances for n samples.

Table 1. Median and range of concentrations for cloudwater samples-Henninger Flats: 1982 and 1983

		Cloudwater		Rainwater		
		1982 ^a	1983 ^b	Site ^c	Pasadena ^d	Mt. Wilson ^d
pH		2.86 2.06-3.65	2.96 2.07-3.87	4.6	4.4	5.0
H ⁺		1365	1100	24	39	10
Na ⁺		224-8710	135-8510	14	24	26
K ⁺		146	285	0.9	1.7	1.7
		5-2465	3-6320			
NH ₄ ⁺		18	22	9.2	21	36
		1-161	3-197			
Ca ²⁺	$\mu\text{eq l}^{-1}$	576	582	4.1	6.7	9.3
		128-3130	62-7420			
		132	142	5.2	7.2	6.6
Mg ²⁺	$\mu\text{eq l}^{-1}$	5-975	3-3020	18	28	28
		54	106			
		2-762	1-1735	17	31	23
Cl ⁻		125	220	19	39	40
NO ₃ ⁻		21-1965	15-9650	na	na	na
		1435	1510	na	na	na
SO ₄ ²⁻	$\mu\text{mol/l}^{-1}$	191-9500	161-16,300	na	223	28
		617	971	na	na	na
		128-7310	133-9300			
S(IV)		15	7			
CH ₂ O		7-85	0.4-94			
		66	50			
		34-920	12-173			
Fe		1055	455			
Pb	$\mu\text{g l}^{-1}$	200-6880	20-4800			
		346	212			
		80-2780	38-2500			

^a Median and range for 38 samples (42 for pH) on 8 days.^b Median and range for 82 samples (86 for pH) on 15 days.^c Volume-weighted mean values for October 1982 to July 1983 (see Table 3).^d Volume-weighted mean values for 1978-79 (Liljestrand and Morgan, 1981).

na = not analyzed.

Hydrogen, ammonium, nitrate, and sulfate dominated the ionic composition in most samples; this is consistent with previous observations for Los Angeles aerosol (Appel et al., 1978). For most samples, non-sea salt sulfate was greater than 90% of measured sulfate, assuming as an upper limit that sodium was solely of marine origin. The nitrate-to-sulfate equivalent ratio for these samples was between 1.5 and 2 (Fig. 3). This ratio is similar to fogwater samples collected in the Los Angeles basin (cf. Munger et al., 1983a) but markedly different from local rainwater with ratios less than 1 (Table 1). The basinwide nitrate-to-sulfate equivalent ratio for precursor emissions has been reported

between 2 and 3 (California Air Resources Board, 1979; 1982).

The low pH values in the cloudwater occurred in a rather narrow range: pH = 2 to 4 (Fig. 4). The degree to which ambient acids have been neutralized in the atmosphere following their formation is indicated by the equivalent ratio of [H⁺] versus [NO₃⁻] plus [SO₄²⁻]. The ratio for Los Angeles stratus cloudwater was generally ~0.5 (Fig. 5). That is, in the cloudwater about half of the acidic anions were not neutralized.

Even for the cases with low aqueous concentrations, sufficient ambient bases were either not available or scavenged to fully neutralize the acid.

Gaseous ammonia should be completely scavenged by acidic cloud droplets (Jacob and Hoffmann, 1983). Basinwide, ammonia emissions are one-third of the SO_2 and NO_x sum on an equivalent basis; however, major source areas are located in San

Bernadino and eastern Los Angeles counties (Russell et al., 1983). The degree of fractional acidity reported herein is similar to coastal fogs collected in southern California (Munger et al., 1983a). However, for sites with very high ammonia emissions (cf. Jacob et al., 1984a), fogwater with similarly high ionic concentrations of acidic anions were largely neutralized. For some of the highly concentrated cloudwater samples, $[\text{Ca}^{2+}]$ and $[\text{Mg}^{2+}]$ were 10–50% lower for filtered ($0.2 \mu\text{m}$ pore size) compared to non-filtered aliquots. Na^+ , K^+ and NH_4^+ showed little difference between aliquots. This suggests that some of these ions in the condensation nuclei do not rapidly or completely dissolve. That is, there may be a kinetic limitation to the neutralization of cloudwater by the dissolution of an alkaline fraction.

The median values of trace metals (Fe, Pb, Mn, Ni and Cu) concentrations for approximately 100 cloudwater samples collected both years were 520, 260, 46, 36, and 20 ppb, respectively. For iron and lead, the values range from ~100 ppb to several ppm. The occurrences of stratus clouds intercepting inland slopes were linked to on-shore pressure gradients. As a whole, the trace metal concentrations and loadings in the cloud samples reflect the transport of anthropogenic pollutants to elevated sites downwind from their sources.

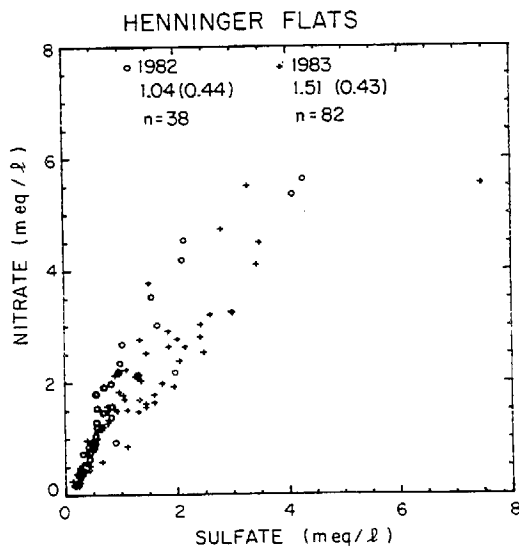


Fig. 3. Concentrations of nitrate versus sulfate in cloudwater samples of 1982 and 1983 with mean (std. dev.) of equivalent nitrate/sulfate ratios.

STRATUS CLOUDWATER pH FREQUENCY HENNINGER FLATS: 1982 & 1983

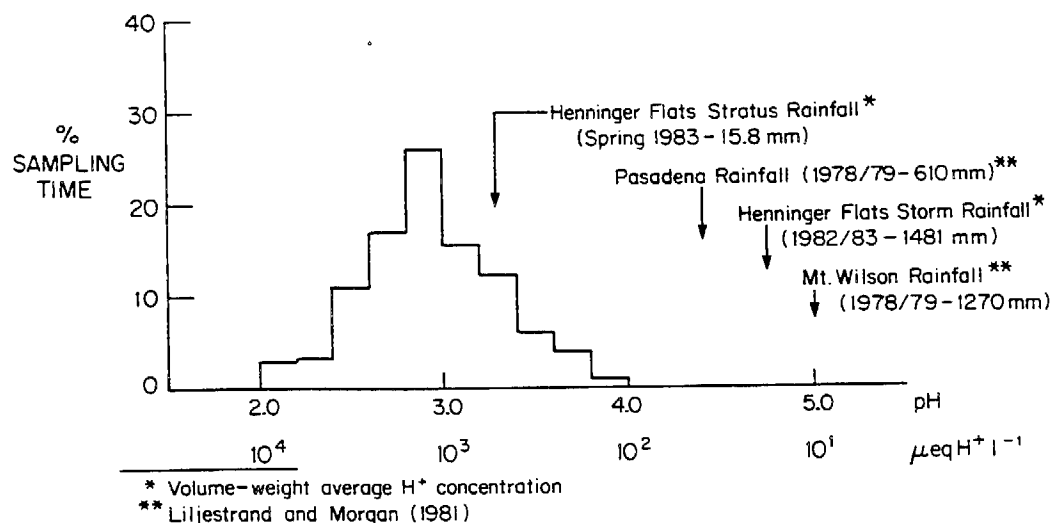


Fig. 4. Frequency histogram of pH for 1982 and 1983 Henninger Flats cloudwater samples.

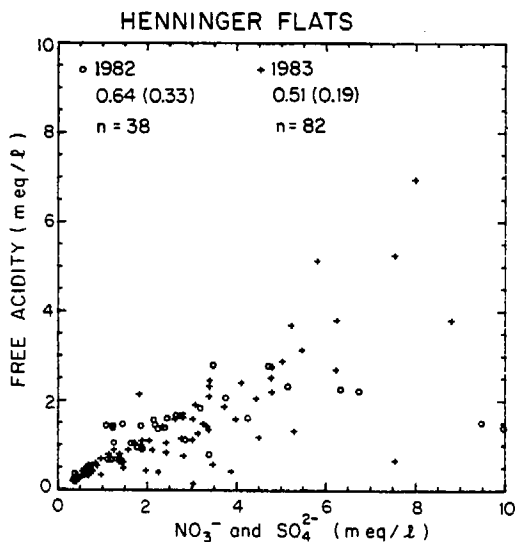


Fig. 5. Free acidity (i.e., $[H^+]$) versus sum of nitrate and sulfate concentrations in cloudwater samples for 1982 and 1983 with mean (std. dev.) of equivalent ratios.

The concentration of S(IV) in cloudwater samples ranged between 1 and $100 \mu\text{mol l}^{-1}$, with a two-season median value of 10. Formaldehyde was measured at concentrations 4 to 10 times greater than for S(IV) (median value = $56 \mu\text{mol l}^{-1}$). These data are given in Munger et al., (1984). Gaseous SO_2 levels at Henninger Flats were measured to be generally 10 ppb or below (Hering and Blumenthal, 1984). Similarly low levels are typical in nearby Pasadena during the spring. The formations of S(IV)-aldehyde adducts in solution led to total aqueous S(IV) concentrations which exceeded the Henry's law solubility for gaseous SO_2 at low pH (Munger et al., 1984), although these were yet a small fraction of aqueous sulfur.

3.2. Examples of specific events

Ambient aerosol was sampled prior, during and following several fog episodes in 1983 (Table 2). Aerosol concentrations ($\mu\text{eq m}^{-3}$ of air) measured on Teflon filters were comparable to those of cloudwater samples (Fig. 6). During fog, these samples included droplets as well. Values for aerosol $[H^+]$ concentration were calculated from the ionic charge deficiency. This procedure is justified by the large excess of anions observed and the resulting low aerosol pH predicted. Several points are suggested from these data.

First, the acidities of the precursor aerosol were somewhat lower than those measured for cloudwater. Filter samples collected wholly during fog were generally more acidic. Daum et al. (1984) found clear-air aerosol to contain much less acidity than the cloudwater in the eastern United States for samples collected aloft, although they make the caveat that the samples they compare were from different days. Our calculations indicate that much of the cloudwater solute was derived from ambient aerosol scavenged by cloud formation; some but not all of the resultant aqueous acidity is measured in the precursor aerosol. Second, the nitrate-to-sulfate ratios of the afternoon and late evening (non-fog) intervals were usually less than one, while the concentrations of nitrate generally showed a large increase immediately following the onset of fog, wherein the ratio was between 1.5 and 2. Shown in Fig. 6, the aerosol nitrate measured after fog formed increased (June 11) while all the other measured species remained unchanged.

A likely source of additional nitrate is the scavenging of nitric acid vapor by the droplets. Compared to levels measured in non-fog aerosol, the increase in nitrate was around 0.1 to $0.2 \mu\text{mol m}^{-3}$, similar to nitric acid values reported for the Los Angeles atmosphere (Spicer et al., 1982). Nitric acid was measured in clear air at Henninger Flats during June 1984 between 0.01 and $0.4 \mu\text{mol m}^{-3}$ (Waldman, 1985). In all aerosol and cloudwater samples, there was unneutralized acidity. Under these conditions, gaseous ammonia would be completely scavenged by acidic sulfate aerosol. Nitric acid would remain unneutralized and, in clear air, in the gas phase. The increase in suspended liquid water upon fog formation results in 100% scavenging of nitric acid (Jacob and Hoffmann, 1983). Conversely, for dissipating fog conditions, nitric acid would be driven back into the gas phase.

The lower pre-fog concentrations measured could have also been caused by particulate nitrate loss due to ammonium nitrate volatilization from the Teflon filter medium (Appel et al., 1979). For cool, humid conditions at Henninger Flats (e.g. $T = 10^\circ\text{C}$ and $\text{R.H.} \geq 90\%$), the equilibrium dissociation constant (K_N) for NH_4NO_3 is below 0.1 ppb² or $1.8 \times 10^{-4} (\mu\text{mol m}^{-3})^2$ (Stelson and Seinfeld, 1982). Therefore, during most sample intervals, K_N would be too low for this to be a significant artifact. It appears that some nitric acid

Table 2. *Ambient aerosol chemical concentrations—Henninger Flats: June 1983*

Date & Time	Size ^a	Fog ^b	$\mu\text{eq m}^{-3}$			"pH" ^c	$\text{NO}_3^-/\text{SO}_4^{2-}$	cloudwater ^d	
			NH_4^+	NO_3^-	SO_4^{2-}			pH	$\text{NO}_3^-/\text{SO}_4^{2-}$
June 8									
0000–0600	T	post	0.196	0.067	0.312	"3.11"	0.22	2.71	1.11
	F		0.189	0.018	0.273				
	(C)		(0.007)	(0.049)	(0.039)	"3.47"	1.26		
2145–0215	T	fog	0.101	0.294	0.213	"2.74"	1.38	3.00	1.68
	F		0.009	0.042	0.086				
	(C)		(0.092)	(0.252)	(0.127)	"2.86"	1.98		
June 10									
1200–1800	T	pre	0.154	0.070	0.284	"3.25"	0.25		
	F		0.159	0.012	0.265				
	(C)		(0.005)	(0.058)	(0.019)	"3.98"	3.05		
2230–0230	T	pre	0.136	0.073	0.195	"3.39"	0.37		
	F		0.188	0.044	0.190				
	(C)		(0.052)	(0.029)	(0.005)	"3.51"	5.80		
June 11									
0630–1030	T	fog	0.154	0.265	0.185	"2.87"	1.43	3.01	1.85
	F		0.050	0.010	0.069				
	(C)		(0.104)	(0.255)	(0.116)	"2.92"	2.20		
1040–1430	T	fog	0.057	0.105	0.109	"3.22"	0.96	3.26	1.36
	F		0.034	0.004	0.045				
	(C)		(0.023)	(0.101)	(0.064)	"3.27"	1.58		
June 12									
0800–1200	T	fog/post	0.200	0.201	0.197	"3.40"	1.02	3.57	1.43
	F		0.041	0.044	0.082				
	(C)		(0.159)	(0.151)	(0.115)	"3.82"	1.31		
June 19									
0045–0600	T	patchy fog	0.027	0.068	0.100	"3.33"	0.68	2.87	1.65
June 21									
0835–1045	T	patchy fog	0.257	0.269	0.480	"2.95"	0.56	2.67	na
	F		0.242	0.057	0.267				
	(C)		(0.015)	(0.212)	(0.213)	"3.05"	1.00		
June 22									
0430–0830	T	fog/post	0.243	0.141	0.262	"3.46"	0.54	3.09	2.50
	F		0.213	0.098	0.229				
	(C)		(0.030)	(0.043)	(0.033)	"4.52"	1.30		

^a T, total particulate (open-faced filter); F, fine particulate ($d_p < 3 \mu\text{m}$); (C), coarse: T minus F.

^b Conditions during sampling relative to fog episode.

^c "pH" calculated assuming H^+ balanced charge deficiency of major ions and $\text{LWC} = 0.2 \text{ g m}^{-3}$.

^d LWC and time-weighted average values for cloudwater samples relative to b; nitrate/sulfate ratios are on equivalent basis.

loss from the filters during patchy and dissipating fogs (e.g., June 21 and 22) led to $\text{NO}_3^-/\text{SO}_4^{2-}$ values below cloudwater ratios. A third possibility exists by which the noted increase in nitrate concentrations were due to its advection to the site. However, there was no increase in measured gaseous pollutants (SO_2 , NO_x and O_3) following

the onset of the fog (Hering and Blumenthal, 1984).

Prior to the fog, most of the particulate solute, especially sulfate, was measured in the fine ($< 3 \mu\text{m}$) size class. In dense fog, very little of the particulate solute remained in the fine-size class. However, the proportion of sulfate found in the

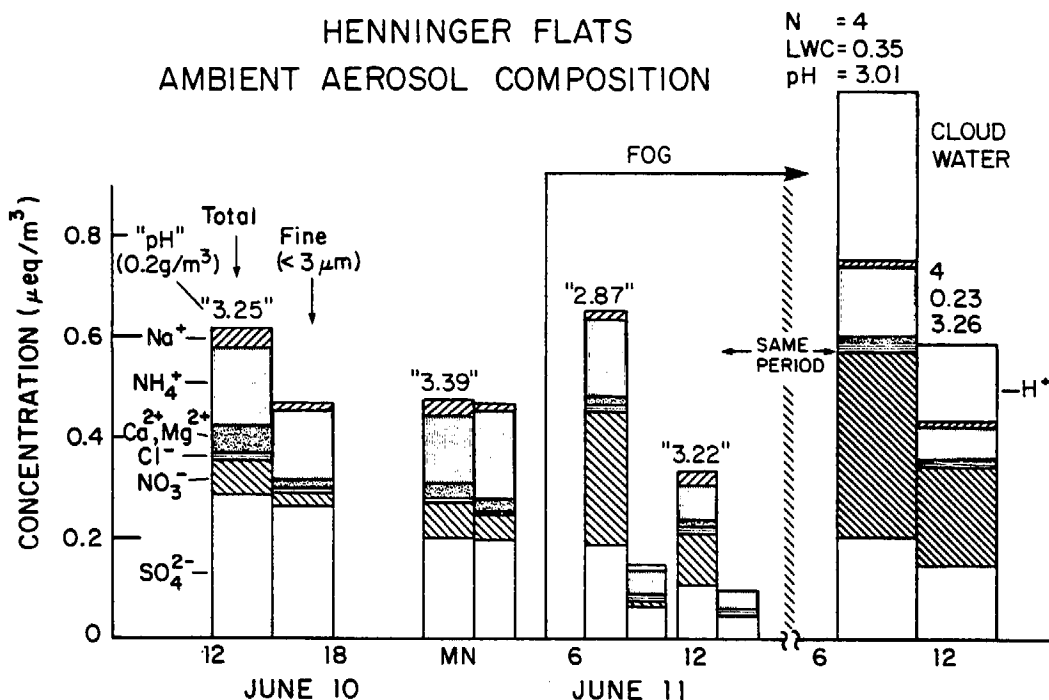


Fig. 6. Ambient aerosol composition for June 10–11, 1983. Total and fine ($d_p < 3 \mu\text{m}$) particulate concentrations given are for each sample interval. Time-weighted solute concentrations for cloudwater samples are shown for the latter two intervals.

fine-size fraction of the filter samples (1/3 to 1/2) was greater than for nitrate. This difference is primarily due to the presence of precursor nitrate in the air as nitric acid which is subsequently absorbed into fog droplets. Also, as nitrate and sulfate salts are highly hygroscopic, the difference in the portion which was activated into droplets would be a function of particle size. The model of Bassett and Seinfeld (1984) predicts that nitric acid will be more favorably absorbed by larger aerosol, due to the Kelvin effect. Previous findings that nitrate is associated with larger-sized aerosol (Appel et al., 1978) would support an interpretation that particulate nitrate was more completely scavenged by droplet activation. Cloudwater samples collected during post-precipitation intervals generally had the lowest nitrate-to-sulfate ratios. As suggested above, this could be caused by mechanisms which scavenge (and deposit) nitrate more effectively than sulfate.

Concentration, LWC, and solute mass loading profiles for cloudwater samples from June 11 and

12, 1983 are shown in Fig. 7. During the first several hours of sampling, as the marine air permeated the forest, the fog was patchy, and the LWC fluctuated dramatically. In addition, there were brief periods of complete dissipation at the onset of this fog episode when deactivation of cloud droplets would remove cloudwater solute mass to the haze-size range, below the collector size-cut. For these first few intervals, the RAC-derived value (estimated from the entire sampling period) underestimated LWC for the fog actually collected. Thus, a representative indication of the cloudwater solute loading is difficult to determine for time-averaged samples in locally patchy fogs.

After 0700, fog became more stable at the site (Fig. 7b), and the solute loading remained fairly constant for the next 4 to 5 hours (Fig. 7c). A slight drizzle began at 0800, intensifying to a measurable rate in the mid-afternoon. Often, drizzle-size drops do not fall far below the cloud base before they evaporate. During the afternoon (June 11), 5.8 mm of rainfall was measured at the site, which was

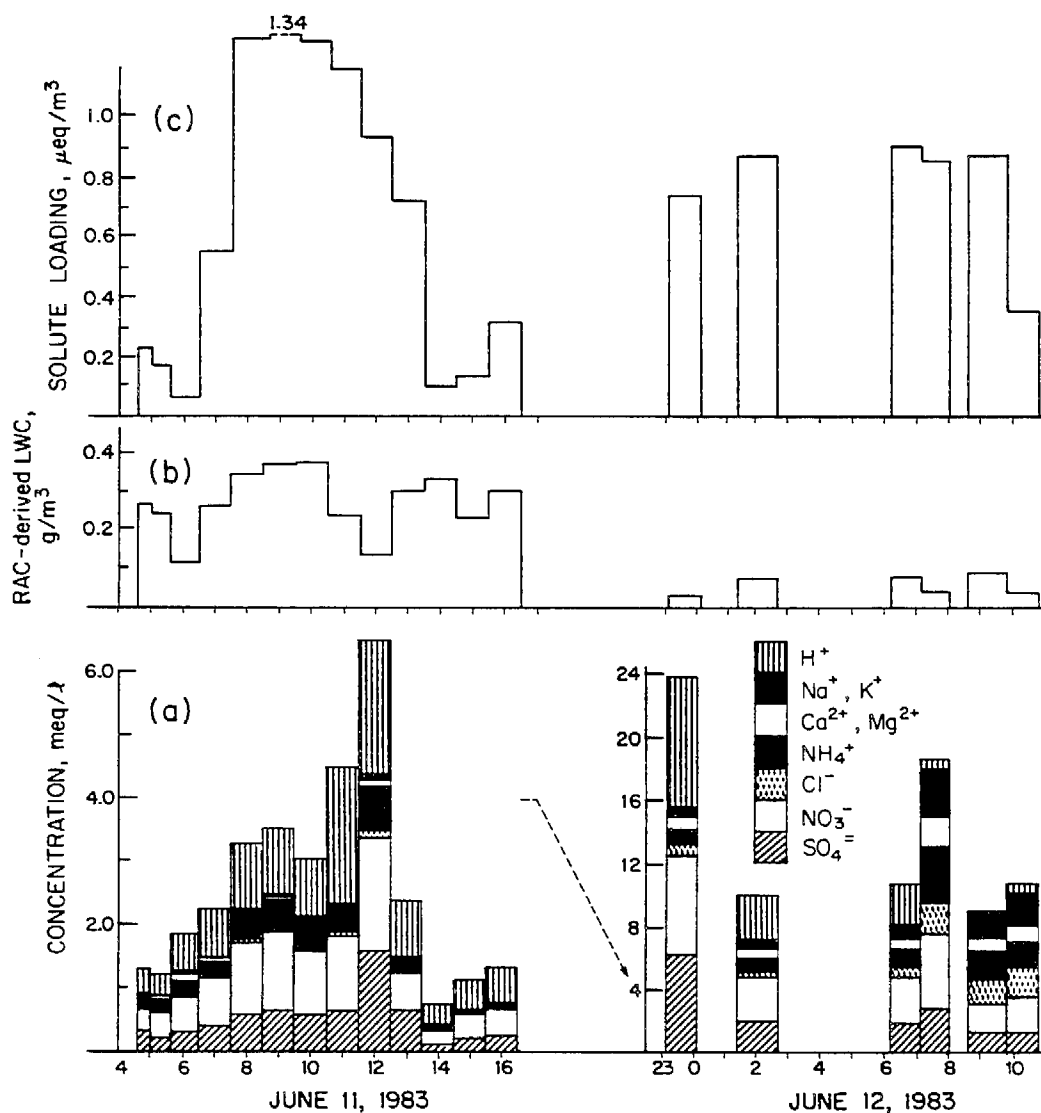


Fig. 7. (a) Concentration, (b) LWC, and (c) ambient solute loading for sequential cloudwater samples on June 11 and 12, 1982. Note the change in scale (a). A slight drizzle began 0800 on June 11, intensifying after 1200 and ending by early evening.

above the cloud base, compared to the trace (<0.25 mm) measured ~ 500 m below the base in Pasadena. Coincident with afternoon drizzle was a drop in ambient solute concentrations (see Fig. 6 and 7c). The total solute deposited in the drizzle (see subsequent section) was several times the product of aerosol concentration and cloud height, which indicates a continuing source of solutes. Advection of pollutant-laden cloud air to the mountain slope

adds to the amount deposited in the rainfall there, while upwind over the lower basin no precipitation was occurring. Also following the onset of rainfall, the mass median diameter for measured cloud droplet spectra became lower. The collection efficiencies of cloud droplets by drizzle-size drops falling to the ground increases for larger droplets (Pruppacher and Klett, 1978). Hudson and Rogers (1984) have shown that a significant fraction of

the larger nuclei are found in the larger droplets. The depletion of larger, cloud droplets, taken with the magnitude of solute deposition measured in the drizzle, lends further support to the interpretation that the drop in cloudwater solute loading was caused by its depletion by precipitation scavenging.

The fog continued with fairly uniform LWC through that day—drizzle ceasing in the late afternoon—and into the following morning. Cloudwater sampling was discontinued until 2300. Two intermittent samples were collected before continuous sampling was resumed at 0600 on June 12. For June 12 samples, the ambient solute loading was elevated to the pre-drizzle level—aqueous concentrations were much higher with fluctuations mirrored by commensurately lower LWC. Similarly, the solute measured in fog on filters was greater (Table 2). The large-scale eddy circulation which had deepened the marine layer in the previous afternoon had weakened. The increase in pollutant levels in the cloud was partially a reflection of this decrease in the mixing depth. Also, as the drizzle had ceased, advected pollutants in the cloud air would not be locally depleted. In the

morning, the cloudwater samples became progressively less acidic, and equimolar Na^+ and Cl^- increases occurred. This latter point suggests that air of greater marine character was advected to the site. The roles of vertical mixing and ventilation within stratus clouds and fogs are major uncertainties. Until we can better quantify the transport component of cloud/fog dynamics at a given sampling site, our explanations remain speculative. Finally, the drop in solute loading for the last sample accompanied evaporation of fog droplets.

3.3 Deposition: measurements and calculations

3.3.1. Storm and stratus rain. Rainfall at Henninger Flats was collected and analyzed from November 1982 to June 1983. In Table 3, the wet deposition is split between storm (A) and (B) spring stratus events. The 1982–83 season (October 1 to September 30) was above average rainfall—the wettest on record at Henninger Flats: 1660 mm compared to an average of 670 mm. Pasadena and Mt. Wilson deposition (from 1978–79 data) are presented for comparison. Because of the high frequency and water flux per storm event, the

Table 3. Wet deposition—Henninger Flats: October 1982 to July 1983

Table 3. Wet deposition—Heminger Falls, October 1982 to July 1983											
			meq m ⁻²								
Month	#	mm	H ⁺	Na ⁺	K ⁺	NH ₄ ⁺	Ca ²⁺	Mg ²⁺	Cl ⁻	NO ₃ ⁻	SO ₄ ²⁻
A. Storms ^a											
Sum (mean ^d)	34	1480	27.8 (18.8)	20.6 (13.9)	1.2 (0.8)	12.1 (8.2)	4.9 (3.3)	7.2 (4.8)	25.2 (17.0)	18.4 (12.4)	23.4 (15.8)
B. Stratus ^b											
Sum (mean ^d)	6	15.8	8.33 (526)	0.87 (55)	0.13 (8)	1.68 (106)	1.24 (78)	0.64 (41)	1.30 (82)	7.40 (467)	5.45 (344)
<hr/>											
$\frac{B}{A+B} \times 100$		1.1	23.1	4.1	9.7	12.2	20.2	8.2	4.9	28.7	18.9
<hr/>											
1978/1979 ^c											
Pasadena (mean ^d)		610	23.8 (39)	14.6 (24)	1.0 (1.7)	12.8 (21)	4.1 (6.7)	4.4 (7.3)	17.1 (28)	18.9 (31)	23.8 (39)
Mt. Wilson (mean ^d)		1270	12.7 (10)	33.0 (26)	2.2 (1.7)	45.7 (36)	11.8 (9.3)	8.4 (6.6)	35.6 (28)	29.2 (23)	30.8 (40)

^a Five major storms (total = 250 mm) and several light rains (<10 mm) between Oct. and Apr. were missed. Standard rainfall gauge values were used to calculate individual storm deposition when portion of rainfall was missed by collector. The volume-weighted concentrations were used to determine total storm deposition.

^b Actually, two stratus events (total = 13.3 mm) were collected; four additional trace events (total = 2.5 mm) were assumed to have similar concentrations to calculate total stratus deposition.

^c Liljestrand and Morgan (1981).

^d Volume-weighted mean concentration ($\mu\text{eq l}^{-1}$).

volume-weighted mean concentrations (A) were lower than in the earlier year. Stratus events (i.e., drizzle or light rainfall) occurred within a developed marine layer, similar to that which led to stratus cloudiness and fog on mountain slopes but with more intense deepening. The ionic concentrations of these light rains were dramatically higher than for the storm events, but in a range somewhat less concentrated and acidic than the cloudwater samples. Morgan and Liljestrand (1980) noted similarly higher concentrations in sparser rains they measured in Pasadena. Brewer et al. (1983) reported a similar relationship between fog and "mist" (i.e. drizzle) samples at several Los Angeles locations.

The meteorology is an important factor to consider in comparing the precipitation types. Most wintertime storms are associated with weather systems which advect moist, unstable oceanic air with fairly intense convective activity extending up to >5000 m (Keith, 1980). On the other hand, drizzle and fog events usually occur within a developed marine layer constrained by a strong temperature inversion aloft. This limits the vertical extent of mixing; thus, stratus cloud droplets form and can have longer residence times in the polluted atmosphere. The mean pH values for stratus and storm rainwater are compared to cloudwater samples in Fig. 4. The fog → drizzle → rain hierarchy of solute concentration also reflects the relationship between droplet size and dilution. The growth of non-freezing cloud droplets to a size with appreciable sedimentation velocity occurs solely by condensation of water vapor for sizes below 50 μm diameter; subsequently both coalescence and condensation lead to drizzle (0.2 to 0.5 mm) and raindrop (>0.05 mm) sizes, depending upon the intensity of vertical motion (Pruppacher and Klett, 1978).

Stratus events led to solute deposition which was disproportionate to the water flux. While accounting for ~1% of measured rainfall, nearly 20% or more of H^+ , NO_3^- and SO_4^{2-} were deposited in less than 16 mm precipitation. Na^+ and Cl^- were much less enhanced in stratus rainfall. The winter storms responsible for most of the precipitation form over the eastern Pacific Ocean. They are more effective at generating and transporting sea salt aerosol due to their greater convective activity. For stratus events, the enhancement of H^+ and NO_3^- was greatest and, for NH_4^+ and SO_4^{2-} , it was somewhat

less. The difference in nitrate/sulfate ratios for stratus (1.4) versus storm (0.8) events is a further indication of the meteorological and seasonal variation in SO_2 and NO_x oxidation and transport.

3.3.2. Bulk deposition and throughfall. For our program, bulk deposition was collected with open buckets. These provided large collection areas, minimized resuspension (relative to flat surfaces) and were convenient to use and rinse. Standard 4-gallon, polyethylene buckets (open area = 566 cm^2) were placed with the rim at least 1 meter above the ground in the vicinity of the nursery (see Fig. 1). One bucket was placed beneath a dense stand of Coulter pine (*Pinus coulteri*). The containers were extracted with 0 to 500 ml of H_2O , depending on the exposure duration and precipitation amount.

Surrogate surface methods, such as flat plates and open containers, remain controversial due to the variability of their results and the uncertainty in extrapolation of specific results to a regional value. From intercomparison of surrogate surfaces (Dolske and Gatz, 1984; Dasch, 1983), buckets were shown to give flux values which were sensitive to ambient aerosol sulfate levels. Dry deposition of SO_2 and NO_x has been reported to be inconsequential for the plastic buckets (Dasch, 1983); however, gaseous nitric acid might be expected to contribute to the measured deposition because of its reactivity.

There are uncertainties in interpreting these data: for example, atmospheric conditions for the sampling intervals were not well known with respect to aerosol size spectra, pollutant fractionation, or micrometeorology. For simple topography, a very detailed data set could be required; for complex terrain, the problem is almost intractable. Rather, the bulk deposition measurements are presented to provide a relative measure of solute deposition under varying ambient conditions.

Overall, bulk deposition for most intervals with precipitation was significantly greater than for intervals with none (Table 4). For example, the deposition rates for H^+ , NH_4^+ , NO_3^- and SO_4^{2-} , averaged for the two intervals with measurable rainfall (May 26–June 3 and June 9–13), were 10 or more times that of the other intervals listed. The dry-only deposition (i.e., with the measured wet-only values subtracted) was also greater for those intervals. These coincided with stratus clouds and fog. This indicated to us, as noted in the previous section, that trace precipitation (not measured in

Table 4. Bulk deposition and throughfall—Henninger Flats: May–July 1983

meq m ⁻² (std. dev.)											
Interval	Location ^a	"H" ^b	Na ⁺	K ⁺	NH ₄ ⁺	Ca ²⁺	Mg ²⁺	Cl ⁻	NO ₃ ⁻	SO ₄ ²⁻	
May 12-19 (168 h)	O (3)	0.0 (0.0)	0.52 (0.08)	0.35 (0.13)	0.39 (0.37)	0.30 (0.11)	0.40 (0.24)	0.16 (0.08)	0.78 (0.10)	0.59 (0.26)	
	C (1)	0.0	0.16	0.09	0.07	0.31	0.19	0.14	0.43	0.17	
May 19-26 (162 h)	O (2)	0.10 (0.10)	0.05 (0.01)	0.10 (0.08)	0.20 (0.23)	0.21 (0.02)	0.09 (0.04)	0.10 (0.10)	0.47 (0.08)	0.10 (0.03)	
	C (1)	0.18	0.05	0.07	0.05	0.21	0.07	0.04	0.45	0.17	
May 26-June 3 (191 h)	O (3)	4.69 (0.87)	2.04 (0.25)	0.30 (0.17)	2.28 (0.69)	0.81 (0.02)	0.91 (0.27)	1.87 (0.04)	5.49 (0.06)	4.42 (0.35)	
	C (1)	4.41	3.71	5.71	3.48	4.35	3.93	2.96	14.5	5.50	
Wet only—15 mm		3.83	0.56	0.09	0.89	0.74	0.42	0.63	3.60	2.80	
June 3-9 (156 h)	O (3)	0.55 (0.60)	0.28 (0.03)	0.19 (0.10)	0.21 (0.17)	0.66 (0.04)	0.34 (0.10)	0.20 (0.03)	1.05 (0.40)	0.73 (0.34)	
	C (1)	0.47	0.16	0.07	0.24	0.36	0.13	0.10	0.80	0.37	
Wet only—0.5 mm ^c		0.26	0.03	0.00	0.05	0.04	0.02	0.04	0.23	0.17	
June 9-13 (94 h)	O (3)	3.34 (0.64)	0.41 (0.15)	0.12 (0.10)	1.28 (0.21)	0.54 (0.20)	0.26 (0.13)	0.33 (0.16)	4.07 (0.99)	2.64 (0.56)	
	C (1)	4.59	1.34	1.65	1.59	2.06	1.44	0.90	8.55	4.04	
Wet only—5.8 mm		3.38	0.18	0.02	0.56	0.42	0.21	0.46	2.76	1.85	
June 13-19 (135 h)	O (1)	0.0	0.09	0.14	0.08	0.20	0.14	0.12	0.22	0.11	
June 19-July 11 (531 h)	O (2)	0.15 (0.08)	1.08 (0.01)	0.15 (0.05)	0.81 (0.02)	0.92 (0.08)	0.85 (0.09)	0.11 (0.0)	1.57 (0.11)	1.55 (0.13)	
	Wet only—2.0 mm ^c	1.05	0.11	0.02	0.21	0.16	0.08	0.16	0.93	0.69	
July 11-25 (342 h)	O (2)	0.05 (0.01)	0.26 (0.0)	0.07 (0.01)	0.16 (0.11)	0.24 (0.18)	0.16 (0.0)	0.13 (0.16)	0.65 (0.05)	0.19 (0.08)	

^a O = Open; C = Under Canopy; (# replicates).^b "H"⁺ deposition from pH of bucket extraction or precipitation sample.^c Wet only deposition calculated from measured trace rainfall × mean stratus (B) concentration (see Table 3).

standard rainfall gages) accompanying these low clouds had enhanced solute flux associated with it.

During dry periods, the below-canopy sample had generally lower pollutant deposition compared to open collectors. This reduction may be due to the interception of material to the canopy alone, or the suppression of turbulent transport below the canopy as well. It also appeared that some of this material eventually was deposited as throughfall when appreciable rainfall occurred (cf. June 3–9 to June 9–13). However, some of the additional cations had likely leached from the pine needles.

3.3.3. Calculation of fog precipitation. Fog droplet capture by the forest canopy has been recognized as an important hydrologic input. Hori (1953) and co-workers conducted extensive research on the mechanisms and efficiency of droplet capture. Lovett (1984) modeled the transfer of liquid water to the forest canopy in fog-laden winds. Compared to the deposition of dry aerosol (Sehmel, 1974), the capture of fog droplets is

significantly more efficient. The parameters that control the rate of deposition are the wind speed and turbulence, canopy and leaf geometries, and fog LWC and droplet size distribution. Lovett calculated water deposition rates, chiefly by impaction to the upper 3 m of the canopy, which varied linearly from 0.2 to 1.2 mm h⁻¹ for canopy-top wind speeds of 2 to 10 m s⁻¹. From collection on natural and surrogate surfaces, Yosida (1953) reported an overall average rate of 0.5 mm h⁻¹ for fogwater capture by the forest canopy. Fog-induced water flux deposition can vary greatly, even tree-to-tree (e.g. Oberlander, 1956). For sparsely forested areas and chaparral, the average would be expected to be lower. Dollard et al. (1983) estimated a mean cloud drop flux of 0.07 mm h⁻¹ to shortgrass by eddy turbulence and sedimentation in fog, based on micrometeorological techniques.

Direct measurement of this deposition was not made during this study. Instead, we assumed a water deposition rate of 0.2 mm h⁻¹ to calculate

approximate values of fog-induced fluxes for cloudwater with the measured composition. Henninger Flats has a relatively dense, tall canopy. Canopy-top data were not measured. The LWC at canopy-top would be somewhat higher than at the ground (Lovett, 1984); aqueous concentrations would be commensurately lower at elevated locations. In the nursery, winds were generally $<1 \text{ m s}^{-1}$; wind speeds measured just downslope of the site were $\sim 1\text{--}2 \text{ m s}^{-1}$, hence a conservative water deposition rate was used. Using the above rate (0.2 mm h^{-1}) with the median $[\text{H}^+]$ of $1150 \mu\text{eq l}^{-1}$ gave an average rate equal to $230 \mu\text{eq m}^{-2} \text{ h}^{-1}$. Also using the median values for 1982 and 1983 data, nitrate and sulfate deposition rates were calculated to be 300 and $170 \mu\text{eq m}^{-2} \text{ h}^{-1}$, respectively.

3.3.4. Comparison of pollutant wet deposition pathways. It is difficult to generalize about the frequency and duration of cloud interception within the Los Angeles basin. It is subject to spatial and temporal variability as well as year-to-year fluctuation. The presence of marine layer clouds and fog are persistent phenomena in coastal southern California, especially during spring and summer (Keith, 1980). From a daily record kept by rangers at Henninger Flats (Los Angeles County Fire Department, Forestry Bureau, unpublished meteorological records, 1983), the median number of times dense fog was observed at 8 a.m. was 30 per year (range = 8 to 55) and 12 during the May/June period for 1970–83. However, clouds are as often observed to intercept the mountain slope less than several hundred meters above or below the site. Further, clearing prior to the morning observation often occurs. Hence, at an inland location, the Henninger Flats observations are likely a conservative estimate of the frequency that low-lying clouds intercept coastal mountain slopes in the Los Angeles area. Both 1982 and 1983 were above normal for fog, with 31 and 18 morning observations of fog during each May/June period, respectively. During our two years of monitoring, over 120 fog-hours were sampled on 23 days or approximately 5 hours per event.

Assuming deposition rates as in the previous section with 150 hours of cloud interception per year (i.e., 30 events times an average of 5 hours per event), the product gave an annual total of $35 \text{ meq H}^+ \text{ m}^{-2}$. Similar calculations for NH_4^+ , NO_3^- , and SO_4^{2-} yield 17, 45, and 24 meq m^{-2} , respectively;

for lead, 8 mg m^{-2} deposition annually is calculated. Though the preceding calculations are based on limited data and rough estimates, they are intended to demonstrate the order of magnitude that cloud droplet processes may contribute to the acidic deposition in this urban-impacted mountain environment. Comparing these with measured precipitation (Table 3), cloud interception could deliver up to half the total wet deposition. At coastal sites with less rainfall and greater fog frequency, the effect could be greater.

4. Cloudwater interactions with foliar surfaces

Part of our motivation to sample cloudwater at Henninger Flats was the observation in the spring 1982 of an unseasonably high number of pine trees, especially Monterey-Knobcone (*Pinus radiata* \times *attenuata* hybrid) which exhibited necrotic needles (M. Gubrud, Senior Deputy Ranger, Los Angeles Fire Department, Forestry Bureau, private communication, 1982). Normally, needle necrosis is observed in the late summer and early autumn, due to the high oxidant levels in the Los Angeles basin (Richards et al., 1968).

4.1. Measurements

To better understand the nature of its interaction with plant tissue, cloudwater was removed from pine needles where it had naturally deposited during several fog events. These samples were aggregated from several hundreds of individual drops ($d = 1$ to 2 mm) taken from the lower reaches ($\sim 1.5 \text{ m}$) of a variety of individual pine trees. All the pine needles from which samples were removed showed some degree of browning at the tips where the cloudwater had collected, but were otherwise green and healthy. In general, these samples were found to be as acidic though often more concentrated than the suspended cloudwater. In Fig. 8, the equivalent ratio of major ions to sulfate are presented for tree drop samples and for cloudwater samples collected simultaneously. The measured concentrations can be derived from comparing the ratio with the $[\text{SO}_4^{2-}]$ given in the figure. Nitrate was 2 or more times greater than sulfate for these samples. The highest ionic con-

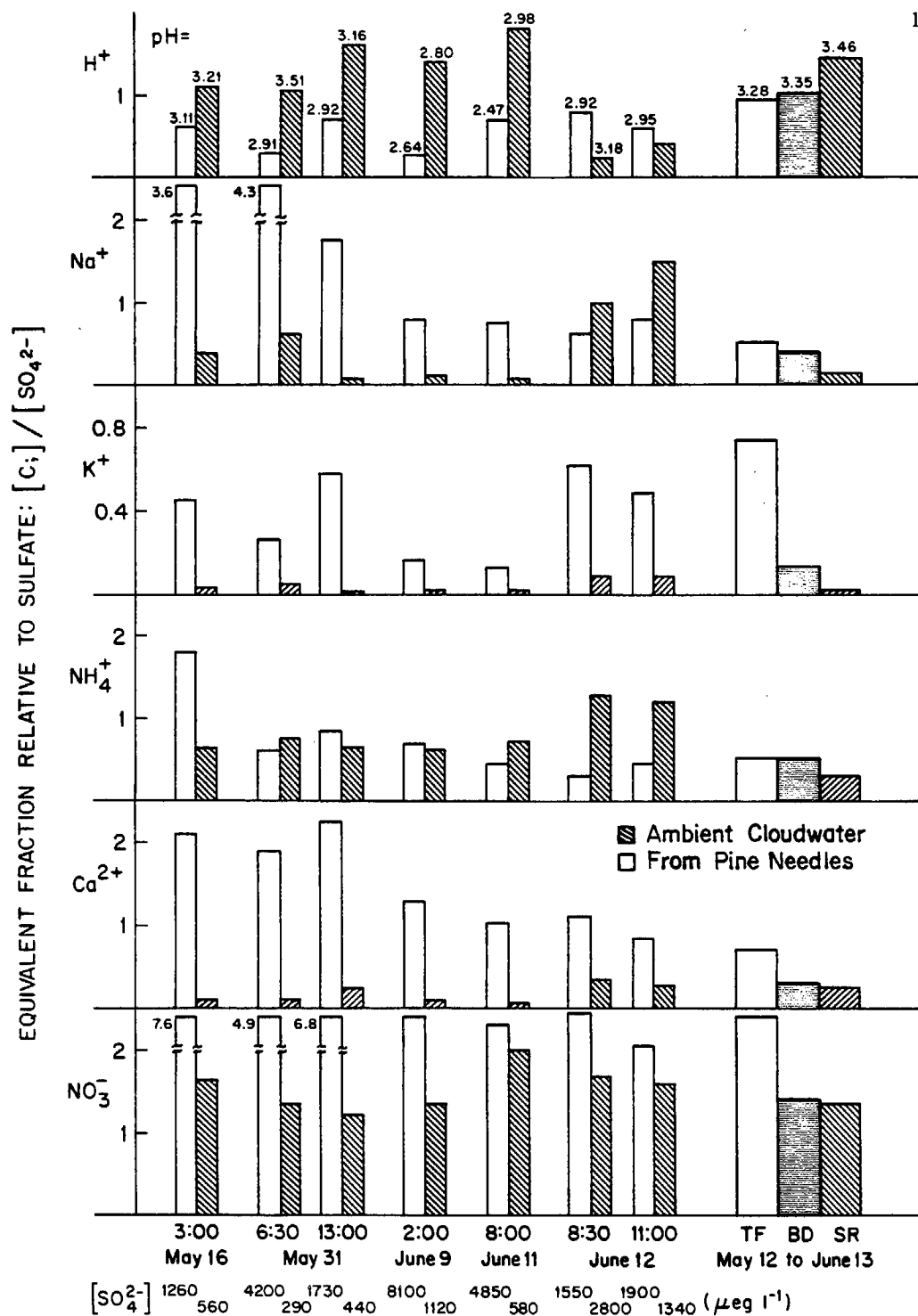


Fig. 8. Equivalent fractions of ionic species relative to sulfate in cloudwater removed from pine needles (open) and ambient cloudwater (shaded) collected simultaneously in 1983. TF is throughfall; BD is bulk deposition; and SR is stratus rainwater (see Table 4).

centrations were found for intervals preceded by dry periods (e.g., May 16 and May 31). Samples for intervals following rainfall or a long duration of fog had concentrations generally lower compared to the earlier samples. The fractions of Na^+ , K^+ , Ca^{2+} , and Mg^{2+} in the fog drops were much higher than in any of the fogwater samples.

4.2. Discussion

Leaching of internal leaf tissue cations, especially K^+ , by aqueous proton could explain their enhanced ratios. Scherbatskoy and Klein (1983) reported leaching of K^+ , Ca^{2+} , and amino acids for birch and spruce foliage exposed to acidic ($\text{pH} = 4.3$ and 2.8) mists. They also suggested that the increase in leachate pH compared to the applied mists involved cation exchange process. Hoffman et al. (1980) indicated that proton exchange with cations was negligible as rain ($\text{pH} \sim 4$) penetrated chestnut canopies, for the total acidity of rainwater was conserved during throughfall, with weak acids exchanging for strong acids. This may be the case for moderate acidity, but at higher $[\text{H}^+]$ specific leaf injury could occur, accompanied or, more likely, caused by proton exchange. Cronan and Reiner (1983) also reported enhancement of basic cations in coniferous and hardwood throughfall with concurrent neutralization of precipitation ($\text{pH} = 4.1$). They proposed both proton exchange and Bronsted base leaching in the canopy as important processes. Throughfall measured during stratus rainfall (see Fig. 8) demonstrated similar enhancement of basic cations, however, with nitrate and acidity enhanced as well. The release of accumulated dry-deposited acidic aerosol and nitric acid was likely important.

Without further research, it is not possible to confirm a direct relationship between acidic cloudwater and needle symptoms observed at Henninger Flats. However, similar damage to leaf surfaces has been reported in exposure studies. In simulated acid rain experiments, Haines et al. (1980) found a threshold of leaf damage for most species tested in a pH range 2.5 to 2.0 and for *Pinus strobus* needles at pH 1.0 to 0.5. Wood and Bormann (1974) observed foliar tissue damage at pH 3 for misting of yellow birch seedlings; significant growth decreases occurred when acidic exposure (pH 2.3) was initiated during the germination stage. Thomas et al. (1952) reported cases in which plant injury was not initially caused

by concentrated H_2SO_4 aerosol—apparently due to its high surface tension—but followed surface wetting by fog.

Cloudwater capture may represent a more severe threat to plant tissue than deposition accompanying rainfall or by dry particle deposition alone, because it subjects plant surfaces to much higher aqueous concentrations and acidities. Dry deposition of pollutant gases (e.g., SO_2) can also lead to acidic solutions, however, these affecting internal tissue (Hallgren, 1978). Leaf surface wetting may be a critical component of the interaction between foliar membranes and deposited pollutants. This potential has been raised by Lindburg et al. (1982) with respect to the wetting of metal particles they monitored on dry leaf surfaces. Furthermore, surface wetting greatly reduces particle rebound (Chamberlain, 1967) and enhances SO_2 uptake by pine needles (Garland and Branson, 1977).

5. Summary

Highly concentrated, acidic stratus cloudwater was monitored as it intercepted a Los Angeles pine forest. Observed pH values ranged from 2.06 to 3.87 for samples ($n = 128$) collected on 8 days in June 1982 and 15 days in May/June 1983. The median value was below pH 3 for both seasons' data. The ratio of nitrate/sulfate in cloudwater samples was between 1.5 and 2; rainwater at the same site had a ratio of approximately 1. About half of the nitrate and sulfate measured in the cloudwater was not neutralized. The solute mass per cubic meter of air in the cloudwater was of the same magnitude as for aerosol samples collected before, during and after fog episodes. The nitrate/sulfate ratio of the dry aerosol was lower than in the cloudwater; the additional nitrate is believed to be derived from dissolution of gaseous nitric acid by cloud droplets. Overall, a higher fraction of precursor nitrate (aerosol and gaseous) than sulfate aerosol appears to be scavenged by the cloud droplets.

Wet deposition at Henninger Flats in 1982–83 was comparable to the value for Pasadena in 1978–79, even though the water flux was more than twice as great. The greater frequency and rainfall amount per storm in the recent year is believed to have led to the lower volume-weighted

mean concentrations in the Henninger Flats precipitation. The solute deposition with several light, spring rains (summing to ~1% of annual rainfall) was a disproportionate fraction of the annual total: H^+ , NO_3^- , and SO_4^{2-} were ~20% or more.

Based on a reasonable estimate of fog precipitation, deposition of sulfate, nitrate and free acidity due to intercepted stratus clouds may be of comparable magnitude as that due to the incident rainfall at Henninger Flats. Fog and stratus precipitation, though not previously considered on the regional scale, appears to be a seasonally important vector for pollutant deposition in the Los Angeles basin.

Cloudwater that had deposited on local pine needles was collected and found to be in general more concentrated and with acidity comparable to suspended cloudwater. Enhancement of cations,

especially K^+ , is believed to be due to leaching from foliar surfaces. Enhancement was also found in throughfall samples collected during stratus rainfall. Injury to sensitive plant tissue has been reported in the literature by exposure to similarly acidic solutions.

6. Acknowledgements

We are grateful to the Los Angeles Fire Department Forestry Bureau for allowing us to conduct our field monitoring at Henninger Flats and to the Rangers at the site for their assistance. This research has been supported by a contract with the California Air Resources Board (Contract No. A2-048-32), with additional support from the Coordinating Research Council.

REFERENCES

- Appel, B. R., Kothny, E. L., Hoffer, E. M., Hidy, G. M. and Wesolowski, J. J. 1978. Sulfate and nitrate data from the California Aerosol Characterization Experiment (ACHEX). *Environ. Sci. Tech.* 12, 418-425.
- Appel, B. R., Wall, S. M., Tokiwa, Y. and Haik, M. 1979. Interference effects in sampling particulate nitrate in ambient air. *Atmos. Environ.* 13, 319-325.
- Azevedo, J. and Morgan, D. L. 1974. Fog precipitation in coastal California forests. *Ecology* 55, 1135-1141.
- Bassett, M. E. and Seinfeld, J. H. 1984. Atmospheric equilibrium model for sulfate and nitrate aerosols—II. Particle size analysis. *Atmos. Environ.* 18, 1163-1170.
- Brewer, R. L., Ellis, E. C., Gordon, R. J. and Shepard, L. S. 1983. Chemistry of mist and fog from the Los Angeles urban area. *Atmos. Environ.* 17, 2267-2271.
- California Air Resources Board 1982. *Emission Inventory: 1979*. Emission Inventory Branch, Sacramento, CA.
- California Air Resources Board 1979. *Emission Inventory: 1974*. Emission Inventory Branch, Sacramento, CA.
- Chamberlain, A. C. 1967. Transport of *Lycopodium* spores and other small particles to rough surfaces. *Proc. Roy. Soc.* 296A, 45-70.
- Cronan, C. S. and Reiners, W. A. 1983. Canopy processing of acidic precipitation by coniferous and hardwood forests in New England. *Oecologia* 59, 261-223.
- Dasch, J. M. 1983. A comparison of surrogate surfaces for dry deposition collection. In *Precipitation scavenging, dry deposition, and resuspension* (ed. H. R. Pruppacher et al.). Amsterdam: Elsevier Science, 883-902.
- Daum, P. H., Schwartz, S. E. and Newman, L. 1984. Acidic and related constituents in liquid water stratiform clouds. *J. Geophys. Res.* 89D, 1447-1458.
- Dollard, G. J., Unsworth, M. H. and Harve, M. J. 1983. Pollutant transfer in upland regions by occult precipitation. *Nature* 302, 241-243.
- Dolske, D. A. and Gatz, D. F. 1984. A field intercomparison of sulfate dry deposition monitoring and measurement methods. In *Deposition both wet and dry* (ed. B. B. Hicks). Boston: Buttonworth Publisher, 121-132.
- Ekern, P. C. 1964. Direct interception of cloud water on Lanaihale, Hawaii. *Soil Sci. Soc. Am. Proc.* 28, 419-421.
- Evans, L. S. 1982. Biological effects of acidity in precipitation on vegetation; a review. *Environ. Exp. Bot.* 22, 155-169.
- Garland, J. A. and Branson, J. R. 1977. The deposition of sulfur dioxide to pine forest assessed by a radioactive tracer method. *Tellus* 28, 445-454.
- Haines, B., Stefani, M. and Hendrix, F. 1980. Acid rain: threshold of leaf damage in eight plant species from a southern Appalachian forest succession. *Water, Air and Soil Pollut.* 14, 403-407.
- Hallgren, J. 1978. Physiological and biochemical effects of sulfur dioxide on plant. In *Sulfur in the environment Part II* (ed. J. O. Nriagu). New York: J. Wiley & Sons, 163-209.
- Hering, S. V. and Blumenthal, D. L. 1984. Fog Sampler Intercomparison Study Final Report (Draft). Project No. STI 11 90063. Available from Coordinating Research Council, 219 Perimeter Center Pkwy. Atlanta, GA.

- Hoffman, Jr., W. A., Lindberg, S. E. and Turner, R. R. 1980. Precipitation acidity: the role of forest canopy in acid exchange. *J. Environ. Qual.* 9, 95–100.
- Hori, T. (ed.) 1953. *Studies on fog in relation to fog-preventing forest*. Sapporo/Japan: Tanne Trading Co., 399 pp.
- Hudson, J. G. and Rogers, C. F. 1984. Interstitial CCN measurements related to mixing in clouds. Proceedings of 9th Intern. Cloud Physics Conference August 21–28, Tallinn, USSR.
- Jacob, D. J. and Hoffmann, M. R. 1983. A dynamic model for the production of H^+ , NO_3^- , and SO_4^{2-} in urban fog. *J. Geophys. Res.* 88C, 6611–6621.
- Jacob, D. J., Waldman, J. M., Munger, J. W. and Hoffmann, M. R. 1984a. A field investigation of physical and chemical mechanisms affecting pollutant concentrations in fog droplets. *Tellus* 36B, 272–285.
- Jacob, D. J., Wang, R.-F. T. and Flagan, R. C. 1984b. Fogwater collector design and characterization. *Environ. Sci. & Technol.* 18, 827–833.
- Katz, U. 1980. A droplet impactor to collect liquid water from laboratory clouds for chemical analysis. In *Communications a la VIII conference internationale sur la physique des nuages* (July 15–19), Clermont-Ferrand/France, 697–700.
- Keith, R. W. 1980. *A climatological/air quality profile: California south coast air basin*. South Coast Air Quality Management District, El Monte, CA.
- Kerfoot, O. 1968. Mist precipitation on vegetation. *For Abst.* 29, 8–20.
- Liljestrand, H. M. 1980. *Atmospheric Transport of Acidity in Southern California by Wet and Dry Mechanisms*. Ph.D. Thesis, California Institute of Technology, Pasadena, CA.
- Liljestrand, H. M. and Morgan, J. J. 1981. Spatial variations of acid precipitation in Southern California. *Environ. Sci. & Technol.* 15, 333–338.
- Lindberg, S. E., Harriss, R. C. and Turner, R. R. 1982. Atmospheric deposition of metals to forest vegetation. *Science* 215, 1609–1611.
- Lovett, G. M. 1984. Rates and mechanisms of cloud water deposition to a subalpine balsam fir forest. *Atmos. Environ.* 18, 361–371.
- Morgan, J. J. and Liljestrand, H. M. 1980. *Measurement and Interpretation of Acid Rainfall in the Los Angeles Basin*. W. M. Keck Laboratory Report AC-2-80. California Institute of Technology, Pasadena, CA.
- Mrose, H. 1966. Measurements of pH and chemical analyses of rain-, snow- and fog-water. *Tellus* 18, 266–270.
- Munger, J. W., Jacob, D. J., Waldman, J. M. and Hoffmann, M. R. 1983a. Fogwater chemistry in an urban atmosphere. *J. Geophys. Res.* 88C, 5109–5121.
- Munger, J. W., Waldman, J. M., Jacob, D. J. and Hoffmann, M. R. 1983b. Vertical variability and short-term temporal trends in precipitation chemistry. In *Precipitation scavenging, dry deposition, and resuspension* (ed. H. R. Pruppacher et al.). Amsterdam: Elsevier Science, 275–282.
- Munger, J. W., Jacob, D. J. and Hoffmann, M. R. 1984. The occurrence of bisulfite-aldehyde addition products in fog- and cloudwater. *J. Atmos. Chem.* 2, 335–350.
- Nagel, J. F. 1956. Fog precipitation on Table Mountain. *Q. J. R. Meteorol. Soc.* 82, 452–460.
- Oberlander, G. T. 1956. Summer fog precipitation on the San Francisco peninsula. *Ecology* 37, 851–852.
- Okita, T. 1968. Concentration of sulfate and other inorganic materials in fog and cloud water and in aerosol. *J. Meteorol. Soc. Japan* 46, 120–126.
- Pruppacher, H. R. and Klett, J. D. 1978. *Microphysics of clouds and precipitation*. Amsterdam: D. Reidel, 714 pp.
- Richards, Sr., B. L., Taylor, O. C. and Edmunds, Jr., G. F. 1968. Ozone needle mottle of pine in southern California. *J. Air Pollut. Control Assoc.* 18, 73–77.
- Russell, A. G., McRae, G. J. and Cass, G. R. 1983. Mathematical modeling of the formation and transport of ammonium nitrate aerosol. *Atmos. Environ.* 17, 949–964.
- Scherbatskoy, T. and Klein, R. M. 1983. Response of spruce and birch foliage to leaching by acidic mists. *J. Environ. Qual.* 12, 189–195.
- Schlesinger, W. H. and Reiners, W. A. 1974. Deposition of water and cations on artificial foliar collectors in fir krummholz of New England mountains. *Ecology* 55, 378–386.
- Sehmel, G. A. 1980. Particle and gas dry deposition: a review. *Atmos. Environ.* 14, 983–1011.
- Spicer, C. W., Howes, J. E., Bishop, T. A. and Arnold, L. H. 1982. Nitric acid measurement methods: an intercomparison. *Atmos. Environ.* 16, 1487–1500.
- Stelson, A. W. and Seinfeld, J. H. 1982. Relative humidity and temperature dependence of the ammonium nitrate dissociation constant. *Atmos. Environ.* 16, 983–992.
- Thomas, M. D., Hendricks, R. H. and Hill, G. R. 1952. Some impurities in the air and their effects on plants. In *Air Pollution: Proc. of US Tech. Conf.* (ed. L. McCabe). New York: McGraw-Hill, 41–47.
- Tukey, Jr., H. B. 1970. The leaching of substances from plants. *Ann. Rev. Plant. Physiol.* 71, 305–324.
- Waldman, J. M. 1985. *Contributions of Fog and Dew to the Depositional Flux of Acidity*. Ph.D. Thesis, California Institute of Technology, Pasadena, CA.
- Vogelmann, H. W. 1973. Fog precipitation in the cloud forests of eastern Mexico. *Bioscience* 23, 96–100.
- Vogelmann, H. W., Siccama, T., Leedy, D. and Ovitt, D. C. 1968. Precipitation from fog moisture in the Green Mountains of Vermont. *Ecology* 49, 1205–1207.
- Wood, T. and Bormann, F. H. 1974. The effects of an artificial acid mist upon the growth of *Betula alleghaniensis* Britt. *Environ. Pollut.* 7, 259–267.
- Yoshida, Z. 1953. General survey of the studies on fog-preventing forest. In *Studies on fog in relation to fog-preventing forest* (ed. T. Hori). Sapporo/Japan: Tanne Trading Co., 1–23.

CHAPTER 19

Environ. Sci. Technol. 1987, 21, 854-863

Field Intercomparison of Five Types of Fogwater Collectors

Susanne V. Hering^{*,†}

University of California, Los Angeles, California 90025

Donald L. Blumenthal

Sonoma Technology Inc., Santa Rosa, California 95401

Robert L. Brewer

Global Geochemistry Corporation, Canoga Park, California 91303

Alan Gertler

Desert Research Institute, Reno, Nevada 89506

Michael Hoffmann

California Institute of Technology, Pasadena, California 91125

John A. Kadlecsek

State University of New York, Albany, New York 12222

Keith Pettus

AeroVironment Inc., Monrovia, California 91051

■ Fog samplers of five different designs were operated simultaneously to assess differences, if any, in measured acidity, analyte concentrations, and liquid water collection efficiencies. Measurements were made at Henninger Flats, a mountainous site at 777 m msl overlooking the Los Angeles, CA, basin. Samplers were operated by AeroVironment, Inc. (Monrovia, CA), the California Institute of Technology (Pasadena, CA), the Desert Research Institute (Reno, NV), Global Geochemistry Corp. (Canoga Park, CA), and the State University of New York Atmospheric Sciences Research Center (Albany, NY). The experimental design included duplicate chemical analyses and data from collocated identical samples, from separated identical samplers, and from the five sampler types. The first three data types represent variability inherent in the experiment, to which the variability among samples types is compared. In general, larger discrepancies were found in the liquid water content data than in the fogwater chemistry. All of the samplers agreed for fogwater pH. Four of the samplers showed reasonable agreement for analyte concentrations. Only three of the samplers showed any agreement for liquid water content.

Field Intercomparison of Five Types of Fogwater Collectors

Susanne V. Hering^{*†}

University of California, Los Angeles, California 90025

Donald L. Blumenthal

Sonoma Technology Inc., Santa Rosa, California 95401

Robert L. Brewer

Global Geochemistry Corporation, Canoga Park, California 91303

Alan Gertler

Desert Research Institute, Reno, Nevada 89506

Michael Hoffmann

California Institute of Technology, Pasadena, California 91125

John A. Kadlecsek

State University of New York, Albany, New York 12222

Kelth Pettus

AeroVironment Inc., Monrovia, California 91051

■ Fog samplers of five different designs were operated simultaneously to assess differences, if any, in measured acidity, analyte concentrations, and liquid water collection efficiencies. Measurements were made at Henninger Flats, a mountainous site at 777 m mal overlooking the Los Angeles, CA, basin. Samplers were operated by AeroVironment, Inc. (Monrovia, CA), the California Institute of Technology (Pasadena, CA), the Desert Research Institute (Reno, NV), Global Geochemistry Corp. (Canoga Park, CA), and the State University of New York Atmospheric Sciences Research Center (Albany, NY). The experimental design included duplicate chemical analyses and data from collocated identical samples, from separated identical samplers, and from the five sampler types. The first three data types represent variability inherent in the experiment, to which the variability among samples types is compared. In general, larger discrepancies were found in the liquid water content data than in the fogwater chemistry. All of the samplers agreed for fogwater pH. Four of the samplers showed reasonable agreement for analyte concentrations. Only three of the samplers showed any agreement for liquid water content.

Introduction

Recent work has shown that fogs, as well as rain, can be a source of acidity. Measurements (1-4) in the Los Angeles basin show that fogwater pH values can be as low as 2.2-2.7. Several groups have developed fogwater collectors, but the calibration of the instruments is difficult. In this study, we wish to compare how the different collectors compared in side by side operation under field conditions.

The objective of the work is to evaluate systematic differences, if any, among the samplers. Parameters that were examined include (1) fogwater acidity, (2) concentrations of ionic species, and (3) liquid water collection rates. Although no absolute standard is available, it is useful to evaluate the relative performance of the samplers to assess design factors affecting fogwater collection and

to enable comparison of data from different research groups.

The intercomparison was conducted during June 1983 at Henninger Flats in the San Gabriel Mountains north of Pasadena, CA. Five different types of fog samplers were operated by the groups that designed them. Samplers were provided by AeroVironment, Inc. (AV, Monrovia, CA), the California Institute of Technology (CIT, Pasadena, CA), the Desert Research Institute (DRI, Reno, NV), Global Geochemistry Corp. (GGC, Canoga Park, CA), and the State University of New York Atmospheric Sciences Research Center (ASRC, Albany, NY). Chemical analyses of all of the fogwater samples were performed by CE Environmental Monitoring Services Inc. (EMSI, formerly Rockwell International Environmental Services, Newbury Park, CA). The study design, field management, and data analyses were performed by Sonoma Technology Inc. (Santa Rosa, CA). Supporting meteorological, gas, and aerosol measurements were made by several additional participants, including CIT, DRI, Southern California Edison (Rosemead, CA), Environmental Research and Technology (Westlake Village, CA), the National Center for Atmospheric Research (Boulder, CO), and University of California at Los Angeles (UCLA).

The experimental design includes data from (I) duplicate chemical analyses, (II) collocated identical samplers, (III) separated identical samplers, and (IV) from the ASRC, AV, CIT, DRI, and GGC sampler types. The first three represent variability inherent in the experiment, to which the variability among sampler types is compared. Data analyses include comparisons of the relative fogwater collection rates and of measured ionic concentrations. The portion of variability attributable to sampler type is assessed with analysis of variance techniques. The variability among sampler types is examined as a function of liquid water content and droplet size. The average bias among sampler types is reported when the differences are statistically significant.

Descriptions of the Fogwater Collectors

Of the five types of samplers that were compared, all of the collectors used impaction and interception to collect

[†]Consultant to Sonoma Technology Inc.

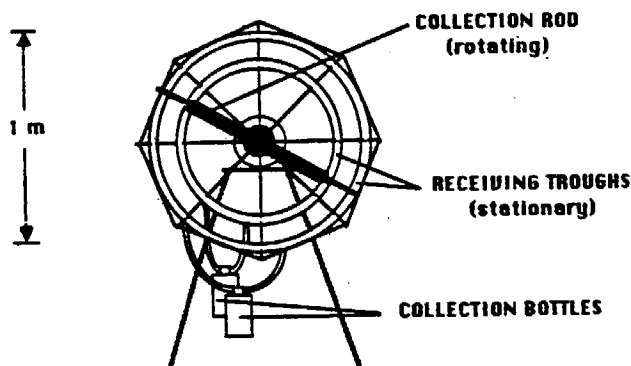


Figure 1. AeroVironment Inc. (AV) fog collector. Fogwater impacts on the cylindrical rotating rod.

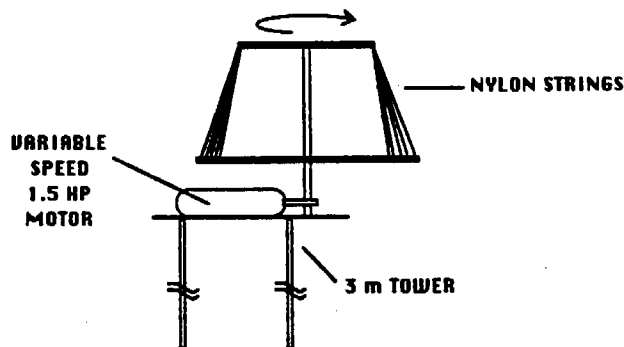


Figure 2. Atmospheric Science Research Center (ASRC) string collector. This samples rotates in the horizontal plane; fogwater is intercepted by the nylon strings.

the fogwater droplets. The California Institute of Technology, ASRC, and AeroVironment instruments are rotating collectors, employing external surfaces for impaction of the droplets. The Global Geochemistry and Desert Research Institute instruments are internal collectors, in which air is drawn into the instrument and extracted by surfaces internal to the device.

AeroVironment Rotating Rod Collector. The AV fog sampler collects droplets by impaction on a Teflon-coated rod rotated in a vertical plane at 3450 rpm (Figure 1). The outer part of the rod is 1.6 mm and the inner part is 19 mm in diameter to provide size cuts of 2.5 and 10 μm , respectively. Water impacting on the rods is transferred by centrifugal force to circular polyethylene troughs that drain to polyethylene collection bottles. Separate troughs and sample bottles are used for the two size fractions.

ASRC String Collector. The ASRC sampler consists of 150 0.41-mm strings mounted between two plates as shown in Figure 2. The sampler rotates about its vertical axis at 100 rpm. Water impacting on the strings collects in traps on the bottom plate. Periodically, the sample rotation is stopped, and fogwater on the strings is coaxed into the traps by trapping the bottom plate with a mallet. At the end of the sampling period, water in the traps is manually transferred to polyethylene bottles.

California Institute of Technology Rotating Arm Collector. The CIT rotating arm collector (5) is an external impactor that sweeps through the air at a high velocity in order to collect large particles. The arm spins in a vertical plane, driven by a 1.5-hp motor, as illustrated in Figure 3. Each end of the arm has a slot milled into its leading edge. Standard 30-mL Nalgene bottles are mounted at the ends of the arm to collect the water that impacts in the slots. Threaded Teflon tubes are screwed on the end of the arm and extend inside the collection bottles, preventing the collected fogwater from running out after the instrument is stopped. Deflectors prevent water

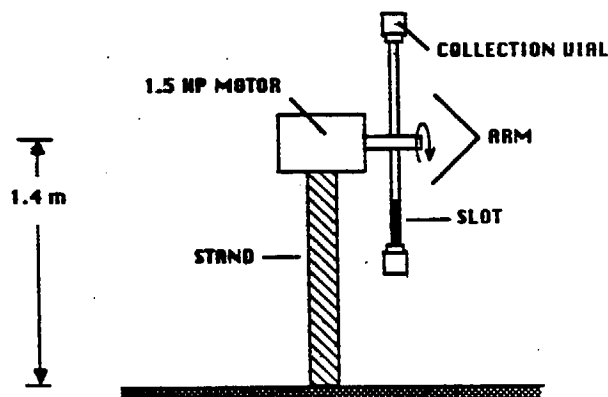


Figure 3. California Institute of Technology (CIT) rotating arm collector. Fogwater impacts in the slots located on the leading edge of the rotating arm.

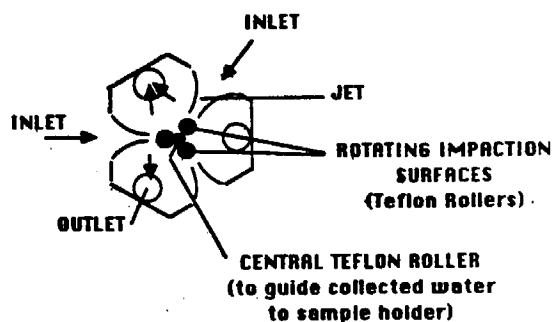


Figure 4. Schematic horizontal cross section of the Desert Research Institute (DRI) linear jet cloudwater collector.

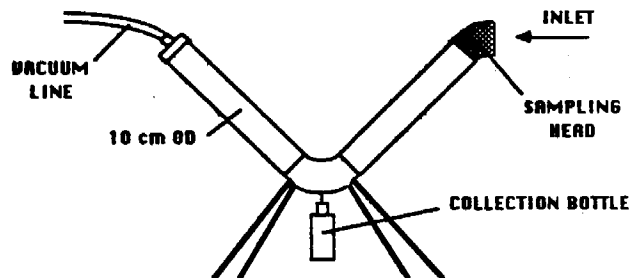


Figure 5. Global Geochemistry Corp. (GGC) fog sampler. Fog droplets are collected by the mesh mounted in the sampling head.

that impacts on the solid part of the arm from entering the slot. Small fins are welded to the back of the arm for extra strength. The entire arm is Teflon-coated to prevent chemical contamination and to facilitate cleaning.

Desert Research Institute Linear Jet Collector. The DRI collector, shown in Figure 4, is based on a jet impaction principle (6). Fog is drawn through three rectangular jets at a total flow rate of 20 L s^{-1} . The accelerated droplets impact on rotating Teflon rollers, and are transferred to a central roller. Here, the fogwater is forced to accumulate in bulk form and is deposited into a polystyrene collection vessel. The impactor has a sharp cut-off at 5- μm diameter to allow efficient collection of droplets while rejecting small interstitial particles. The collector is housed in a shelter consisting of an inverted, insulated 55-gallon drum to prevent collection of precipitation. Airflow up to the collector is provided by a fan.

Global Geochemistry Mesh Sampler. The Global Geochemistry fog sampler (Global Geochemistry Corp., Canoga Park, CA) is an internal impaction sampler that collects fogwater on a 10 cm diameter by 4 cm thick polypropylene mesh located at the entrance of a V-shaped Teflon-lined PVC pipe (Figure 5). The mesh consists of a pad of interlaced 410- μm filaments and has a void volume

of 96%. Air is drawn through the mesh at 1.7 m³/min. Fogwater impacts on the mesh, coalesces, and then drains into a polyethylene bottle at the bottom of the V tube. The sampler, calibrated by McFarland and Ortiz (7), has a 50% cut point of 2.4 μ m and a collection efficiency of $\geq 98\%$ for particles larger than 5 μ m. Liquid holdup on the mesh depends on the mass of liquid sampled. If ≤ 1 g of water is sampled, all of it remains on the mesh. If 100 g is sampled, less than 5% remains.

Experimental Design

Although the purpose of the experiment was to assess systematic differences in measurements due to sampler type, there are other sources of variability within the field measurements. These include precision of the chemical analysis, consistency of sampling for a specified sampler type, and variability due to sampler siting. The experiments were designed to account for these variables, in order to distinguish variations due to sampler type.

The five types of data collected in the study include (I) replicate chemical analyses of individual samples, (II) simultaneous samples collected by collocated identical samplers, (III) simultaneous samples collected by identical samplers sited at different locations within the sampling area, (IV) simultaneous samples collected by all five sampler types, and (V) ancillary measurements of the fog liquid water content, using principally the CO₂ laser transmissometer and Particle Measuring Systems optical particle counter.

The replicate chemical analyses (type I data) are a direct measure of the precision of the chemical assays. The replicate sample collection by collocated samplers of the same design (type II data) is a measure of the sum of the variability due to the imprecision of sample collection and of chemical analysis. Similarly, type III data, the simultaneous collection by separated sampler pairs of the same design, give a measure of the overall variability within the experiment not attributable to sampler type. These data include the effects of fog inhomogeneity across the sampling area as well as reproducibility of sample collection and chemical analysis.

Replicate chemical analyses (type I data) were obtained by sample splitting in the field, followed by blind replicate analysis by the central laboratory (CE Environmental Services). Additionally, pH measurements were made both in the field, within 2 h of collection, and again in the central laboratory, a few days later. Duplicate samplers from Global Geochemistry and the California Institute of Technology allowed us to obtain the type II and type III data. Simultaneous collection by all five (sampler) types gave the type IV data. With the exception of the replicate sampler pairs described above, the sampler locations were fixed throughout the project. Ideally, the siting of the different samplers would have been changed to randomize the effects of location. However, the immobility of some of the samplers precluded this possibility.

Sampling Procedure

The Henninger Flats sampling site is located at 2550 ft (777 m) msl north of Pasadena, CA, overlooking the Los Angeles Basin. The area is operated by the Forestry Division of the Los Angeles County Fire Department as a tree nursery and public campground. Samplers were sited in an area measuring approximately 18 \times 35 m. One sampler each of the ASRC, DRI, and AV designs was operated along with two samplers each of the CIT and GGC designs.

During a fog event, all samplers were operated simultaneously. Due to inherent differences in sampler design

and collection rates, the required times for sample collection varied. In general, half of the samplers would collect several 1-h samples during the same time others collected a single 2- or 3-h sample. The sampling time for a "run" was determined by the slower collectors and set at either exactly 2 or exactly 3 h. Collection vials from samplers with large collection rates were changed at 1-h intervals and analyzed separately. For the statistical analyses, data from the sequential 1-h samples are combined to allow comparison with single samples obtained from other samplers in the same time period. The 1-h ion concentration data are weighted in proportion to the mass of fog-water collected and then averaged to give the effective concentration.

Immediately after collection, samples were weighed to determine the mass of water collected. Sample pH was determined on-site with a 0.5-mL aliquot by a Radiometer Microelectrode meter. Occasionally, aliquots were also taken for conductivity and hydrogen peroxide determinations. Samples were split for analyses by both the central laboratory (EMSI) and the participating groups. Eight percent of samples for EMSI were split again to provide blind replicates for quality control. Samples for the central laboratory were transferred to polyethylene bottles provided by the lab and stored on ice. These sample manipulations were all handled on-site within 2 h of collection. The day following collection, the samples were transported in an ice chest to the central laboratory for analysis of pH, strong acid, total acid, nitrate, sulfate, chloride, ammonium, sodium, potassium, calcium, magnesium, and conductivity. The total acid measurement employed titration to pH 8.3 and approximates the sum of strong acids, organic acids, dissolved SO₂, and HONO.

For the duplicate sampler pairs from CIT and GGC, two different sampling configurations were used. The first configuration placed the two CIT samplers side by side, with the GGC samplers separated by a distance of 10 m. The second configuration placed the GGC samplers together, with the CIT samplers separated by a distance of about 30 m. Collocated identical samplers were used to assess measurement precision, and split sampler pairs were used to assess the homogeneity of the fog in the sampling area.

Independent from the fogwater collectors, the liquid water content of the air was measured at the site with a CO₂ laser transmissometer, a Particle Measurement System (PMS, Boulder, CO) CASP-100-HVSP laser optical particle counter, and three high-volume samplers. Gas and aerosol measurements included ozone, sulfur dioxide, carbon monoxide, peroxyacetyl nitrate, nitric acid, ammonia, carbonyl compounds, sulfate, nitrate, chloride, and cloud condensation nuclei. Wind speed, wind direction, temperature, humidity, and inversion height were also measured. Details of the sample handling and experimental protocol are given by Hering and Blumenthal (8).

Average Fog Composition and Sampling Conditions

In this work, all measurements were made in June 1983, under conditions of very light winds of 0.1–0.4 m/s and temperatures of 10–13 °C. Ozone levels were 0.02–0.06 ppm, CO was 0.6–1.5 ppm, and SO₂ was 2–6 ppb. The liquid water content, as determined by sampler collection rates, was 20–200 mg of H₂O/m³ of air. Volume-median droplet diameters determined by the PMS optical particle counter were 18–28 μ m.

The total ionic strength of fogwaters collected during the study varied by over an order of magnitude. The most dilute samples had a total ionic strength, on an equivalence basis, of 1100 μ equiv/L; the most concentrated samples

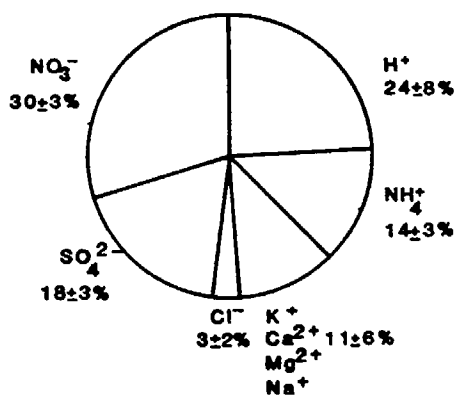


Figure 6. Average equivalence percent of major analytes in collected fogwater. Hydrogen ion is based on field pH measurements.

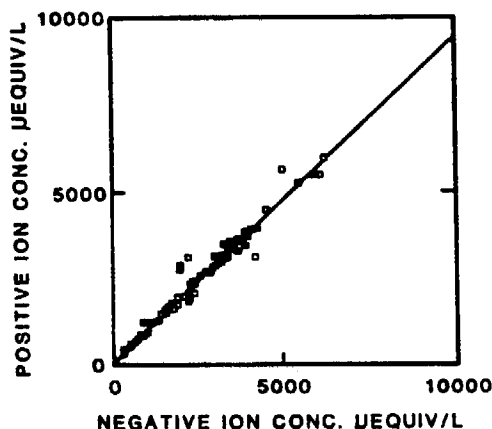


Figure 7. Ion balances for all fogwater samples, except those too small to permit complete chemical analyses. Hydrogen ion concentrations are taken from the field pH measurements. The line is the least-squares linear fit, $y = 0.95x + 150$, $r = 0.98$.

were 17 000 $\mu\text{equiv/L}$. In contrast, the relative composition of the major analytes was quite consistent. As shown in Figure 6, ammonium, sulfate, and nitrate were respectively $14 \pm 3\%$, $18 \pm 3\%$, and $30 \pm 3\%$ on an equivalence basis of the total ions measured. The proportion of hydrogen ion calculated from field pH measurements was more variable at $24 \pm 8\%$. Ion and conductivity balances, shown in Figures 7 and 8, indicate most of the major species have been measured.

The concentrations of the major analytes fall within the range previously reported for the Los Angeles urban area. Our pH values varied from 2.4 to 3.5, whereas Jacob et al. (2) report values from 1.7 to 6.2; Brewer et al. (3) report 2.7–7.1. The maximum ammonium, sulfate, and nitrate levels we observed were 2700, 4800, and 6700 $\mu\text{equiv/L}$, respectively. Minimum levels were 100–200 $\mu\text{equiv/L}$. These levels are intermediate to those reported by Jacob and by Brewer.

We note that the dominant anion is nitrate. For this work, the average nitrate to sulfate ratio, on an equivalence basis, is 1.8 ± 0.4 . This is similar to other data for the Los Angeles Basin (1–4, 9, 10) but much higher than that measured at Whiteface Mountain, NY (11–13), in northern England (14), and in Oildale, CA (1).

Fogwater Collection Rates and Estimates of Liquid Water Content

Both the liquid water content (LWC) and chemistry of fogs are of interest. Knowledge of LWC is required to assess atmospheric burdens of analytes found in the fogwater. This is important for modeling pollutant scavenging and reactions in fog droplets or for assessing total acid

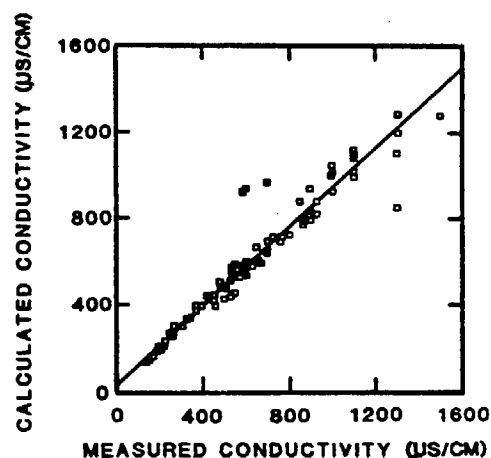


Figure 8. Comparison of calculated and measured conductivity. Hydrogen ion concentrations taken from the field pH measurements. The line is a least-squares linear fit to the data.

deposition. Each of the samplers can be used to estimate a liquid water content on the basis of the rate of water collection and the air sampling rate. Ancillary measurements of LWC included in this study are CO_2 laser transmissometer and an optical particle counter.

Even in a dense fog, most of the water present is in the vapor phase. For example, for the 10–13 $^{\circ}\text{C}$ temperatures encountered in this study, the equilibrium vapor pressure of water is equivalent to 9–11 g of water vapor/ m^3 of air. The highest liquid water contents of the study were on the order of 0.2 g/ m^3 , or less than 3% of the vapor water. As a result, small changes in the vapor equilibrium at the sampler, induced by adiabatic expansion or compression of the sampled air, could cause a large change in the observed liquid water content. Other factors that affect the sampler LWC measurements are the droplet collection efficiency and loss of water after collection. In the discussion that follows we have made no correction for these effects. We simply compare the different samplers on the basis of the rates of water collection normalized by the volumetric air sampling rate.

Collocated Identical Samplers (Type II Data). Reproducibility of the fogwater collection is examined by comparing the rates of water collection for collocated samplers of the same design. For side by side sampling with the CIT samplers, the mass of water collected per minute of sampling agrees well. Our data set of 12 pairs of CIT samples gives a pooled standard deviation of 0.017 g/min, or 2% of the mean value. For the GGC mesh sampler pairs, the standard deviation in water collection rates is 0.011 g/min, corresponding to 6% of the mean. Data for the GGC samplers is shown by the open symbols in Figure 9.

Separated Identical Samplers (Type III Data). One concern in the intercomparison study was the significance of variations in fog intensity across the sampling area. Especially in light fog conditions, visual observation showed spatial as well as temporal variations in the fog density. The question we address here is whether those observed spatial variations persist when averaged over the 1- or 2-h sampling periods. Data for the fogwater collection rates for simultaneous sampling by GGC samplers at different locations are shown by the solid symbols in Figure 9. The simultaneous split sampling data still show good agreement. The pooled standard deviations (including the outlier points) are 0.033 g/min (10%) and 0.022 g/min (6%) for the CIT and GGC samplers, respectively. The agreement between separated samplers is as good as between collocated samplers of the same design. We con-

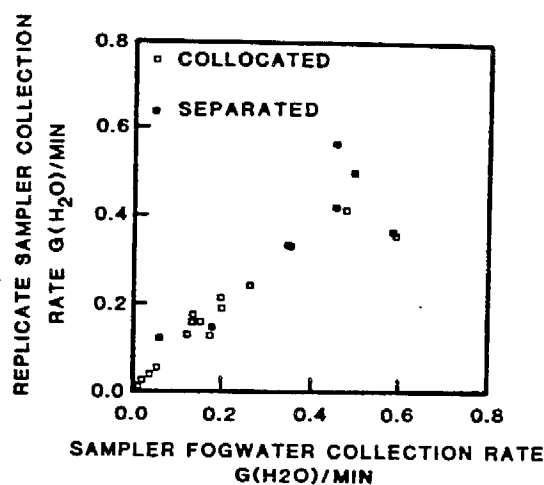


Figure 9. Comparison of fogwater collection rates for replicate GGC fog samplers located side by side (□) and separated (■).

cluded that the fog is sufficiently homogeneous to allow us to evaluate differences between sampler types.

Comparison of Sampler Types (Type IV Data). Different samplers have different effective volumetric collection rates. To compare different sampler types, we wish to know the ratio of the amount of water collected to the volume of air sampled. For collectors with 100% efficiency, this would be the same as the liquid water content (LWC). Calculation of this ratio allows comparison with the other measures of LWC, including the laser transmissometer and the optical particle counter (OPC).

The volume of air sampled by the internal collectors, namely, the GGC mesh and the DRI impactor, is readily determined because the volumetric airflow rates were measured to be 1.7 and 1.2 m³/min, respectively. For the external collectors, several factors enter into the effective air sampling rate, including (1) the volume of air intercepted by the collection surface per unit time and (2) the rate of replacement of air sampled. In this discussion we only consider the first factor, the volume of air intercepted by the collection surface, to give effective sampling rates. The values used here are 5 m³/min for the CIT rotating arm collector, 6.5 m³/min for the ASRC string collector, and 3.4 and 8 m³/min for the AV >2.5- and >10-μm samples, respectively.

With these values for the effective air volumetric sampling rates, the liquid water content indicated by each sampler, expressed as grams of water per cubic meter of air sampled, is compared with the mean value from the DRI, ASRC, CIT, and GGC samplers excluding replicate samplers from CIT and GGC. The AV sampler was not included in the mean because it was not on-site during a large portion of the study. Had it been possible, the laser transmissometer would have been chosen as the basis of comparison, but these data too were available for only part of the project. The LWC calculated from the OPC droplet size distributions was not considered a good basis of comparison because of the large discrepancies from other measurements described below.

Scatter in the data can be seen in Figure 10, which shows the water collection by each sampler with respect to the mean of the DRI, ASRC, CIT, and GGC samplers. Note that the correlations are quite good, although there are systematic differences between the samplers. Analysis of variance shows that the sampler liquid water content values differ at the 99.5% confidence level. For all of the sampling periods, the pooled standard deviation is 79 mg/m³, corresponding to a coefficient of variation of 109%. This is considerably larger than the 6–10% variability for

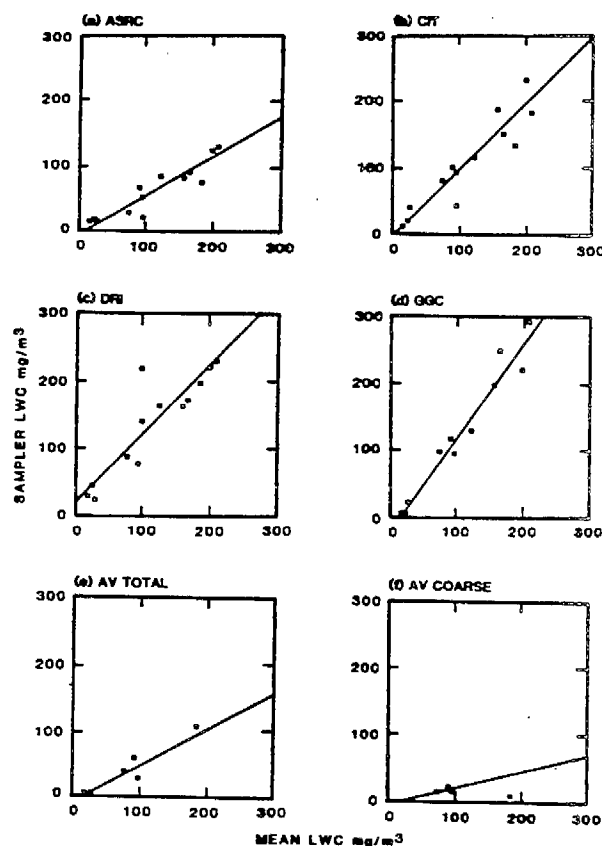


Figure 10. For each sampler the mass of fogwater collected per cubic meter of air sample is compared with the mean value for the ASRC, CIT, DRI, and GGC samplers. Values are from the (a) ASRC rotating string, (b) CIT rotating arm, (c) DRI linear jet, (d) GGC mesh, (e) AV-total fog (>2 μm), and (f) AV-coarse fog (>10 μm) samplers. Lines are least-squares linear fits (see text).

simultaneous sampling by separated samplers of the same type.

A least-squares fit to the data of Figure 10 gives significant results for the inferred liquid water content for the AV total, CIT, DRI, and GGC samplers, as follows:

$$AV = (0.5 \pm 0.2)M - (8 \pm 10) \quad r = 0.873$$

$$CIT = (1.0 \pm 0.1)M - (0.3 \pm 14.0) \quad r = 0.945$$

$$DRI = (1.0 \pm 0.2)M - (21 \pm 21) \quad r = 0.889$$

$$GGC = (1.4 \pm 0.1)M - (20 \pm 12) \quad r = 0.975$$

Here M represents the mean LWC value from the ASRC, CIT, DRI, and GGC samplers (excluding replicate samplers), and r is the correlation coefficient. For the ASRC and AV-coarse samplers, the errors in the slope of the line are as large as the slope itself and are therefore not reported.

The regression slope is largest for the GGC mesh sampler; however, its intercept is negative. It is the only sampler for which the intercept is significantly different from zero. The mesh sampler tends to give lower values at low liquid water content levels and higher values at high LWC. This is explained by the calibration data of McFarland and Ortiz, who find a significant fraction of the water is retained by the mesh at low LWC and is not transferred to the collection bottle. At high LWC, this is not a large factor in sample recovery.

The DRI and CIT samplers agree fairly well throughout the range of LWC observed here. Calibration data indicate that the particle sizes collected by the samplers differ. Measured 50% efficiency cutoffs for the CIT (5), DRI (6),

and GGC (7) samplers are 20, 5, and 2.4 μm , respectively. With a volume-median fog droplet diameter of 20 μm , one would expect almost twice as much liquid as water would be collected by the DRI and GGC samplers than by the CIT sampler. This was not observed. In fact, these data indicate very similar collection efficiencies for the CIT and DRI samplers.

The ASRC and AV samplers give systematically lower values of LWC than the four-sampler mean. Correlation coefficients for regressions against the mean are above 0.82. Errors in the regression coefficient (i.e., the slope) are large, but inspection shows that the inferred liquid water contents are lower than with the other sampler types. One would expect the AV-coarse sample cut, which was designed to collect only those droplets greater than 10 μm , to collect less fogwater, but the decrease seen here is greater than can be explained on the basis of the size cut alone. The optical particle counter gave volume-median droplet diameters of 18–28 μm , which implies that substantially more than half of the water mass was in droplets greater than 10 μm . Yet the AV-coarse LWC is less than one-third of the AV-total (>2.5 μm) collection and only about one-fourth of the mean.

Comparison with Ancillary Measurements of LWC. Both the laser transmissometer and the PMS optical particle counter gave continuous measurements of liquid water content. These have been averaged over each of the time periods for the sampler fogwater collection. The optical counter LWC and the four- (ASRC–CIT–DRI–GGC) sampler mean LWC are compared with the laser transmissometer LWC. The correlations are good for both the optical counter ($r = 0.99$) and the sampler mean ($r = 0.93$), but there are significant biases between the measurement methods. Linear regression with respect to the laser transmissometer (LT) gives

$$\text{OPC} = (6.5 \pm 0.5)\text{LT} - (450 \pm 120)$$

$$\text{M} = (0.57 \pm 0.07)\text{LT} - (19 \pm 17)$$

where OPC and M, respectively, are the optical counter and the four-sampler mean observations of liquid water content. The sampler mean LWC is about 40% lower than the laser transmissometer observation. The optical counter data are higher than the laser transmissometer data by a factor of 4.5–7.5 and higher than the sampler mean LWC by a factor of 6–11. A large discrepancy between OPC and sampler liquid water content has also been reported by Katz and Miller (12). They saw a difference of a factor of 4.5 between the PMS optical counter and the DRI collector. Baumgardner (15) has also reported poor LWC estimates from optical counter data, with the optical counter about a factor of 2 higher than a hot-wire probe.

Fogwater Chemistry

The fogwater collected from each sampler was analyzed on-site for pH and then sent to a central laboratory for determinations of pH, conductivity, total acid by Gran's titration, sulfate, nitrate, ammonium, sodium, chloride, potassium, calcium, and magnesium. The data include (1) replicate chemical analyses or individual samples and analysis of samples from (2) collocated identical samplers, (3) separated identical samplers, and (4) simultaneous collection by all sampler types. The data from the different samplers are also examined for systematic biases. Because of the large volume of data, only illustrative examples are presented here. The complete data set is presented by Hering and Blumenthal (8).

Replicate Chemical Analyses (Type I Data). Of the 183 samples collected during the project, 14 were split

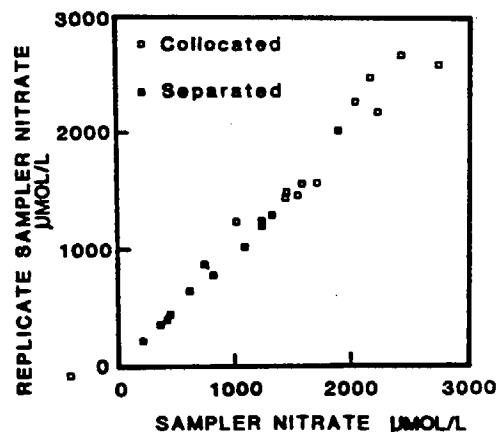


Figure 11. Comparison of simultaneous nitrate measurements for replicate CIT samplers located side by side (□) and separated (■).

on-site to provide blind replicate analyses by the central laboratory. The coefficients of variation for the replicate analyses of sulfate, nitrate, ammonium ion, hydrogen ion (by pH), total acidity (Gran's titration), sodium, and chlorine are 3–5%. Greater variabilities of 14% and 26% (2–10 $\mu\text{M/L}$) were found for potassium and calcium. This larger error is attributed to the low concentrations of these ions in the samples.

Sample pH measurements were made both in the field and at the central laboratory. The average pH value for the 122 measurements is 3.08; the pooled standard deviation between field and laboratory measurements is 0.06 pH unit, corresponding to an error in the hydrogen ion concentration of 15%. The laboratory data show systematically higher pH values than measured in the field. On the basis of the Wilcoxon signed rank test (16), the bias is significant at the >99% confidence level. This difference could be due to either a systematic difference in calibration between the pH meters or a slight loss of acidity during the 1–2-day storage. We note that the pH meters were compared side by side at the beginning of the project, and the buffer solutions used for the daily calibrations were all provided by CE Environmental Services. Other investigators (17) have reported an increase of pH with sample storage.

Identical Samplers (Type II and Type III Data). For collocated identical samplers, the fogwater chemistry data were generally in good agreement. The nitrate data from the two collocated CIT samplers are shown by the open symbols in Figure 11. Data from the GGC sampler and data for other major analyses are similar. The pooled standard deviations (coefficients of variation) are 0.02 unit (0.8%) for field pH, 130 μM (11%) for total acid, 184 μM (13%) for nitrate, 60 μM (14%) for sulfate, and 102 μM (15%) for ammonium.

Similarly, reasonable agreement is also found for simultaneous sampling with identical samplers located at different sites within the Henninger Flats sampling area. Figure 11 also compares nitrate concentrations for the separated CIT samplers. For most species, the variation between separated samplers of the same design is about the same as for side by side sampling. A direct comparison of simultaneous collocated and separated sampling with the same sampler type was not possible because there were no more than two samplers of each type. The comparison that is made is between collocated sampling on some days and separated sampling on other days. For the separated sampling with identical sampler types, the pooled standard deviations (and coefficients of variation) for nitrate, sulfate, ammonium, and total acid are 216 μM (12%), 48 μM (9%),

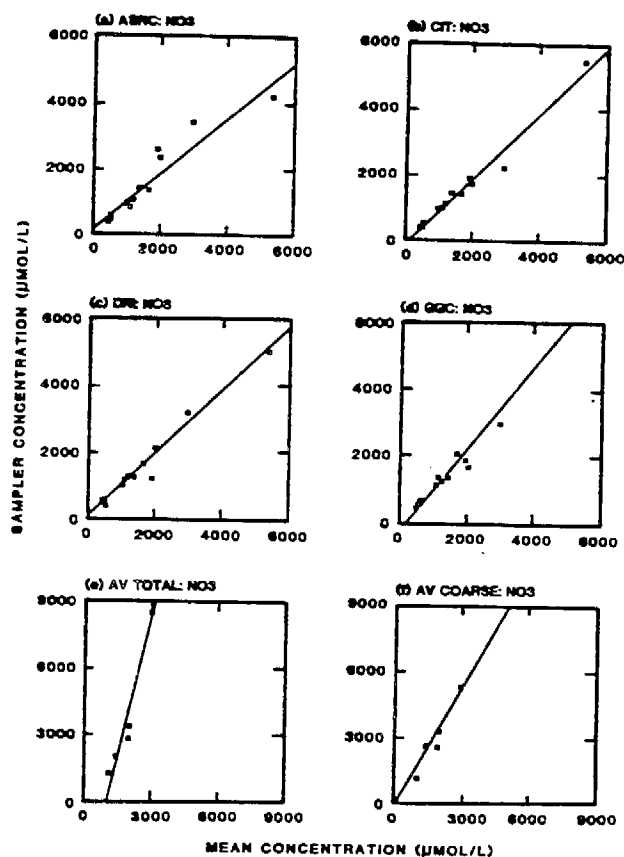


Figure 12. Fogwater nitrate concentration data from each sampler is compared with the mean value from the ASRC, CIT, DRI, and GGC samplers. Values are from the (a) ASRC rotating string, (b) CIT rotating arm, (c) DRI linear jet, (d) GGC mesh, (e) AV-total fog, and (f) AV-coarse ($>10\text{ }\mu\text{m}$) fog samplers. Lines are least-squares linear fits, as follows: ASRC = $(0.84 \pm 0.09)M + (160 \pm 190)$ ($r = 0.96$); CIT = $(0.93 \pm 0.05)M - (76 \pm 120)$ ($r = 0.99$); DRI = $(0.96 \pm 0.03)M + (110 \pm 80)$ ($r = 1.00$); GGC = $(1.22 \pm 0.07)M - (190 \pm 160)$ ($r = 0.99$); AV-T = $(4.2 \pm 0.8)M - (4200 \pm 1900)$ ($r = 0.98$); AV-C = $(1.71 \pm 0.26) + (100 \pm 570)$ ($r = 0.99$).

61 μM (8%), and 297 μM (17%) respectively.

Comparison of All Five Sampler Types. The different sampler types are compared for simultaneous sampling. Sequential 1-h samples obtained from some collector types have been averaged to allow direct comparison with the single 2–3-h samples obtained from other collector types. The replicate CIT and GGC samplers are not included in this analysis. Of the two samples collected by the AV sampler, namely, coarse ($>10\text{-}\mu\text{m}$ drops) and total ($>2.5\text{-}\mu\text{m}$ drops), we include only the total sample in this analysis. Thus, each sampler type is represented once.

In Figure 12 the nitrate concentrations from each sampler are plotted against the mean values. As the data set including the AV sampler is much smaller, its values were not included in the calculation of the mean. The mean value is the average from ASRC, CIT, DRI, and GGC, excluding replicate samplers.

Most notable in Figure 12 are the high nitrate data from the AV rotating rod sampler. Sulfate, ammonium ion, Na^+ , K^+ , Mg^{2+} , and Ca^{2+} data from the AV sampler were also high. In contrast, the hydrogen ion concentration calculated from the field pH measurement is in agreement with the mean value from the other four samplers. This can be seen both by inspection of scatter plots (not shown) and by analysis of variance.

Systematic difference among the sampler types is evaluated with a Friedman analysis of variance by rank (16). This is a nonparametric statistical test that ranks the species concentrations obtained by the different sam-

plers for each sampling period and then tests whether the rankings are random. The Friedman rank sums were also analyzed by a distribution-free multiple-comparisons test to assess which samplers are outliers. This statistical treatment does not require the data to be normally distributed; it is equally valid for any distribution.

For the five sampler types, the Friedman tests show no systematic differences for pH or hydrogen peroxide. Differences are found at the $>95\%$ level for ammonium, sulfate, nitrate, chloride, and metals. That a difference was found with a small data set of only four or five sampling periods is indicative of a large bias among the data. Inspection of the data shows consistently high values from the AV sampler for these analytes. Pairwise comparisons based on the sampler rankings show this bias toward high species concentrations from the AV sampler is statistically significant at the 95% confidence level. Specifically, for this five sampling period data set, we find sulfate, nitrate, and ammonium concentrations from the AV sampler are significantly higher than those from any of the other four samplers, whereas there is no apparent difference among the ASRC, CIT, DRI, and GGC samplers. For the metals sodium, potassium, calcium, and magnesium, we again find the AV sampler concentrations are higher (at the 95% confidence level) than those of the other samplers. Additionally, metals concentrations from the DRI sampler are lower (at the 95% confidence level) than those from either ASRC, GGC, or AV. Metals concentrations from the CIT samplers are intermediate between DRI and ASRC or GGC. These results may be summarized as follows:

- (1) For pH there are no apparent differences.
- (2) For SO_4^{2-} , NO_3^- , and NH_4^+ :
 AV > ASRC
 AV > CIT
 AV > DRI
 AV > GGC
- (3) For Na^+ , K^+ , Ca^{2+} , and Mg^{2+} :
 AV > ASRC
 AV > CIT
 AV > DRI
 AV > GGC
 DRI < ASRC
 DRI < AV
 DRI < GGC
- (4) For H_2O_2 there are no apparent differences.

Examination of Analyte Burdens. The consistently high concentrations measured by the AV rotating rod sampler, coupled with the low values for liquid water content inferred from the AV collection volumes, lead one to suspect evaporative losses. Thus, the samplers were also compared on the basis of burdens, i.e., mass of analyte collected per volume of air sampled. We found that the nitrate burdens obtained with the AV sampler are compared with the mean burdens from the other four sampler types. The higher analyte concentrations are partially offset by the lower liquid water collection. For the other samplers we found systematic differences in the species burdens, attributable to the differences in inferred liquid water content discussed previously. Friedman ranking tests show systematic differences in calculated burdens at the $>99\%$ confidence level. The ASRC string collector, which gives low LWC, also gives low burdens. Regression slopes from the GGC, DRI, and CIT samplers are no significantly different from one.

We conclude that evaporative losses are a problem for the AV rotating rod collector. For the ASRC string collector the analyte concentrations are in agreement, but the

LWC calculated is not. The assumption of 100% collection and retention of intercepted fog used to calculate LWC is probably incorrect for this sampler.

Comparison of ASRC, CIT, DRI, and GGC Samplers. The data comparing the four sampler types, ASRC, CIT, DRI and GGC, were also analyzed with the Friedman tests. This is a much larger data set, which allows us to detect differences among these four samplers that may not be apparent from the above analyses. For these four sampler types, we find no significant differences in the results of the Gran's titration acidity, field pH, conductivity, hydrogen peroxide, nitrate, or sulfate. Differences are found for ammonium ion, chlorine, sodium, potassium, calcium, and magnesium.

Pairwise comparisons based on the Friedman rank sums show the ammonium ion concentrations measured by the CIT sampler are lower than those from the GGC sampler. Sulfate and nitrate concentrations also tend to be lower, but the difference is not significant. For chlorine, the GGC sampler is consistently high, with other samplers reporting equivalent values. For the metals, we find concentrations from the DRI sampler are lower at the 95% confidence level than those from the CIT sampler, which in turn are lower than those from either the GGC or ASRC sampler. In other words, only the GGC and ASRC samplers give equivalent metals concentrations. Those from the DRI sampler are the lowest; those from the CIT sampler are intermediate. We infer from these data that the DRI sampler did not collect as much soil dust as the other samplers. The statistically significant biases among sampler types are summarized as follows:

- (1) For pH there are no apparent differences.
- (2) For SO_4^{2-} and NO_3^- there are no apparent differences.
- (3) For NH_4^+ :
GGC > CIT
- (4) For Cl^- :
GGC > ASRC
GGC > CIT
GGC > DRI
- (5) For Na^+ , K^+ , Ca^{2+} , and Mg^{2+} :
DRI < CIT < ASRC or GGC

Summary of Pooled Standard Deviations. For ammonium, sulfate, and nitrate, the variability among sampler types is greater than for separated identical sampler types. This is shown graphically in Figure 13, which gives the pooled standard deviations for each of the four data types discussed here, namely, (1) duplicate chemical analyses, (2) collocated identical samplers, (3) separated identical samplers, and (4) different sampler types (not including AV). The corresponding coefficients of variation, calculated as the pooled standard deviation over the average species concentration for the particular data set, are also given. As the average values vary from type I to type II to type III, etc. data sets, these coefficients of variation are not always in the same proportion to σ . For ammonium, sulfate, and nitrate, the coefficients of variation vary from 3.6% to 4.6% for duplicate chemical analyses, from 8% to 12% for separated identical sampler pairs, and from 24% to 33% for the four sampler types. Each added factor in the experiment such as replicate sampler collocation, sampler location, and sampler design increased the standard deviation in the measurement.

Acidity measurements are more consistent (Figure 14). The total and strong acid from Gran's titration show 11-16% variation for collocated identical samplers, 17% for separated identical samplers, and 21-23% among sampler types. Hydrogen ion concentrations calculated



Figure 13. Comparison of pooled standard deviations (σ) and coefficients of variation (%) for all four data types for nitrate, sulfate, and ammonium.

from pH showed 28% variability for the different sampler types, as compared with 22% variability among separated samplers of the same design. These acidity measurements were the most reproducible in the study and were not detectably influenced by sampler design. For the metals, the variability is quite large for separated identical samplers. The respective coefficients of variation for Na^+ , Ca^{2+} , K^+ , and Mg^{2+} are 30%, 70%, 38%, and 34%. This is approximately twice the variability observed for collocated identical samplers. The variability among sampler types is not significantly greater than the variability due to sampler location. For the four different sampler types, the coefficients of variation are 46% (Na^+), 80% (Ca^{2+}), 71% (K^+), and 34% (Mg^{2+}).

Comparison of CIT and GGC Samplers. Here we considered the data subset of GGC and CIT samplers for which there is one replicate during each sampling period. No distinction is made between the collocated and separated siting of replicate samplers. Once again, this provides us with a larger data set, which allows us to detect differences not apparent in the foregoing analyses.

We applied the analysis of variance to apportion the variance between the effects of sampler type, sampler duplicate, and the random (sampling) error. The random error includes discrepancies due to sampler operation. It is what would be found for repeated sampling with the same sampler under identical conditions. This analysis was applied to 11 sampling periods for which we have complete data sets of field pH, ammonium, sulfate, nitrate, chloride, sodium, potassium, calcium, and magnesium.

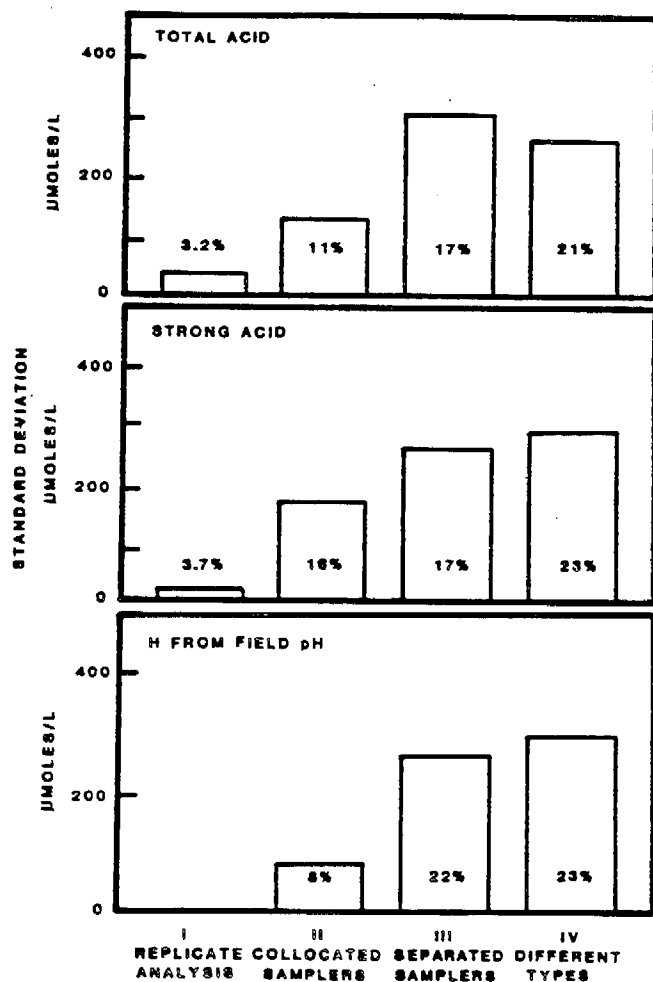


Figure 14. Comparison of pooled standard deviations (σ) and coefficients of variation (%) for all four data types for acid measurements.

Field pH values were converted to hydrogen ion concentrations.

We found the variance attributable to sampler replicates was insignificant. On the other hand, the variance between the two sampler types was significant for all analytes except pH. The variance in analyte concentration for the two sampler types may thus be apportioned between effect due to sampler type, σ_{type} , and effect due to random error, σ_e . For ammonium concentrations, we find random error $\sigma_e = 22 \mu\text{M/L}$, and the variance due to sampler type $\sigma_{\text{type}} = 67 \mu\text{M/L}$. Values for nitrate are $\sigma_e = 83 \mu\text{M/L}$, and $\sigma_{\text{type}} = 92 \mu\text{M/L}$; for sulfate, $\sigma_e = 17 \mu\text{M/L}$ and $\sigma_{\text{type}} = 26 \mu\text{M/L}$. With the exception of hydrogen ion and potassium, the effects due to sampler type are of the same size as the random error. For hydrogen, all of the error is random, $\sigma_e = 260 \mu\text{M/L}$, with no difference attributed to sampler type.

With this larger data set we found some significant differences between the CIT and GGC sampler types. For nitrate, sulfate, and ammonium ion, we find the values for GGC are systematically higher than those of CIT. The average nitrate from the GGC sampler is $66 \mu\text{M/L}$ (5%) higher than the mean value of $1408 \mu\text{M/L}$. For sulfate, GGC is $19 \mu\text{M/L}$ (5%) higher than the mean of $422 \mu\text{M/L}$. For ammonium ion, GGC is $47 \mu\text{M/L}$ (7%) higher than the mean. There is no difference for hydrogen ion calculated from field pH.

Effects of Droplet Size, Liquid Water Content, and Analyte Concentration. For the ASRC, CIT, DRI, and GGC samplers, we have examined the variance among samplers as a function of liquid water content, mean

droplet size, and analyte concentration. For hydrogen ion, ammonium ion, nitrate, sulfate, and metals, the standard deviation among the four sampler types is greater at large concentrations. On the other hand, the coefficients of variation are independent of analyte concentration. Standard deviations among sampler types appear to be independent of droplet diameter.

The standard deviation among sampler types is larger at low liquid water contents. To examine the effect of LWC more closely, the data set was divided into two classes at high and low liquid water contents. Analysis of variance was applied to each class. For the CIT and GGC replicate samplers we find no differences attributable to liquid water content. Replicates of the same sampler give the same results, within statistical error, as before. The difference among sampler types is seen at both high and low liquid water contents. In both cases, the reported concentrations of ammonium, nitrate, sulfate, and chloride are higher for the GGC sampler. Hydrogen ion concentrations taken from field pH are the same within statistical error. The total variance and the magnitude of variance attributable to sampler type are greater at the low liquid water contents.

Similar results are found for the four sampler types, ASRC string collector, DRI impactor, GGC mesh, and CIT rotating arm collectors. Analysis of variance tests shows that for hydrogen ion (from field pH), ammonium, sulfate, nitrate, or chloride there is no effect attributable to liquid water content. This is to say, there is no systematic difference among sampler types that is seen only at low liquid water contents.

Summary and Conclusions

Fog samplers were compared both on the basis of their water collection rates per volume of air sampled and on the basis of the chemistry of the collected water. For all of these parameters, we compared the variability among sample types with the variability inherent in the experiment, as determined from replicate chemical assays and simultaneous sampling with identical collectors.

Three of the samplers gave reasonable agreement for liquid water content. The CIT and DRI samplers agreed throughout. The GGC sampler was close but gave 40% higher LWC in heavy (high LWC) fogs and lower LWC in light fogs. The ASRC and AV samplers gave consistently low values for LWC. The mean liquid water content from the samplers correlates well with the transmissometer data but is consistently lower by 40%.

Four of the samplers, ASRC, CIT, DRI, and GGC, agreed in the concentrations of the major analyses. There were no systematic differences in sulfate, nitrate, or hydrogen ion levels. The GGC sampler was slightly higher for chloride and ammonium ion. The metal ions Na^+ , K^+ , Ca^{2+} , and Mg^{2+} were more variable. Higher values are obtained by the GGC and ASRC samplers and lower values from the DRI samplers. The variability in these metals is likely due to differences in the amount of soil dust collected.

For the AV sampler, fogwater pH values agreed with those from other samplers. For all other analytes, concentrations were significantly higher. Since this sampler also gave low values for liquid water content, it is apparent that evaporative losses are significant.

Overall, of the five samplers, reasonably consistent data were obtained from the CIT, DRI, and GGC samplers. Each of these samplers still has its limitations, and improved samplers are forthcoming. The CIT sampler is no longer in use, in part because of the safety hazard. Also, calibration work shows it is not an efficient collector for

small droplets ($<10\ \mu\text{m}$). The GGC sampler is not effective in light fogs because of the low sampling rate and fogwater retention on the mesh. The DRI sampler experienced some mechanical difficulties and has a low air sampling rate, which may limit its applications. The ASRC sampler gave consistent values for analyte concentrations but not for liquid water content.

To summarize, discrepancies were much greater for liquid water content than for analyte concentrations. All of the samplers agreed for fogwater pH; most samplers agreed for fogwater nitrate and sulfate. Evaporative losses of fogwater can be a very important factor and must be considered in fog sampler design.

Acknowledgments

This work was sponsored by the Coordinating Research Council, the Southern California Edison Company, and the Western Oil and Gas Association. The field coordination and data analyses were performed by Sonoma Technology under contract to the Coordinating Research Council CAPA-21 Committee, under the direction of Robert Gorse. The sampling site was provided by the Forestry Division of the Los Angeles County Fire Department. Laboratory facilities were provided by CIT. Logistics support, meteorological forecasting, and many ancillary measurements were provided by Southern California Edison personnel under the direction of Carol Ellis. The project was possible only through the efforts and contributions of the many participants. These include George Colovos and Susanne Ozdemir of the Combustion Engineering Environmental Services Laboratory, who provided the fogwater chemical analyses. William Munger, Jed Waldman, and Daniel Jacob of the California Institute of Technology operated the laser transmissometer and an optical counter in addition to their fog samplers. Greg Kok of the National Center for Atmospheric Research provided on-site measurements of hydrogen peroxide. Many people dedicated their nighttime hours to the operation of the instrumentation, including Bradley Muller of AeroVironment, Win Proctor, John Word, and Jack Dea of the Desert Research Institute, Richard Brewer of Global Geochemistry, John Del Santo, Ken Webster, and Nancy Camarota of Atmospheric Sciences Research Center, and Stan Marsh, Larry Bregman, Andrew Huang, and Laura Games of Edison. On-site pH and fogwater mass measurements were made with the able assistance of Diane Austin (STI) and Don Buchholz (STI). Mel Zeldin (SCE) and Stan Marsh (SCE) provided meteorological forecasting. Suzanne Twiss, Willard Richards, and Mel Widawski assisted in the statistical analyses, and Bruce Appel helped design the chemical protocol and quality-assurance procedures. For their enthusiastic cooperation and assistance, we thank the Forestry personnel, including Clyde Bragden, Robert Johnson, Martin Gebrude, and Karl Fisher, and the California Institute of Technology staff, especially Elton Daly, Elaine Granger, Joan Mathews, and Sandy Brooks. We also thank Dave Wilbur, Dave Miller, and Ted Smith for their advice in the program planning, and Stephanie Duckhorn, Phyllis Gilbert, and the late J. A.

McDonald for their able assistance in the manuscript preparation.

Registry No. H_2O , 7732-18-5; H^+ , 12408-02-5; NH_4^+ , 14798-03-9; Cl^- , 16887-00-6; K^+ , 24203-36-9; Ca^{2+} , 14127-61-8; Mg^{2+} , 22537-22-0; Na^+ , 17341-25-2; NO_3^- , 14797-55-8; SO_4^{2-} , 14808-79-8.

Literature Cited

- (1) Munger, J. W.; Jacob, D. W.; Waldman, J. M.; Hoffman, M. R. *J. Geophys. Res.* 1983, 88, 5109-5121.
- (2) Jacob, D. J.; Waldman, J. M.; Munger, W. J.; Hoffmann, M. E. *Environ. Sci. Technol.* 1985, 19, 730-736.
- (3) Brewer, R. L.; Gordon, R. J.; Shepard, L. S. *Atmos. Environ.* 1983, 17, 2267-2270.
- (4) Waldman, J. M.; Munger, J. W.; Jacob, D. G.; Hoffmann, M. R. *Tellus, Ser. B* 1985, 37B, 91-105.
- (5) Jacob, D. J.; Wang, R. F. T.; Flagan, R. C. *Environ. Sci. Technol.* 1984, 18, 827-833.
- (6) Katz, U. A. *Droplet Impactor to Collect Liquid from Laboratory Clouds for Chemical Analysis*; Communications a la VIII^{ème} Conference International sur la Physique des Nauges Clermont-Ferrand, France; 1980; pp 697-700.
- (7) McFarland, A. R.; Ortiz, C. A. "Characterization of the Mesh Impactor Fog Sampler"; report to Southern California Edison (Research & Development); Texas Engineering Experiment Station Project 32525 1107; May 1984.
- (8) Hering, S. V.; Blumenthal, D. L. "Fog Sample Intercomparison Study"; Data Volume; Sonoma Technology: Santa Rosa, CA, 1983; Hering, S. V.; Blumenthal, D. L. "Fog Sampler Intercomparison Study"; final report; Sonoma Technology; Santa Rosa, CA, 1985.
- (9) Richards, L. W.; Anderson, J. A.; Blumenthal, D. L.; Duckhorn, S. L.; McDonald, J. A. "Characteristics of Reactants, Reaction Mechanisms, and Reaction Products Leading to Extreme Acid Rain and Acid Aerosol Conditions in Southern California"; final report to the California Air Resources Board; CARB Agreement AO-140-32; STI Report 83 ES-200; Sonoma Technology: Santa Rosa, CA, 1983.
- (10) Hegg, D. A.; Hobbs, P. V. *Atmos. Environ.* 1981, 15, 1597-1604.
- (11) Castillo, R. A.; Jiusto, J. E. In *Precipitation Scavenging, Dry Deposition, and Resuspension*; Pruppacher, H. R.; Semonin, R. G.; Slinn, W. G. N., Eds.; Elsevier: New York, 1983; Vol. 1, pp 115-123.
- (12) Katz, U.; Miller, D. "Development and Evaluation of Cloud Water Collectors"; final report; Atmospheric Sciences Center, Desert Research Institute: Reno, NV, 1985.
- (13) Kadlecsek, J.; McLaren, S.; Camarota, N.; Mohnen, V.; Wilson, J. In *Precipitation Scavenging, Dry Deposition, and Resuspension*; Pruppacher, H. R.; Semonin, R. G.; Slinn, W. G. N., Eds.; Elsevier: New York, 1983; Vol. 1, pp 102-113.
- (14) Dollard, G. J.; Unsworth, M. H. In *Precipitation Scavenging, Dry Deposition, and Resuspension*; Pruppacher, H. R.; Semonin, R. G.; Slinn, W. G. N., Eds.; Elsevier: New York, 1983; Vol. 1, pp 161-169.
- (15) Baumgardner, D. *J. Clim. Appl. Meteorol.* 1983, 22, 891-910.
- (16) Hollander, M.; Wolfe, D. *Nonparametric Statistical Methods*; Wiley: New York, 1973.
- (17) Peden, N. E.; Skowron, L. M. *Atmos. Environ.* 1978, 12, 2343-2349.

Received for review March 17, 1986. Revised manuscript received October 20, 1986. Accepted February 27, 1987.

00000002



ASSET